Alma Mater Studiorum – Università di Bologna

DOTTORATO DI RICERCA IN

CHIMICA

Ciclo 34

Settore Concorsuale: 03/C1 - CHIMICA ORGANICA

Settore Scientifico Disciplinare: CHIM/06 - CHIMICA ORGANICA

β-LACTAMS: FROM THEIR STRUCTURAL FEATURES TO THEIR BIOLOGICAL APPLICATIONS

Presentata da: Martina Cirillo

Coordinatore Dottorato

Prof. Luca Prodi

Supervisore

Prof. Daria Giacomini

Co-supervisore

Prof. Pier Giorgio Cozzi

Esame finale anno 2022

Table of content

Abstract

β-lactam compounds represent an important class of four-membered cyclic amides (azetidin-2-ones) thanks to their valuable and varied biological activities. The presence of a β-lactam ring in a series of bioactive molecules targeting different proteins, allows us to consider the azetidin-2-one a privileged structure. In particular, β-lactams have two definite structural features that are of interest with regard to biological activity: a constrained four-membered cyclic amide which could easily undergo ring-opening reactions by nucleophilic residues in the active sites of enzymes (mechanism suggested for antibacterial activity and for the inhibition of β-lactamases and elastases); and a rigid core structure that, by reducing the conformational degrees of freedom, could favour and actually enhance directional noncovalent bonding for an effective ligand−receptor recognition.[1] Nowadays monocyclic β-lactams are known as anticancer, antidiabetic, anti-tubercular, anti-inflammatory, antiparkinsonian and anti-HIV agents[2-4] and as ligands of integrin receptors.[1,5]

In order to consider different facets of 4-azetidin-2-ones, this report will be divided into two sections: the first one will be dedicated to the design, synthesis and characterization of biological active β-lactams (new β-lactam based integrin ligands and their different applications and novel N-thio-alkyl substituted azetidinones for the treatment of Tuberculosis); the second one instead, will be based on two projects which consider two different proprieties of β-lactams: stereochemistry, evaluated by biocatalytic methods and reactivity at C-4 position. In the first case we want to obtain enantiomerically pure 4-acetoxy-2-azetidinone, useful for synthesis of stereo-chemically defined bioactive β-lactams, while in the second case we want to study in which conditions the nucleophilic substitutions occur.

A final section will be instead dedicated to the research project that I followed during my period abroad in Philochem AG, Zurich, under the supervision of Prof. Dario Neri and Dr. Samuele Cazzamalli, based on the study of new cleavable disulfide linkers for small molecule drug conjugates targeting Fibroblast activation protein (FAP).

Section 1

Integrins are heterodimeric transmembrane receptors constituted by two protein chains, α and β, and particularly attractive as pharmacological targets. These cell adhesion glycoproteins have a fundamental role in increasing invasion, migration, and proliferation; moreover, they have been linked to tumor angiogenesis, which is an essential process for tumor growth and metastasis.[6] Previous studies provided a novel series of β-lactam-based molecules able to modulate cell adhesion on targeting different integrins, mainly RGD-binding and leukocyte-integrins such as $\alpha_v\beta_3$, $\alpha_v\beta_5$, $\alpha_v\beta_6$, $\alpha_5\beta_1$, $\alpha_{II}b\beta_3$, $\alpha_4\beta_1$, and $\alpha_L\beta_2$. The chemical structure of the new integrin ligands was designed with the β-lactam ring as a site of conformational restriction to provide a favourable alignment on the receptor and to satisfy the crucial requirements for integrin affinity and selectivity. Some ligands behave as agonists promoting cell adhesion and intracellular signaling, while others acting as integrin antagonists may inhibit integrin-dependent cell functions.[1,7]

As previously anticipated, integrin receptors play an important role in tumor angiogenesis and metastasis, and they are overexpressed in many types of cancer cells. For all these reasons, their potential as a therapeutic target is now widely recognized.[7] In addition, integrins can be internalized upon agonist ligand binding[9-11] and therefore they may be used as shuttle to selectively release the antineoplastic drug only inside integrin expressing cancer cells; so integrin ligand can be used as carrier in the development of drug delivery systems.[6] Starting from a previously studied selective agonist (**A**) for $\alpha_4\beta_1$ integrin,[1] we designed and realized first two fluorescent compounds **B** and **C** (*Figure 1*) to get evidence on ligands internalization. Then, the chemotherapeutic agent 5-fluorouracil (5-FU), chosen as model drug, was conjugated to the integrin ligand using different linkers, and the new conjugates **D**, **E**, and **F** (*Figure 1*) were studied in cell-based assays in order to ascertain their activity and selectivity against tumor cells.[12]

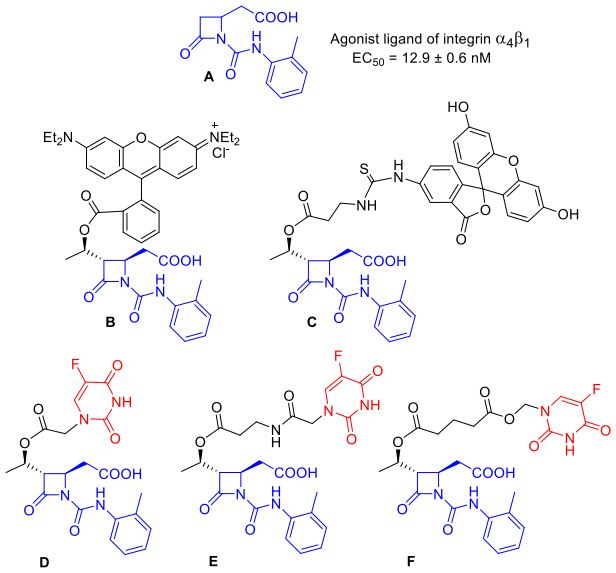

Figure 1. Compound **A** is the reference compound as model of integrin agonist ligand, **B** and **C** are new fluorescent compounds for internalization analyses, **D**, **E**, and **F** are new 5-FU-conjugates designed to evaluate the selectivity of the anticancer effect.

After demonstrating that these fluorescent-integrin ligand conjugates (**B** and **C**) displayed internalization properties required to deliver cytotoxic drugs into cancer cells in integrin-selective manner, the three conjugates composed by the β-lactam ligand, suitable linkers, and **5-FU** were realized. The best compound **E**, acting as $\alpha_5\beta_1$ integrin agonist, is able to selectively deliver 5-FU into tumor cells, successfully leading to cancer cell death.[12]

Thanks to these good results, in order to continue this project, we decided to use the same β-lactam-based integrin compound as drug-cargo for the selective delivery of theranostic agents. Theranostic systems permit to combine diagnostic and therapeutic functions into one integrated platform.

We developed two different systems, following two different strategies: the first is called "One for all"[13] (*Figure 2*) in which the β-lactam derivative is linked to a BODIPY, which is a particular photosensitizer that, upon interaction with light, brings out the formation of a cytotoxic

event, combining both imaging and therapeutic application. The second, instead, is an "All in one"[13] system in which the β-lactam carrier is conjugated with 3-azido-7-hydroxy coumarin, which acts as a fluorophore, suitably functionalized with 5-Fluorouracil, chosen as cytotoxic drug (*Figure 2*).

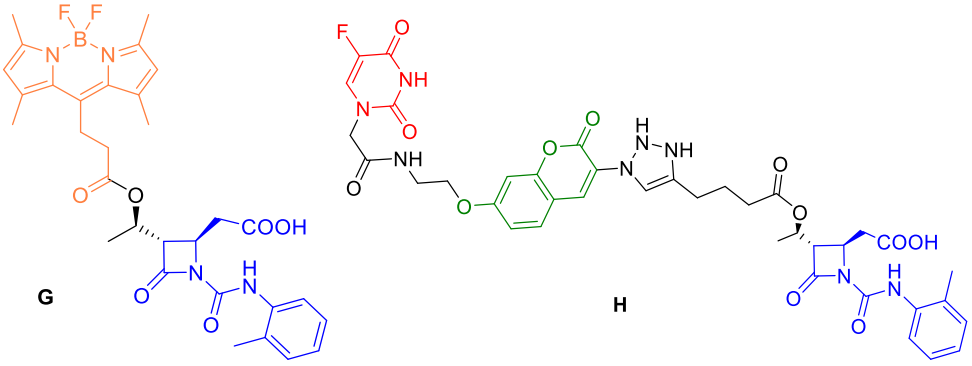

Figure 2. "One for All" system (**G**) and "All in One" system (**H**).

These two compounds will be tested in adhesion assays, cytotoxicity assays and finally the diagnostic proprieties will be evaluated.

Two β-lactam integrin agonists (*Figure 3*) from the library developed by the research group were selected on the basis of their activities towards specific integrins and have been used for the functionalization of Stronzium substituted Hydroxyapatite (SrHA) to develop materials able to enhance mesenchymal cells adhesion and to promote bone regeneration.

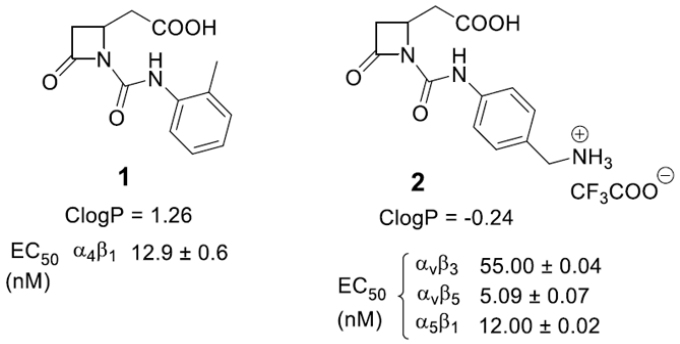

Figure 3. Selected β-lactam integrin agonists.

The amount of azetidinones loaded on SrHA could be modulated on changing the polarity of the loading solution, from 3.5 to 24 w% for compound **1** and from 3.2 to 8.4% for compound **2**. Studies on the release of the β-lactams from the functionalized SrHA in aqueous medium showed an initial burst followed by a steady-release that ensures a small but constant amount of the compounds over time. The new composites were fully characterized. Co-culture of human primary mesenchymal stem cells (hMSC) and human primary osteoclast (OC) demonstrated that the presence of β-lactams on SrHA favours hMSC adhesion and viability, as well as differentiation towards osteoblastic lineage. Moreover, the azetidinones were found to enhance the inhibitory role of Strontium on osteoclast viability and differentiation.[8]

Moreover, following the good results obtained for β-lactam **I** (*Figure 4*) towards leukocyte integrins (antagonist toward $\alpha_L\beta_2$, IC_{50} = 0.39 nM) evaluated in the aforementioned work[1], we also decided to develop a new library of compounds able to be recognized by the same class of receptors. These molecules are now being tested in adhesion assays in order to evaluate their real activity.

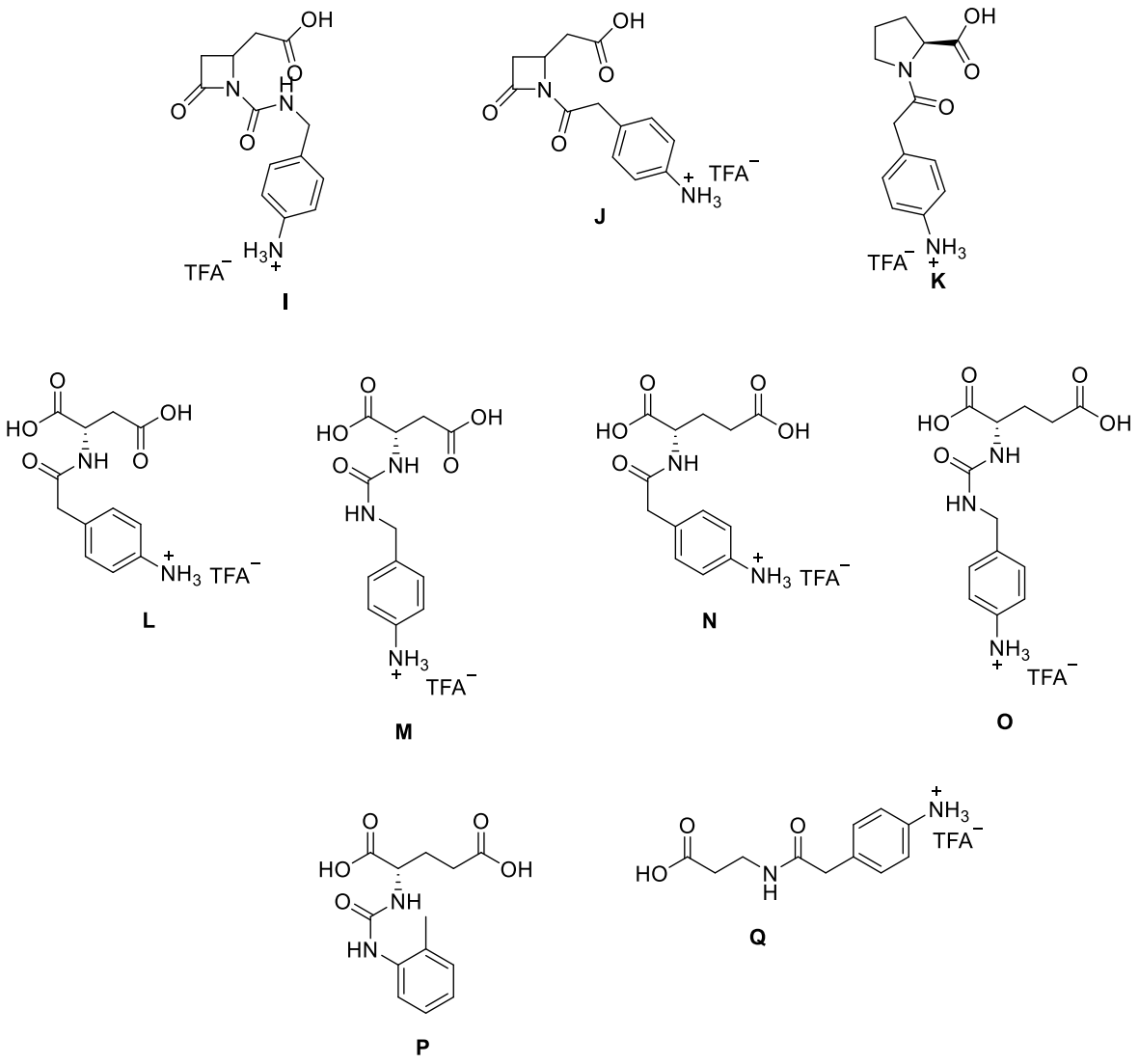

Figure 4. Novel leukocyte integrin ligands.

Besides these new applications, it is important to remember that the main medical use of β-lactam is the antibiotic one. They are in fact, still the main class of agents used today to treat bacterial infections, and a plethora of monocyclic β-lactams available today exhibit potent antimicrobial effects and diverse biological activities.[14] Several human pathogens including Mycobacterium tuberculosis, the agent responsible for Tuberculosis (TB), represents a serious problem with the increased occurrence of antimicrobial resistance and with the emergence of multidrug-resistant (MDR) infections observed in the clinic. Consequently, the World Health Organization considers the development of novel and effective antibiotics against MDR M. tuberculosis a high-priority issue.[15] About that, my research group conducted the design, synthesis, and characterization of novel antibiotic candidates targeting M. tuberculosis in collaboration with Prof. Schnell of Karolinska Institutet of Stockholm and Prof. Dal Monte of

Azienda Ospedaliero-Universitaria of Bologna. These compounds demonstrated to inhibit a cell wall remodelling protein using an unconventional mechanism of action acting effectively as carbapenem-type antibiotics. Furthermore, they kill M. tuberculosis including drug-resistant variants in vitro.[16] We decided to widen this library and in particular I focused on the synthesis of three series of new N-thioalkyl-β-lactams, with different groups at the C-4 position of the ring (4-SAc, 4-SO2Ph, 4-SPh). The synthesis of all compounds started with a nucleophilic substitution reaction on the commercially available starting materials (**SM1**, **SM2**). Then, for each series N-thioalkyl group were introduced; the last step, for compounds containing TBS group, was the deprotection reaction to give the free alcohol (*Figure 5*).

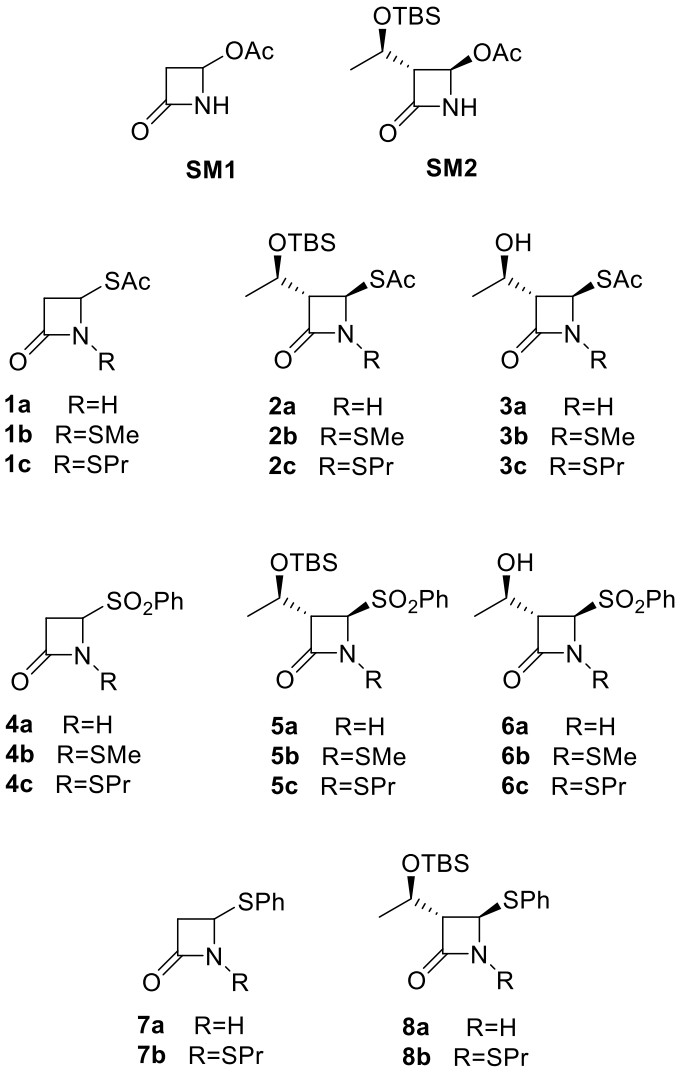

Figure 5. N-thio-alkyl β-lactams: target molecules of this thesis project.

Section 2

A useful β-lactam intermediate for the synthesis the aforementioned bioactive compounds is 4-acetoxy azetidin-2-one (**SM1**) and it is commercially available. However, **SM1** is purchased only as a racemic mixture so it can only provide racemic derivatives. It is well known that two enantiomeric drugs could give different pharmacologic responses and diverse pharmacokinetic,

pharmacodynamic and therapeutic profiles, or could even reveal adverse effects[17], therefore the possibility to gain access to the enantiopure form of 4-acetoxy-azetidinone **SM1** would be of utmost importance in the synthesis of stereo-chemically defined bioactive β-lactams. To the best of our knowledge, only (+) 4-acetoxy-azetidinone has been reported and obtained by chiral recognition process upon separation of chiral host-guest inclusion complexes.[18] We instead, decided to use lipases in a kinetic resolution (KR) process to finally obtain 4-acetoxy azetidin-2-one as separated pure enantiomers (*Figure 6*). From a preliminary screening on a set of commercial enzymes, *Pseudomonas Fluorescens* emerged as the most suitable lipase that allowed to obtain good conversions and excellent enantiomeric excesses. On the enantiomerically pure 4-acetoxy-azetidin-2-ones some nucleophilic substitutions and N-thio-alkylation reactions were tested in order to evaluate the stereochemical integrity at the C-4 position.[19]

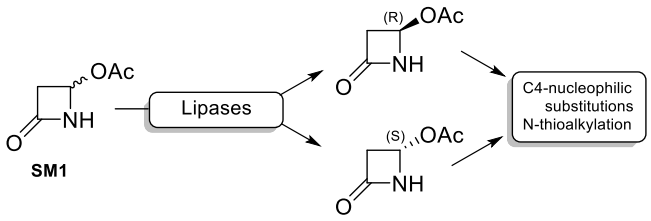

Figure 6. Enzymatic kinetic resolution on 4-acetoxy-2-azetidinone and evaluation of the stereochemical outcome in C-4 and N-functionalization.

Another interesting aspect to explore is the reactivity at the C-4 position of β-lactam based compounds toward nucleophilic substitutions (S_N1) under different conditions.

Initially, we decided to use benzyl alcohol or 4-methoxybenzylamine as nucleophiles in two different solvents: water and DCM, without any catalyst. In addition, selected alcohols were employed both as nucleophile and solvent. Then we employed acid resins as catalysts, while several amines having different basicity were employed as base catalysts. Even in this case the nucleophiles employed are benzyl alcohol and various amines.
Finally, the C-4 position of β-lactams was compared to the reactivity at the anomeric position of glycosides. Therefore, S_N1 reactions were conducted on selected β-lactam compounds under reaction conditions characteristic of glycosidation reactions (lewis acids as $BF_3{\cdot}Et_2O$, $TiCl_4$, and $AlCl_3$, promoters as NBS and triflates).

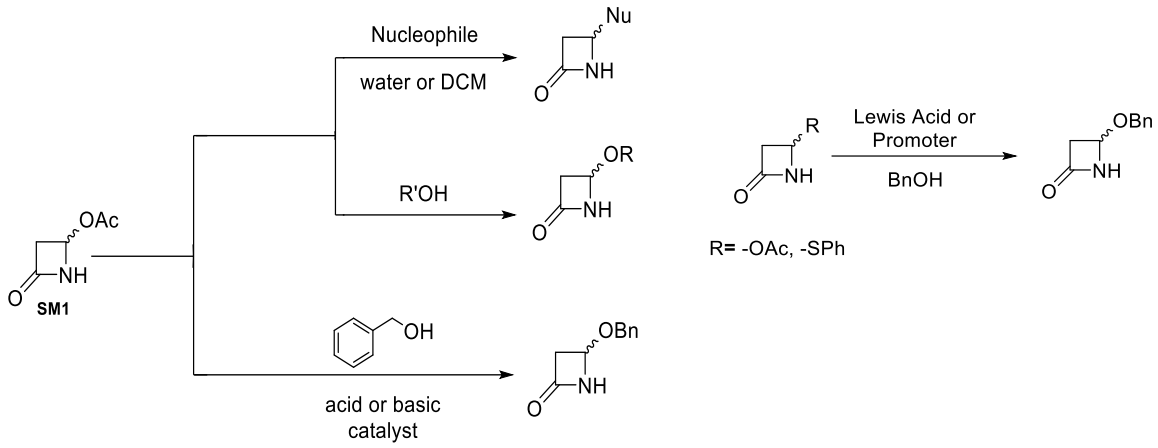

Figure 7. Nucleophilic substitutions at C-4 position of β-lactams under different conditions.

Section 3

Section 3 is dedicated to the study of disulfide linkers for the design and synthesis of new small molecule drug conjugates (*Figure 8*). I had the great opportunity to join the research group of Philochem AG during my PhD period abroad, and to work on this project under the supervision of Prof. Dario Neri and Dr. Samuele Cazzamalli.

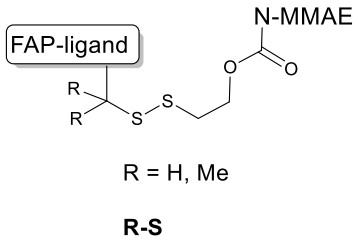

Figure 8. Study of new dipeptide linkers for small molecule drug conjugates.

Bibliography

1. M. Baiula, P. Galletti, G. Martelli, R. Soldati, L. Belvisi, M. Civera, S. D. Dattoli, Santi M. Sampinato, D. Giacomini, *J. Med. Chem.*, 2016, **59**, 9721-9742;
2. D. J. Fu, Y. F. Zhang, A. Q. Chang, J. Li. *Eur. J. Med. Chem*, 2020, **201**, 11251;
3. P. Galletti, D. Giacomini, *Curr. Med. Chem.*, 2011, **18**, 4265-4283;
4. P.D. Mehta, N. P. Sengar, A. K. Pathak, *Eur. J. Med. Chem.*, 2010, **45**, 5541-5560;
5. G. Martelli, M. Baiula, A. Caligiana, P. Galletti, L. Gentilucci, R. Artali, S. Spampinato, D. Giacomini, *J. Med. Chem.*, 2019, **62**, 10156-10166;
6. M. Cirillo, D. Giacomini, *Cancers*, 2021, **13**, 299;
7. P. Galletti, R. Soldati, M. Pori, M. Durso, A. Tolomelli, L. Gentilucci, S. D. Dattoli, M. Baiula, S. Spampinato, D. Giacomini, Eur. *J. Med. Chem.*, 2014, **83**, 284-293;
8. M. Cirillo, G. Martelli, E. Boanini, K. Rubini, M. Di Filippo, P. Torricelli, S. Pagani, M. Fini, A. Bigi, D. Giacomini, *Colloids Surf. B Biointerfaces.*, 2021, **200**, 111580;
9. L. Ferrazzano, D. Corbisiero, E. Potenza, M Baiula, S. D. Dattoli, S. M. Spampinato, L. Belvisi, M. Civera, A. Tolomelli, *Sci Rep.*, 2020, **10**, 7410;
10. N. De Franceschi, H. Hamidi, J. Alanko, P. Sahgal, J. Ivaska, *J. Cell. Sci.*, 2015, **128**, 839-852;

11. P. T. Caswell, J. C. Norman, *Traffic*, 2006, **7**, 14-21;
12. M. Baiula, M. Cirillo, G. Martelli, V. Giraldi, E. Gasparini, A. C. Anelli, S. M. Spampinato, D. Giacomini, *ACS Pharmacol. Transl. Sci.*, 2021, **4**, 1528-1542;
13. K. Kenry, K. C. Chong, B. Liu, *Acc. Chem. Res.*, 2019, **52**, 3051-3063;
14. P. Galletti; D. Giacomini, *Curr. Med. Chem.*, 2011, **18**, 4265-4283;
15. E. Tacconelli, E. Carrara, A. Savoldi, S. Harbarth, M. Mendelson, D. L. Monnet, C. Pulcini, G. Kahlmeter, J. Kluytmans, Y. Carmeli, M. Ouellette, K. Outterson, J. Patel, M. Cavaleri, E. M. Cox, C.R. Houchens, M. L. Grayson, P. Hansen, N. Singh, U. Theuretzbacher, N. Magrini, *Lancet Infect Dis.*, 2018, **18**, 318-327;
16. G. Martelli, T. B. Pessatti, E. M. Steiner, M. Cirillo, C. Caso, F. Bisognin, M Landreh, P. Dal Monte, D. Giacomini, R. Schnell, *Cell Chem Biol.*, 2021, **28**, 1321-1332;
17. S. W. Smith, *Toxicol. Sci.*, 2009, **110**, 4-30;
18. F. Toda, K. Tanaka, M. Yagi, Z. Stein, I. Goldberg, *J. Chem. Soc. Perkin Transactions I*, 1990, **4**, 1215-1216;
19. G. Martelli, M. Cirillo, V. Giraldi, D. Giacomini, *Bioorg. Chem.*, 2022, **120**, 105580;

Introduction

The main topic of this PhD thesis concerns the design and synthesis of new monocyclic β-lactam compounds, differently functionalized in order to express a specific biological activity. Moreover, other two projects are presented: the first one provides the use of biocatalysis and the other one is based on the study of nucleophilic substitutions at C-4 position of 4-acetoxy-2-azetidinones.
All these projects have been performed during my three year-PhD-program under the supervision of Prof. Daria Giacomini at the Department of Chemistry, University of Bologna.
Finally, I will also present the project performed during my six months-period abroad in Philochem AG (Zurich), under the supervision of Prof. Dario Neri and Dr. Samuele Cazzamalli.

A first section of this thesis will be therefore dedicated to the design, synthesis and characterization of new biological active β-lactams. This section will be further divided into two main sections: new β-lactam based integrin ligands and their different applications (bone regeneration, immune response, and cancer treatment), and novel N-thio-alkyl substituted azetidinones for the treatment of Tuberculosis. Moreover, biological data, obtained in collaboration with other research groups, as specified in the main body text, will be reported.

The second section instead, will be based on the two projects which consider two different properties of β-lactams: stereochemistry, evaluated by biocatalytic methods and reactivity at C-4 position. In the first case we want to obtain enantiomerically pure 4-acetoxy-2-azetidinone, useful for the synthesis of stereo-chemically defined bioactive β-lactams, while in the second case we want to study in which conditions the nucleophilic substitutions occur.

My research group is a pioneer in the development of novel active azetidinone compounds within since more than 15 years. This thesis work aims at amplifying the different biological activities and innovative promising applications that these kinds of compounds can present.

As previously anticipated, a final section is instead dedicated to the study of disulfide linkers for design and synthesis of new small molecule drug conjugates conducted at Philochem AG during my PhD period abroad.

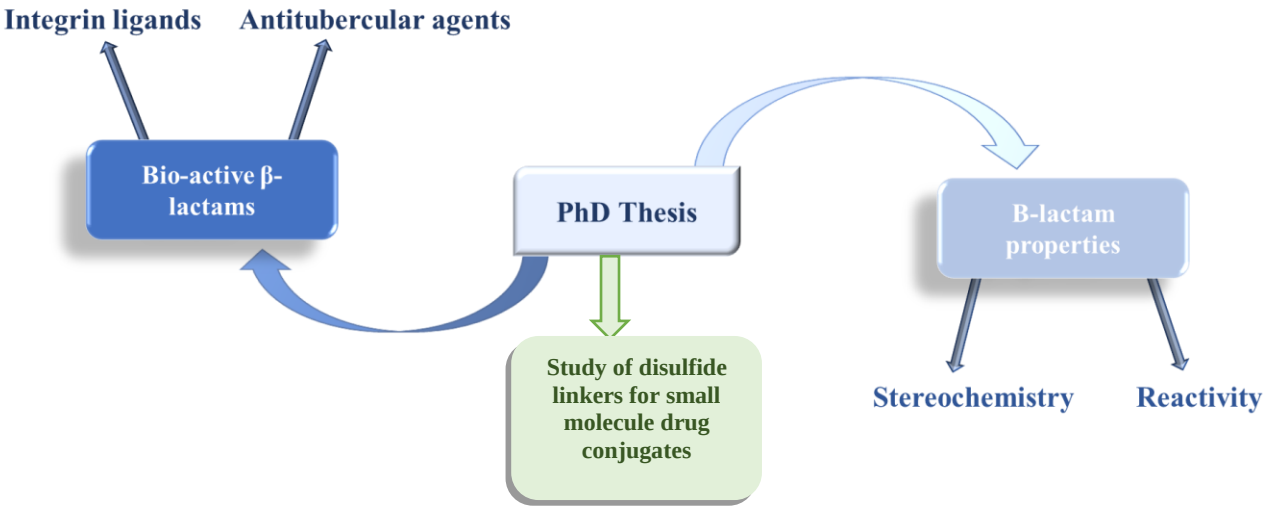

Figure 1. Phd thesis scheme.

Section 1. Novel bio-active β-lactam compounds

β-lactam (2-azetidinone), arguably one of the most acclaimed heterocycles studied over the last century, has a great impact in different fields, such as chemistry, biology, and medicine.[1] Azetidinone derivatives first attracted attention for their antibacterial properties, but recently they have been demonstrated by several studies that structural modifications with specific substituents are valid procedures for the detection of varied pharmacological activities different from the antibacterial one.[2] For example β-lactams can act as anticancer, antidiabetic, anti-tubercular, anti-inflammatory, antiparkinsonian and anti-HIV agents[1-3] and as inhibitors of a wide range of enzymes.[4]

About that, in this first section, we will explore the different pharmacological activities of the β-lactam-based compounds developed during these three years of PhD and we will also deepen their design, synthesis and biological evaluation. In particular, two main areas will be evaluated: the development β-lactam-based integrin ligands and their different fields of application and the study of novel N-thio substituted azetidinones with a potential activity as antitubercular agents.

1.1 New β-lactam based integrin ligands and their applications

1.1.1 Integrins

Integrins are adhesion receptors able to mediate dynamic adhesive cell-cell and cell-matrix interactions,[5] but they are also involved in the regulation of several crucial aspects of cellular functions, including migration, adhesion, differentiation, growth and survival, acting as bidirectional signalling transducers between the extracellular and intracellular environments.[6] From a structural point of view they are heterodimeric transmembrane receptors made of a non-covalent combination of α and β subunits and both subunits are type I transmembrane glycoproteins with a relatively large extracellular domain, a single transmembrane domain, and a short cytoplasmic tail (*Figure 2*).[7]

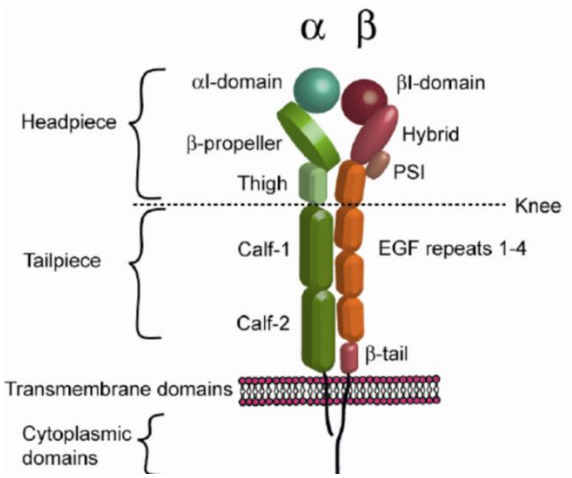

Figure 2. Integrin structure.

In mammals are known 18 α-subunits and 8 β-subunits, which assemble into 24 different integrins, which can be divided into 4 groups in relation to their ligand-binding specificity.[8,10] The first group involves integrins that recognize collagen (α_1, α_2, α_{10}, and α_{11}), then we have

integrins that recognize laminin (α_3, α_6, and α_7), leukocyte integrins (α_4, α_L, α_M, α_X, and α_D) and finally RGD (arginine-glycine-aspartic acid) binding integrins (α_{IIb}, α_V, α_5, and α_8) (*Figure 3*).

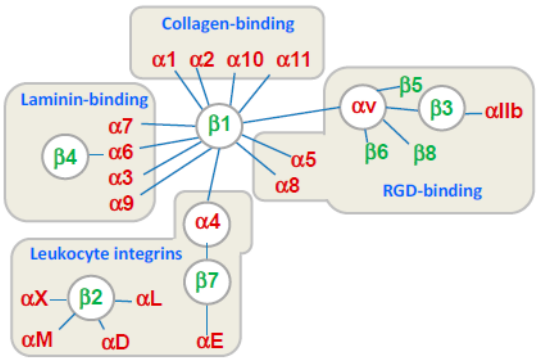

Figure 3. Integrin classification. Figure adapted from ref. 9.

Each integrin has a selective affinity for a particular ligand and performs different tasks depending on the type of cell in which is located.[10] The β subunit of the cytoplasmic domain plays an important role in integrin function as it acts as a binding site for some regulatory proteins. The α subunit, on the other hand, generates different families of integrins based on the type of ligand they interact with (*Figure 3*). Concerning the integrin binding site, it is important to distinguish the two types of α-subunits: those with or those without the αI domain. The αI domain is the binding site for ligands, whereas in integrins without it, the ligand-binding site is formed at the interface between the α-subunit and the β-subunit, and it is called βI domain.[11] The αI and βI domains are structurally homologous and contain metal ion-dependent adhesion sites (MIDAS) which are able to bind Asp, Glu, or carboxylic acid residues in ligands. In RGD-binding integrins (without αI), the Arg of RGD binds the α-subunit while the Asp of RGD coordinates to the Mg^{2+} ion in the βI domain MIDAS.[9]

From a structural point of view, all integrins may adopt three possible limit conformations: a bent-closed, an extended-closed, and an extended-open. These are related to a low affinity conformation, an activated and an activated together with ligand-bounded integrin conformations, respectively[12] (*Figure 4*).

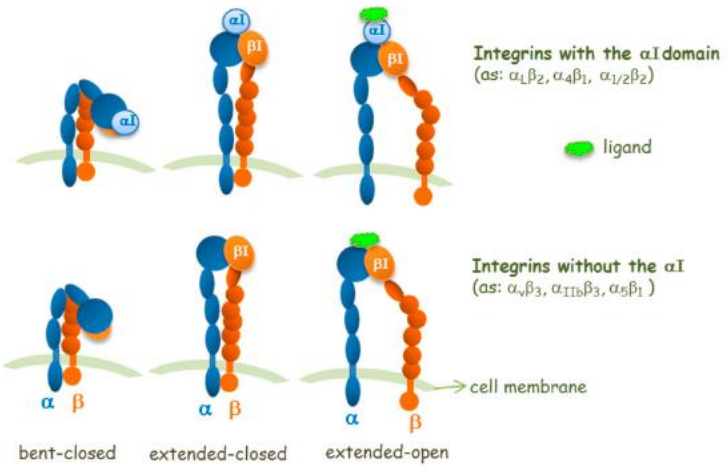

Figure 4. The three limit conformations of integrins and ligand interaction sites. Figure adapted from ref. 13.

Integrins are normally inactive with low affinity for their endogenous ligands, but they rapidly undergo activation upon various stimuli.[14] In fact, they can shift from one conformation to another after the recognition of the ligand[15] present in the extra-cellular matrix, through non-covalent interactions or after the interaction of the cytoplasmic tails with intracellular factors, such as talin.[16] So, after the interaction with a specific ligand, the integrin changes its conformation and together with this change there is the transmission of signals from the outside to the inside of the cell (outside-in, *Figure 5*), while due to the interaction of the cytoplasmic tails with some proteins, the conformational change induces a signal that has the opposite direction, from the inside to the outside of the cell (inside-out, *Figure 5*).[17] Integrin capacity to activate, integrate and distribute information identifies this family of adhesion receptors as valuable drug targets.[18] In fact, integrins are involved in immune responses, leukocyte traffic, haemostasis, and their potential as a therapeutic target is now widely recognized.[14]

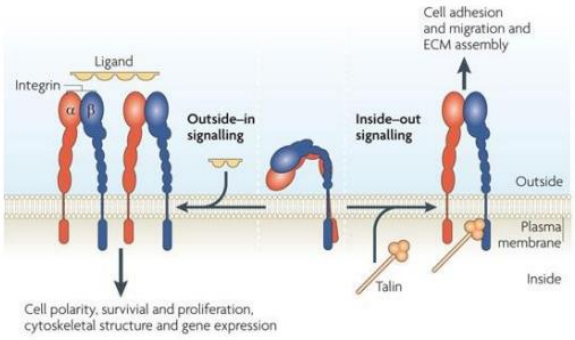

Figure 5. Integrin outside-in and inside-out signalling. Figure adapted from ref. 19.

The interaction with the ligand not only activates the integrin itself, but also induces a series of important processes for cellular activity such as integrin trafficking and endocytosis.[20]

Integrin trafficking is a process consisting of complex intracellular internalization and recycling pathways. These cycles of endocytosis and re-exocytosis can control the availability of integrins at the plasma membrane.[15] This process is regulated by members of the Ras-associated binding (Rab) family of small GTPases, which function as molecular switches is to control vesicular transport in eukaryotic cells.[21] This process consists of a complex intracellular internalization, through which integrin heterodimers are brought into the cytoplasm by modifying the shape of the plasma membrane (endocytosis), and are later re-send back to the cell surface (exocytosis).[22] As this mechanism plays such an important role in modulating the migratory activity of normal cells, it seems reasonable to suppose that it also will have a major impact upon a similar behavior on transformed cells. Thus, individual cell migration and invasive activity appear to be inextricably linked in regulating cancer invasion.[23] Understanding the molecular mechanisms of integrin trafficking is so fundamental for monitoring tumor progression and for the development of anticancer drugs. Several studies indeed demonstrated that tumor cells overexpress integrin receptors and their signal transduction occur in an anomalous way.[24] Especially the process of internalization of integrins, known as endocytosis, has a great impact on the behavior of cancer cells. Specifically, endocytosis is characterized by the internalization of protein receptors from the plasma membrane into internal membrane compartments before sorting to different cellular locations. Generally, endocytic processes are classified as clathrin-dependent endocytosis (CDE) or clathrinin-independent endocytosis (CIE) (*Figure 5*).[25] Cell surface receptors are endocytosed

by one of these routes, but it is also possible that a given type of integrin could follow more than one pathway depending on regions within a cell, cell conditions, and cell type.[26] Clathrin-mediated endocytosis, the best-characterised internalisation route, involves the recruitment of small vesicles that have a crystalline coat made up of a complex of proteins associated with the cytosolic protein clathrin, called clathrin-coated pit (CCP).[27] In contrast, less is known about the mechanisms involved in CIE, and, in particular, how cargoes are recruited, but most common reported non-clathrin-coated plasma membrane buds is Claveolae, which exist on the surface of many, but not all, cell types.[28]

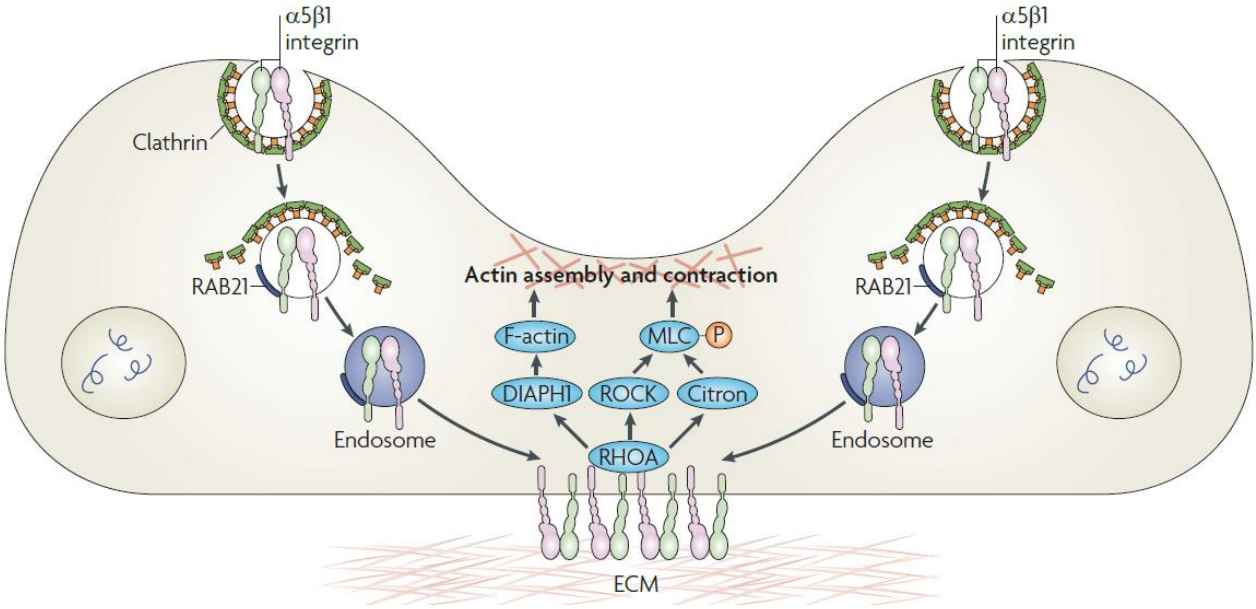

Figure 6. General scheme of integrin trafficking. Figure adapted from ref. 29.

1.1.2 Integrin ligands

In pharmacology ligands can be generally classified according to their action at the receptor. Agonists are compounds which bind to receptors and mimic the signaling of endogenous compounds; antagonists instead, bind to the receptor and block its interaction with endogenous agonists, but do not induce any receptor activation and signal transduction, and this means that they do not possess any intrinsic activity. Moreover, we can define as partial agonists the ligand which possess less ability to activate the receptor and associated signal transduction, while inverse agonists are compounds that are able to stabilize the receptor in its inactive conformation. In addition, there are ligands that can modulate receptor activity or binding of agonists/antagonists acting allosterically on a topographically distinct position from the site of activity or ligand binding and they are called allosteric agonists/antagonists.[9] Recently, it has been recognized that not all agonists behave in the same manner, introducing the hypothesis of biased agonism for integrins.[30] Among non-natural ligands, particular attention was attributed to cyclic peptides containing the RGD sequence into the cycle (cRGDs, *Figure 7*) and initial studies, showed that they have higher potency than linear RGD sequences in the inhibition of integrin receptor.[31]

This result could be ascribed to a lower flexibility due to conformational constrains by the cyclic structure and thus a higher directionality of the non-covalent interactions engaged by the cyclic molecules in the integrin-binding site.[32]

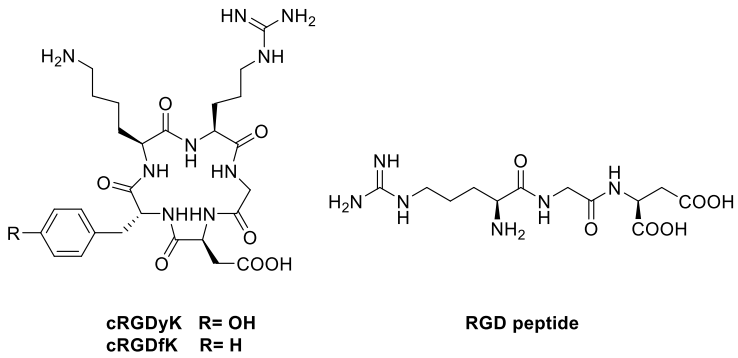

Figure 7. Cyclic and linear RGD peptide.

Initially, numerous efforts have been made to discover and develop integrin antagonists, for clinical applications,[33-34] active on specific type of integrins: $\alpha_v\beta_{3/5}$ and $\alpha_5\beta_1$, which have been implicated in tumor development; $\alpha_4\beta_{1/7}$ and $\alpha_L\beta_2$, which have been implicated in the regulation of immune functions, and finally $\alpha_{IIb}\beta_3$ (GpIIbIIIa), implicated in platelet aggregation.[35] Unfortunately, the antagonists of $\alpha_v\beta_3$, $\alpha_v\beta_5$ and $\alpha_5\beta_1$ integrins that have entered clinical trials as antiangiogenic agents for cancer treatment, such as the well-known Cilengitide (*Figure 8*), have generally been unsuccessful.[9] Cilengitide structurally is a small RGD containing cyclic pentapeptide developed by Kessler[36], studied in clinical phase III for glioblastoma and in phase II for other types of cancers.

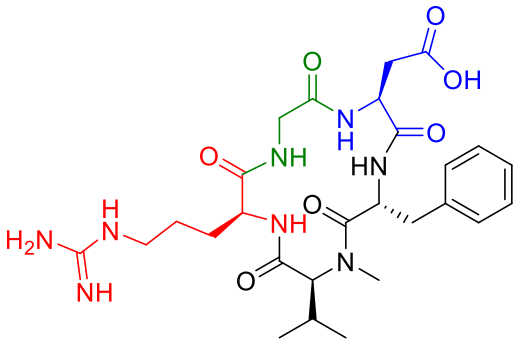

Figure 8. Cilengitide.

Recently, several studies have suggested that small molecules that act as integrin agonists may open novel opportunities for therapeutics, increasing rather than decreasing integrin-dependent adhesion. These include an agonist of $\alpha_M\beta_2$ integrin[37] that ameliorates kidney transplantation,[38] an agonist of $\alpha_L\beta_2$ integrin that inhibits lymphocyte trans-endothelial migration,[39] and an agonist of $\alpha_4\beta_1$ integrin that induces progenitor cell adhesion.[40] Recent research efforts have tentatively improved the pharmacological parameters of the developed derivatives mainly by altering their polarity and rigidity. Among several heterocyclic structures, Palomo et al. and Aizpurua et al. embedded an azetidinone scaffold in cyclic peptides or pseudopeptides containing the RGD recognition motif or a RGD-like sequence (*Figure 9*).[41] The incorporation of a conformational

constrain, such as the introduction of an unsaturated β-amino acid or a β-lactam scaffold in a cyclic structure, was in general intended to enhance selectivity and modulate the affinity toward the receptor.

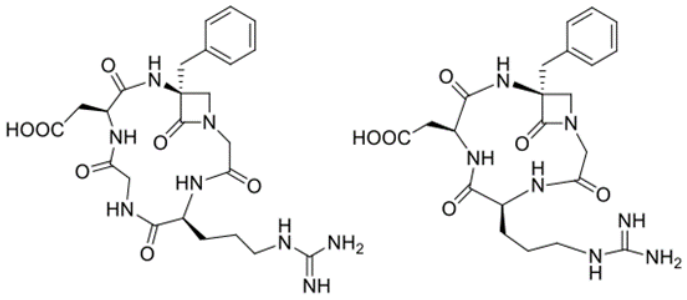

Figure 9. Azetidinone scaffold in cyclic peptides or pseudopeptides containing the RGD (or RGD like) recognition motif.[41]

According to this, the ability of azetidinones to target integrins was recently evaluated by my research group. A preliminary study on the synthesis of three new azetidinones as potential integrin ligands was reported (*Figure 10*).[42]

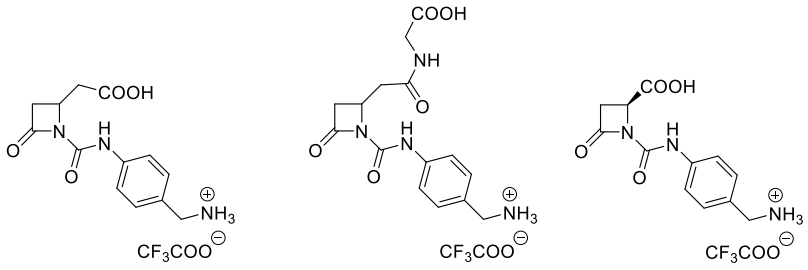

Figure 10. β-lactam-based integrin ligands developed by Giacomini's research group.[42]

The approach used was based on rationalization from known integrin ligands and the novel molecules were designed with the azetidinone as a rigid cyclic central core, with two arms holding a carboxylic acid and a basic moiety, as in the RGD sequence. The 4-amidobenzylamine residue was chosen as a basic terminus that was directly linked to the β-lactam nitrogen atom as in urea derivatives, and a carboxylic acid was located on the C-4 side chain and differently spaced from the ring. The C-3 position was not substituted in order to mimic the methylene residue of glycine in the RGD peptide. The two side chains anchored on the β-lactam provided a favourable alignment on the receptor, thus meeting the crucial requirements for integrin affinity. When these new molecules were tested on cell lines K562 (human erythroleukemia expressing $\alpha_5\beta_1$ integrin) and SK-MEL-24 (human malignant melanoma expressing $\alpha_v\beta_3$ integrin), a concentration dependent enhancement of fibronectin-mediated adhesion was observed.[42]
Subsequently my research group developed an entire library of novel β-lactam derivatives designed to target integrins (*Figure 11*). From a structural point of view, to ensure interaction with integrins, these compounds, as aforementioned, must necessarily have a basic/o-tolyl group and an acid portion at a certain distance, thus mimicking the behaviour of endogenous ligands such as the RDG sequence.[43]

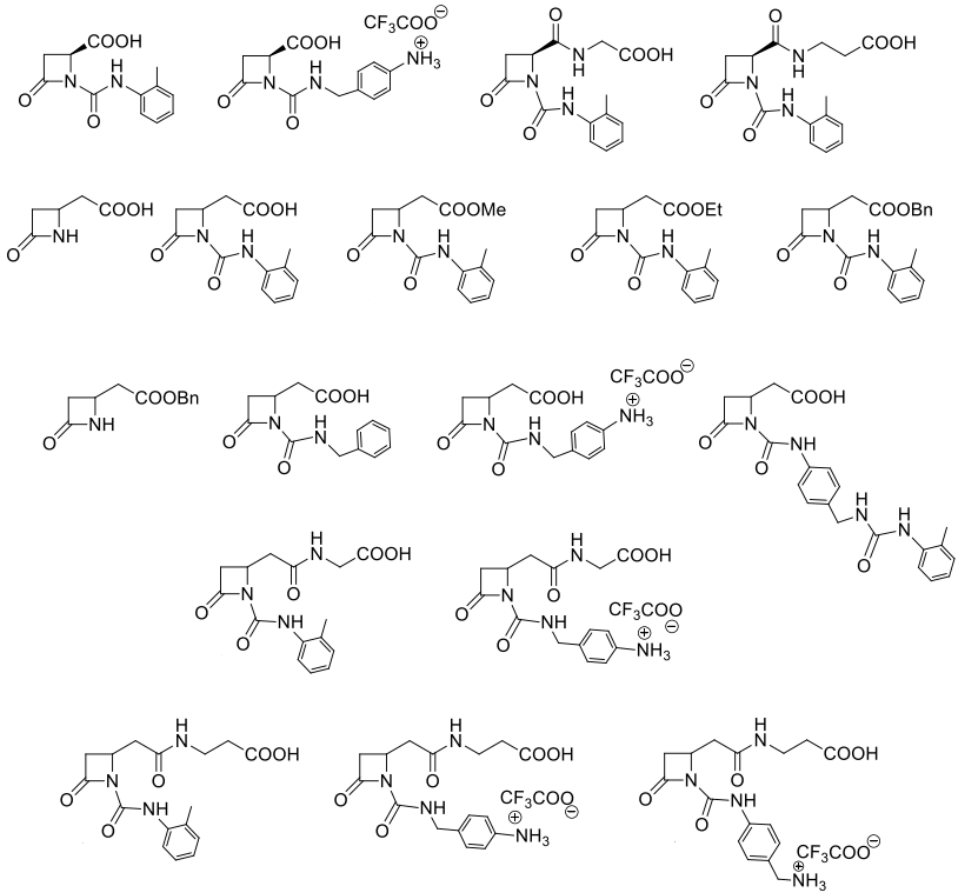

Figure 11. Novel β-lactam compounds designed to target integrins.[43]

Selective and potent agonists have been so obtained; they could promote cell adhesion mediated by $\alpha_v\beta_3$, $\alpha_v\beta_5$, $\alpha_5\beta_1$, or $\alpha_4\beta_1$ integrins. Also antagonist compounds active towards these RGD-binding integrins have been developed, as well as antagonists that bound to $\alpha_v\beta_6$, $\alpha_4\beta_1$, and $\alpha_L\beta_2$ integrins.[43]

The next step was to investigate how these ligands could eventually promote or inhibit trafficking processes. Therefore, in collaboration with the group of Prof. Spampinato of the Department of Pharmacology of the University of Bologna, integrin internalization mediated by the developed synthetic β-lactams was evaluated through confocal microscopy analysis using HEK293 cell lines expressing fluorescent α_5 integrin. For these experiments, a plasmid of α_5 integrin fused with an Enhanced Green Fluorescent Protein (EGFP) was transfected in HEK293 cells (*Figure 12a*), and its expression was monitored with fluorescence microscopy. Control cells expressed fluorescent α_5 integrin that was localized primarily on cell membrane. Following fibronectin (FN) exposure (10 μg/mL), after 15 minutes integrin was internalized into the cytoplasm and consequently the cell appeared completely green-coloured (*Figure 12b*). The same behaviour was found when the cells were treated with one of our $\alpha_5\beta_1$ agonist compounds, able to promote internalization in a 1 μM concentration (*Figure 12c*). Conversely, a $\alpha_5\beta_1$ antagonist from our library, showed to prevent integrin endocytosis mediated by fibronectin. As shown in *Figure 12d* in fact, the fluorescence remained confined along the cell membrane and the internalization was inhibited, in both absence and presence of fibronectin.

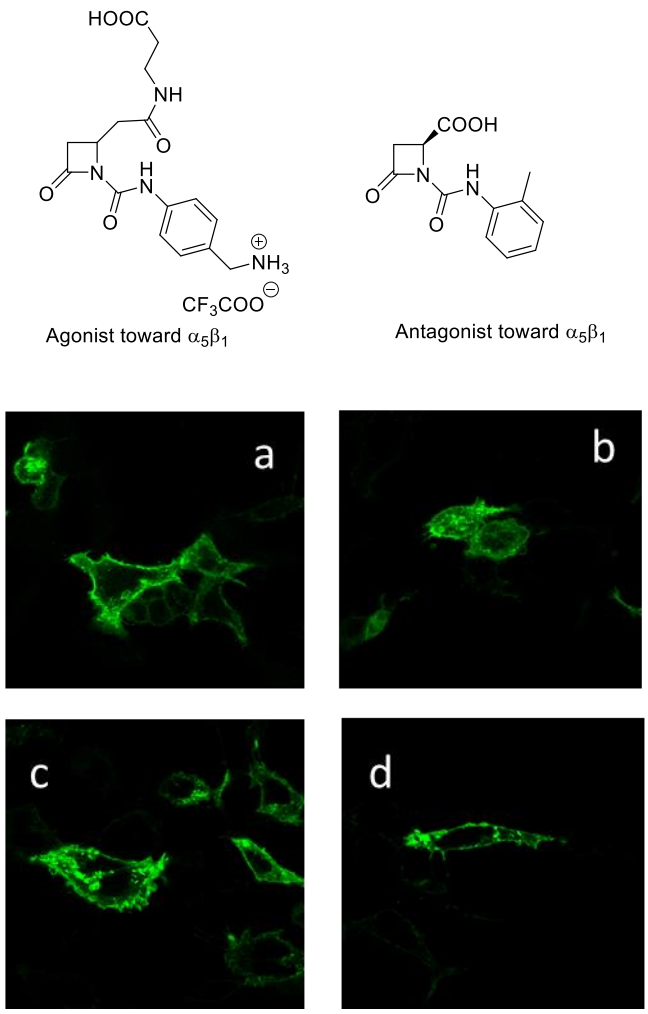

Figure 12. Confocal microscopy analysis of HEK293 cells expressing fluorescent α_5 integrin: a) control cells; b) fibronectin-treated cells; c) internalization mediated by $\alpha_5\beta_1$ agonist; d) internalization inhibited by $\alpha_5\beta_1$ antagonist compound**.**

1.1.3 Selective integrin ligands conjugated to the antineoplastic agent Fluorouracil

Cancer is the second cause of death after heart diseases in the world.[44] Chemotherapy refers to cancer treatment by the use of one or more anticancer drug, but most of them are often associated with serious and life-threatening side effects that arise from toxicities to healthy cells, because of lack of selectivity toward cancer cells. As a result, in the past decade significant research efforts has been focused on the development of targeted drug delivery systems (TDDs). The new agents could enhance the efficacy of the drug and minimize the side effects.[45]

The TDDs usually consist of a carrier, that ensures a selective transport of the drug, a linker, that acts as a spacer between the carrier and the drug, and a cytotoxic agent (*Figure 13*).

Figure 13. General TDDs.

The carrier ensures the selective delivery of the drug to cancerous cells. To obtain an efficient carrier it is necessary to pay attention to some crucial points such as chemical synthesis, kinetic parameters and avidity of the conjugate towards the target cell, i.e. the strength with which the conjugate binds to the biological target, and the penetration into the tissues. Different TDDs have been developed depending on the carrier type:

- Nanocarriers
- Antibody
- Peptide
- Small molecules

The development of drug delivery systems based on nanoparticles with adaptable shape, size, chemical surface and physical properties, has been a real revolution in the therapeutic area, and is still a very active research field.[44] Having high surface area and tunable morphology, nanoparticles can cause excellent pharmacokinetics and passive accumulation at the desired site and enhance permeation and retention (EPR) effect. Especially magnetic nanoparticles (MNPs) have been widely used for targeted drug delivery, thanks to the fact that the drug is directed to the target site and accumulate by an external magnetic field, without effect to the healthy cells.[46]

Also monoclonal antibodies were considered as a possible vehicle for the selective transport of drugs, based on their high binding specificity, which could in fact favor the selective accumulation of the drug in the site affected by the disease. Specifically, the ability to release the cytotoxic agent only in the proximity of tumor cells derives from the presence, on these cells, of a specific antigen that will be recognized by the antibody. Obviously, in order to have selective delivery, it is necessary to find an antigen expressed only by cancerous cells and not by healthy ones.[47]

Inversely, the use of peptides as carriers derived from the evidence that many cancer cells over-express certain receptors, whose ligands are peptides. These peptides can therefore have a promising vector role in targeted drug delivery systems. Furthermore, since they generally have a very high affinity in the nano-molar range, a small amount is required.[48]

In addition to peptides as carriers, a number of small ligands to tumor-associated antigens have been characterized in terms of their tumor targeting properties and for pharmacodelivery applications.[47] Some of the most promising compounds include folate derivatives,[49] glutamic acid urea derivatives[50-52], somatostatin analogues[53] and certain aromatic sulfonamides specific to carbonic anhydrase IX.[54-58]

Another fundamental portion in TDDs is the linker; it defines a suitable distance between the cytotoxic and the carrier. The linkage between the linker and the cytotoxic can occur both

through amide and ester bond; the amide bonds appear to be less susceptible to hydrolysis in physiological conditions,[23] while the ester bonds can be hydrolyzed more easily by enzymes such as lipases or esterases. If the stability of the conjugated system is sufficient to make it reach the biological target, the hydrolysis of the bonds with the linker can guarantee a controlled release of the drug inside sub-cellular compartments. Thus, the linker structure defines the exact breaking point between carrier and cytotoxic agent, mediated by internal or external stimuli. In this way the drug is inactive during transport, but extremely effective once it reaches the diseased cell.[48,59]

Finally, in a TDDs it is also important the choice of the cytotoxic agent. Generally, with the term cytotoxic we refer to any drug capable of damaging or killing cells. In practice it serves to define the category of drugs that inhibit cell division and therefore are potentially useful for anticancer chemotherapy.

They can be divided into the following categories:

• Cytotoxic drugs which include:

- alkylating agents and related compounds, which act by forming covalent bonds with DNA and preventing its replication.

-antimetabolites, which block or alter one or more metabolic pathways involved in DNA synthesis.

- cytotoxic antibiotics, such as substances of microbial origin that prevent the division of mammalian cells.

- plant derivatives such as vinca alkaloids, taxanes, camptothecins; most of these act specifically on microtubules.

• Hormones, of which the most important are steroid ones (glucocorticoids, oestrogens and androgens).

• Monoclonal antibodies, which are typically used only for particular types of cancer.

• Protein kinase inhibitors, which inhibit protein kinases, enzymes responsible for the transduction of growth signals in rapidly dividing cells.

In this study we will deepen the antimetabolite class and in particular our attention will be focused on 5-Fluoro Uracil (5-FU). 5-FU is an analogue of uracil (*Figure 14*), which is one of the four nucleobases and thanks to this structure, it interferes with some metabolic pathways linked to the synthesis of DNA. 5-FU, after conversion into deoxyribonucleotide triphosphate, can be incorporated into DNA and, as ribonucleotide triphosphate, also into RNA with alterations of its process and functionality. It is usually administered parenterally;[60] pharmacokinetic studies have in fact shown that 5-FU is hardly absorbed after oral administration with an irregular bioavailability. It has also been observed that the derivatives functionalized in N-1 and / or N3 of the pyrimidine ring have good characteristics, both from the pharmacokinetic and pharmacodynamic point of view. These derivatives are in fact used in the synthesis of 5-FU pro-drugs.[61] The main undesirable effects of this cytotoxic agent are gastrointestinal epithelial damage and myelotoxicity.

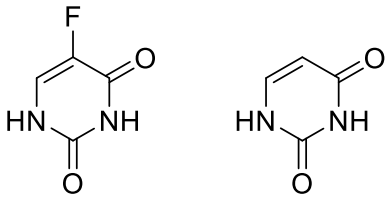

Figure 14. 5-Fluoro uracil (on the left) and uracil (on the right).

In this project, 5-FU was used as a model drug for the development of an effective anticancer drug delivery therapy, exploiting its conjugation to novel and selective integrin ligands for promoting an active tumor targeting.[62]

Conjugation of anticancer drugs with integrin-specific ligands may in fact lead to higher selectivity toward cancer cells and to payload accumulation within tumor cells through integrin trafficking.[32] Therefore, we have hypothesized that integrin agonists, conjugated with anticancer drugs, could be exploited as a targeting unit to promote selective drug internalization only into cancer cells. In the project, starting from the previously studied compound **A** (*Figure 16*) as a selective agonist for $\alpha_4\beta_1$ integrins,[43] we first designed and realized two fluorescent compounds **B** and **C** to get evidence on ligands internalization (*Figure 16*).

For our purpose, we selected two fluorophores among the most employed for bioimaging: fluorescein isothiocyanate (FITC), with a green light emission[63] and Rhodamine B, with a red light emission[64] (*Figure 15*). Both compounds are commercially available, easy to handle and derivatize, and stable in cellular conditions. FITC is easily accessible and due to its absorption wavelength (492 nm) does not interfere with the absorption of cellular proteins and does not require sophisticated microscopic tools.[65] On the other hand, Rhodamine B is a low-cost fluorophore widely used because of its high photostability and chemostability in aqueous media.[66] Moreover, emitting in the near infrared region, Rhodamine B can be widely exploited for biological applications.[67]

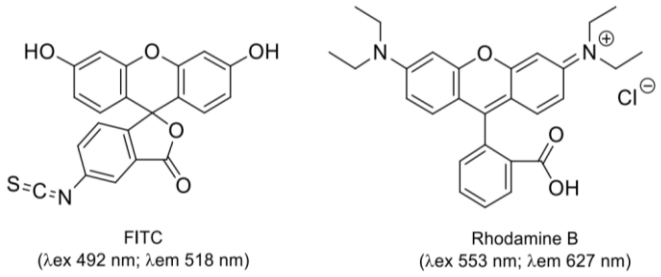

Figure 15. FITC (on the left) and Rhodamine B (on the right).

Finally, as previously anticipated, the chemotherapeutic agent 5-FU, chosen as model drug, was conjugated to the integrin ligand **A** by means of different linkers and the so obtained new conjugates **D**, **E**, and **F** were studied in cell-based assays in order to ascertain their activity and selectivity against tumor cells (*Figure 16*).[68]

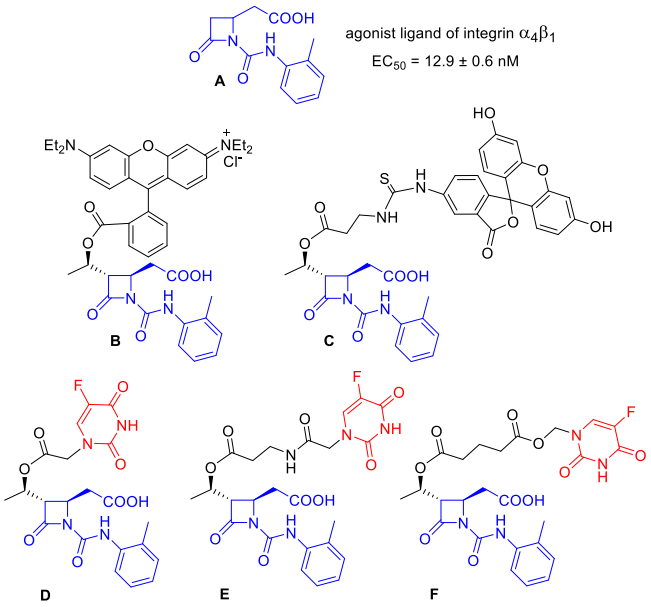

Figure 16. A series of β-lactam compounds evaluated in this study. Compound **A** is the reference compound as model of integrin agonist ligand; **B** and **C** are new fluorescent compounds for internalization analyses; **D**, **E**, and **F** are new 5-FU-conjugates designed to evaluate the selectivity of the anticancer effect.[68]

Results and discussion

Compound **A** was chosen as a model for the design of the new ligands that should keep a carboxylic acid terminal on the C4 position of the β-lactam scaffold to target the integrin metal ion-dependent adhesion site (MIDAS), and a *o*-tolyl-urea moiety for a selective activation of $\alpha_4\beta_1$ integrins. To trace the integrin-mediated internalization of the compounds into the cell it would be necessary to introduce a fluorescent tag to the integrin ligand and hence we modified the model compound **A**. Tags were anchored on the C3 side chain of a 3-hydroxyethyl β-lactam, and Rhodamine B or fluorescein isothiocyanate (FITC) were chosen to obtain compounds **B** and **C**, respectively (*Scheme 1*).[68]

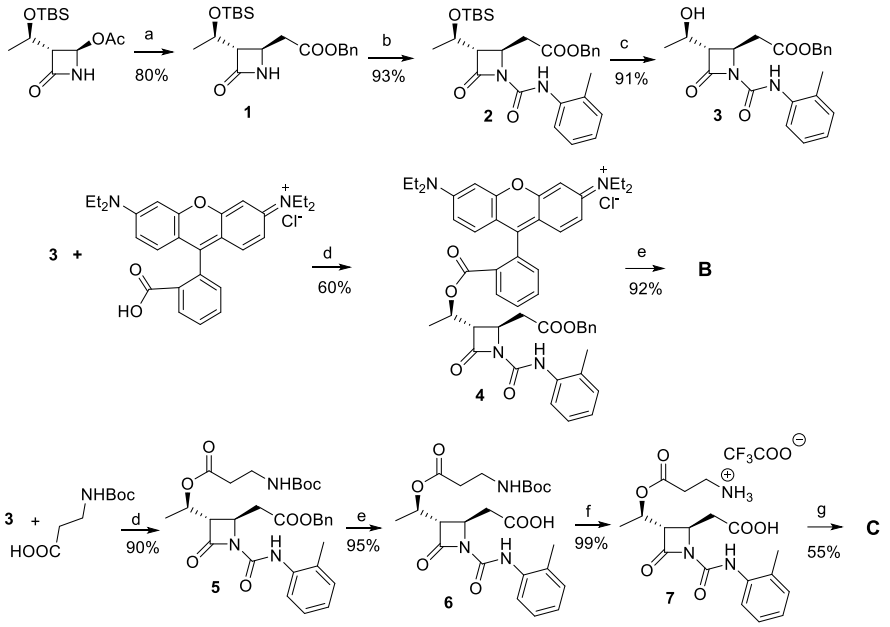

Scheme 1. Synthesis of fluorescent compounds **B** and **C**; Reagents and conditions: a) Zn, TMSCl, benzylbromoacetate, THF, 0 °C then rt, 3 h; b) o-tolylisocyanate, TEA, CH_2Cl_2, rt, 16 h; c) $BF_3{\cdot}OEt_2$, CH_3CN, 0 °C then rt, 2 h; d) DCC, TEA, DMAP, Rhodamine B or N-Boc-beta alanine, CH_2Cl_2, 0 °C then rt, 24 h; e) H_2, Pd/C (10%), THF/CH_3OH 1:1, rt, 2 h; f) TFA, CH_2Cl_2, 0 °C then rt, 16 h; g) FITC, TEA, CH_2Cl_2, rt, 4 h. Yields % refer to isolated compounds.[68]

The synthesis of fluorescent compounds **B** and **C** started with a nucleophilic substitution reaction at the C-4 position on the commercially available *(2R,3R)-3-((R)-1-((tbutyl dimethylsilyl)oxy) ethyl)-4-oxoazetidin-2-yl acetate*, by a Reformatsky reagent obtained in turn from benzyl bromo-acetate and a pre-activated zinc with t-butyldimethylsilylchloride (*Scheme 1*). The substitution of the 4-acetoxy group occurred with a complete control of the stereoselectivity obtaining exclusively the trans diastereoisomer **1**.[69] Compound **1** was acylated on the β-lactam nitrogen atom with the commercially available *o*-tolylisocyanate to give **2**, in order to get the specific *o*-tolylureidic residue necessary for modulating the affinity toward the integrin receptor. The *t*-butyldimethylsilyl group on the C-3 side chain was then removed with $BF_3{\cdot}OEt_2$ as Lewis acid affording alcohol **3** in good yields.

For the synthesis of compound **B**, the alcohol **3** was exploited for inserting Rhodamine B by DCC and DMAP-mediated amidation reaction to give intermediate **4**. The final deprotection of benzyl ester on the C-4 side chain catalyzed by Pd/C, yielded the free carboxylic acid needed for integrin recognition at the MIDAS.

To obtain compound **C**, in order to have an amine group for the insertion of the FITC fluorophore, alcohol **3** was subjected to a DCC-mediated esterification with the commercial N-Boc-β-alanine, obtaining compound **5** in excellent yields. Following hydrogenolysis for benzyl ester deprotection and Boc removal, compound **7** was obtained in quantitative yields. Coupling of **7** with FITC isothiocyanate gave the target compound **C** in 55 % yields after flash chromatography.

To conjugate 5-FU to the selected β-lactam scaffold we designed three different anchoring systems: a short ester linkage to give compound **D**, a longer diester generated from glutaraldehyde to obtain **F**, and an ester-amide linker derived from β-alanine to get **E** (*Scheme 2*).[68]

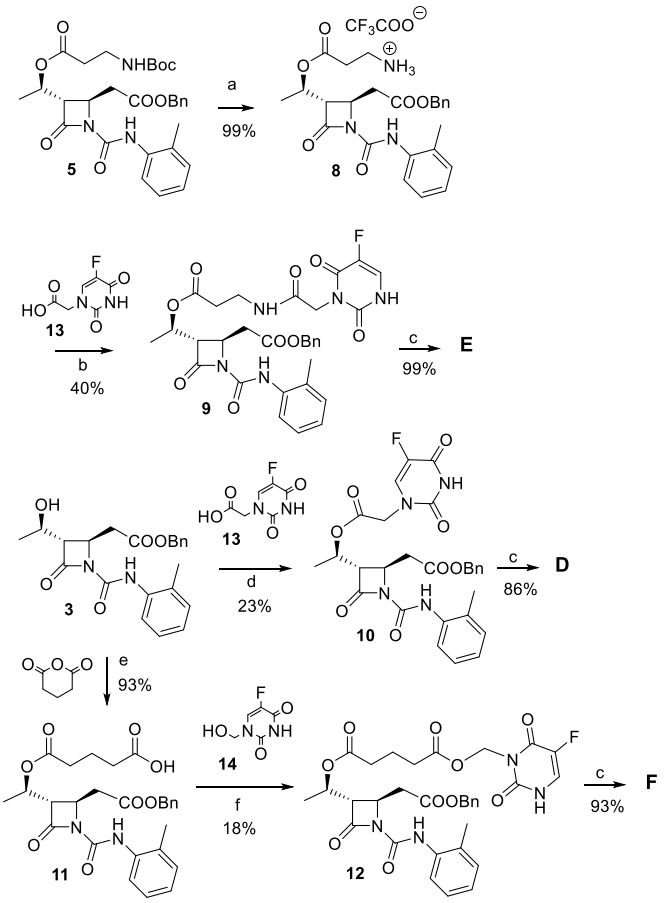

Scheme 2. Synthesis of 5-FU conjugate compounds **D**, **E**, and **F**; a Reagents and conditions: a) TFA, CH_2Cl_2, 0 °C then rt, 5 h; b) TEA, CH_2Cl_2, HOBt, EDC, DMF, 0 °C then rt, 18 h; c) H_2, Pd/C (10%), THF/CH_3OH 1:1, rt, 2 h; d) DCC, DMAP, CH_3CN, DMF, rt, 48 h; e) TEA, DMAP, CH_2Cl_2, rt, 18 h; f) EDC, DMAP, CH_3CN, rt, 18 h. Yields % refer to isolated. [68]

Synthesis of compound **D** started from alcohol **3** by DCC and DMAP-mediated esterification with the fluorouracil acid **13**, prepared as previously reported.[70] The final hydrogenolysis of the benzylester group gave **D** in good yields.

Compound **E** was obtained from intermediate **5** which was subjected to Boc deprotection with TFA to give **8**. A coupling reaction with **13** mediated by TEA, HOBt and EDC gained **9** and a final hydrogenolysis quantitatively yielded compound **E**.

In order to obtain compound **F**, a coupling between alcohol **3** and glutaric anhydride under mild conditions[71] gained acid **11** in excellent yields, without the need of purification. The N-hydroxymethylene-5-fluorouracil **14**, obtained as reported in the literature,[72] was then esterified with **11** in the presence of EDC and DMAP. Finally, hydrogenolysis of the benzyl ester gained compound **F** with the free carboxylic acid required for integrin recognition at MIDAS. [68]

Stability assays

The stability of the three new 5-FU conjugates **D**, **E**, and **F** was tested in Phosphate Buffer Solution (PBS) 0.1 M (pH = 7.4) and in Fetal Bovine Serum (FBS) as models for physiological conditions and was evaluated by HPLC-UV analysis. The compounds (1 mg/mL) were dissolved

in PBS or FBS and incubated at 30°C in thermostat. Aliquots were taken at different time points from 0 to 72 h since the analysis of apoptosis induction by compounds **D**-**F** in cells is measured after 72 h exposure. The results are summarized in *Figure 17* and reported as mol% of intact compound respect to mol% at the initial time (mol0). Compound **E** showed a good stability in both PBS and FBS with a recovery of the intact conjugate after 72 h of 89 and 78 mol/mol0(%), respectively. Compounds **D** and **F** are rather stable in PBS, whereas in FBS the stability underwent a sudden decrease, after 72 h the intact compounds **D** and **F** were recovered in 60 and 30 %, respectively. In order to recognize any possible fragment obtained from the decomposition of **D** and **F**, HPLC-MS analyses of the samples have been conducted. In test solutions of **D** in FBS, traces of compounds **13** and **3** appeared just after 2 hours, due to an ester hydrolysis; in FBS solutions of compound **F** significant amounts of 5-FU and the acid **11** appeared after 24 hours due to a hydrolysis of the aminal group of 5-FU. [68]

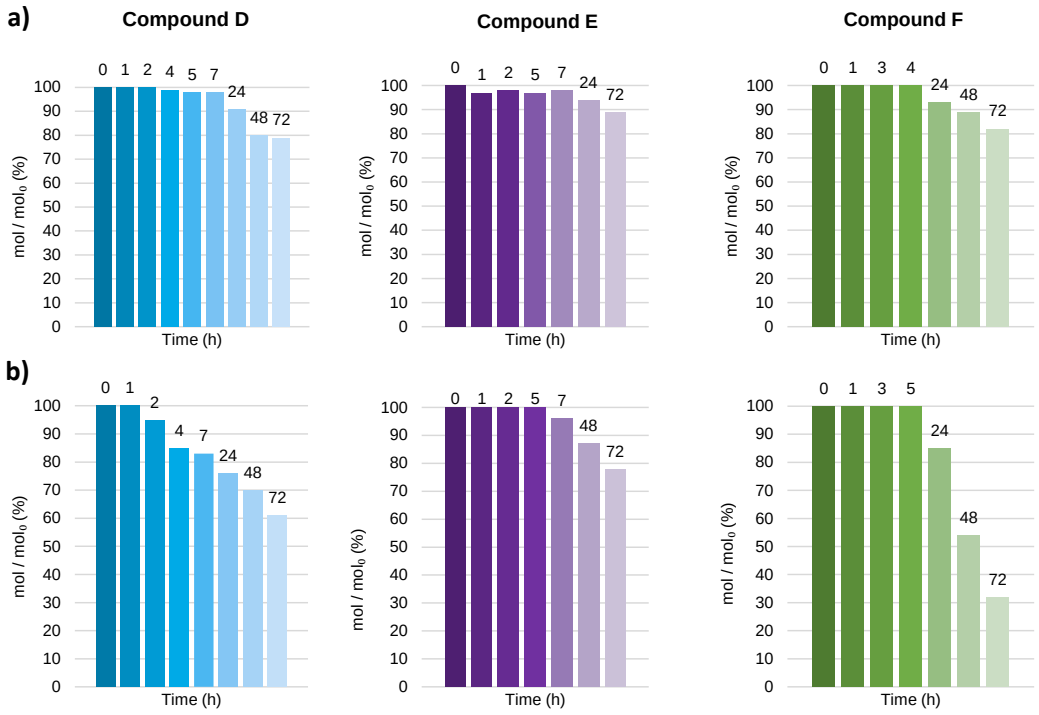

Figure 17. Stability study for compounds **D** (blue), **E** (violet) and **F** (green); panel a) stabilities in phosphate buffer solution (PBS) 0.1 M pH = 7.4; panel b) stabilities in fetal bovine serum (FBS). The quantity of intact compounds is reported as mol% respect to mol% at time = 0 (mol_0).[68]

Cell adhesion assays

To investigate the ability of new fluorescent compounds and 5-FU-conjugates **D**, **E**, and **F** to modulate integrin-mediated cell adhesion in comparison with the parental agonist **A**, we employed cell adhesion assays using Jurkat E6.1 cells (mainly expressing $\alpha_4\beta_1$ integrin)[43] and K562 cells (mainly expressing $\alpha_5\beta_1$ integrin).[73] Both $\alpha_4\beta_1$ and $\alpha_5\beta_1$ integrins are expressed in several types of cancer cells and their expression, as those of other integrins, has been correlated with metastasis and poor patient prognosis.[74] Specifically, $\alpha_5\beta_1$ integrin is known to increase

tumor progression and cancer invasion and to mediate resistance to radiotherapy,[75] whereas $\alpha_4\beta_1$ is involved in cancer cell ability to invade basement membranes and metastasize.[76] In addition, β_1 integrins mediate drug resistance and stimulate metastasis of several different tumor types. [77, 78] Cell adhesion results are summarized in *Table 1*.[68]

Table 1. Effects of compounds **A-F** on $\alpha_5\beta_1$ or $\alpha_4\beta_1$ integrin-mediated cell adhesion.[a–c]

Entry	compound	K562/FN $\alpha_5\beta_1$	Jurkat/VCAM-1 $\alpha_4\beta_1$
1	**A**	> 100 [d]	0.0129 ± 0.0006 [d] agonist
2	**B**	0.332 ± 0.047[c] agonist	0.549 ± 0.066 agonist
3	**C**	11.1 ± 1.7 agonist	41.1 ± 7.3 agonist
4	**D**	0.717 ± 0.070 agonist	0.372 ± 0.052 agonist
5	**E**	1.30 ± 0.31 agonist	2.99 ± 0.41 antagonist
6	**F**	0.058 ± 0.006 antagonist	2.36 ± 0.23 antagonist

[a] Data are presented as EC_{50} for agonists and as IC_{50} for antagonists (μM). [b] Cell adhesion mediated by $\alpha_5\beta_1$ for K562 cell adhesion to FN, and by $\alpha_4\beta_1$ evaluating Jurkat cell adhesion to VCAM-1. [c] Values represent the mean ± SD; n = 3. [d] Data of parental compound **A** were already published, see ref. 43.

Integrin agonists are considered those compounds able to promote cell adhesion to fibronectin or VCAM-1, conversely antagonists are defined as compounds capable of inhibiting cell adhesion to fibronectin or VCAM-1 in a concentration-dependent manner.

Parental compound **A** has been analyzed in a previous study,[43] and it showed a potent and selective activity as agonist towards $\alpha_4\beta_1$ integrin; moreover, it was completely inactive towards all the other integrins investigated ($\alpha_v\beta_3$, $\alpha_v\beta_5$, $\alpha_v\beta_6$, $\alpha_{IIb}\beta_3$, $\alpha_L\beta_2$). For comparison purposes, cell adhesion data of compound **A** on $\alpha_4\beta_1$ and $\alpha_5\beta_1$ integrins have been added to *Table 1* (entry 1). Both fluorescent compounds **B** and **C** behaved as agonist in cell adhesion assays involving $\alpha_4\beta_1$ or $\alpha_5\beta_1$ integrin (*Table 1*, entries 2 and 3). In particular, integrin agonist-FITC-conjugated **C** was less potent than both parental compound **A** and Rhodamine B-conjugate compound **B**, when employed in cell adhesion assays. Regarding 5-FU-integrin ligand-conjugates, compound **D** behaved as a less effective agonist in cell adhesion assays on $\alpha_4\beta_1$ integrin compared to parental

compound **A**, albeit it maintained an interesting activity in the sub-micromolar range (EC_{50}: 0.372 ± 0.052 μM, *Table 1,* entry 4). In addition, compound **D** acted as an agonist also in $\alpha_5\beta_1$ integrin-mediated cell adhesion assay (*Table 1,* entry 4), conversely to parental compound **A**, which was reported to be highly selective for $\alpha_4\beta_1$.[22] The elongation of the anchoring system onto the β-lactam scaffold with an ester-amide linker, as in compound **E**, induced a reduction in the potency towards $\alpha_5\beta_1$ integrin if compared to compound **A** and **D**, but still maintaining the agonist behavior. On the contrary, compound **E** was able to reduce $\alpha_4\beta_1$-mediated cell adhesion with potency in the micromolar range (*Table 1,* entry 5). Compound **F**, which possesses a long diester as anchoring system, showed potency and behavior similar to compound **E** toward $\alpha_4\beta_1$ integrin, acting as an antagonist, while demonstrated an opposite and more potent activity toward $\alpha_5\beta_1$ if compared to agonists **D** and **E** (*Table 1*, entries 4, 5, and 6). Overall, cell adhesion assays showed that 5-FU-conjugates, when compared to the parental compound **A**, retain the ability to modulate cell adhesion towards $\alpha_4\beta_1$ integrin but with a reduced potency and with opposite activity for compounds **E** and **F**. Moreover, all the 5-FU-conjugated compounds acquired an interesting activity towards $\alpha_5\beta_1$ integrin, as agonists for **D** and **E**, and as antagonist in case of **F**.[68]

Cellular uptake

In order to determine the capacity of internalization of the novel integrin ligands, two fluorescent compounds **B** and **C** were synthesized and the extent of their internalization into cancer cells, expressing $\alpha_4\beta_1$ or $\alpha_5\beta_1$ integrins (Jurkat and K562, respectively), or non-cancer cells, expressing only β_1 integrin subunit (HEK293), was quantified by flow cytometry.
Fluorescent-FITC-conjugated **C**, which behaves as an integrin agonist for both $\alpha_4\beta_1$ and $\alpha_5\beta_1$, is highly internalized in a concentration-dependent manner, both in Jurkat and in K562 cells (*Figure 18*, panel a). In Jurkat cells, cellular uptake of compound **C** was prevented by pre-treatment with agonist **A** or an antibody anti-α_4 integrin. The blockade of α_5 integrin with a specific antibody was ineffective in reducing the internalization of fluorescent conjugate **C** in Jurkat cells. These data suggest that compound **C** internalization in Jurkat cells is $\alpha_4\beta_1$ integrin-dependent. In K562 cells, intra-cellular uptake of compound **C** was mediated by $\alpha_5\beta_1$ integrin, as demonstrated by a strong reduction of internalization induced by pre-treatment with an antibody anti-α_5. Superimposable results were obtained for compound **B** (*Figure 18*, panel b): it was internalized in a concentration-dependent manner in both Jurkat and K562 cancer cells, and its intra-cellular uptake was mediated by α_4 integrin in Jurkat cells and by α_5 integrin in K562 cells. No cellular uptake was observed for both compounds **C** and **B** in HEK293 non-cancer cells (*Figure 18*, panel a and b, respectively). Altogether, these results demonstrated that fluorescent-integrin ligand conjugates displayed internalization properties required to deliver cytotoxic drugs into cancer cells in integrin-selective manner.[68]

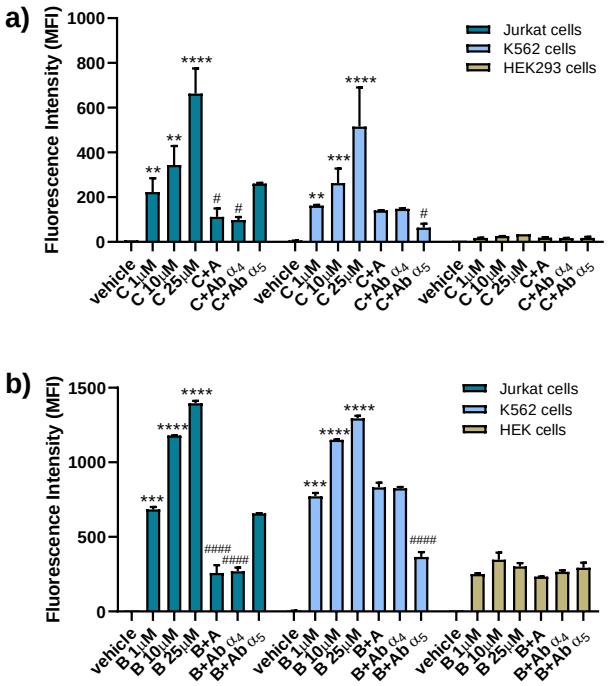

Figure 18. Cellular uptake of integrin agonist-FITC-conjugated **C** (panel a) and Rhodamine B-conjugate **B** (panel b) by Jurkat, K562 and HEK293 cells. Cells were incubated with fluorescent conjugates (1 - 10 - 25 μM) or medium containing the vehicle alone (vehicle) for 1 h. To demonstrate integrin involvement, cells were pretreated with anti-α_4 (10 μg/mL) or anti-α_5 (10 μg/mL) antibody or $\alpha_4\beta_1$ selective agonist **A** (100 μM) for 30 minutes, before the addition of the fluorescent compound (1 μM). The fluorescence intensity of the cells (MFI: mean fluorescence intensity, arbitrary units) corresponds to fluorescent conjugates intracellular uptake and was quantified by flow cytometry. [68]

Apoptosis assays

The in vitro activity of 5-FU conjugates **D**, **E**, and **F** was evaluated by apoptosis assays in Jurkat, K562 and HEK293 cells. Previous studies[79,80] have demonstrated that Jurkat cells present mutations in BAX and TP53 genes, leading to the lack of these proteins or to the production of a truncated isoform, respectively. Although these alterations impair crucial components of apoptotic process, it has been shown that 5-FU is able to trigger apoptosis in a time- and concentration-dependent manner in Jurkat cells.[80] HEK293 cells were employed as non-cancerous control cells; moreover, this cell line does not express α_4 nor α_5 integrin subunit whereas it endogenously expresses the integrin subunit β_1.[43,81,82]

Jurkat, K562 and HEK293 cell lines were exposed to 5-FU and compounds **D**-**F** (10 – 50 – 100 μM) for 72 h and apoptosis was evaluated by Annexin V assay as described in the experimental section.

As shown in *Figure 19*, 5-FU was able to induce apoptosis in all the three cell lines considered; interestingly, the pro-apoptotic effect of 5-FU was concentration-dependent. In Jurkat cells, which express $\alpha_4\beta_1$ integrin, only compound **F** induced a significant increase of apoptosis (*Figure 19a*), only at the highest concentration (100 μM). As regards K562 cells, expressing $\alpha_5\beta_1$ integrin, compounds **E** and **F** increased significantly apoptotic levels (*Figure 19b*). The effect of **F** was strongly concentration-dependent and effective as that of 5-FU, at least at the highest concentration (100 μM) (5-FU 100 μM vs F 100 μM: not significant). Compound **D** did not

induce apoptosis neither in Jurkat nor in K562 cells (*Figure 19a* and *b*). In addition, neither of the 5-FU conjugates **D** and **E** were able to exert pro-apoptotic effects in HEK293 cells (*Figure 19c*). On the contrary, we observed a significant increment of apoptotic levels in HEK293 cells induced by **F** (*Figure 19c*); this effect could be probably due to the degradation of conjugated compound **F** leading to 5-FU release, as above mentioned. These results show that 5-FU-conjugates exhibit a more selective integrin-mediated antitumor activity than unconjugated 5-FU. [68]

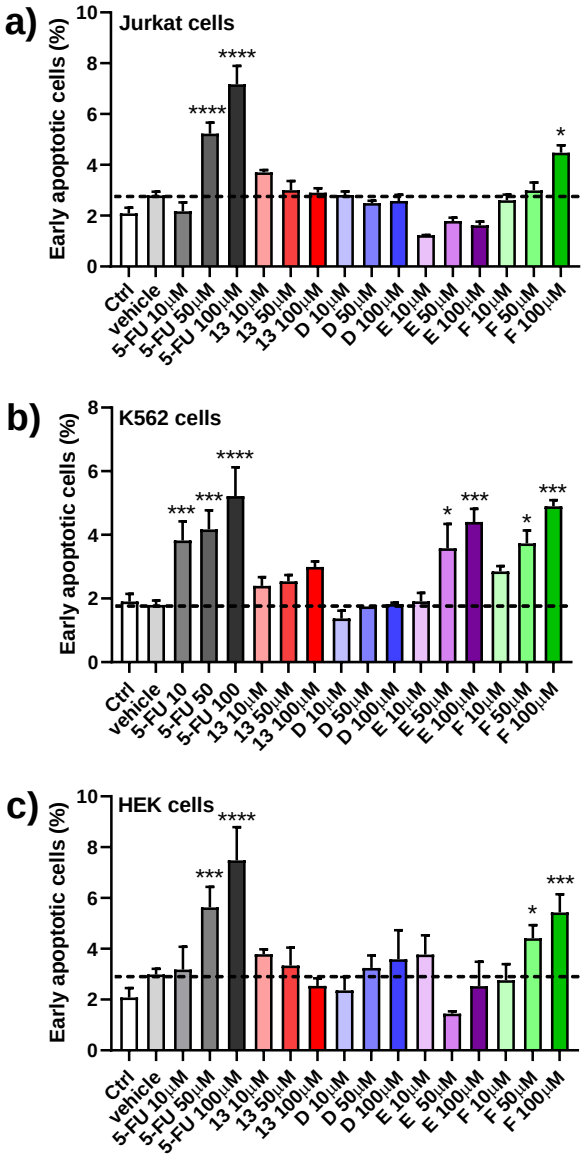

Figure 19. Analysis of apoptosis induced by 5-FU conjugate compounds **D**, **E**, and **F** and of precursor compound **13** (10 - 50 - 100 µM) in Jurkat (panel a) and K562 (panel b) cancer cells and in HEK293 (c) cell line after 72 h exposure. Apoptosis was determined by flow cytometry to evaluate the ability of the cells to bind annexin V, and the results are presented as the percentage of early apoptotic cells. Values are mean ± SD from three independent experiments conducted in triplicate. [68]

Conclusions

A selective and effective drug delivery is essential for antitumor drugs to selectively target tumor cells and thus lowering the toxicity against non-cancerous cells. Tumor-selective targeting may improve drug delivery through the increment of anti-neoplastic drug concentration in tumor cells avoiding distribution to other tissues and through the improved distribution of the drug within cancer cells. Moreover, tumor-selective conjugates may surmount anticancer drug resistance possibly through drug conjugate endocytosis.[83-85] It has been already studied the action of some peptide- or peptidomimetic-conjugates as tumor-penetrating molecules.[83,86,87] To provide a specific receptor targeting for the conjugates, integrins have been identified because essential for physiological development and feature in some diseases, particularly in cancer.[32,77,88] An active targeting via integrins has been accomplished by including specific integrin ligands in the drug-conjugate, for example RGD peptide, or Cilengitide, or others.[89] Moreover, the use of integrin-targeting small molecule for intracellular delivery of an associated cargo maximizes endocytosis as compared to an integrin-targeting monoclonal antibody.[90] However, notwithstanding the efforts in the design and realization of the conjugates, less attention was paid to the effective action of the targeting ligand, if it would act at the receptor as an antagonist or an agonist .

Our study was conceived to investigate this point. The design of the new derivatives has the β-lactam **A** as the model of a potent and selective agonist of integrins $\alpha_4\beta_1$. The substituents on the nitrogen atom and on the C-4 position of the β -lactam ring of the new compounds must be an o-tolyl-urea and a carboxylic acid, respectively, because crucial for integrin recognition as previously demonstrated.[43,91] To covalently anchor fluorescent tags or 5-FU, a β-lactam skeleton with a C-3 hydroxyethyl side chain was selected and five new β-lactam compounds were obtained.

Preliminary adhesion assays on K562 and Jurkat cells confirmed for all five molecules a lower potency than compound **A**, but unexpectedly, compounds **E** showed agonist activity against integrin $\alpha_5\beta_1$ and antagonist towards integrin $\alpha_4\beta_1$, whereas compound **F** proved to be an antagonist for both integrins (*Table 1*). These results show that also the substituent on the C-3 position of the β-lactam could play an active role on the receptor response. The antagonism of the ligand increases for longer C-3 side chains and, moreover, the C-3 substituent switches on the activity towards $\alpha_5\beta_1$ integrins.

It was then demonstrated by flow cytometry that the two fluorescent agonists **B** and **C** are internalized in a concentration-dependent manner in Jurkat and K562 cells, selectively addressed by integrin binding because upon treatment with the agonist **A** or neutralizing antibodies specific for α_4 or α_5 chains, they were no more able to enter within the cells.

The absence of internalization of the two fluorescent β-lactam derivatives in non-cancer HEK 293 cells demonstrated the privileged selectivity of the two ligands for cancer cells expressing $\alpha_5\beta_1$ or $\alpha_4\beta_1$ integrin. This result is quite important because may help to find a positive answer to the meaningful issue to discover drugs with a cell-selective toxicity.

Finally, the three 5FU-conjugates **D**, **E**, and **F** were evaluated by apoptosis assays in Jurkat, K562, and HEK 293 cells. Compound **D** is a bad apoptosis inducer in all three cell lines considered. This behavior could be ascribed to the less stability of compound **D** (*Figure 19, panel b*) due to the labile ester linkage and the release of 5-FU-acetic acid **13** which, in turn, was less toxic than 5-FU.[92] Compound **E**, showed a selective response with a concentration-dependent behavior against K562 cells. This could account for the opposite receptor responses of

E as agonist of $\alpha_5\beta_1$ and antagonist of $\alpha_4\beta_1$ integrins (*Table 1*). The conjugate **E** is quite stable and it does not release **13**. The good result of **E** gives evidence that the conjugates of **13** were more cytotoxic than the parent compound as already reported.[92] Compound **F** instead, showed apoptotic effects all over the three cell lines although its activity as antagonist towards both $\alpha_5\beta_1$ or $\alpha_4\beta_1$ integrins; this could be due, rather than to its profile at the receptor, to the lower stability of **F** sustained by the release of 5-FU in cell medium. Accordingly, **F** induced a significant increase in apoptosis levels in non-cancer cells (HEK 293 cells), which do not express $\alpha_5\beta_1$ nor $\alpha_4\beta_1$ integrins. Moreover, the apoptotic effect is particular evident for K562 cells where at 100 μM the early apoptotic cells % are comparable to that of the unconjugated 5-FU (*Figure 19*, panel b). On the basis of these results, it seems that integrin ligands that behave as antagonists towards $\alpha_5\beta_1$ or $\alpha_4\beta_1$ integrins are not suitable as targeting group to effectively and selectively deliver anti-neoplastic drug (such as 5-FU) only to cancer cells. On the contrary, integrin agonists seem to selectively deliver the anti-neoplastic drug intracellularly, leading to cancer cell death. Nevertheless, further studies are needed to better clarify which are the most suitable integrin ligands for selective intracellular delivery of an associated cargo.[68]

Experimental

Commercial reagents were used as received without additional purification. ^{1}H and ^{13}C-NMR spectra were recorded with INOVA 400 instrument with a 5 mm probe. All chemical shifts were quoted relative to deuterated solvent signals (δ in ppm and J in Hz). Polarimetric analyses were conduct-ed on Unipol L 1000 "Schmidt−Haensch" polarimeter at 598 nm. FTIR spectra: Bruker Alpha instrument, measured as films between NaCl plates, wave numbers are reported in cm^{-1}. The purities of the target compounds **D**, **E**, and **F** were assessed as being >95% using HPLC. HPLC-MS: Agilent Technologies HP1100 instrument, equipped with a ZOBRAX-Eclipse XDB-C8 Agilent Technologies column; mobile phase, H_2O/CH_3CN, 0.4 mL/min; gradient from 30 to 80% of CH_3CN in 8 min, 80% of CH_3CN until 25 min, coupled with an Agilent Technologies MSD1100 single-quadrupole mass spectrometer, full scan mode from m/z = 50 to 2600, in positive or negative ion mode. Compounds **1**,[43] **13**,[70] and **14**[72] are known and were synthesized according to reported procedures, spectroscopic data of the compounds were in accordance to those reported in literature.

General procedure for hydrogenolysis (GP1)

A β-lactam benzyl ester (1 equiv) was dissolved in a mixture of THF and CH_3OH (22 mL/mmol, 1:1 v/v) and Pd/C (10% w/w) was added. The solution was then stirred under a H_2 atmosphere (1 atm) at room temperature. After a complete consumption of the starting material (TLC monitoring, 2 h) the reaction mixture was filtered through celite and concentrated in vacuum. The crude was then triturated with few drops of pentane to afford the desired carboxylic acid.

General procedure for N-Boc-deprotection (GP2)

A N-Boc-protected β-lactam (1 equiv) was dissolved in CH_2Cl_2 (18.5 mL/mmol) under a nitrogen atmosphere and trifluoroacetic acid (TFA) (4 equiv) was added dropwise at 0 °C. New TFA aliquots were added each 60 mins at 0 °C until a complete conversion (HPLC or TLC

monitoring). The solvent was removed under reduced pressure and the crude was triturated with few drops of pentane to afford the resulting deprotected compound.

*Benzyl 2-((2R,3S)-3-((R)-1-((t-butyldimethylsilyl)oxy) ethyl)-4-oxo-1-(o-tolylcarbamoyl)azetidin-2yl)acetate (**2**)*

Compound **1** (80 mg, 0.21 mmol, 1 equiv) was dissolved in anhydrous CH_2Cl_2 (2.3 mL) under a nitrogen atmosphere. Anhydrous TEA (148 µL, 1.05 mmol, 5 equiv) was added dropwise, followed by a dropwise addition of *o*-tolylisocyanate (130 µL, 1.05 mmol, 5 equiv). The mixture was stirred at room temperature until a complete consumption of the starting β-lactam (16 h, TLC monitoring) and then quenched with a saturated solution of NH_4Cl. The mixture was extracted with CH_2Cl_2 (3 × 10 mL), the organic layers were collected, dried over anhydrous Na_2SO_4, concentrated in vacuum and purified by flash-chromatography (Cyclohexane/EtOAc 90:10) affording the desired compound **2** as a colorless oil (100 mg, 93%). ^{1}H NMR: (400 MHz; $CDCl_3$) δ = 0.06 (s, 3H), 0.08 (s, 3H), 0.84 (s, 9H), 1.20 (d, J = 6.3 Hz, 3H), 2.27 (s, 3H), 2.93 (dd, J = 15.5, 7.7 Hz, 1H), 3.10 – 3.24 (m, 2H), 4.29 – 4.35 (m, 1H), 4.58 – 4.61 (m, 1H), 5.16 (s, 2H), 7.05 (t, J = 7.3 Hz, 1H), 7.20 (dd, J = 14.3, 7.3 Hz, 2H), 7.29 – 7.38 (m, 5H), 7.91 (d, J = 8.1 Hz, 1H), 8.41 (bs, 1H) ppm. ^{13}C NMR: (100 MHz; $CDCl_3$) δ = -4.9, -3.8, 18.0, 18.1, 22.3, 25.9, 37.3, 49.9, 62.9, 65.0, 67.1, 121.5, 124.7, 127.1, 127.9, 128.7, 128.8, 128.9, 130.7, 135.7, 135.8, 148.2, 168.6, 170.1 ppm. HPLC-MS (ESI+): Rt = 18.1 min, m/z = 511 $[M+H]^+$. IR (film): ν = 3341, 3034, 2857, 1766, 1737, 1718, 1548, 1459, 1252 cm^{-1}. $[\alpha]^D_{20}$ = - 72 (c=1, CH_2Cl_2).

Benzyl 2-((2R,3S)-3-((R)-1-hydroxyethyl)-4-oxo-1-(o-tolycarbamoyl)azetidin-2-yl)acetate (**3**)

$BF_3{\cdot}OEt_2$ (35 µL, 0.28 mmol, 1.15 equiv) was added to a solution of β-lactam **2** (124 mg, 0.24 mmol, 1 equiv) in CH_3CN (5 mL) at 0 °C under nitrogen atmosphere. After 30 minutes, the reaction was allowed to warm to room temperature and stirred until a complete consumption of the starting material (2 h, TLC monitoring). The mixture was then quenched with phosphate buffer (0.1M, pH 7.4, 10 mL) and extracted with CH_2Cl_2 (3 × 15 mL). The organic layers were collected, dried over Na_2SO_4 and concentrated in vacuum. The crude was purified by flash-chromatography (Cyclohexane/EtOAc 70:30) yielding compound **3** as a colorless oil (76 mg, 91%). ^{1}H NMR: (400 MHz; $CDCl_3$) δ = 1.37 (d, J = 6.3 Hz, 3H), 2.28 (s, 3H), 2.77 (dd, J = 17.1, 9.8 Hz, 1H), 3.12 (dd, J = 7.9, 2.6 Hz, 1H), 3.3 (bs, 1H), 3.52 (dd, J = 17.1, 3.6 Hz, 1H), 4.21 (dq, J = 12.7, 6.3 Hz, 1H), 4.38 (dt, J = 9.8, 3.2 Hz, 1H), 5.16 (d, J_{AB} = 12.2 Hz, 1H), 5.19 (d, J_{AB} = 12.2 Hz, 1H), 7.04 (t, J = 7.5 Hz, 1H), 7.15 – 7.25 (m, 2H), 7.28 – 7.41 (m, 5H), 7.93 (d, J = 7.9 Hz, 1H), 8.43 (bs, 1H) ppm. ^{13}C NMR: (100 MHz; $CDCl_3$) δ = 18.2, 21.7, 37.0, 52.5, 64.0, 66.4, 67.8, 121.4, 125.0, 127.4, 127.9, 129.0, 129.1, 129.2, 131.0, 135.5, 135.7, 148.3, 167.5, 171.7 ppm. HPLC-MS (ESI^+): Rt = 10.0 min, m/z = 397 $[M+H]^+$. IR (film): ν = 3475, 3340, 2971, 1764, 1735, 1715, 1548, 1459, 1306, 1187 cm^{-1}. $[\alpha]^D_{20}$ = - 81 (c=1, CH_2Cl_2).

N-(9-(2-(((R)-1-((2R,3S)-2-(2-(benzyloxy)-2-oxoethyl)-4-oxo-1-(o-tolylcarbamoyl)azetidin-3yl)ethoxy)carbonyl)phenyl)-6-(diethylamino)-3H-xanthen-3-ylidene)-N-ethylethanaminium chloride (**4**)

To a solution of alcohol **3** (57 mg, 0.14 mmol, 1 equiv) in CH_2Cl_2 (2.5 mL) under nitrogen atmosphere, Rhodamine B (67 mg, 0.14 mmol, 1 equiv) and DMAP (3.4 mg, 0.03 mmol, 0.2 equiv) were added. The mixture was then cooled to 0 °C and DCC (29 mg, 0.14 mmol, 1 equiv) was added; the system was allowed to reach room temperature in 15 minutes and left under stirring overnight. After 24 h (TLC monitoring) the reaction mixture was filtered washing with CH_2Cl_2 (5 mL) and evaporated. The crude was suspended in EtOAc at 0°C and the solid residual dicyclohexylurea was eliminated by filtration. The organic layer was concentrated in vacuum and purified by flash-chromatography (CH_2Cl_2/EtOAc 50:50 then EtOAc 100% then EtOAc/CH_3OH 80:20) yielding compound **4** as a purple solid (72 mg, 60%). ^{1}H NMR: (400 MHz; $CDCl_3$) δ = 1.14 (d, J = 6.4 Hz, 3H) 1.29 (t, J = 6.9 Hz, 12H), 2.18 (s, 3H), 2.77 (dd, J = 16.4, 8.2 Hz, 1H), 3.15 (dd, J = 16.3, 4.0 Hz, 1H), 3.31 (dd, J = 6.2, 2.7 Hz, 1H), 3.53 – 3.68 (m, 8H), 4.11 – 4.17 (m, 1H), 5.07 (s, 2H), 5.22 – 5.30 (m, 1H), 6.79 (d, J = 9.5 Hz, 1H), 6.82 – 6.90 (m, 3H), 7.01 – 7.10 (m, 3H), 7.15 – 7.23 (m, 2H), 7.27 – 7.36 (m, 6H), 7.70 (t, J = 7.7 Hz, 1H), 7.78 -7.83 (m, 2H), 8.20 (d, J = 7.8 Hz, 1H), 8.27 (bs, 1H), ppm. ^{13}C NMR: (100 MHz; $CDCl_3$) δ = 12.8, 17.7, 17.8, 36.5, 46.3, 51.4, 60.0, 66.9, 68.5, 96.3, 96.5, 113.5, 113.5, 114.3, 114.6, 121.1, 124.8, 126.9, 127.6, 128.4, 128.6, 128.7, 129.9, 130.4, 130.5, 130.6, 131.2, 131.3, 133.5, 133.6, 135.1, 135.4, 147.5, 155.5, 155.6, 155.7, 157.7, 157.9, 158.3, 164.3, 166.0, 169.5 ppm. HPLC-MS (ESI$^+$): Rt = 9.10 min, m/z = 821 [M-Cl-]$^+$. IR (film): ν = 3338, 3062, 2976, 2929, 2855, 1766, 1720, 1647, 1592, 1548, 1413, 1338, 1250, 1181, 1133, 1076 cm^{-1}.

N-(9-(2-(((R)-1-((2R,3S)-2-(carboxymethyl)-4-oxo-1-(o-tolylcarbamoyl)azetidin-3yl)ethoxy)carbonyl)phenyl)-6-(diethyl amino)-3H-xanthen-3-ylidene)-N-ethylethanaminium chloride (**B**)

Following GP1 compound **4** (38 mg, 0.04 mmol) yielded compound **B** as a purple solid (31 mg, 92%). ^{1}H NMR: (400 MHz; CD_3OD) δ = 0.99 (d, J = 6.4 Hz, 3H), 1.28 – 1.32 (m, 12H), 2.17 (s, 3H), 2.45 (dd, J = 14.9, 8.7 Hz, 1H), 2.94 (dd, J = 14.9, 3.6 Hz, 1H), 3.30 – 3.32 (m, 1H), 3.60 – 3.70 (m, 8H), 3.90 – 3.93 (m, 1H), 5.28 – 5.34 (m, 1H), 6.98 – 7.09 (m, 6H), 7.14 – 7.20 (m, 3H), 7.43 (d, J = 7.4 Hz, 1H), 7.68 – 7.78 (m, 2H), 7.83 (t, J = 7.5 Hz, 1H), 8.25 (d, J = 7.7 Hz, 1H) ppm. ^{13}C NMR: (100 MHz; CD_3OD) δ = 12.8, 17.4, 17.8, 34.6, 46.7, 52.5, 61.1, 69.2, 97.5, 97.6, 114.4, 115.4, 116.0, 122.9, 126.0, 127.5, 129.9, 131.3, 131.9, 132.3, 133.4, 134.1, 136.2, 149.1, 152.8, 156.8, 157.0, 158.7, 159.1, 165.7, 167.9, 168.7, 168.9 ppm. HPLC-MS (ESI$^+$): Rt = 8.03 min, m/z = 731 [M-Cl-]$^+$. IR (film): ν = 3341, 2975, 2931, 1765, 1716, 1648, 1590, 1339, 1250, 1133, 1011 cm^{-1}.

(R)-1-((2R,3S)-2-(2-(benzyloxy)-2-oxoethyl)-4-oxo-1-(o-tolylcarbamoyl)azetidin-3-yl)ethyl 3-((tert-butoxycarbonyl) amino)propanoate (**5**)

Following the procedure reported for **4**, alcohol **3** (98 mg, 0.25 mmol, 1 equiv) was treated with Boc-β-alanine (76 mg, 0.4 mmol, 1.6 equiv), DMAP (6 mg, 0.05 mmol, 0.2 equiv) and DCC (83 mg, 0.4 mmol, 1.6 equiv). Purification by flash-chromatography (Cyclohexane/EtOAc 80:20)

yielded compound **5** as a colorless oil (127 mg, 90%). ^{1}H NMR: (400 MHz; $CDCl_3$) δ = 1.38 (d, J = 4.3 Hz, 3H) 1.43 (s, 9H), 2.28 (s, 3H), 2.52 (t, J = 4.5 Hz, 2H), 2.86 (dd, J = 15.3, 7.4 Hz, 1H), 3.28 – 3.45 (m, 4H), 4.39 – 4.46 (m, 1H), 5.08 (bs, 1H), 5.15 (s, 2H), 5.29 – 5.39 (m, 1H), 7.05 (t, J = 7.4 Hz, 1H), 7.15 – 7.25 (m, 2H), 7.28 – 7.38 (m, 5H), 7.92 (d, J = 8.0 Hz, 1H), 8.38 (bs, 1H) ppm. ^{13}C NMR: (100 MHz; $CDCl_3$) δ = 17.8 18.4, 27.1, 28.6, 36.3, 36.7, 51.8, 60.3, 67.1, 67.6, 79.6, 121.2, 124.8, 127.0, 127.6, 128.6, 128.7, 128.8, 130.7, 135.3, 135.5, 147.7, 156.0, 166.4, 169.7, 171.7, ppm. HPLC-MS (ESI^+): Rt = 12.0 min m/z = 468 $[M\text{-}Boc+H]^+$. IR (film): ν = 3344, 2977, 2932, 1766, 1736, 1718, 1594, 1546, 1459, 1252, 1170 cm^{-1}. $[\alpha]^{D}_{20}$ = - 25 (c=0.6, CH_2Cl_2).

2-((2R,3S)-3-((R)-1-((3-((tert-butoxycarbonyl)amino) propanoyl)oxy)ethyl)-4-oxo-1-(o-tolylcarbamoyl)azetidin-2-yl)acetic acid (**6**)

Following GP1, compound **5** (107 mg, 0.19 mmol) yielded compound **6** as a colorless oil (86 mg, 95%). ^{1}H NMR: (400 MHz; CD_3OD) δ = 1.35 (d, J = 6.4 Hz, 3H) 1.37 (s, 9H), 2.22 (s, 3H), 2.48 (t, J = 6.7 Hz, 2H), 2.79 (dd, J = 15.9, 8.4 Hz, 1H), 3.17 – 3.21 (m, 1H), 3.23 – 3.29 (m, 2H), 3.48 (dd, J = 6.3, 2.1 Hz, 1H), 4.35 – 4.42 (m, 1H), 5.27 – 5.36 (m, 1H), 7.01 (t, J = 7.4 Hz, 1H), 7.12 - 7.20 (m, 2H), 7.74 (d, J = 7.9 Hz, 1H) ppm. ^{13}C NMR: (100 MHz; CD_3OD) δ = 17.8, 18.5, 28.7, 35.6, 37.3, 53.1, 61.3, 68.9, 80.2, 123.0, 126.0, 127.6, 130.0, 131.5, 136.4, 149.6, 158.2, 168.2, 172.5 ppm. HPLC-MS (ESI^+): Rt = 9.58 min m/z = 378 $[M\text{-}Boc+H]^+$. IR (film): ν = 3343, 2979, 2936, 1766, 1738, 1714, 1615, 1593, 1252, 1171 cm^{-1}. $[\alpha]^{D}_{20}$ = - 45 (c=1, CH_2Cl_2).

2,2,2-trifluoroacetate, 3-((R)-1-((2R,3S)-2-(carboxymethyl)-4-oxo-1-(o-tolylcarbamoyl)azetidin-3yl)ethoxy)-3-oxopropan-1-aminium salt (**7**)

Following GP2, compound **6** (51 mg, 0.11 mmol, 1 equiv) yelded compound **7** as a colorless oil (54 mg, 99%). ^{1}H NMR: (400 MHz; CD_3CN) δ = 1.40 (d, J = 6.4 Hz, 3H), 2.25 (s, 3H), 2.67 – 2.78 (m, 3H), 3.12 – 3.42 (m, 5H), 4.36 (dt, J = 9.7, 3.1 Hz, 1H), 5.39 – 5.51 (m, 1H), 7.0 (bs, 2H), 7.07 (t, J = 7.5 Hz, 1H), 7.17 – 7.25 (m, 2H), 7.83 (d, J = 8.1 Hz, 1H), 8.39 (bs, 1H) ppm. ^{13}C NMR: (100 MHz; CD_3CN) δ = 17.9, 18.8, 32.1, 36.9, 37.1, 53.7, 61.6, 69.5, 122.5, 125.7, 127.7, 129.5, 131.6, 136.7, 149.3, 167.4, 171.6, 173.4 ppm. HPLC-MS (ESI^+): Rt = 1.7 min m/ z = 378 $[M\text{-}TFA+H]^+$. IR (film): ν = 3340, 3067, 2984, 2940, 2727, 2575, 1771, 1733, 1726, 1718, 1678, 1594, 1337, 1308, 1182 cm^{-1}. $[\alpha]^{D}_{20}$ = - 34 (c=1, CH_2Cl_2).

2-((2R,3S)-3-((R)-1-((3-(3-(3',6'-dihydroxy-3-oxo-3H-spiro[isobenzofuran-1,9'-xanthen]-5yl)thioureido)propanoyl)oxy) ethyl)-4-oxo-1-(o-tolylcarbamoyl)azetidin-2-yl)acetic acid (**C**)

Compound **7** (46 mg, 0.09 mmol, 1 equiv) was dissolved in anhydrous CH_2Cl_2 (1 mL) under a nitrogen atmosphere. Anhydrous TEA (50 µL, 0.36 mmol, 4 equiv) was added dropwise, followed by a dropwise addition of FITC (32 mg, 0.08 mmol, 0.9 equiv). After complete consumption of the starting β-lactam (4 h), the solvent was evaporated in vacuum and the crude was re-dissolved in CH_3OH (1 mL), then water and HCl (1M) were added until pH = 3 to litmus. The aqueous solution was extracted with EtOAc (3 × 10 mL). The organic layers were collected, dried over Na_2SO_4 and concentrated in vacuum. Purification by flash chromatography (EtOAc/CH_3OH 80:20 then 70:30) yielded compound **C** as an orange solid (38 mg, 55%). ^{1}H

NMR: (400 MHz; CD_3OD) δ = 1.39 (d, *J* = 6.4 Hz, 3H), 2.21 (s, 3H), 2.63 (dd, *J* = 15.3, 9.1 Hz, 1H), 2.70 (t, *J* = 6.2 Hz, 2H), 3.14 (dd, *J* = 15.3, 3.6 Hz, 1H), 3.47 (dd, *J* = 7.2, 2.4 Hz, 1H), 3.80 – 3.90 (m, 2H), 4.43 (dd, *J* = 5.8, 3.1 Hz, 1H), 5.33 – 5.42 (m, 1H), 6.51 (d, *J* = 8.7, 2H), 6.60 – 6.70 (m, 4H), 6.99 (t, *J* = 7.4 Hz, 1H), 7.05 – 7.18 (m, 3H), 7.70 – 7.76 (m, 2H), 8.18 (bs, 1H) ppm. ^{13}C NMR: (100 MHz; CD_3OD) δ = 18.1, 18.8, 34.9, 39.3, 41.3, 54.2, 61.7, 69.4, 103.8, 112.0, 114.4, 116.9, 120.7, 123.4, 126.1, 126.3, 127.8, 129.6, 130.4, 130.7, 131.7, 136.36 142.6, 148.6, 150.0, 154.7, 162.5, 168.6, 171.6, 173.1, 176.1, 183.0 ppm. HPLC-MS (ESI^+): Rt = 8.4 min m/z = 767 $[M+H]^+$. IR (film): ν = 3374, 2972, 2936, 1764, 1710, 1688, 1594, 1545, 1460, 1310, 1205 cm^{-1}.

2,2,2-trifluoroacetate,3-((R)-1-((2R,3S)-2-(2-(benzyloxy)-2-oxoethyl)-4-oxo-1-(otolylcarbamoyl)azetidin-3-yl)ethoxy)-3-oxopropan-1-aminium salt (**8**)

Following GP2, the beta-lactam **5** (59 mg, 0.10 mmol, 1 equiv) yielded compound **8** as a colorless oil (56 mg, 96%). ^1H NMR: (400 MHz, CD_3CN) δ = 1.36 (d, *J* = 6.4 Hz, 3H), 2.25 (s, 3H), 2.71 (t, *J* = 6.3 Hz, 2H), 2.82– 3.08 (m, 4H), 3.17 – 3.26 (m, 3H), 3.46 (dd, *J* = 7.3, 2.7 Hz, 1H), 4.39 (ddd, *J* = 8.1, 4.0, 2.7 Hz, 1H), 5.12 (d, *J* = 12.4 Hz, 1H), 5.16 (d, *J* = 12.4 Hz, 1H), 5.34 – 5.42 (m, 1H), 7.05 – 7.10 (m, 2H), 7.17 – 7.26 (m, 2H), 7.32 – 7.40 (m, 4H), 7.82 (d, *J* = 8.1 Hz, 1H), 8.36 (bs, 1H) ppm. ^{13}C NMR: (100 MHz, $CDCl_3$) δ = 17.5, 18.1, 30.7, 36.3, 36.6, 52.1, 60.7, 67.3, 68.9, 122.0, 125.6, 127.0, 128.2, 128.7, 128.8, 130.8, 134.5, 135.2, 148.3, 165.9, 170.5, 171.3 ppm. ESI-MS (ESI^+): Rt = 1.7 min, m/z = 468 $[M-TFA]^+$. IR (film): ν = 3342, 3064, 2930, 1768, 1734, 1680, 1594, 1460, 1203 cm^{-1}. $[\alpha]^D_{20}$ = - 16 (c = 0.9, CH_2Cl_2).

(R)-1-((2R,3S)-2-(2-(benzyloxy)-2-oxoethyl)-4-oxo-1-(o-tolyl carbamoyl) azetidin-3-yl)ethyl 3-(2-(5-fluoro2,6-dioxo-2,3-dihydropyrimidin-1(6H)-yl)acetamido)propanoate (**9**)

In a round-bottom flask, compound **8** (51 mg, 0.09 mmol, 1.2 equiv) was dissolved in CH_2Cl_2 (0.5 mL) under a nitrogen atmosphere and anhydrous TEA (15 µL, 0.108 mmol, 1.4 equiv) was added dropwise. The reaction was left for 20 minutes in order to desalt compound **8**. At the same time, in a second round-bottom flask, compound **13** (14 mg, 0.075 mmol, 1 equiv) was dissolved in DMF (0.1 mL), and the solution of the first round-bottom flask was dropped. Then HOBt (10 mg, 0.075 mmol, 1 equiv) and EDC (14, 0.075 mmol, 1 equiv) were added at 0 °C. After 1 h the solution was warmed to rt and left under stirring after complete consumption of the starting material (18 h, TLC monitoring). The mixture was quenched with H_2O and extracted with CH_2Cl_2 (3 × 10 mL). The organic layers were collected, dried over Na_2SO_4 and concentrated in vacuum. Purification by flash-chromatography (Cyclohexane/EtOAc 3:7 than 2:8) yielded compound **9** as a waxy white solid (19 mg, 40%). ^1H-NMR: (400 MHz, $CDCl_3$) δ = 1.39 (d, *J* = 6.3 Hz, 3H), 2.28 (s, 3H), 2.45 – 2.62 (m, 2H), 2.79 (dd, *J* = 16.2, 9.1 Hz, 1H), 3.32 (dd, *J* = 7.8, 2.1 Hz, 1H), 3.38 (dd, *J* = 16.3, 3.6 Hz, 1H), 3.47 – 3.57 (m, 2H), 4.16 (d, *J* = 15.6 Hz, 1H), 4.26 (d, *J* = 15.6 Hz, 1H), 4.38 – 4.44 (m, 1H), 5.14 (s, 2H), 5.32 – 5.42 (m, 1H), 6.90 - 7.09 (m, 2H), 7.18 - 7.22 (m, 2H), 7.30 - 7.37 (m, 5H), 7.91 (d, *J* = 8.1 Hz, 1H), 8.35 (bs, 1H), 9.48 (bs, 1H) ppm. ^{13}C-NMR: (100 MHz, $CDCl_3$) δ = 18.1, 18.7, 34.1, 35.6, 37.2, 51.1, 52.1, 60.7, 67.5, 68.2, 121.6, 122.5, 125.3, 125.9, 127.3, 128.1, 128.7, 129.0 (d, J = 33 Hz), 130.0, 135.5, 139.8 (d, J = 219 Hz) 148.2, 150.2, 157.5 (d, J = 26.5 Hz), 166.7, 170.4, 171.9 ppm. HPLC-MS (ESI^+): Rt=

8.2 min, m/z = 638 $[M+H]^+$. IR (film): ν = 3367, 3060, 2990, 1765, 1693, 1662, 1615, 1543, 1241, 1169, 1133 cm^{-1}. $[\alpha]^D_{20}$ = - 43 (c = 1, CH_3OH).

2-((2R,3S)-3-((R)-1-((3-(2-(5-fluoro-2,6-dioxo-2,3-dihydro pyrimidin-1(6H)yl)acetamido)propanoyl)oxy)ethyl)-4-oxo-1-(o-tolylcarbamoyl)azetidin-2-yl)acetic acid (**E**)

Following GP1, compound **9** (13 mg, 0.02 mmol) yielded compound **E** as a waxy white solid (11 mg, 99%). ^{1}H-NMR: (400 MHz, CD_3OD) δ = 1.41 (d, *J* = 7.4 Hz, 3H) 2.28 (s, 3H), 2.59 (dd, *J* = 10.9, 6.0 Hz, 1H), 2.68 (dd, *J* = 15.3, 8.9 Hz, 1H), 3.17 – 3.22 (m, 1H), 3.38 – 3.54 (m, 3H), 4.37 (s, 2H), 4.40 – 4.43 (m, 1H), 5.31 – 5.43 (m, 1H), 7.03 – 7.08 (m, 1H), 7.19 (m, 2H), 7.74 (d, *J* = 6.2 Hz, 1H), 7.76 (d, *J* = 8.2 Hz, 1H) ppm. ^{13}C NMR: (100 MHz, CD_3OD) δ = 18.1, 18.8, 35.2, 36.8, 38.0, 51.5, 53.7, 61.8, 69.5, 123.6, 126.5, 128.0, 130.7, 131.9, 132.1 (d, *J* = 33.9 Hz), 136.8, 141.9 (d, *J* = 232.0 Hz), 150.1, 151.9, 160.3 (d, J = 25.9 Hz), 168.6, 169.6, 172.7 ppm. HPLC-MS (ESI^+): Rt= 5.01 min; m/z = 548 $[M+H]^+$. IR (film): ν = 3352, 2930, 1763, 1697, 1664, 1592, 1542, 1244, 1176 cm^{-1}. $[\alpha]^D_{20}$ = - 45 (c = 1.1, CH_3OH).

Benzyl 2-((2R,3S)-3-((R)-1-(2-(5-fluoro-2,4-dioxo-3,4-dihy dropyrimidin-1(2H)-yl)acetoxy)ethyl)-4-oxo-1-(o-tolylcarbamoyl) azetidin-2-yl)acetate (**10**)

Compound **3** (65 mg, 0.17 mmol, 1 equiv) was dissolved in MeCN (1.6 mL) under a nitrogen atmosphere. Compound **13** (31 mg, 0.17 mmol, 1 equiv) was dissolved in DMF (1.7 mL) and added dropwise, followed by the addition of DCC (38 mg, 0.18 mmol, 1.1 equiv) and DMAP (4 mg, 0.033 mmol, 0.2 equiv). The reaction was left under stirring after complete consumption of the starting material (48 h, TLC monitoring). The reaction mixture was filtered washing with CH_2Cl_2 (5 mL) and evaporated. The crude was suspended in EtOAc at 0°C and the solid residual dicyclohexylurea was eliminated by filtration. The organic layer was concentrated in vacuum and purified by flash-chromatography (CH_2Cl_2/EtOAc 7:3) yielded compound **10** as a waxy solid (21 mg, 23%). ^{1}H-NMR: (400 MHz, $CDCl_3$) δ = 1.46 (d, *J* = 6.4 Hz, 3H), 2.28 (s, 3H), 2.74 (dd, *J* = 17.2, 9.9 Hz, 1H), 3.24 (dd, *J* = 8.9, 2.4 Hz, 1H), 3.55 (dd, *J* = 17.1, 3.3 Hz, 1H), 4.17 (d, *J* = 17.6 Hz, 1H), 4.43 (dt, *J* = 9.9, 2.8 Hz, 1H), 4.65 (d, *J* = 17.5 Hz, 1H), 5.14 (d, *J* = 12.5 Hz, 1H), 5.17 (d, *J* = 12.5 Hz, 1H), 5.47 (dq, *J* = 12.8, 6.4 Hz, 1H), 7.05 (t, *J* = 7.5 Hz, 1H), 7.15 – 7.20 (m, 2H), 7.32 - 7.38 (m, 6H), 7.91 (d, *J* = 8.1 Hz, 1H), 8.36 (s, 1H), 9.29 (s, 1H) ppm. ^{13}C-NMR: (100 MHz, $CDCl_3$) δ = 17.8, 18.6, 36.7, 48.7, 52.1, 61.2, 67.2, 69.4, 121.2, 124.9, 127.0, 127.7, 128.1, 128.8, 129.0 (d, J = 19 Hz), 130.6, 135.2, 135.3, 140.6 (d, *J* = 237 Hz), 147.6, 149.6, 157.1 (d, *J* = 26 Hz), 165.5, 166.9, 170.4 ppm. HPLC-MS (ESI^+): Rt = 9.81 min; m/z = 567 $[M+H]^+$. IR (film): ν = 3338, 3204, 3067, 2933, 1764, 1703, 1669, 1616, 1593, 1548, 1460, 1381, 1249, 1210 cm^{-1}. $[\alpha]^D_{20}$ = - 6.5 (c = 1.3, CH_2Cl_2).

2-((2R,3S)-3-((R)-1-(2-(5-fluoro-2,4-dioxo-3,4-dihydro pyrimidin-1(2H)-yl)acetoxy)ethyl)-4-oxo-1-(o-tolylcarbamoyl) azetidin-2-yl)acetic acid (**D**)

Following GP1, compound **10** (21 mg, 0.04 mmol) yielded compound **D** as a waxy white solid (15 mg, 86%). ^{1}H-NMR: (400 MHz, CD_3OD) δ = 1.45 (d, *J* = 6.4 Hz, 3H) 2.28 (s, 3H), 2.79 (dd, *J* = 16.0, 9.0 Hz, 1H), 3.23 (dd, *J* = 16.0, 3.1 Hz, 1H), 3.52 (dd, *J* = 7.2, 2.4 Hz, 1H), 4.40 (dd, *J*

= 5.9, 2.8 Hz, 1H), 4.48 (d, *J* = 17.5 Hz, 1H), 4.58 (d, *J* = 17.5 Hz, 1H), 5.38 - 5.46 (m, 1H), 7.06 (t, *J* = 7.4 Hz, 1H), 7.14 – 7.24 (m, 2H), 7.80 (d, *J* = 8.0 Hz, 1H), 7.85 (d, *J* = 6.1 Hz, 1H) ppm. ^{13}C-NMR: (100 MHz, CD_3OD) δ = 17.8, 18.5, 37.9, 50.2, 53.7, 61.5, 70.5, 123.0, 126.0, 127.6, 130.0, 131.1, 131.4 (d, *J* = 3.6 Hz), 136.5, 141.6 (d, *J* = 232.8 Hz), 149.7, 151.3, 159.8 (d, *J* = 53 Hz), 167.8, 168.6 ppm. HPLC-MS (ESI^+): Rt = 6.69 min; m/z = 477 $[M+H]^+$. IR (film): ν = 3424, 1762, 1641, 1551, 1460, 1250, 1214 cm^{-1}. $[\alpha]^D_{20}$ = -14 (c = 1, CH_2Cl_2).

5-((R)-1-((2R,3S)-2-(2-(benzyloxy)-2-oxoethyl)-4-oxo-1-(o-tolylcarbamoyl)azetidin-3-yl)ethoxy)-5-oxopentanoic acid (**11**)

Compound **3** (49 mg, 0.12 mmol, 1.0 equiv) was dissolved in CH_2Cl_2 (3.5 mL) under a nitrogen atmosphere. Glutaric anhydride (28 mg, 0.24 mmol, 2.0 equiv), DMAP (3 mg, 0.024 mmol, 0.2 equiv) and TEA (34 µL, 0.24 mmol, 2 equiv) were then added. The solution was left under stirring after complete consumption of the starting material (18 h, TLC monitoring). The mixture was quenched with H_2O (1 mL) and HCl 2N (2 mL) and extracted with CH_2Cl_2 (3 × 10 mL). The organic layers were collected, dried over Na_2SO_4 and concentrated in vacuum to afford compound **11** as a colorless oil (60 mg, 95%). ^{1}H NMR: (400 MHz, $CDCl_3$) δ = 1.36 (d, *J* = 6.4 Hz, 3H) 1.87 – 1.98 (m, 2H), 2.27 (s, 3H), 2.45 – 2.32 (m, 4H), 2.88 (dd, *J* = 16.2, 8.2 Hz, 1H), 3.29 (dd, *J* = 16.1, 4.0 Hz, 1H), 3.35 (dd, *J* = 6.3, 2.7 Hz, 1H), 4.36 – 4.50 (m, 1H), 5.13 (s, 2H), 5.33 (p, *J* = 6.4 Hz, 1H), 7.01 – 7.10 (m, 1H), 7.11 – 7.22 (m, 2H), 7.29 – 7.38 (m, 5H), 7.92 (d, *J* = 8.1 Hz, 1H), 8.38 (bs, 1H) ppm. ^{13}C NMR: (100 MHz, $CDCl_3$) δ = 17.6, 18.1, 19.7, 32.6, 33.1, 36.6, 51.4, 60.1, 66.9, 67.1, 120.9, 124.5, 126.8, 127.8, 128.0, 128.2, 128.6, 130.2, 135.2, 135.4, 147.6, 166.3, 169.5, 171.8, 177.5 ppm. HPLC-MS (ESI^+): Rt = 10.01 min, m/z = 511 $[M+H]^+$. IR (film): ν = 3344, 3055, 2984, 2928, 1769, 1736, 1719, 1710, 1614, 1593, 1545 cm^{-1}. $[\alpha]^D_{20}$ = -36 (c= 1, CH_2Cl_2).

(R)-1-((2R,3S)-2-(2-(benzyloxy)-2-oxoethyl)-4-oxo-1-(o-tolylcarbamoyl)azetidin-3-yl)ethyl ((5-fluoro-2,4-dioxo-3,4-dihy dropyrimidin-1(2H)-yl)methyl) glutarate (**12**)

In a first round-bottom flask, 5-FU (55 mg, 0.42 mmol, 1.8 equiv) was dissolved in H_2O (3.5 mL) and paraformaldehyde (19 mg, 0.64 mmol, 2.7 equiv) was added. The reaction was left 6 h at 60°C and then H_2O was concentred in vacuum. The mixture was dissolved in MeCN (5.8 mL) and transferred in a second round-bottom flask, under nitrogen atmosphere, and then compound 11 (115 mg, 0.23 mmol, 1 equiv) was added followed by EDC (61 mg, 0.32 mmol, 1.4 equiv) and DMAP (39 mg, 0.32 mmol, 1.4 equiv). The mixture was left under stirring after complete consumption of the starting material (18 h, TLC monitoring). The mixture was quenched with H_2O and extracted with CH_2Cl_2 (3 × 10 mL). The organic layers were collected, dried over Na_2SO_4 and concentrated in vacuum. Purification by flash-chromatography (Cyclohexane/EtOAc 45:55) yielded compound **12** as a waxy white solid (27 mg, 18%). ^{1}H NMR: (400 MHz, $CDCl_3$) δ = 1.35 (d, *J* = 6.2 Hz, 3H), 1.86 – 1.98 (m, 2H), 2.27 (s, 3H), 2.31-2.48 (m, 4H), 2.88 (dd, J = 16.0, 8.0 Hz, 1H), 3.25 – 3.35 (m, 2H), 4.42 - 4.47 (m, 1H), 5.16 (s, 2H), 5.25 – 5.39 (m, 1H), 5.54 (s, 2H), 7.05 (t, *J* = 7.1 Hz, 1H), 7.16 - 7.24 (m, 2H), 7.30 - 7.36 (m, 5H), 7.53 (d, *J* = 4.8 Hz, 1H), 7.92 (d, *J* = 7.9 Hz, 1H), 8.38 (bs, 1H), 8.83 (bs, 1H) ppm. ^{13}C NMR: (100 MHz, $CDCl_3$) δ = 17.8. 18.3, 19.8, 32.9, 33.1, 36.8, 51.4, 60.2, 67.1, 67.3, 70.0, 121.1, 124.8, 127.0, 127.6, 128.5, 128.6, 128.8, 130.3 (d, *J* = 30Hz), 135.2, 135.8, 140.8 (d, *J* =

289 Hz), 147.8, 149.2, 156.5 (d, *J* = 28Hz), 166.5, 169.7, 171.8, 173.0 ppm. HPLC-MS (ESI^+): Rt = 9.91 min, m/z = 653 $[M+H]^+$. IR (film): ν = 3210, 3088, 2986, 1763, 1719, 1709, 1677, 1252, 1126 cm^{-1}. $[\alpha]^D_{20}$ = -24 (c= 0.9, CH_2Cl_2).

2-((2R,3S)-3-((R)-1-((5-((5-fluoro-2,4-dioxo-3,4-dihydro pyrimidin-1(2H)-yl)methoxy)-5-oxopentanoyl)oxy)ethyl)-4-oxo-1-(o-tolylcarbamoyl)azetidin-2-yl)acetic acid (**F**)

Following GP1, compound **12** (27 mg, 0.04 mmol) yielded compound **F** as a waxy white solid (21 mg, 93%). ^1H NMR: (400 MHz, $CDCl_3$) δ = 1.42 (d, *J* = 6.0 Hz, 3H), 1.89 - 2.0 (m, 2H), 2.29 (s, 3H), 2.31 – 2.56 (m, 4H), 2.74 (m, 1H), 3.35 (d, *J* = 6.5 Hz, 1H), 3.41 (d, *J* = 14.9 Hz, 1H), 4.40 - 4.43 (m, 1H), 5.29 – 5.37 (m, 1H), 5.56 (d, *J* = 10.6 Hz, 1H), 5.64 (d, *J* = 10.4 Hz, 1H), 7.05 (dd, *J* = 20.6, 13.2 Hz, 1H), 7.13 – 7.26 (m, 2H), 7.59 (d, *J* = 4.9 Hz, 1H), 7.91 (d, *J* = 8.1 Hz, 1H), 8.43 (bs, 1H), 10.04 (bs, 1H) ppm. ^{13}C NMR: (100 MHz, $CDCl_3$) δ = 17.6, 18.3, 19.6, 30.3, 32.7, 36.9, 51.9, 60.4, 67.6, 70.2, 121.1, 124.8, 125.5, 126.8, 127.7, 128.6 (d, *J* = 34 Hz), 130.5, 135.0, 140.4 (d, *J* = 238 Hz), 147.8, 149.7, 157,2 (d, *J* = 26 Hz), 166.2, 171.8, 172.9, 173.2 ppm. HPLC-MS (ESI^+): Rt = 6.36 min, m/z =563 $[M+H]^+$. IR (film): ν = 3192, 3059, 2963, 1735, 1718, 1701, 1686, 1250, 1124, 1082 cm^{-1}. $[\alpha]^D_{20}$ = -32 (c = 0.7, CH_2Cl_2).

Stability tests

Compounds **D**, **E**, and **F** were dissolved in PBS 0.1 M pH = 7.4 (1 mg/mL) and incubated at 30°C in a thermostat. Aliquots (0.5 mL) were taken at different time points (from 0 to 72 h) and analyzed by HPLC-UV using Zorbax-Eclipse XDB column – C18, 4.6x150 mm, 5 microns for **D** and **E**, and Gemini column – C18, 100x2 mm, 3 micron for **F**. Peaks relative to the intact compound were integrated and their concentration was determined at the established times to obtain a stability profile of the compounds in PBS.
Compounds **D**, **E** and **F** were dissolved in Fetal Bovine Serum (1 mg/mL) and incubated at 30°C in a thermostat. Aliquots of 0.15 mL were taken at different time points (from 0 to 72 h) and diluted with 0.6 mL of MeOH. After centrifugation for 3 min at 50 rpm, 0.4 mL of the supernatant were taken and for compound **D** and **E** directly analyzed in HPLC-UV using Gemini column – C18 100x2 mm 3 micron; for compound **F** instead, the supernatant was concentrated and the resulting solid material was re-dissolved in 0.2 mL of MilliQ water and 0.2 mL of MeCN and analyzed as described above. Peaks relative to the intact compound were integrated and their concentration was determined at the established times to obtain a stability profile of the compounds in FBS. [68]

Cell culture

Jurkat E6.1 human T and K562 cells were grown in RPMI-1640 (Life Technologies, Carlsbad, CA, USA) supplemented with L-glutamine and 10% FBS (fetal bovine serum; Life technologies). K562 cells were treated with 25 ng/mL PMA (Phorbol 12-myristate 13-acetate, Sigma-Aldrich SRL, Milan, Italy) 40 h prior to the experiments in order to induce differentiation and consequently to increase $\alpha_5\beta_1$ integrin expression. HEK293 cells were routinely cultured in EMEM (Cambrex, Walkersville, MD, USA) with the addition of L-glutamine, nonessential aminoacids and 10% FBS. Cells were kept at 37 °C under 5% CO_2 humidified atmosphere. All

cell lines were obtained from American Type Culture Collection (ATCC, Rockville, MD, USA). The cell lines employed in this study are considered as useful in vitro models to investigate potential ligands acting as integrin agonists or antagonists.[43, 91, 93,68]

Cell adhesion assays

The adhesion assays were performed as previously described.[43] Briefly, regarding adhesion assays on Jurkat E6.1 cell, black 96-well plates (Corning Costar, Celbio, Milan, Italy) were coated overnight at 4 °C with VCAM-1 (5 μg/mL) to investigate $\alpha_4\beta_1$ integrin-mediated cell adhesion. Jurkat E6.1 cells were stained by incubation with CellTracker green CMFDA (12.5 μM, 30 min at 37 °C, Life Technologies). After three washes, various concentrations of each compound (10^{-4} – 10^{-10} M) or the vehicle (methanol) were added to Jurkat E6.1 cells and incubated for 30 min at 37 °C. Cells were then plated (500000/well) on VCAM-1-coated wells and incubated for 30 min at 37 °C. After three washes, adhered cells were lysed with 0.5% Triton X-100 in PBS for 30 min at 4 °C and green fluorescence was measured (Ex485 nm/Em535 nm). Experiments were carried out in quadruplicate and repeated at least three times. Data analysis and IC_{50} or EC_{50} values were calculated using GraphPad Prism 5.0 (GraphPad Software, San Diego, CA, USA).

For adhesion assay on K562 cells, clear 96-well plates were coated by passive adsorption with fibronectin (10 μg/mL) overnight at 4 °C. K562 cells were then pre-incubated with various concentrations of each compound (10^{-4} – 10^{-10} M) or with the vehicle (methanol) for 30 min at room temperature. Then the cells (50000 cells/well) were plated and incubated at room temperature for 1 h. After washing away nonadherent cells with 1% BSA (bovine serum albumin) in PBS, 50 μL of hexosaminidase substrate were added and incubated for 1 hour at room temperature. After the addition of stopping solution, plates were read at 405 nm in an EnSpire Multimode Plate Reader (PerkinElmer, Waltham, MA, USA).[68]

Cellular uptake

Intracellular uptake of fluorescent-conjugated compounds was evaluated by flow cytometry as previously described,[43] with the following modifications. Jurkat, K562 and HEK293 cells were seeded in 12 well plates and treated with fluorescent conjugates (1 - 10 - 25 μM) for 1 h at 37°C. To determine integrin involvement in fluorescent conjugates cell internalization, cells were pretreated with anti-α^4 (10 μg/mL, Abcam, #Ab220) or anti-α_5 (10 μg/mL, BD Bioscience, #555651) antibody or $\alpha_4\beta_1$ selective agonist **A** (100 μM) for 30 minutes. Afterward, the cells were washed three times with cold PBS and cellular uptake was quantified by flow cytometry on a Guava® easyCyte 5 flow cytometer (Merck Millipore, Vimodrone, Italy).[68]

Cell apoptosis detection

Phycoerythrin-conjugated annexin V (annexin-PE) and 7-amino-actynomicin D (7-AAD; Guava Nexin Reagent, Merck Millipore, Darmstadt, Germany) were employed to determine the percentage of viable, early-apoptotic and late apoptotic/necrotic cells by flow cytometry.[43,94] After 72 hours treatments with different concentrations of compounds (10 - 50 - 100 μM), cells were collected by centrifugation, the supernatant were discarded, and the cell pellets were resuspended in 100 μL of complete medium. Then, the cells were stained with 100 μL of Nexin

reagent for 20 min at room temperature in the dark, following manufacturer's instructions. Cells were analyzed on a Guava® easyCyte 5 flow cytometer. At least 10,000 cells/sample were analyzed. Three populations of cells can be identified by this assay: viable cells (annexin V-PE and 7-AAD negative), early apoptotic cells (annexin V-PE positive and 7-AAD negative), and late stages apoptosis or necrotic cells (annexin V-PE and 7-AAD positive).[68]

1.1.4 Conjugation of integrin ligands to two different theranostic systems

In the past decade, significant research efforts have been focused on the development of new technologies that permit to combine diagnostic and therapeutic functions into one integrated platform. These studies led to the development of theranostic systems.
This strategy seems to be very profitable, indeed the combination of diagnostic and therapeutic agents within a single formulation allows to localize the target site, to evaluate the in vivo biodistribution and accumulation of drugs and to monitor in real time the pharmacokinetic profile through drug release. Theranostics is a highly interdisciplinary field, in fact, in order to ensure the development of suitable systems for monitoring the delivery, release and efficacy of drugs, it is required a close collaboration between different scientific disciplines such as chemistry, biology, pharmacy and medicine (Figure 20).[95]

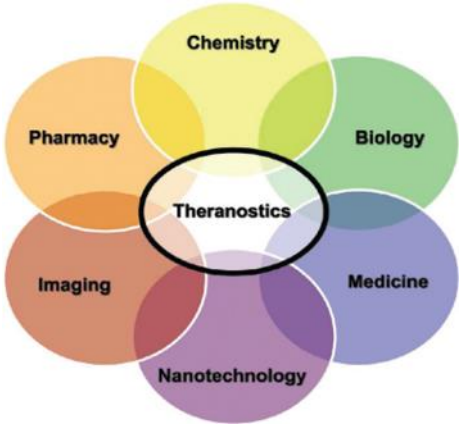

Figure 20. Schematic theranostic field representation. Figure adapted from ref. 95.

In this work, we want to develop new targeted drug delivery systems for theranostic applications, following two different strategies: “All in one” and “One for all”.

In the first case, i.e. “All in One”, the fluorophore, appropriately functionalized to allow the target recognition, is conjugated with a therapeutic agent[96] (i.e. cytotixic drugs); the latter can be released at the target site after breaking of the bond between the fluorophore and the pharmacologically active moiety, thus activating the fluorophore (*Figure 21*).

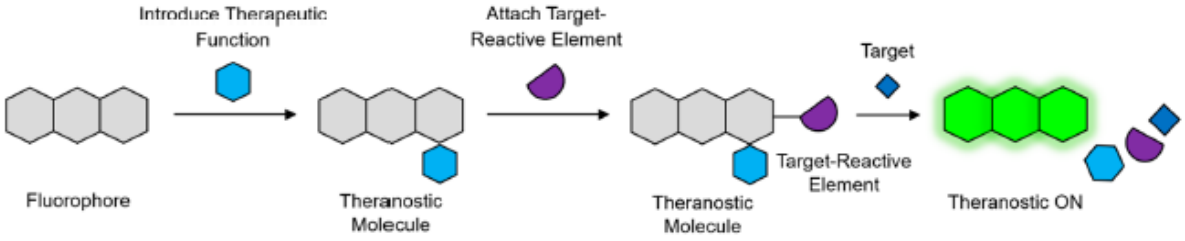

Figure 21. “All in one” system. Figure adapted from ref. 96.

Several organic fluorophores mainly belong to two classes: xanthene derivatives and phenazine derivatives (*Figure 22*). Currently, great attention has been put on a new class of compounds which can be used as fluorophores: coumarins[97] (*Figure 22).* They are natural compounds and are divided into different classes based on their structural properties, although they still have the benzopyranic structure in common. These compounds are characterized by the presence of aromatic rings which, thanks to the extensive delocalization and the coplanarity of the structure, give to these molecules excellent photophysical properties, such as high molar absorption coefficients ($\varepsilon \approx 80000\ M^{-1}cm^{-1}$) and quantum yields close to 100 %.[97,98] In particular, it has been shown that structural variations on the coumarin skeleton, such as the insertion of electron-donor auxochromic groups, can considerably influence the photophysical properties of these compounds.[97,99,100]

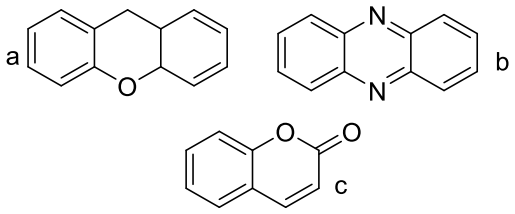

Figure 22. Organic fluorophores: a) xantene base structure; b) phenzine base stucture; c) coumarin base structure.

A fluorophore to be efficient, must possess foundamental characteristics for its detection. First of all, it is essential that the absorption and emission have a maximum in a region of the spectrum in which interference phenomena with the biological matrix are minimal. This parameter significantly affects the sensitivity of the detection. Furthermore, an important aspect to consider is the phenomenon of the autofluorescence of biological molecules; this generates a background signal that can compromise the sensitivity of the detection of the fluorophore effect.[101-102] It is therefore important to choose a class of fluorophores whose spectral characteristics can be easily modulated through small structural variations, which are photochemically stable, which have a high quantum yield value, which do not give specific binding with the other molecules present in the sample and which are highly biocompatible. Furthermore, another factor that must be taken into account is solubility; it is a crucial aspect to prevent self-aggregation phenomena that can turn off the fluorescence.[96]

In the " All for one " systems, on the other hand, the fluorophores need to be engineered to simultaneously possess imaging and therapeutic functions.[96] These systems are used for the application of phototherapy that involves the local exposure of patients to light to treat disease, including photodynamic therapy (PDT) and photothermal therapy (PTT) (*Figure 23*).[103]

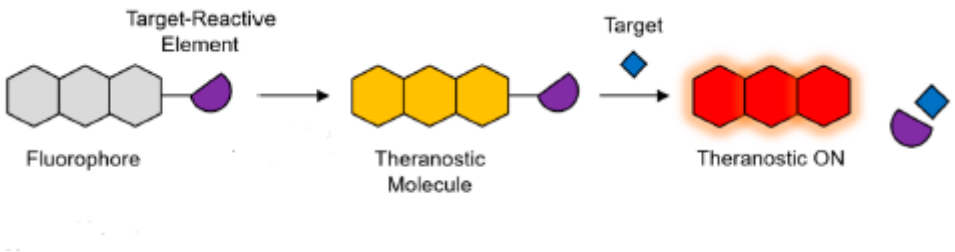

Figure 23. "All for one" systems. Figure adapted from ref. 96.

Both these therapies have been widely studied for cancer treatments in recent years, as they can eliminate tumor cells without damaging normal tissues. PDT is a minimally invasive technique and provides the use of photosensitizer (PS) and light activation. The PS that selectively accumulates in the tumor tissue can be activated by light of a specific nonthermal wavelength to produce reactive oxygen species (ROS), known as singlet oxygen, which can oxidize with nearby biological macromolecules in the tumor cells; this can cause cytotoxicity and cell death. PTT is also a minimally invasive and highly efficient antitumor approach, which is based on photothermal agent (PTA) with high photothermal conversion efficiency.[103]

A new class of PDT agents has emerged over the past decade: these are based on the 4,4-difluoro-4-bora-3a,4a-diaza-s-indacene (BODIPY) core. BODIPYs have many ideal photosensitizer characteristics including high extinction coefficients and environment insensitivity resistance to photobleaching. Fluorescence occurs via relaxation from singlet excited states, so high quantum yields for fluorescence are undesirable since this means that much of the energy absorbed on excitation does not cross to triplet states. Consequently, BODIPYs for PDT have to be modified to depress fluorescence and enhance singlet-to-triplet intersystem crossing.[104]
Some examples of these compounds are shown in *Figure 24*. Tetramethyl BODIPY (compound X) shows a poor quantum yield, this implies a poor production of reactive oxygen species. This can be improved by making changes such as inserting a heavy atom such as a halogen. (Compound Y). However, experimental evidence has shown that further incorporation of an acid group (compound Z) improved ROS production, thus increasing the phototoxicity of the system.[104-105]

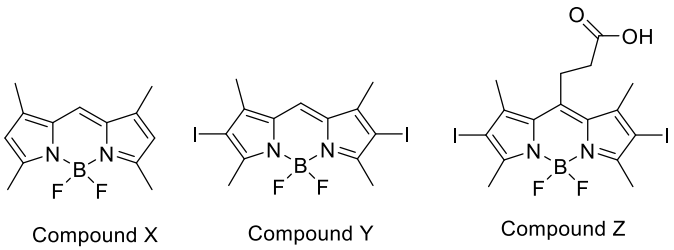

Figure 24. Examples of BODIPYs.

In our work, as previously anticipated, we want to develop two new different theranostic systems. Thanks to the good results obtained whit the development of TDDs[68], now our aim is to conjugate our β-lactam-based integrin ligand, which acts as drug-cargo for a selective delivery into cancerous cells, to theranostic agents.

The first system developed is **G** ("One for all", *Figure 25*) in which the β-lactam derivative is linked to a BODIPY, responsible of both imaging and therapeutic effect.

Compound **H**, on the other hand, is an "All in one" system in which the β-lactam carrier is conjugated with 3-azido-7-hydroxy coumarin, which acts as a fluorophore, suitably functionalized with 5-Fluorouracil, as a cytotoxic drug (*Figure 25).*

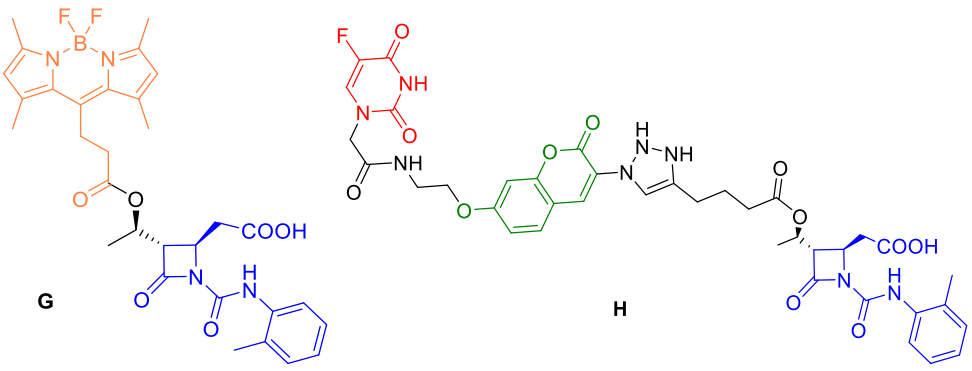

Figure 25. "One for All" system (**G**) and "All in One" system (**H**).

Results and discussion

For the development the two new theranostic agents **G** and **H**, we start from the synthesis of a common carrier, the β-lactam based integrin ligand developed by my research group; subsequently two different strategies will be used for the functionalization of the hydroxyethyl side chain at C3 position of the azetidinone in order to obtain the "All for one" theranostic compound **G** and the "All in one" theranostic compound **H**. We can start discussing the synthesis of compound **G**.

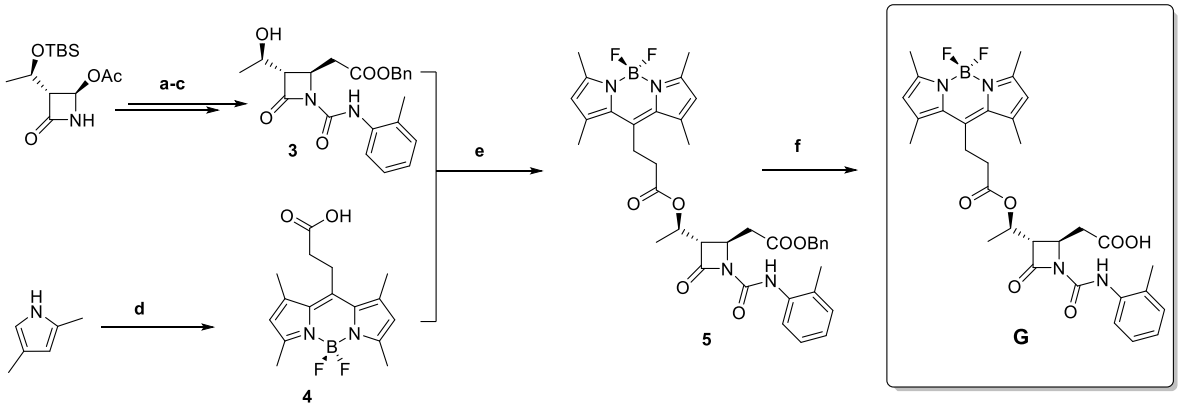

Scheme 3. Synthesis of Theranostic compound **G**; Reagent conditions: a) Zn, TMSCl, benzylbromoacetate, THF, 0°C then rt, 3 h; b) *o*-tolylisocyanate, TEA, CH_2Cl_2, rt, 16 h; c) $BF_3{\cdot}Et_2O$, CH_3CN, 0°C then rt, 2 h; d) Succinic anhydride, $BF_3{\cdot}OEt_2$, TEA, DCM, reflux, 5h; e) DCC, DMAP, DCM, 0°C then rt rt, 18 h; f) H_2, Pd/C (10%), THF/CH_3OH 1:1, rt, 2 h.

The synthesis of compound **G** started with a nucleophilic substitution reaction at the C-4 position[69] on the commercially available *(2R,3R)-3-((R)-1-((tbutyl dimethylsilyl)oxy) ethyl)-4-oxoazetidin-2-yl acetate*, by a Reformatsky reagent obtained in turn from benzyl bromo-acetate and a pre-activated zinc with *t*-butyldimethylsilylchloride. The β-lactam scaffold was acylated on nitrogen atom with the commercially available *o*-tolylisocyanate, in order to get the specific *o*-tolylureidic residue necessary for modulating the affinity toward the integrin receptor. The *t*-butyldimethylsilyl group on the C-3 side chain was then removed with $BF_3{\cdot}OEt_2$ as Lewis acid affording alcohol **3** in good yields.

For the synthesis of compound **G**, the hydroxy ethyl side chain of **3** was exploited for inserting the BODYPY, previously synthetized starting from 2,4-dimethyl pyrrole. This reaction is conducted in DCM in presence of $BF_3{\cdot}Et_2O$ and TEA to obtain the typical BODYPY structure and with succinic anhydride in order to add the side chain with the terminal carboxylic acid, necessary to anchor the β-lactam scaffold.
The coupling reaction between **3** and **4** is conducted in presence of DCC and DMAP to give intermediate **5**. The final deprotection of benzyl ester on the C-4 side chain catalyzed by Pd/C, yielded the final molecule **G** with the free carboxylic acid needed for integrin recognition at the MIDAS.

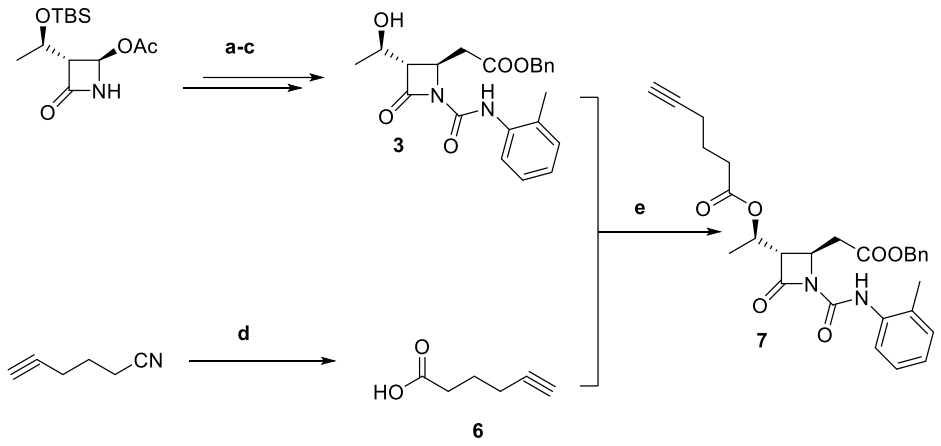

Scheme 4. Synthesis of intermediate **7**; Reagent conditions: a) Zn, TMSCl, benzylbromoacetate, THF, 0°C then rt, 3 h; b) *o*-tolylisocyanate, TEA, CH_2Cl2, rt, 16 h; c) $BF_3{\cdot}Et_2O$, CH_3CN, 0 °C then rt, 2 h; d) KOH, MeOH, H_2O, reflux, 6 h; e) DCC, DMAP, DCM, 0°C then rt, 18 h.

For the synthesis of theranostic compound **H**, we prepared the β-lactam scaffold as previously seen for compound **G**, obtaining **3** ready to react with an appropriate spacer. This spacer is constituted by compound **6**, having a free carboxylic acid moiety able to anchor the alcohol **3** and a terminal alkyne that will be necessary in future steps. It is obtained from the hydrolysis of 5-hexynenitrile in presence of KOH in a mixture of MeOH and water. Once obtained compounds **3** and **6** we have the coupling reaction mediated by DCC and DMAP, yielding compound **7**.

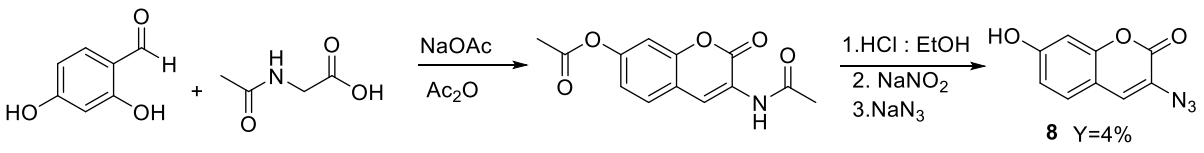

Scheme 5. Synthesis of intermediate **8**.

Separately, it is necessary to synthesize the coumarin, that is the imaging agent of our theranostic system. So the first step for the synthesis of the luminescent marker involved the reaction between 2,4-dihydroxybenzaldehyde and N-acetylglycine. The reaction was conducted under inert atmosphere in presence of sodium acetate and acetic anhydride and refluxed for 4 hours, then it was brought at 0°C to permit the precipitation of the desired compound. The second step consisted instead in the removal of the acetyl group obtaining a free amine in position 3 and a hydroxyl in position 7 using hydrochloric acid and ethanol and refluxing for 4 hours. After this

$NaNO_2$ was added to the mixture and the reaction with the amine gave a diazonium salt. Finally, sodium azide was added to solution, removing the diazonium salt and forming the azide group in position 3. The desired compound **8** is obtained in a low yield of 4%.

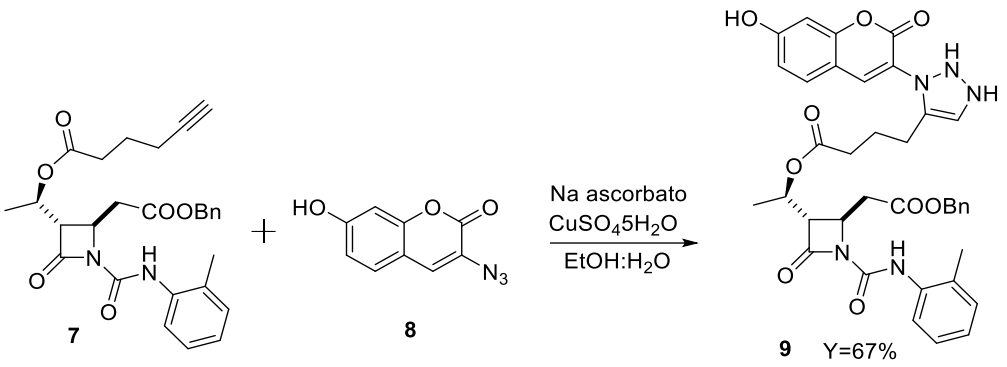

Scheme 6. Synthesis of intermediate **9**.

To link the imaging agent to the β-lactam scaffold we decided to do a copper catalysed click reaction between compound **7** and **8** in presence of Na ascorbate.
At this point we decided to study the coupling between the cytotoxic portion (5-FU) and the fluorophore using umbelliferone as a model for compound **9**. The first strategy we used is shown in the *Scheme 7*.

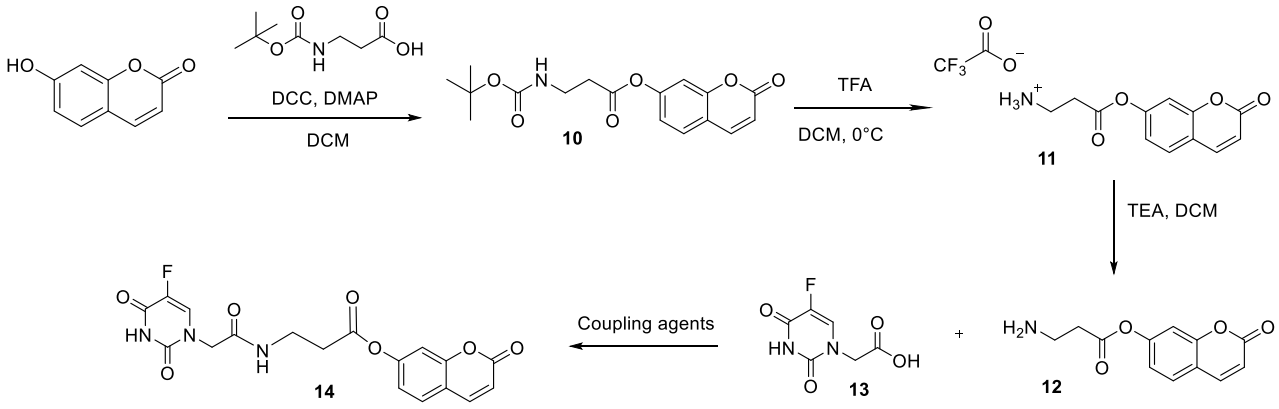

Scheme 7. Synthesis with β-alanine as a linker.

A coupling reaction between Umbelliferone and N-Boc-β-alanine with DCC and DMAP was done to synthetise compound **10**, and then elimination of Boc group with trifluoroacetic acid gave **11** in quantitative yield. Subsequently we tried different coupling conditions between compound **12**, obtained from the desalification in situ of **11** in presence of TEA, and **13** (See *Table 2*). A first attempt was made with HOBt and EDC, then HOBt and DCC and finally EDC and DMAP. The main product present in all the reactions was umbelliferone.

Table 2. Coupling reaction conditions between **12** and **13**.

Entry	Coupling agent (mmol, eq)	Solvent	mmol 5-FUCH$_2$COOH	Yield
1	HOBt (0.10 mmol, 1 equiv) EDC (0.10 mmol, 1 equiv)	DCM, DMF	0.10 (1 equiv)	-
2	HOBt (0.18 mmol, 1.1 equiv) DCC (0.24 mmol, 1.5 equiv)	DCM, DMF	0.16 (1 equiv)	-
3	EDC (0.005 mmol, 0.03 equiv) DMAP (0.32 mmol, 2 equiv)	DCM, DMF	0.16 (1 equiv)	-

Due to those negative results, we decided to invert the strategy, connecting first the linker to the 5-fluorouracil acetic acid **13** and then doing the coupling reaction with umbelliferone to avoid the generation of a free ammine on the coumarin, which can induce the breaking of the ester bound.

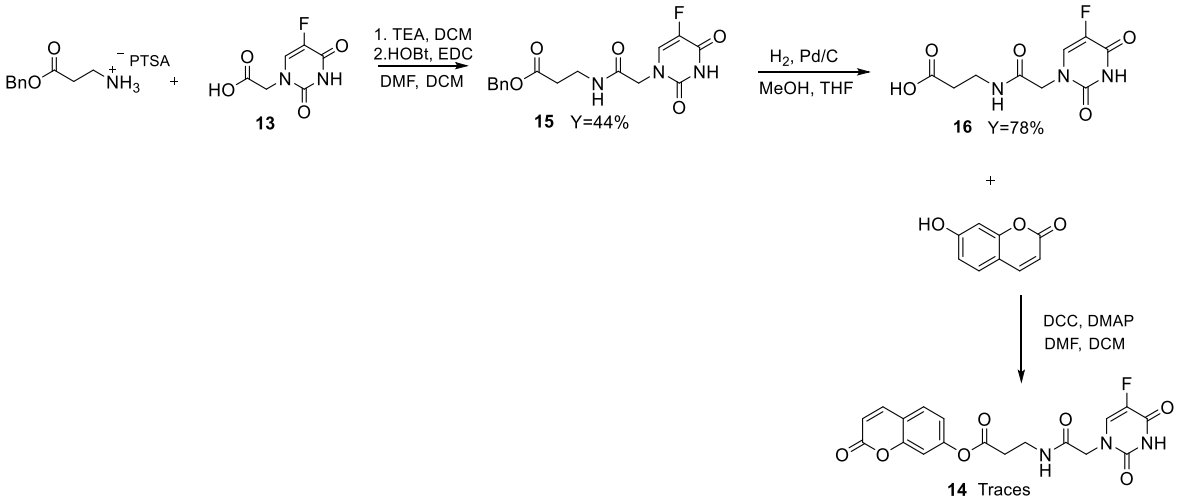

Scheme 8. Inverted strategy with β-alanine as a linker.

This time we started with a coupling reaction between the linker and the 5-fluorouracil acetic acid **13**. The β-alanine was used as *p*-toluene sulfonate salt, so the amine needed to be desalificated with TEA. Then the coupling reaction was conducted in presence of HOBt and EDC using a mixture of DCM and DMF as solvents. Finally, the removal of the benzyl protection was then obtained with the typical conditions of hydrogenolysis. A coupling reaction between umbelliferone and compound **16** was done, using DCC and DMAP as coupling agents. The solvents used were DCM and DMF and the reaction was left under stirring at room temperature for 72 hours. The crude obtained was analysed and only traces of the desired compound **14** were obtained.

Because of the problem encountered with the synthesis of compound **14** in both strategies, we thought that the problem is related to the formation of an ester-linkage. Therefore, the strategy was modified to form a carbamate between the linker and the umbelliferone using 1,3-propane diamine as a linker.

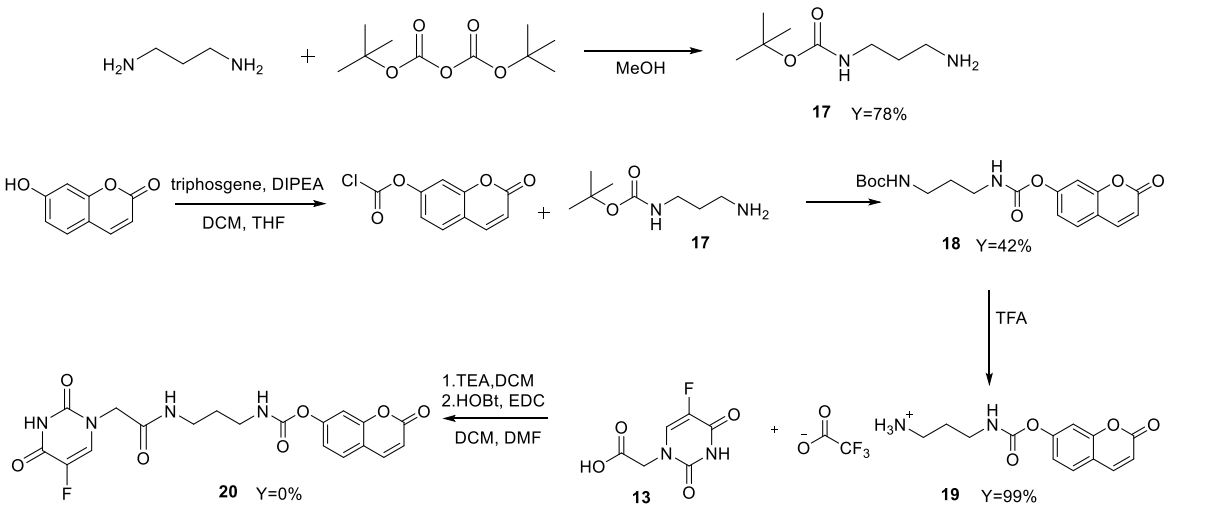

Scheme 9. Synthetic strategy with 1,3-propane diamine as a linker.

The first thing to do is the mono-protection of the diamine, carried out in methanol in defect of Boc-anhydride to disfavour the formation of the di-protected compound. Then, umbelliferone was treated with triphosgene to give a reactive acyl chloride in position 7, ready to react in situ with the free amine of compound **17**.

For the coupling reaction with the cytotoxic compound **13** is necessary the removal of Boc protection with TFA in order to repristinate the free amine. The final step was so conducted in presence of HOBt, EDC, giving as main product the free ubelliferone.
The choice of functionalising umbelliferone with the diamine linker was not successful, so even in this case we decided to try the opposite strategy.

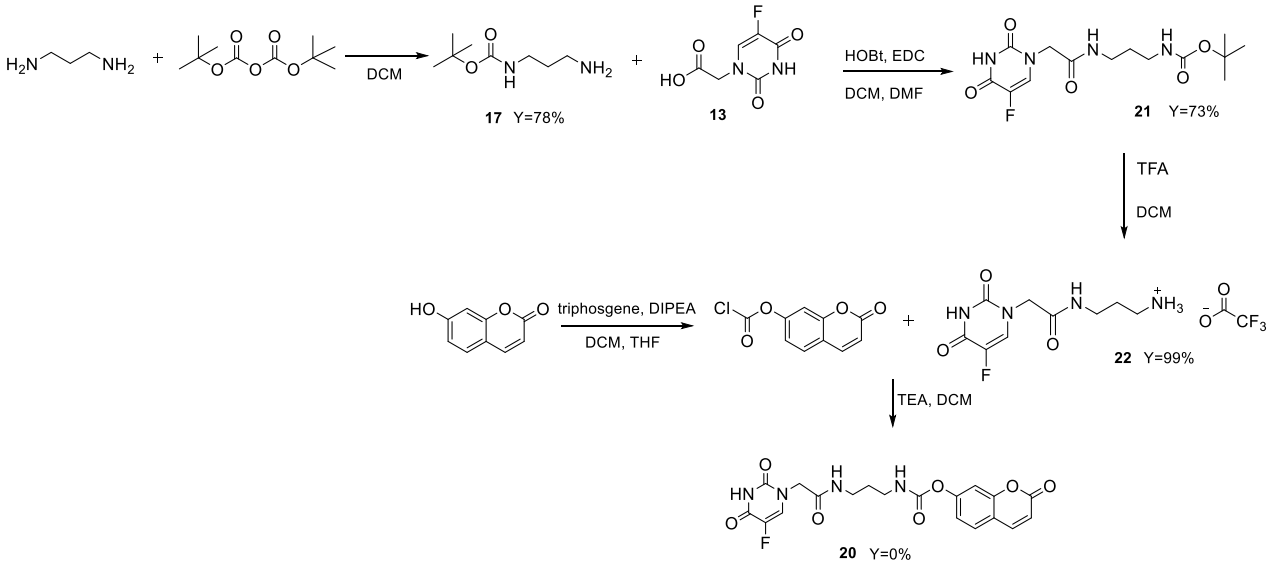

Scheme 10. Opposite strategy with 1,3-propane diamine as a linker.

To form the amide linkage between compound **13** and **17**, HOBt and EDC were chosen as coupling agents and the reaction gave compound **21** in good yield. Then, after the Boc deprotection with TFA we finally have the reaction between **22** and umbelliferone previously treated with triphosgene to give the acyl chloride. Unfortunately, even in this case, the final product was not observed in the crude mixture, and the only compound present was umbelliferone.

As last strategy we decided to change again the type of linkage between the umbelliferone and the spacer, trying an eterification reaction with N-Boc-2-Bromoethylamine hydrobromide in presence of K_2CO_3 in DMF at 60°C overnight. Compound **24** is so obtained with a yield of 34% and was treated with TFA to eliminate the Boc group. For the final coupling reaction between **13** and **26** we used as coupling reagents EDC and NHS and target compound **26** was identified in the crude as the main product by HPLC and ^{1}H NMR analysis.

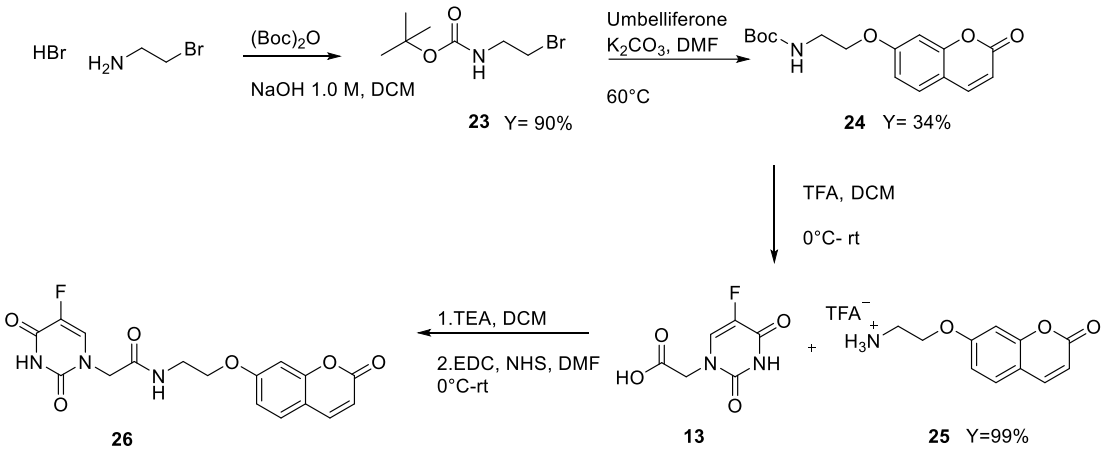

Scheme 11. Strategy with 2-Bromoethylamine as a linker.

This last strategy resulted the best one, therefore we decided to apply this one to our molecule **9**. We did a fist attempt with the same conditions seen for umbelliferone (K_2CO_3 in DMF at 60°C) but from HPLC analysis and ^{1}H NMR we observed that in the crude we did not have the desired molecule **27** but the product of decomposition **28** (*Scheme 12*).

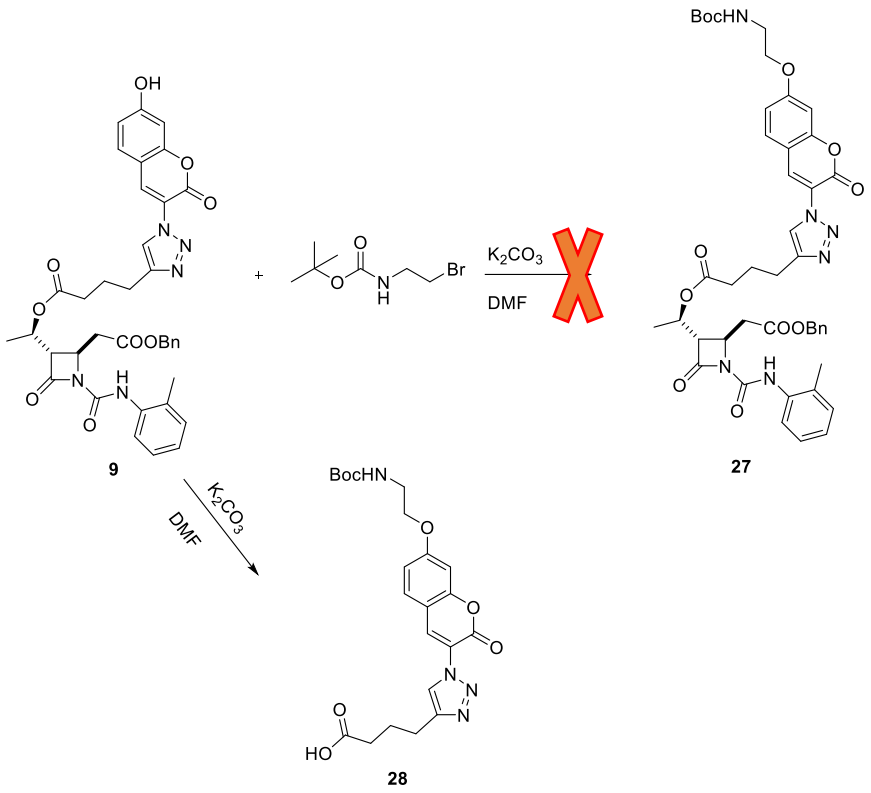

Scheme 12. Synthesis of compound **27**.

Due to this result we decided to lower the temperature of the reaction to avoid the fragmentation of the molecule and so the brake up of the ester bound. Therefore, the reaction was conducted at 0°C and then at rt overnight, but even in this case we observed the same product **28**.

Conclusions

The research group is now still trying to find a new strategy to complete the synthesis of the theranostic molecule **H**; then the two final compounds **G** and **H** will be tested in adhesion assays to evaluate their activity toward integrins and then photophysical evaluation will be also conducted in collaboration with Prof. De Cola of Instituto Mario Negri of Milan.

Experimental

Commercial reagents were used as received without additional purification. ^{1}H and ^{13}C-NMR spectra were recorded with INOVA 400 instrument with a 5 mm probe. All chemical shifts were quoted relative to deuterated solvent signals (δ in ppm and J in Hz). Polarimetric analyses were conduct-ed on Unipol L 1000 “Schmidt−Haensch” polarimeter at 598 nm. FTIR spectra: Bruker Alpha instrument, measured as films between NaCl plates, wave numbers are reported in cm^{-1}. The purity of the target compound **G** was assessed as being >95% using HPLC. HPLC-MS: Agilent Technologies HP1100 instrument, equipped with a ZOBRAX-Eclipse XDB-C8 Agilent Technologies column; mobile phase, H_2O/CH_3CN, 0.4 mL/min; gradient from 30 to 80% of CH_3CN in 8 min, 80% of CH_3CN until 25 min, coupled with an Agilent Technologies MSD1100 single-quadrupole mass spectrometer, full scan mode from m/z = 50 to 2600, in positive or negative ion mode.

Compounds **8**[106] and **13**[70] are known and were synthesized according to reported procedures, and their spectroscopic data were in accordance to those reported in literature.

*Benzyl 2-((2R,3S)-3-((R)-1-((t-butyldimethylsilyl)oxy) ethyl)-4-oxo-1-(o-tolylcarbamoyl)azetidin-2yl)acetate (**2**)*

Compound **1** (80 mg, 0.21 mmol, 1 equiv) was dissolved in anhydrous CH_2Cl_2 (2.3 mL) under a nitrogen atmosphere. Anhydrous TEA (148 μL, 1.05 mmol, 5 equiv) was added dropwise, followed by a dropwise addition of o-tolylisocyanate (130 μL, 1.05 mmol, 5 equiv). The mixture was stirred at room temperature until a complete consumption of the starting β-lactam (16 h, TLC monitoring) and then quenched with a saturated solution of NH_4Cl. The mixture was extracted with CH_2Cl_2 (3 × 10 mL), the organic layers were collected, dried over anhydrous Na_2SO_4, concentrated in vacuum and purified by flash-chromatography (Cyclohexane/EtOAc 90:10) affording the desired compound **2** as a colorless oil (100 mg, 93%). ^{1}H NMR: (400 MHz; $CDCl_3$) δ = 0.06 (s, 3H), 0.08 (s, 3H), 0.84 (s, 9H), 1.20 (d, J = 6.3 Hz, 3H), 2.27 (s, 3H), 2.93 (dd, J = 15.5, 7.7 Hz, 1H), 3.10 – 3.24 (m, 2H), 4.29 – 4.35 (m, 1H), 4.58 – 4.61 (m, 1H), 5.16 (s, 2H), 7.05 (t, J = 7.3 Hz, 1H), 7.20 (dd, J = 14.3, 7.3 Hz, 2H), 7.29 – 7.38 (m, 5H), 7.91 (d, J = 8.1 Hz, 1H), 8.41 (bs, 1H) ppm. ^{13}C NMR: (100 MHz; $CDCl_3$) δ = -4.9, -3.8, 18.0, 18.1, 22.3, 25.9, 37.3, 49.9, 62.9, 65.0, 67.1, 121.5, 124.7, 127.1, 127.9, 128.7, 128.8, 128.9, 130.7, 135.7, 135.8, 148.2, 168.6, 170.1 ppm. HPLC-MS (ESI+): Rt = 18.1 min, m/z = 511 $[M+H]^+$. IR (film): ν = 3341, 3034, 2857, 1766, 1737, 1718, 1548, 1459, 1252 cm^{-1}. $[\alpha]^D_{20}$ = - 72 (c=1, CH_2Cl_2).

Benzyl 2-((2R,3S)-3-((R)-1-hydroxyethyl)-4-oxo-1-(o-tolycarbamoyl)azetidin-2-yl)acetate (**3**)

$BF_3{\cdot}OEt_2$ (35 μL, 0.28 mmol, 1.15 equiv) was added to a solution of β-lactam **2** (124 mg, 0.24 mmol, 1 equiv) in CH_3CN (5 mL) at 0 °C under nitrogen atmosphere. After 30 minutes, the reaction was allowed to warm to room temperature and stirred until a complete consumption of the starting material (2 h, TLC monitoring). The mixture was then quenched with phosphate buffer (0.1M, pH 7.4, 10 mL) and extracted with CH_2Cl_2 (3 × 15 mL). The organic layers were collected, dried over Na_2SO_4 and concentrated in vacuum. The crude was purified by flash-chromatography (Cyclohexane/EtOAc 70:30) yielding compound **3** as a colorless oil (76 mg, 91%). ^{1}H NMR: (400 MHz; $CDCl_3$) δ = 1.37 (d, J = 6.3 Hz, 3H), 2.28 (s, 3H), 2.77 (dd, J = 17.1, 9.8 Hz, 1H), 3.12 (dd, J = 7.9, 2.6 Hz, 1H), 3.3 (bs, 1H), 3.52 (dd, J = 17.1, 3.6 Hz, 1H), 4.21 (dq, J = 12.7, 6.3 Hz, 1H), 4.38 (dt, J = 9.8, 3.2 Hz, 1H), 5.16 (d, J_{AB} = 12.2 Hz, 1H), 5.19 (d, J_{AB} = 12.2 Hz, 1H), 7.04 (t, J = 7.5 Hz, 1H), 7.15 – 7.25 (m, 2H), 7.28 – 7.41 (m, 5H), 7.93 (d, J = 7.9 Hz, 1H), 8.43 (bs, 1H) ppm. ^{13}C NMR: (100 MHz; $CDCl_3$) δ = 18.2, 21.7, 37.0, 52.5, 64.0, 66.4, 67.8, 121.4, 125.0, 127.4, 127.9, 129.0, 129.1, 129.2, 131.0, 135.5, 135.7, 148.3, 167.5, 171.7 ppm. HPLC-MS (ESI^+): Rt = 10.0 min, m/z = 397 $[M+H]^+$. IR (film): ν = 3475, 3340, 2971, 1764, 1735, 1715, 1548, 1459, 1306, 1187 cm^{-1}. $[\alpha]^D_{20}$ = - 81 (c=1, CH_2Cl_2).

*3-(5,5-difluoro-1,3,7,9-tetramethyl-5H-4λ^4,5λ^4-dipyrrolo[1,2-c:2',1'-f][1,3,2]diazaborinin-10-yl)propanoic acid (**4**)*

To a solution of 2,4-dimethyl pyrrole (120 µL, 0.6 mmol, 1 equiv) in 10 mL of DCM, under a nitrogen atmosphere, succinic anhydride (60 mg, 0.6 mmol, 1 equiv), $BF_3 \cdot Et_2O$ (500 µL, 4 mmol, 6.6 eq) and TEA (420 µL, 3 mmol, 5 equiv) were added. The mixture was refluxed for 5 hours until consumption of starting materials (TLC monitoring). The reaction was quenched with H_2O and extracted with DCM (x3) and the organic layers were collected and dried over Na_2SO_4, filtered off and concentrated to dryness under vacuum. The crude was purified by flash chromatography (From 50:50 = CicloHex:EtOAc to 0: 100 = CicloHex : EtOAc) to give compound **4** (40 mg, 20.8%) as an orange solid.
Spectroscopic data are in accordance to those reported in literature.[107]

*1-((2R,3R)-2-(2-(benzyloxy)-2-oxoethyl)-4-oxo-1-(o-tolylcarbamoyl)azetidin-3-yl)ethyl 3-(5,5-difluoro-1,3,7,9-tetramethyl-5H-4λ^4,5λ^{4}4-dipyrrolo[1,2-c:2',1'-f][1,3,2]diazaborinin-10-yl)propanoate (**5**)*

To a solution of **3** (23 mg, 0.058 mmol, 1 eqiv) in 2.5 mL of DCM, under a nitrogen atmosphere, compound **4** (29.8 mg, 0.093 mmol, 1.6 equiv) and DMAP (2.7 mg, 0.018 mmol, 0.2 equiv) were added. Subsequently, DCC (19.2 mg, 0.093 mmol, 1.6 equiv) was added at 0°C. The system was left under stirring at 0°C for ten minutes, then left overnight at retention time. After the consumption of starting materials (TLC monitoring), the white precipitate (DCU) was filtered off and the solution was concentrated to dryness under vacuum. The crude was then dissolved in EtOAc at 0°C for 15 minutes to further eliminate DCU and then another filtration was conducted, and the filtrate was dried under vacuum. After purification by flash chromatography (95: 5 = DCM: Et_2O) the product **5** (16.7 mg, 41.4 %) was obtained as an orange solid. ^{1}H NMR (400 MHz, $CDCl_3$): δ = 8.39 (s, 1H), 7.93 (d, J = 8.0 Hz, 1H), 7.42 – 7.00 (m, 8H), 6.07 (s, 2H), 5.46 – 5.34 (m, 1H), 5.16 (s, 2H), 4.44-4.49 (m, 1H), 3.44 – 3.23 (m, 4H), 2.88 (dd, J = 16.5, 8.8 Hz, 1H), 2.63 (dd, J = 15.6, 7.0 Hz, 2H), 2.54 (s, 6H), 2.44 (s, 6H), 2.30 (s, 3H), 1.42 (d, J = 5.8 Hz, 3H).^{13}C NMR (100 MHz, $CDCl_3$): δ = 171.08, 169.70, 166.33, 155.01, 147.77, 143.25, 140.65, 135.55, 135.35, 130.78, 128.89, 128.75, 128.52, 127.66 , 127.16, 124.93, 122.26 , 121.24, 67.94 , 67.16 , 60.52, 56.05 , 51.73 , 36.83 , 35.67, 23.75 , 16.60 , 14.78 .HPLC-MS (ESI$^+$): Rt= 14.0 min, m/z = 679 [M-F]$^+$. IR (film): ν=3475, 3334, 2926, 2851,1763, 1734, 1718, 1546, 1508, 1306, 1196 cm^{-1}.

*2-((2R,3R)-3-(1-((3-(5,5-difluoro-1,3,7,9-tetramethyl-5H-4λ^4,5λ^{4}4-dipyrrolo[1,2-c:2',1'-f][1,3,2]diazaborinin-10-yl)propanoyl)oxy)ethyl)-4-oxo-1-(o-tolylcarbamoyl)azetidin-2-yl)acetic acid (**G**)*

To a solution of compound **5** (16.7 mg, 0.024 mmol, 1.0 eq) in 1:1 MeOH/THF (3 mL), under a nitrogen atmosphere, 1.7 mg of Pd/C (10% w/w) were added. The reaction was left under stirring under a hydrogen atmosphere for 2 hours until consumption of starting materials (TLC monitoring). The crude was then filtered on celite and dried under vacuum. Final product **G** (10.7 mg, 73.2%) was so obtained as a red solid without any purifications. ^{1}H NMR (400 MHz, $CDCl_3$): δ = 8.39 (s, 1H), 7.89 (d, J = 8.2 Hz, 1H), 7.24 – 7.03 (m, 3H), 6.04 (s, 2H), 5.45 – 5.33

(m, 1H), 4.41 – 4.32 (m, 1H), 3.52 – 3.12 (m, 4H), 2.71 (dd, J = 16.4, 9.0 Hz, 1H), 2.64 – 2.54 (m, 2H), 2.50 (s, 6H), 2.41 (s, 6H), 2.26 (s, 3H), 1.40 (d, J = 6.3 Hz, 3H).^{13}C NMR (100 MHz, CDCl3): δ 172.66, 170.48 , 165.67 , 154.47 , 147.36 , 142.69, 134.67, 130.87, 130.22, 128.34 – 127.91 (m), 127.25, 126.58, 125.36 – 125.04 (m), 124.46, 121.73, 120.80 , 67.57, 59.99 , 51.23 , 49.32 , 36.00 , 35.04 , 23.08 , 17.30 , 16.03 , 14.18. IR (film): ν=3334, 2925, 2853, 1765, 1714, 1715, 1592, 1458, 1306,1253, 1196, 982 cm^{-1}. HPLC-MS (ESI$^+$): Rt= 4.1 min, m/z = 631 [M+Na]$^+$.

1-((2R,3S)-2-(2-(benzyloxy)-2-oxoethyl)-4-oxo-1-(o-tolylcarbamoyl) azetidin-3-yl) ethyl pent-4-ynoate (**7**)

To a solution of β-lactam **3** (72.2 mg, 0.18 mmol, 1 equiv) in 3.2 ml of DCM, compound **4** (20.6 mg, 0.18 mmol, 1equiv) and DMAP (4.39 mg, 0.036 mmol, 0.2 equiv) were added. The mixture was cooled to 0°C and DCC (55.62 mg, 0.27 mmol, 1.5 equiv) was added. The reaction was left under stirring at 0°C for 15 minutes then left under stirring overnight at room temperature. At completion (TLC monitoring), the precipitate was filtered and then the solvent was evaporated. The crude was purified by flash-chromatography (8:2= cyclohexane: ethyl acetate). The product **7** (71.7mg, 89%) was obtained as a white solid. ^{1}H NMR (400 MHz, $CDCl_3$) δ= 8.37 (s, 1H), 7.91 (d, J = 8.1 Hz, 1H), 7.36 – 7.27 (m, 4H), 7.21 – 7.12 (m, 2H), 7.03 (td, J = 7.5, 1.3 Hz, 1H), 5.32 (p, J = 6.3 Hz, 1H), 5.14 (s, 2H), 4.48 – 4.41 (m, 1H), 3.37 – 3.23 (m, 2H), 2.87 (dd, J = 16.1, 8.1 Hz, 1H), 2.43 (td, J = 7.3, 2.7 Hz, 2H), 2.29 – 2.17 (m, 5H), 1.90 – 1.75 (m, 3H), 1.34 (d, J = 6.4 Hz, 3H) ppm. ^{13}C NMR (100 MHz, $CDCl_3$) δ= 171.96, 169.43, 166.33, 147.59, 135.31, 135.22, 130.43, 128.60, 128.46, 128.40, 127.36, 126.80, 124.49, 120.88, 82.97, 69.28, 66.90, 66.84, 60.05, 51.27, 36.57, 32.87, 32.74, 30.89, 26.31, 25.49, 25.32, 24.69, 23.82, 23.48, 18.13, 17.83, 17.70, 17.60 ppm. HPLC-MS (ESI$^+$): Rt = 11.96 min, m/z = 491.6 [M+H] $^+$. IR (film): ν = 3341.00, 3295.11, 2934.91, 2856.47, 1764.27, 1731.64, 1655.95, 1614.47, 1592.80, 1458.33, 1381.99, cm^{-1}. $[\alpha]^{20}_D$ = -47.2 (c=0.96, MeOH).

Synthesis of 1-((2R,3S)-2-(2-(benzyloxy)-2-oxoethyl)-4-oxo-1-(o-tolylcarbamoyl) azetidin-3-yl) ethyl 3-(3-(7-hydroxy-2-oxo-2H-chromen-3-yl)-2,3-dihydro-1H-1,2,3-triazol-4-yl) propanoate ***(9)***

To a solution of compound **7** (116.3 mg, 0.24 mmol, 1 equiv), in 2.8 ml of EtOH, compound **8** (48.12 mg, 0.24mmol, 1 equiv) was added in 2.8 ml of H_2O. Then a solution of sodium ascorbate 1M (50 µL, 0.05 mmol, 0.2 equiv) and a solution of 7,5% $CuSO_4 \cdot 5H_2O$ (40 µL, 0.012 mmol, 0.05 equiv) were added. The reaction left under vigorous stirring overnight. At completion (TLC monitoring) the ethanol was evaporated and the acqueous layer was extracted with EtOAc (x3). The organic phase was dried with Na_2SO_4, and the solvent was removed under vacuum. The crude was purified by flash-chromatography (from 7:3= cyclohexane: ethyl acetate to 4:6= cyclohexane: ethyl acetate) to give product **9** (113.2 mg, 67%) as a colourless oil. ^{1}H NMR (400 MHz, $CDCl_3$) δ 8.34 (d, J = 7.3 Hz, 3H), 7.85 – 7.78 (m, 1H), 7.48 – 7.41 (m, 1H), 7.28 (m, 5H), 7.13 (t, J = 7.7 Hz, 2H), 7.02 – 6.88 (m, 2H), 6.92 (s, 1H), 5.34 (p, J = 6.3 Hz, 1H), 5.11 (s, 2H), 4.45 (m, 1H), 4.11 (q, J = 7.1 Hz, 1H), 3.37 (dd, J = 6.2, 2.7 Hz, 1H), 3.26 (dd, J = 16.2, 4.0 Hz, 1H), 2.89 (dd, J = 16.2, 8.1 Hz, 1H), 2.83 (t, J = 7.5 Hz, 2H), 2.51 – 2.40 (m, 1H), 2.43 – 2.33

(m, 1H), 2.11 – 1.99 (m, 3H), 1.36 (d, J = 6.4 Hz, 3H), 1.25 (t, J = 7.1 Hz, 1H) ppm. ^{13}C NMR (100 MHz, $CDCl_3$) δ 172.24, 169.51, 166.36, 161.88, 156.34, 154.68, 147.77, 146.91, 135.22, 134.94, 134.30, 130.46, 130.29, 128.58, 128.44, 128.35, 127.71, 126.76, 124.69, 122.37, 121.16, 119.54, 114.88, 110.93, 103.15, 67.11, 66.89, 60.54, 60.07, 51.41, 36.52, 33.46, 24.60, 24.29, 21.86, 21.06, 18.17, 17.56, 14.15 ppm. HPLC-MS (ESI^+): Rt = 10.0 min, m/z = 397 $[M+H]^+$. IR (film): ν = 3319.29, 3171.74, 2952.49, 2929.84, 2853.96, 1763.99, 1724.78, 1609.88, 1592.24 cm^{-1}. $[\alpha]^{20}_D$ = -28 (c=1, MeOH).

*Tert-butyl (2-bromoethyl)carbamate (**23**)*

To a solution of 2-Bromoethylamine hydrobromide (250 mg, 1.2 mmol, 1.2 equiv) in 1 mL of DCM, 0,5 mL of NaOH 1 M and $(Boc)_2O$ (200 mg, 1 mmol, 1 equiv) were added. The reaction was left under stirring overnight. At completion (TLC monitoring), the reaction was quenched with HCl 2 N and extracted (x3) with DCM. The organic layers collected were dried with Na_2SO_4, and the solvent was removed under vacuum. Compound **23** (200 mg, 90%) was so obtained without any purification.
Spectroscopic data are in accordance to those reported in literature.[108]

*Tert-butyl (2-((2-oxo-2H-chromen-7-yl)oxy)ethyl)carbamate (**24**)*

Compound **23** (200 mg, 0.29 mmol, 1.0 equiv) was treated with 7-hydroxy-2*H*-chromen-2-one (300 mg, 0.29 mmol, 1.0 equiv) and K_2CO_3 (350 mg, 0.87 mmol, 3.0 equiv) in in the same conditions using dry DMF (1.5 mL) as solvent and under N_2 atmosphere. The reaction mixtures were stirred at 60 °C overnight until the starting materials had been consumed (TLC monitoring), then cooled to room temperature and treated as follows.The reaction was quenched with a 2.0 M aqueous hydrochloric acid solution to give a precipitate which was collected by filtration and triturated with diethyl ether to afford **24** (30 mg, 34 %) as an orange solid.
Spectroscopic data are in accordance to those reported in literature.[109,110]

*2-((2-oxo-2H-chromen-7-yl)oxy)ethan-1-aminium trifluoroacetate (**25**)*

Compound **24** (30 mg, 0.098 mmol, 1.0 equiv) were dissolved in CH_2Cl_2, and TFA (30 µL, 0.59 mmol, 6.0 equiv) was added dropwise to the suspension. The solution was stirred at 0 °C and then at room temperature until starting materials were consumed (TLC monitoring). The solvent was evaporated and the obtained residue dried under vacuo to afford the title compound **25** (30 mg, 99%) as a yellow solid.
Spectroscopic data are in accordance to those reported in literature. [109,110]

*2-(5-fluoro-2,4-dioxo-3,4-dihydropyrimidin-1(2H)-yl)-N-(2-((2-oxo-2H-chromen-7-yl)oxy)ethyl)acetamide (**26**)*

To a solution of **13** (25 mg, 0.13 mmol, 1 equiv) in DMF (0.5 mL) under a nitrogen atmosphere, EDC Cl (38 mg, 0.20 mmol, 1.5 equiv) and NHS (23 mg, 0.20 mmol, 1.5 equiv) in DMF (1 mL) were added dropwise. The reaction was left under stirring overnight. The solution was then added under a nitrogen atmosphere to a mixture of **25** (30 mg, 0.098 mmol, 1.5 equiv) and TEA

(40 µL, 0.3 mmol, 3 equiv) in DMF (0.5 mL). The reaction was left under stirring overnight and then quenched with water and extracted (x3) with EtOAc. The organic layers collected were dried with Na_2SO_4, and the solvent was removed under vacuum. From ^1H NMR of the crude we can see the formation of the desired compound **26**.

1.1.5 Strontium substituted hydroxyapatite with β-lactam integrin agonists to enhance mesenchymal cells adhesion and to promote bone regeneration

A biomaterial is defined as a substance or a combination of substances able to treat or replace any tissue, organ or body function and their biomedical need is growing up continuously.
Particularly interesting is the biological characterization of the new materials in order to verify, beyond the chemico-physical and mechanical properties, their applications in the biomedical field.
Moreover, an ideal biomaterial should have:

- excellent chemical stability
- biocompatibility and biodegradability
- absence of toxic/carcinogenic elements
- the possibility of being repeatedly sterilized without degradation.

Most biomaterials employed to solve problems related to disorders of the muscolo-skeletal system are based on calcium orthophosphates (CaPs), and in particular on hydroxyapatite (HA), which is the most similar to bone inorganic phase. Recently, the interest toward this class of compounds has stimulated a number of studies which aim is enhance their already good biological performances through functionalization with specific additives, including ions, polyelectrolytes and drugs.[111,112] According to the literature,[113] the highest number of studies on HA functionalization with inorganic ions has been performed on Strontium. The trend of interest toward this ion has been continuously increasing because of its influence on bone cells. Sr ion is known to counteract abnormal bone resorption by promoting osteoblast proliferation and differentiation and inhibiting osteoclast activity,[114,115] being effective also when incorporated into HA.[116–121] Further specific activities towards bone cells can be achieved through multi-functionalization of the calcium phosphate.[111,122,123] To improve tissue/bone regeneration, it is important to improve efficacy of cell adhesion and differentiation, and in this aspect, integrins could represent an important cellular target.[124] In osteoclasts, for instance, integrin $\alpha_v\beta_3$ is essential for the attachment to matrix proteins of bone and for cell spreading necessary for the bone-resorbing activity.[125] Other integrins might also be involved in osteoclast attachment and function, such as the $\alpha_v\beta_5$ and those with β_1 and β_2 chains. In addition, also osteoblasts express some integrins able to control their differentiation and fate.[126] One is integrin $\alpha_5\beta_1$, which upon interaction with fibronectin activates pre-osteoblasts to adhere to the extracellular matrix (ECM) and to differentiate into mature osteoblasts.[127] On the contrary, signalling disruption by β_1 integrins results in skeletal defects, and impairment of this signalling in mature osteoblasts decreases osteoblast activity, bone formation and bone mass in growing mice.[127,128] Interestingly, the individual components of $\alpha_5\beta_1$ integrin heterodimer are upregulated in osteoblasts by several anabolic factors, including oestrogens,[129] with an implication in the osteoblastogenesis.[130] Biomaterials for bone regeneration should exhibit high cell adhesion to retain effectively anchorage-dependent osteo-progenitors, such as human bone marrow-derived mesenchymal stem cells (MSCs). Furthermore, it has been demonstrated that an adequate number of osteo-progenitors is a requisite for an efficient bone repair.[131] MSCs express high levels of several integrin classes,[132–134] in particular, integrin α_5 is required for MSC osteogenic differentiation,[135]

and overexpression of integrin α_4 has been reported to increase the bone-homing of MSCs.[136] Thus, a therapy for bone regeneration could be directed toward integrin receptors on MSCs with a better adhesion to the bone surface.[137] As an alternative to those proteins that are natural ligands of integrins, some cell adhesion peptides containing specific amino acid sequences, such as the RGD tripeptide, were used to functionalize biomaterials for improving tissue integration of artificial implants.[138] In particular, RGD-containing peptides have been shown to augment osteoblasts adhesion to coated surface.[139] The hexapeptide GRGDSP (Gly–Arg–Gly–Asp–Ser–Pro) is another example that demonstrated adhesion activity both in vitro and in vivo in various osteoblastic cells.[140] However, the use of a RGD motif has two main issues: i) mimetic peptides may act as partial agonists as well as competitive antagonists of integrins, displaying, in vivo, interactions or competition with endogenous processes;[140] ii) the RGD motif can bind to multiple integrin classes, so that the specificity and selectivity of cell activation could be highly limited.[141] To avoid this problem, in this work, we decided to load two β-lactam integrin agonists from our library[43], onto Strontium substituted hydroxyapatite (SrHA) in order to get innovative materials able to couple the promotion of cell adhesion and activation of intracellular signalling by β-lactam integrin agonists with the beneficial influence of Strontium ion on osteointegration and bone regeneration.[142]

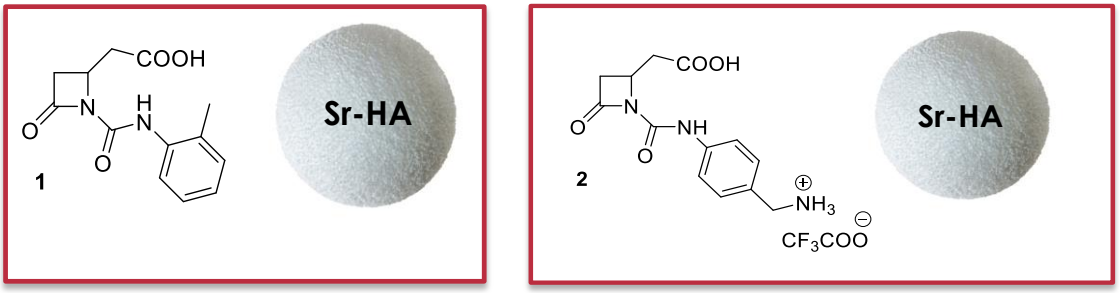

Figure 26. B-lactam-based integrin agonists **1** and **2** loaded onto SrHA.

Results and discussion

Compounds **1** and **2** were selected, among the series of integrin ligands previously synthesized by the research group[43], for this study on the basis of their integrin specificity, agonism, and lipophilicity/hydrophilicity character. According to this aspect, the *N*-substituent on the lactam ring confers a specific behaviour: compound **1** with the *o*-tolylurea is quite lipophilic as indicated by its ClogP, whereas **2** with a *p*-aminobenzyl moiety is more hydrophilic (*Figure 27*).

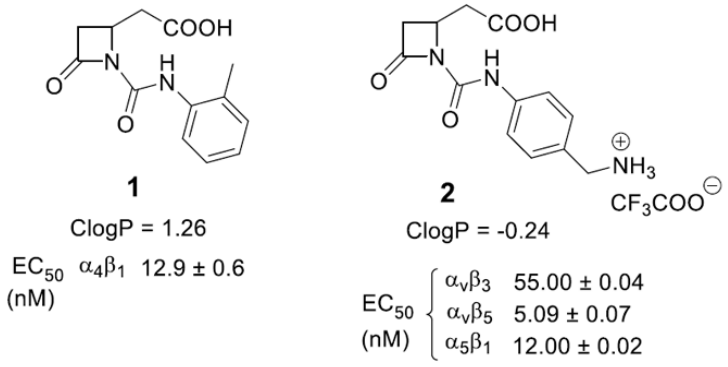

Figure 27. Compounds **1** and **2** evaluated in this study. The agonist activity of the two β-lactams is reported as EC_{50} values obtained in cell adhesion test mediated by integrins. Calculated logP (CLogP) values were obtained with ChemDraw 15.0 program.[142]

The synthesized SrHA was characterized by the powder X-ray diffraction pattern (*Figure 28*) that showed the characteristic peaks of hydroxyapatite shifted towards smaller angles, in agreement with greater lattice parameters. Indeed, the values of the calculated lattice parameters (a = 9.453 (3) Å, c = 6.903(4) Å) indicated an enlargement of the unit cell in comparison to that characteristic of pure HA coherently with a partial substitution of Sr ion to Ca ion into the hydroxyapatite structure. Moreover, SrHA nanocrystals, which contain about 7.5±0.2 at % of Strontium, displayed a plate-like shape with mean dimensions of about 150 nm x 30 nm.[142]

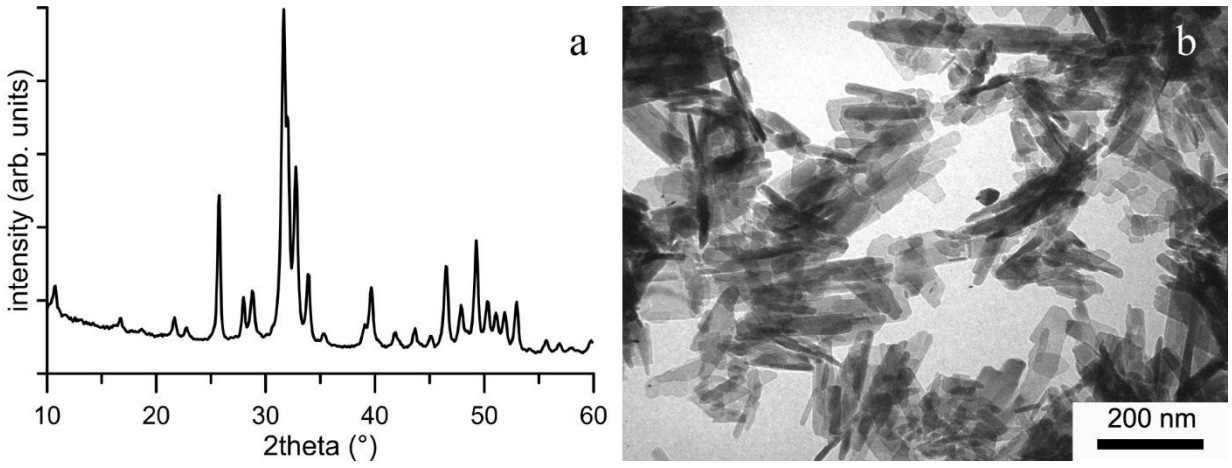

Figure 28. X-ray diffraction pattern (a) and TEM image (b) of SrHA nanocrystals. [142]

Azetidinone loading on SrHA

Azetidinones **1** and **2** were loaded on SrHA as follows: the azetidinone (10 mg) was diluted in a 10 mL flask in the appropriate H_2O/MeCN mixture (0.6 mL) (see *Table 3*), then SrHA nanoparticles (60 mg) were added at room temperature (or 70 °C, see *Table 3*). After selected time (*Table 3*) the mixture was centrifuged for 5 mins at 1200 rpm. Then, the solid phase was dried at 48 °C for 48 h, and maintained in desiccator ($CaCl_2$) for 24 h before the analyses.

Determination of the quantity of the β-lactams loaded on SrHA was assessed by thermogravimetric analysis (TGA) on the dried samples and data were reported in *Table 3*.
The samples are indicated as SrHA**Y**-X, where **Y** indicate the two different azetidinones (**1** and **2**) and X their amount expressed as w%.[142]

Table 3. Effects of medium on loading of azetidinones **1** and **2** on SrHA.[a]

Entry	Compound (mg)	Solvent (0.6 mL)	Polarity index (PI)[b]	Loading (w%)[c]
1	**1** (10)	CH_3CN	5.8	9.0
2	**1** (10)	H_2O/CH_3CN 1:3	6.9	5.3
3	**1** (10)	H_2O/ CH_3CN 1:1	8	9.6
4	**1** (20)	H_2O/ CH_3CN 1:1	8	24.0
5	**1** (6)	H_2O/ CH_3CN 1:1	8	6.2
6	**1** (3)	H_2O/ CH_3CN 1:1	8	3.5
7	**1** (10)	H_2O/ CH_3CN 3:1	9.1	12.9
8	**1** (10)	H_2O/ CH_3CN 10:1	9.8	14.4
9	**2** (10)	H_2O/ CH_3CN 1:5	6.5	8.4
10[d]	**2** (10)	H_2O/ CH_3CN 1:5	6.5	4.4
11	**2** (30)	H_2O/ CH_3CN 1:5	6.5	8.1
12	**2** (10)	H_2O/ CH_3CN 1:1	8	4.5
13[e]	**2** (5)	H_2O/ CH_3CN 2:1	8.7	3.2
14[e]	**2** (10)	H_2O	10.2	4.2

[a] Loading conditions: compound, SrHA (60 mg), solvent (0.6 mL), time (4 h), room temperature.
[b] PI of mixtures was calculated from the Snyder polarity indexes of H_2O and acetonitrile. [ref. 37]
[c] The loaded amount of compounds was evaluated by TGA analysis.
[d] Loading at 70 °C.
[e] Loading overnight.

The loading of β-lactams **1** and **2** on SrHA nanocrystals was screened in H_2O or H_2O/acetonitrile mixtures to evaluate the medium effect on the loading. Acetonitrile was chosen as co-solvent upon the good results obtained in a previous study with antibacterial *N*-methylthio-β-lactams loaded on hydroxyapatite nanocrystals.[143] The influence of the compound concentration and on the polar character of the loading solution[144] was also explored (*Table 3*).
The amount (w%) of azetidinones loaded on SrHA was evaluated through TGA analysis on dried samples. When the loading was carried out in acetonitrile, a good uptake from the solution was observed (9 w%, *Table 3*, entry 1), the loading in water alone, instead, was hindered by the insolubility of **1**. The polarity of the medium polarity was varied through variation of the composition of the H_2O/acetonitrile mixtures at constant concentration (0.063 M). Data in *Table 3* showed that the loading amount of compound **1** increased as the polarity raised (*Table 3*, entries 2, 3, 7 and 8), from 5.3 w% in H_2O/CH_3CN=1:3 (PI = 6.9) to 14.4 w% in H_2O/CH_3CN=10:1 (PI = 9.8). This could be rationalized considering that the molecule **1** is quite apolar (ClogP = 1.26) with high affinity to acetonitrile, so that the adsorption of compound **1** on SrHA was more favoured from a water enriched solution. Compound **1** is hydrophobic and its solvation in acetonitrile is destabilized by an increase of water amount in the loading solution,

which promotes its adsorption on SrHA.[145] Moreover, in H_2O/CH_3CN 1:1 mixture the loaded w% of **1** is proportional to the β-lactam concentration, resulting higher on increasing the amount of the compound in the starting solution (*Table 3*, entries 3-6). In particular, charging 20 mg of **1** per 0.6 mL of the 1:1 solvent mixture gave the highest loading amount, 24 w% (*Table 3*, entry 4).

Conversely, SrHA**2** composites settled around a medium-low loading (3.2-8.4%) that decreased on increasing the solvent polarity (*Table 3*, entries 9, 12, and 13). To notice, the lowest value of loaded azetidinone (3.2 w% *Table 3*, entry 13) arose from a half content of β-lactam **2** in an enriched water solution, balanced by a prolonged loading time (overnight). Compound **2** is more polar and hydrophilic (CLogP = -0.24) than **1**, and hence it tends to be better distributed in solutions at higher water content than to be adsorbed on SrHA. Neither tripling concentration (*Table 3*, entry 11), nor increasing of the loading temperature (70 °C, *Table 3*, entry 10) enhanced loading. The absorption in H_2O alone gave a loading of 4.2% (*Table 3*, entry 14), even if conducted overnight, whereas the experiment in acetonitrile alone was not feasible due to the insolubility of **2** in this solvent.

As a general comment on the loading, the two β-lactam compounds **1** and **2** were adsorbed on SrHA as a function of their partition between the solid phase and the loading solution: SrHA in fact competes with the solvent for the recruitment of azetidinones, which in turn depends on the polarity of the compound and of the loading solution.[142]

Characterization of SrHA composites with the β-lactams

The new azetidinone-functionalized SrHA composites were characterized by ATR-FTIR spectroscopy that shed light on the interactions between β-lactams **1**-**2** and hydroxyapatite. Infrared spectra of SrHA**1**-12.9 in comparison with compound **1** alone, and SrHA**2**-8.4 in comparison with compound **2** alone are reported in *Figure 29*. IR spectra of SrHA composites display the O-H stretching and bending modes of hydroxyapatite at 3572 and 630 cm^{-1} respectively, the strong bands due to phosphate absorption at 550-630 and 900-1100 cm^{-1}, together with the bands of the β-lactam compounds. *Figure 29* reports a selected range of ATR-FTIR spectra (2000-400 cm^{-1}) for a better comparison between the SrHA composites and the compounds alone. Compound **1** showed three C=O stretching bands at 1761 (β-lactam), 1715 (COOH), and 1695 cm^{-1} (urea). In the composite SrHA**1** the band corresponding to the C=O stretching of the COOH was no longer observed, as well as the band at 1309 cm^{-1} relative to the CO stretching of the carboxylic acid dimer. Conversely, two new intense bands appeared in the composite: one at 1570 cm^{-1} (near the ureidic amide band II at 1551 cm^{-1}), and another at 1440 cm^{-1} that could be both attributed to the asymmetric and symmetric stretching of a carboxylate anion, respectively. This analysis supported the hypothesis that β-lactam **1** could have been absorbed onto the SrHA as a carboxylate anion through ionic interactions with Sr^{2+} or Ca^{2+}. Moreover, since we detected a gap between the two bands of the carboxylate anion minor than 200 cm^{-1}, in our case $\Delta\nu = 130$, it could be formulated a hypothesis of a monodentate coordination of the carboxylate on the apatite.[146] In compound **2** the three C=O bands were observed at 1773 (β-lactam), 1703 (COOH), and 1658 cm^{-1} (urea), respectively, whereas in the composite SrHA**2** only the C=O of the urea slightly moves to 1680 cm^{-1}. This could account for a less tendency of **2** to form a carboxylate anion upon the adsorption on SrHA if compared to compound **1**, maybe because **2** could establish interactions between the ammonium cation

residue and the negatively charged phosphate groups on SrHA surface. The consistency of the β-lactam C=O stretching in pure compounds with those in Sr-HA composites provides strong evidence of the integrity of β-lactam compounds upon adsorption on Sr-HA.[142]

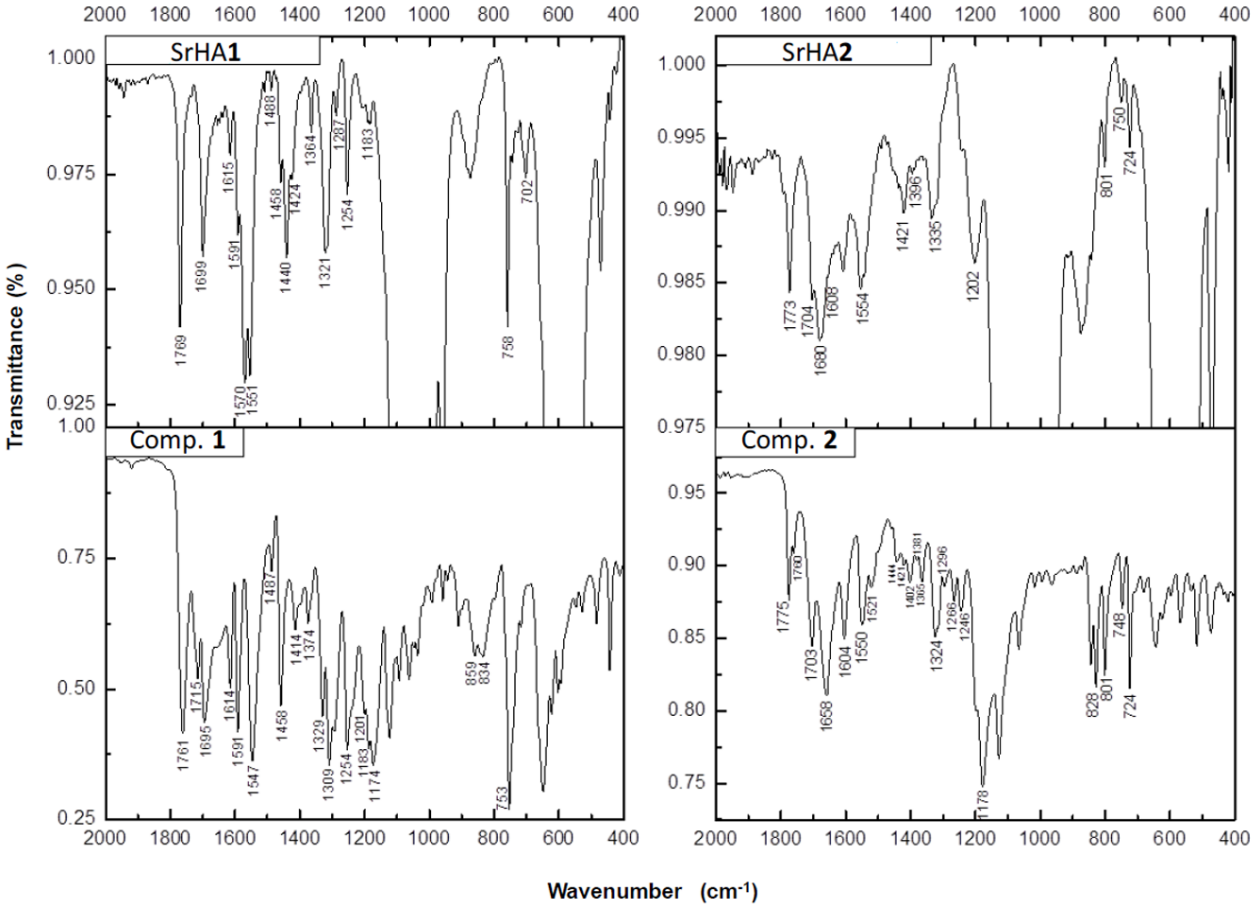

Figure 29. ATR-FTIR spectra in the selected range 2000-400 cm^{-1}: SrHA**1**-12.9 comparison with compound **1** alone, and SrHA**2**-8.4 in comparison with compound **2** alone.[142]

*Release studies from SrHA**1** and SrHA**2** composites*

The in vitro release of β-lactams **1** and **2** from the SrHA composites at different w% loading was determined through HPLC-UV analysis on supernatant solutions after each refresh (*Figure 30*). Two aqueous solutions were analysed: a saline solution and a phosphate buffered solution at pH = 7.4 as models for physiological conditions. At first, it was observed that a new release occurred just after refreshing the aqueous solution, thus the release was determined as cumulative amount over the refresh number.

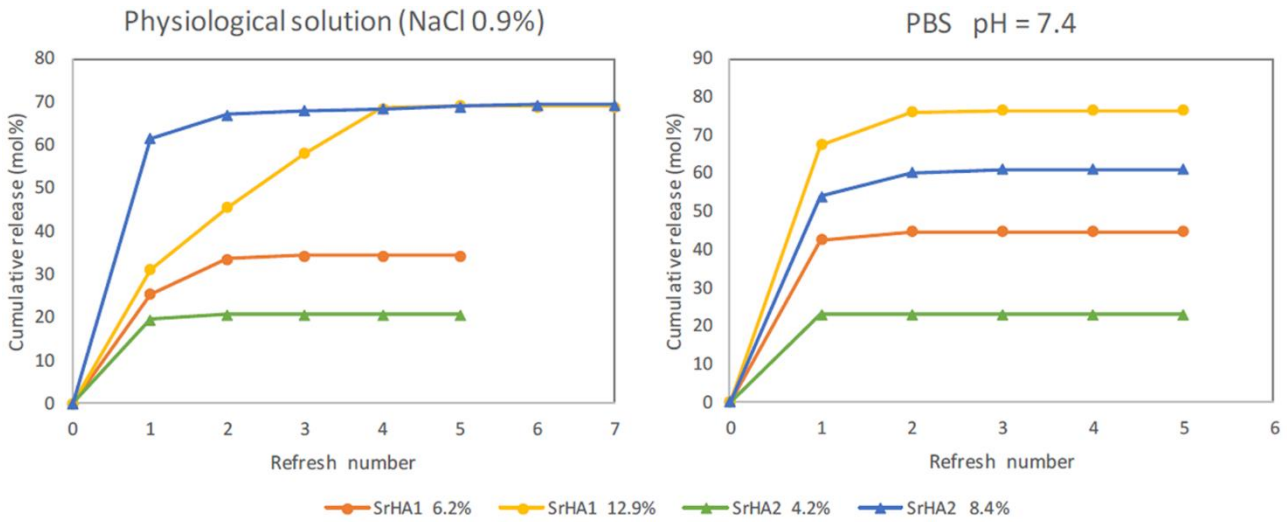

Figure 30. Release of β -lactams compound 1 (●) from SrHA1 and compound 2 (▲) from SrHA2 samples. The different w% loading of the composites are in the legend. The cumulative release is reported as mol% respect to the loaded amount.[142]

The release of both compounds in the aqueous media showed an initial burst followed by a steady concentration-dependent profile. Higher concentrations in the SrHA-β-lactam composite released higher amounts of compounds, except for SrHA**1**-12.9 that has a cumulative release similar to SrHA**2**-8.4 in physiological solution. A further peculiarity of SrHA**1**-12.9 in saline solution regards its more gradual release over time than the other composites; a steady concentration-dependent profile is indeed gained at the fourth refresh, compared to the second in the other SrHA-β-lactams. Generally, for compound **1** the saline solution allowed slightly slower release from SrHA**1** compared to the phosphate buffer. For compound **2** instead, the release rates are comparable in both aqueous solutions. Noteworthy, compounds **1** and **2** were not completely released from the composites even for the lowest loaded concentrations, thus significant amounts of the β-lactams remained adsorbed on SrHA allowing a persistent bioactivity over time (*Figure 31*).

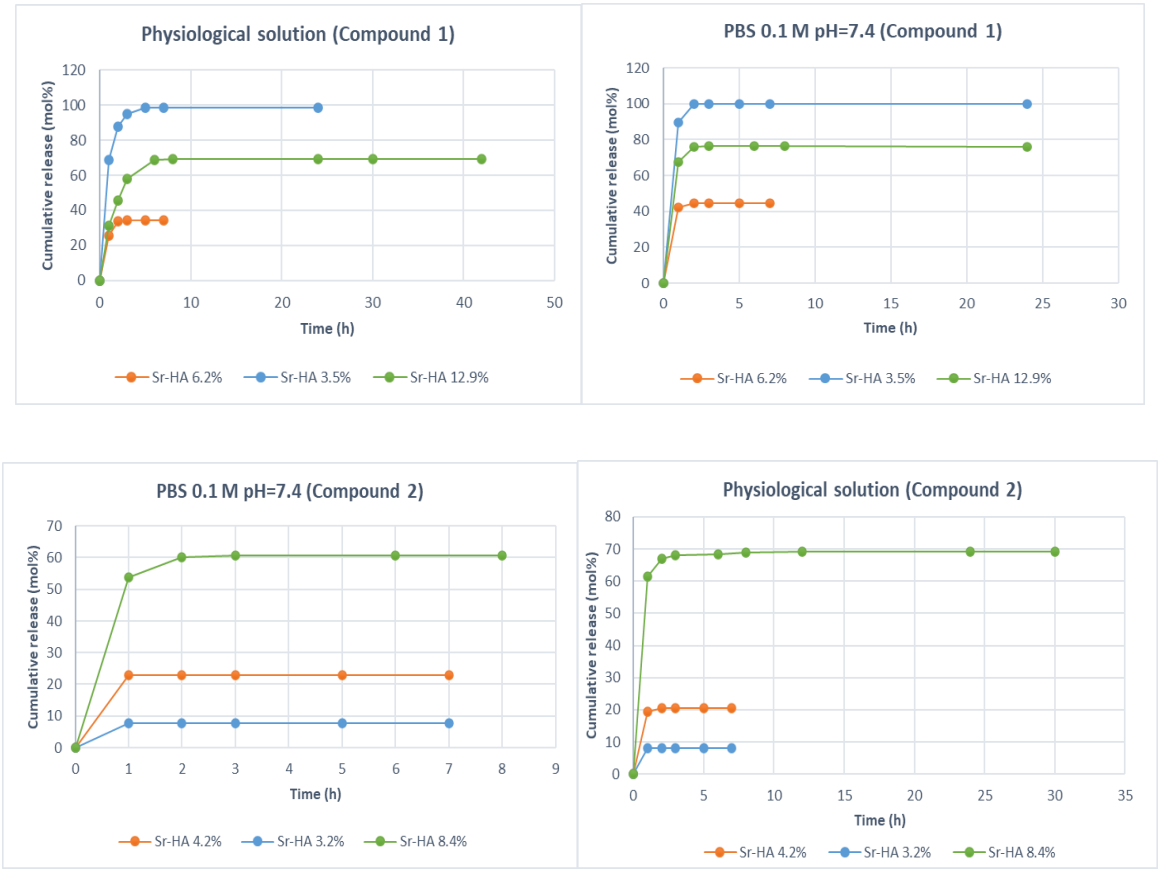

Figure 31. Time-dependent release of compound **1** from SrHA**1** composites and compound **2** from SrHA**2** composites.[142]

Structural, morphological and chemical investigations of the samples after β-lactams release indicate no significant modifications. After release, the crystals appear just a bit fractured in comparison with pristine powders, as shown in the TEM images of two typical samples reported in *Figure 32*. In agreement, the diffraction peaks present in the X-ray patterns of the same samples (*Figure 32*) appear just slightly broader than those reported in *Figure 28*. Furthermore, the results of chemical analysis showed no significant variation of Strontium content.[142]

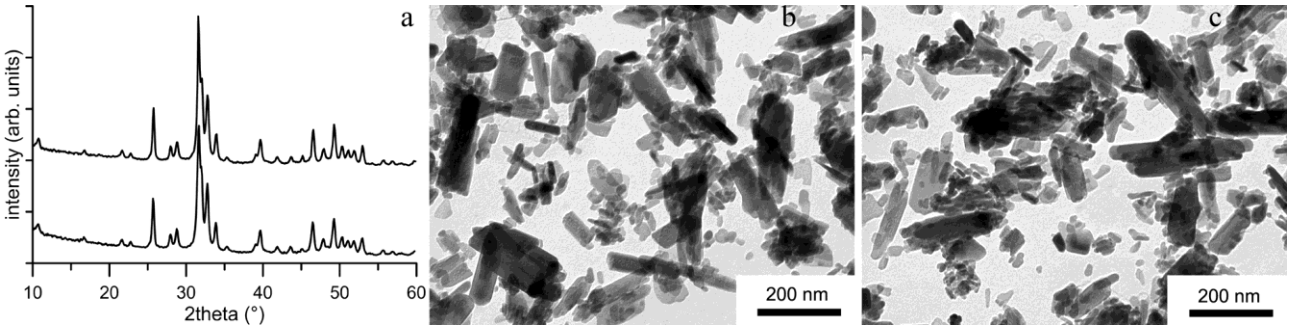

Figure 32. XRD and TEM images of typical samples after β-lactams release. (a) XRD patterns of SrHA**1**-3.5 (bottom) and SrHA**2**-3.2 (top); (b) TEM images of SrHA**1**-3.5; (c) SrHA**2**-3.2.[142]

In vitro tests

Some selected samples of SrHA functionalized with different contents of β-lactam integrin agonists were submitted to *in vitro* cell tests. Low content samples in β-lactams were selected to avoid interfering toxicity effects, and a co-culture model of human primary mesenchymal stem cells (hMSC) and human primary osteoclasts (OC) were chosen in order to investigate the influence of the functionalized materials on hMSC adhesion, viability and differentiation, as well as on OC viability and activity.[142]

Osteoblast and osteoclast viability

hMSC proliferated regularly in control wells as well as in those with the functionalized materials. Considering CTR-hMSC as 100% of viability, samples reached higher values of viability when co-cultured on SrHA, SrHA**1**-3.5 and SrHA**2**-3.2 at both 7 and 14 days, and on SrHA**1**-6.2 and SrHA**2**-4.2 at 14 days (*Figure 33a*). Moreover, hMSC viability was significantly higher on SrHA**1**-3.5 than on SrHA (7 and 14 days). The data showed that in comparison with CTR-hMSC, cells grown onto the new biomaterials demonstrated a significant enhancement of proliferation. In particular, it was observed a greater hMSC viability on those functionalized SrHA materials with a lower content of β-lactams.[142]

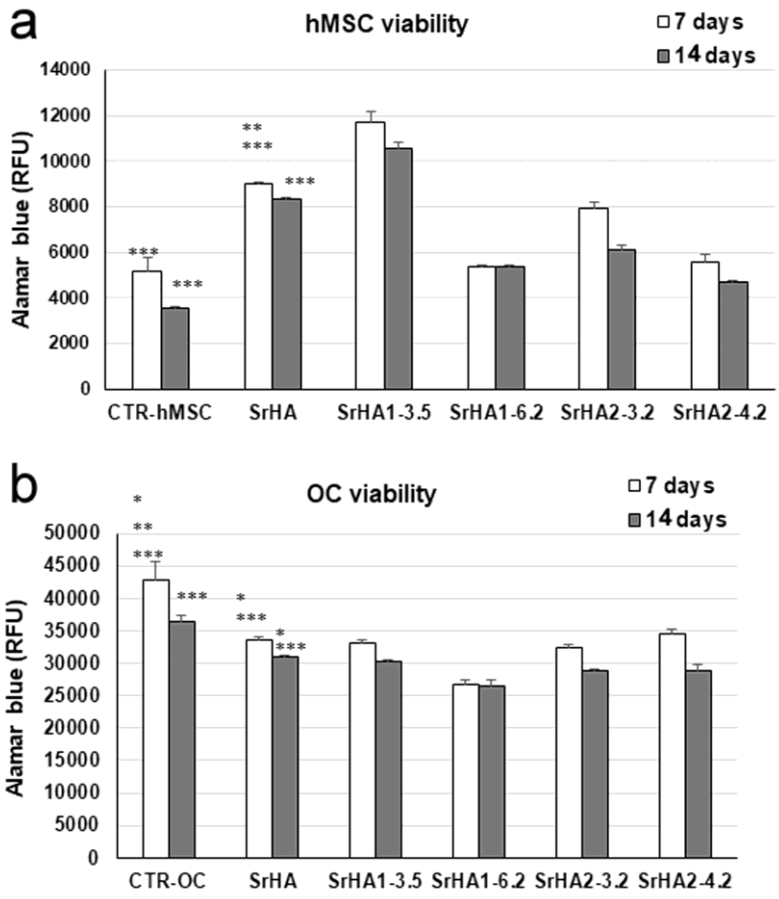

Figure 33. Viability of hMSC (**a**) and OC (**b**) after 7 (light bars) and 14 (dark bars) days of co-culture with biomaterials and controls (cells only) by Alamar blue test.[142]

Moreover, cell adhesion was evaluated by DAPI: onto all biomaterials, cells nuclei (DAPI staining) appeared well defined and covered the surface, suggesting that cells colonized all samples (*Figure 34*).

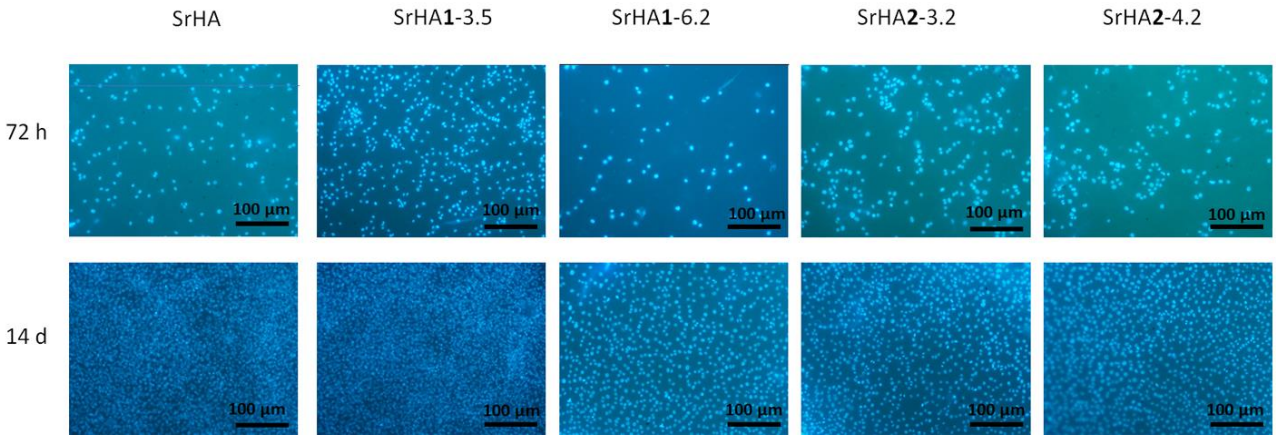

Figure 34. Cell adhesion onto SrHA and functionalized samples by DAPI staining. Fluorescent nuclei of cell adhering to samples surface can be appreciated. Bars =100 µm. [142]

Results were in line with viability data obtained by Alamar Blue test and demonstrated that all samples promote cell adhesion and proliferation. In agreement, SEM images show that cells are rich of filopodia and well attached and spread on samples SrHA**1**-3.5 and SrHA**2**-3.2 (*Figure 35*).

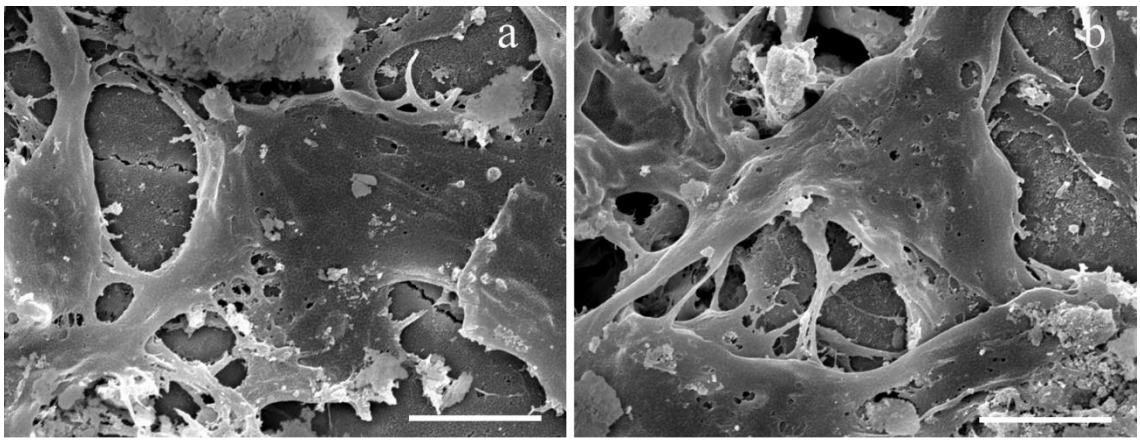

Figure 35. SEM images of hMSC cell grown on (a) SrHA**1**-3.5 and (b) SrHA**2**-3.2. Scale bars = 10 µm.[142]

All samples, as expected, exhibited lower viability of OC than CTR-OC, both at 7 and at 14 days of culture (*Figure 33b*). The values recorded for SrHA**1**-6.2, SrHA**2**-3.2 (7 and 14 days), and SrHA**2**-4.2 (14 days) were also lower than that of SrHA. These data not only confirm the inhibiting effect of Sr on osteoclasts viability,[117-118] but also indicate that this effect is enhanced by the presence of the functionalizing molecules.[142]

Osteoclast differentiation

Osteoclast of CTR group were stained with Phalloidin / DAPI after 3 weeks of culture. Images in *Figure 36a* show the formation of large multinucleated cells (fluorescent green, nuclei blue). After further 7 days, TRAP (Tartrate-resistant acid phosphatase) staining (*Figure 36b*) confirmed that the isolated mononucleated cells have fused forming polynucleated purple TRAP positive cells, characteristics of differentiated osteoclasts. At the end of experimental time, also co-cultured cells of different groups, with or without biomaterials, were stained with TRAP. Results are shown in *Figure 36c*. When compared to CTR group, considered as 100%, all other groups (reference SrHA and different β-lactam-composite groups) showed significantly lower percentage of TRAP positive cells, as a direct effect of Sr presence in the samples.[142]

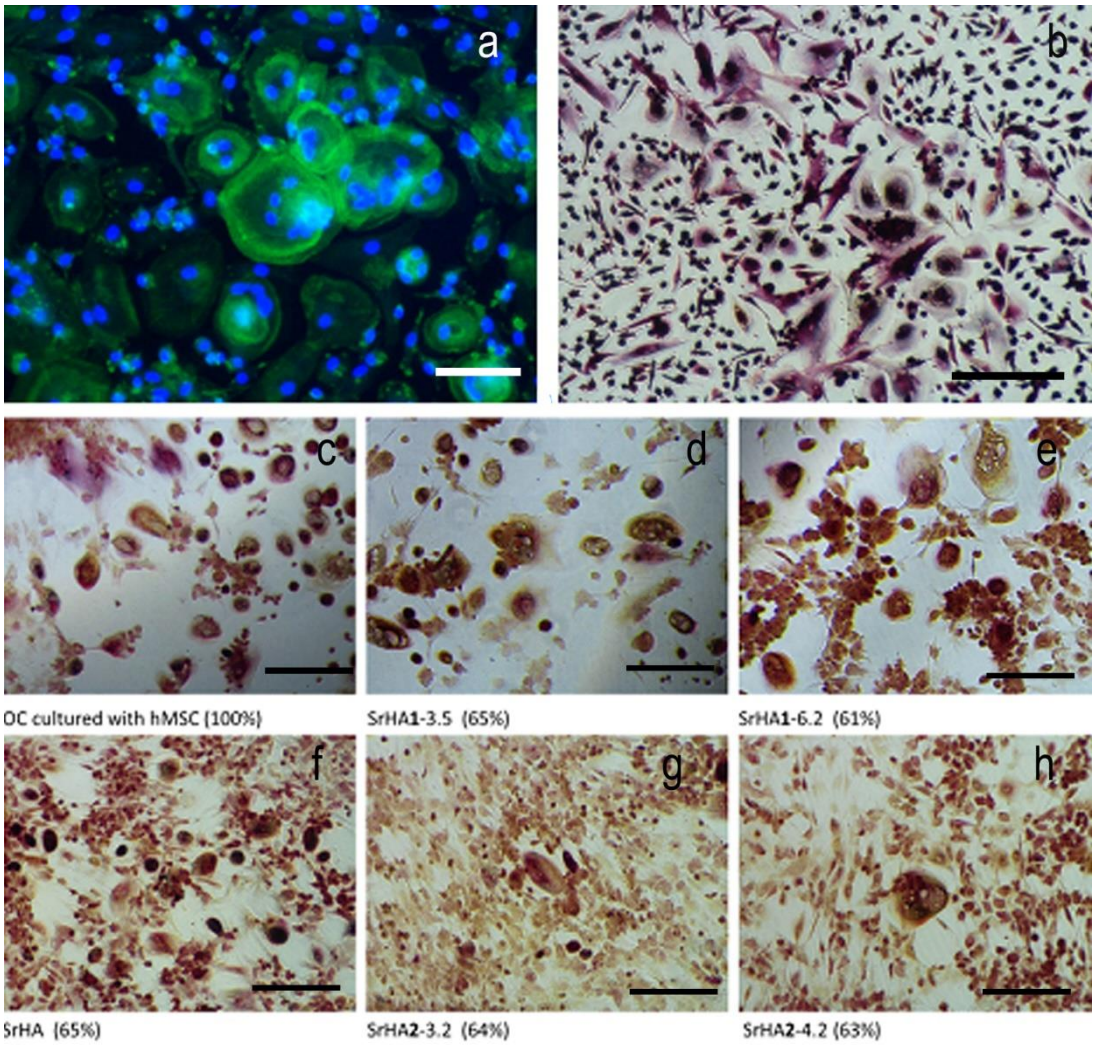

Figure 36. Osteoclast control group differentiation. (a) Phalloidin/DAPI staining after 3 weeks of culture; (b) TRAP staining after 4 weeks. Both images show big multinucleated cells that can be recognized as osteoclasts, differentiated from the originally isolated mononucleated blood cells. (c-h) TRAP staining (10x) of OC co-cultured with hMSC without (c) and with (d-h) materials at the end of experimental time (14 days of co-culture). The percentage of differentiated cells is reported in the figure. It was calculated as the number of cells with more than 3 nuclei, in respect of culture without materials, considered as 100%. Bars = 100 μm.[142]

qPCR

The most common genes for osteoclast and osteoblast differentiation and activity were analyzed to assess the effects of biomaterials on co-cultured cells behavior. All results were normalized to *GAPDH* expression and data are given as fold change relative to the reference group (SrHA), considered as 1.

The effect on osteoclast differentiation of mononucleated cells was studied comparing Cathepsin K (CTSK) and Acid phosphatase 5 (ACP5) gene expression in CTR-OC, SrHA and β-lactam-composite groups. CTSK is highly expressed in osteoclast and contribute to bone resorption with degradation of type I collagen.[147] ACP5 that encodes for TRAP, under the stimulation of RANKL affects different pathways related to bone resorption and osteoclast activity.[148] Both CTSK and ACP5 were highly expressed in CTR-OC, whereas they were significantly reduced in SrHA already at 7 days, with no changes at 14 days, confirming the inhibiting effect of Strontium on osteoclast differentiation (*Figure 37*). The levels of activation of the two genes were also significantly lower on β-lactam functionalized samples than on CTR-OC; moreover, the values of CTSK in SrHA**1**-3.5 and SrHA**2**-4.2, and of ACP5 in SrHA**1**-3.5 and SrHA**2**-3.2, were even significantly lower than on SrHA.[142]

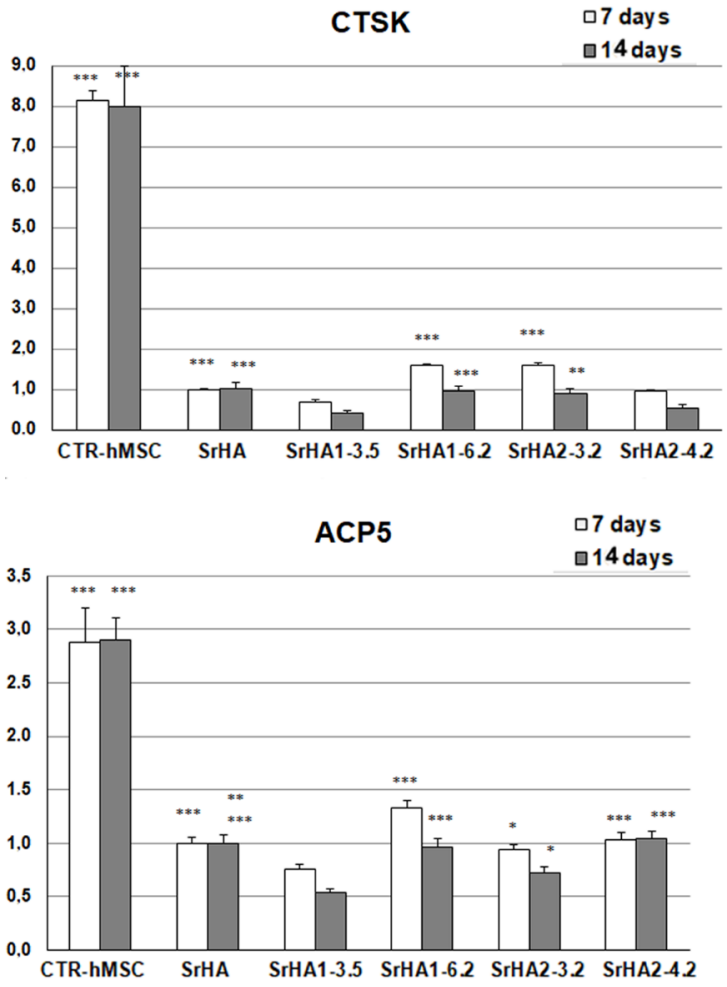

Figure 37. *Gene* expression of common markers CTSK and ACP5 of osteoclast differentiation by qPCR, after 7 (light bars) and 14 (dark bars) days. Results were normalized to GAPDH expression and data are given as fold change relative to the reference group (SrHA), considered as 1. Results are the mean (+/- sd) of six replicates.[142]

Osteoblastic differentiation of hMSC was investigated through evaluation of the gene expression of Runt-related transcription factor 2 (RUNX2). RUNX2 is a transcriptional factor that induces mesenchymal stem cell toward osteoblast lineage and its expression is upregulated in immature osteoblasts.[149] The evaluation of RUNX2 in SrHA and CTR-hMSC groups showed that Sr did not influence hMSC differentiation toward osteoblastic lineage. Indeed, no differences in RUNX2 gene expression were found between SrHA and CTR-hMSC, both at 7 (1.00+/-0.10 and 1.035+/-0.09 respectively) and at 14 (1.005+/-0.15 and 0.86+/-0.10 respectively) days. On the contrary, the comparison between the results obtained on β-lactam functionalized samples and on SrHA demonstrated that all the different formulations positively influenced RUNX2 expression, even if with different statistical significance (*Figure 38*). Osteoblastic activity was also investigated through analysis of further representative genes, such as ALPL, COLL1A1, and BGLAP, which encodes for alkaline phosphatase (ALP), type I collagen (COLL1) and osteocalcin (OSTC), respectively. ALP is an early marker of differentiation, COLL1 is the major constituent of the extracellular bone matrix and OSTC is one of the most abundant non-collagen proteins produced by differentiated osteoblasts.[142]

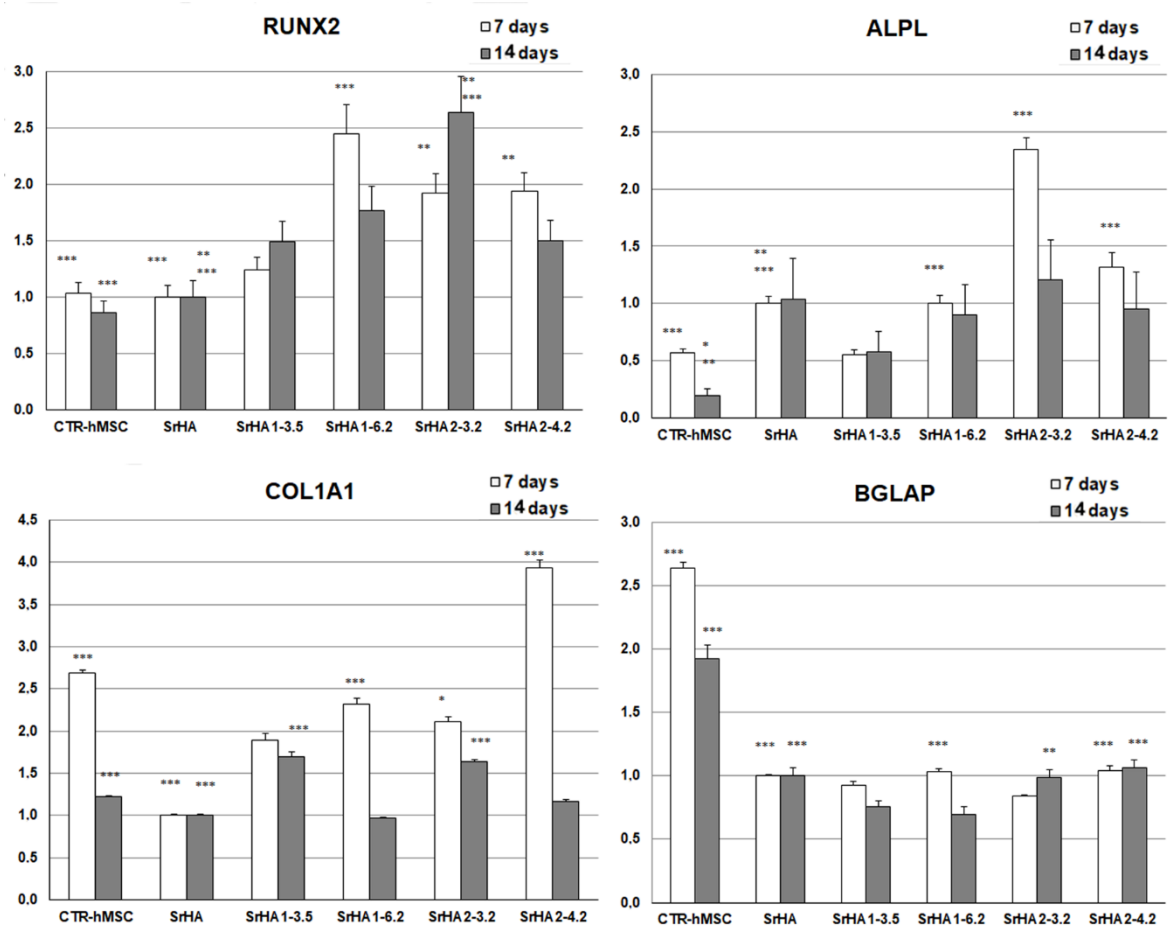

Figure 38. Gene expression of common markers of osteoblast differentiation RUNX2, ALPL, COL1A1, and BGLAP by qPCR, after 7 (light bars) and 14 (dark bars) days. Results were normalized to *GAPDH* expression and data are given as fold change relative to the reference group (SrHA), considered as 1. Results are the mean (+/- sd) of six replicates.[142]

The results indicate that all the samples promote ALPL expression. In particular, ALPL expression on SrHA was significantly greater than on CTR-hMSC. Moreover, all the functionalized samples, with the only exception of SrHA**1**-3.5, displayed significantly higher ALPL than SrHA at 7 days, whereas at 14 days the values for all the functionalized groups were not statistically different from SrHA.
COL1A1 expression showed lower levels on SrHA group than on CTR-hMSC both at 7 and 14 days. However, results of all β-lactam functionalized groups were significantly higher in comparison with SrHA at 7 days, and the value measured on SrHA**2**-4.2 was also significantly higher than on CTR-hMSC. At 14 days COL1A1 expression on all functionalized materials was greater or not significantly different than on SrHA, with SrHA**1**-3.5 and SrHA**2**-3.2, exhibiting even higher values than CTR-hMSC.
BGLAP also was lower on SrHA when compared to CTR-hMSC (7 and 14 days). The results obtained on functionalized materials were similar to those on SrHA, with the exception of a lower BGLAP expression on SrHA**2**-3.2 at 7 days and on SrHA**1**-3.5 and SrHA**1**-6.2 at 14 days (*Figure 38*).
It can be concluded that the presence of β-lactams on functionalized samples positively influenced gene expression, which generally reached levels of activation higher than or equal to the reference SrHA group.[142]

Conclusions

Functionalized materials were obtained by loading β-lactam integrin agonists on Strontium substituted hydroxyapatite. The amount of azetidinones onto Sr-hydroxyapatite could be modulated through variation in the polarity of the loading solution. After an initial burst, the release of both β-lactams in aqueous solution reached a steady state, maintaining a significant local concentration over time.
The results of in vitro tests showed that functionalized samples promoted adhesion and enhanced the viability of human mesenchymal stem cells. Regarding the effect of β-lactams on mesenchymal stem cells differentiation into osteoblastic lineage, results showed that after 14 days of co-culture, mesenchymal stem cells were directed to osteoblast differentiation, as stated by Runt-related transcription factor 2 (RUNX2) activation, which reached higher levels than control and reference groups. The higher expression of alkaline phosphatase ALPL and collagen type I alpha 1 chain (COL1A1), and the lower levels of bone gamma-carboxyglutamate protein (BGLAP) in comparison to control and/or reference group suggested that cells after 14 days were in the first phases of differentiation. Moreover, the presence of β-lactam integrin agonists enhanced the inhibiting influence of Sr-hydroxyapatite on osteoclast viability and activity, suggesting that these multi-functionalized materials can be employed locally to promote osteointegration and counteract abnormal bone loss.[142]

Experimental

Synthesis of Sr-hydroxyapatite (SrHA)

SrHA crystals were prepared under nitrogen atmosphere using 50 mL of solution with Sr/(Ca + Sr) ratio of 0.1. The total concentration of $[Ca^{2+}] + [Sr^{2+}]$ was 1.08 M. The solution was adjusted

to pH 10 with NH_4OH, then heated at 90°C. Afterwards 50 mL of 0.65 M $(NH_4)_2HPO_4$ was added dropwise under stirring. The resulting slurry was kept at 90 °C for 5 h, then the precipitate was isolated by centrifugation (10,000 rpm, 10 min), washed twice with distilled water, and air-dried at 37 °C.

*Synthesis of azetidinones **1** and **2***

Compounds **1** and **2** were synthesized according to an optimized multi-step procedure.[43] Structures of the compounds were assessed by ^1H NMR, purities resulted to be ≥ 95% by HPLC-UV analyses.

*Stabilities of compound **1** and **2***

The stabilities of compounds **1** and **2** in buffered water solutions at pH = 7.4 and in physiological solution at 30 °C were studied by HPLC-UV analysis at 254 nm (*Figure 39*).

HPLC analyses: Eclipse XDB-C18 column, 4.6 x 150 mm 5 micron, 0.5ml/min flux, 30°C.

Compound 1
Eluent phase: from 70% H_2O+TFA 0.08% – 30% CH_3CN + TFA 0.08% to 30% H_2O+TFA 0.08% – 70% CH_3CN + TFA 0.08% in 15min.
Retention time: 9.5 min

Compound 2
Eluent phase: from 100% H_2O+TFA 0.08% to 30% H_2O+TFA 0.08% – 70% CH_3CN + TFA 0.08% in 10min
Retention time: 8 min

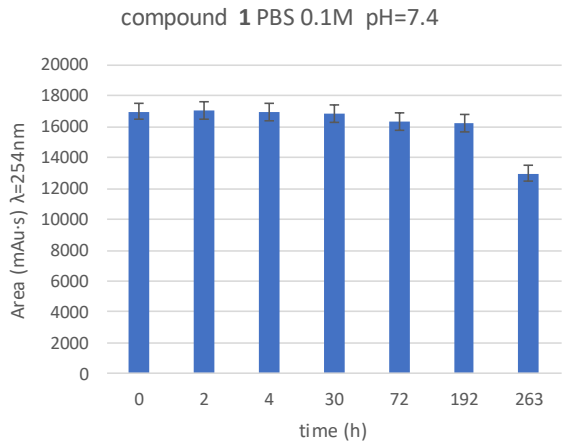

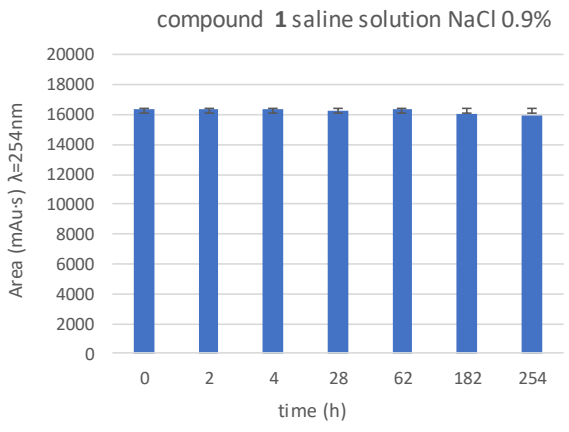

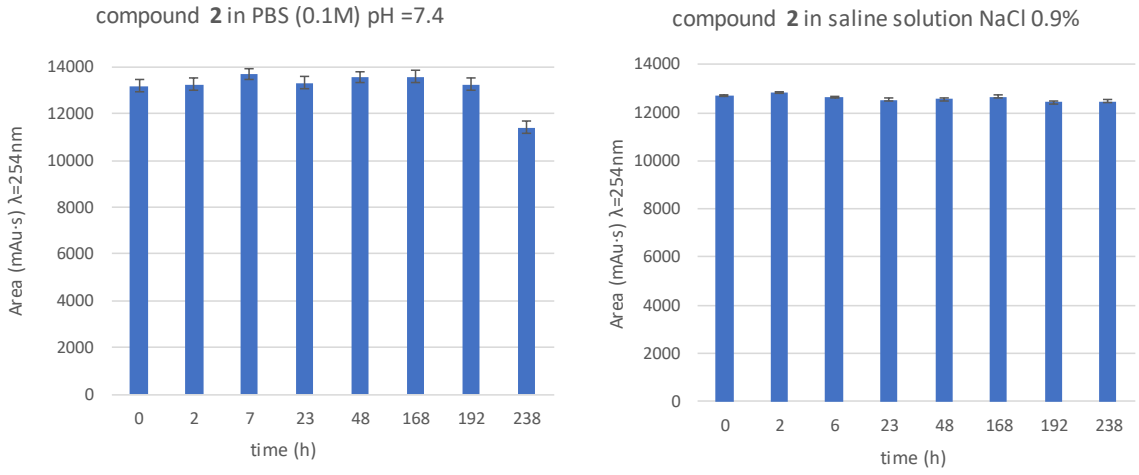

Figure 39. HPLC-UV analysis of absolute areas on testing the stability of **1** and **2** in PBS pH= 7.4 and in physiological solution (saline solution NaCl 0.9%).[142]

Release studies

The in vitro release profiles of β-lactams **1** and **2** from the corresponding SrHA samples were evaluated at 37°C in triplicate by HPLC-UV analysis, using linear calibration curves obtained at 254 nm. Release studies were performed on samples with a compound loading of 12.9 and 6.2 w% for SrHA**1**, and of 8.4 and 4.2 w% for SrHA**2**. Measurements were performed at selected times on the supernatant, which was separated and substituted with fresh solution (refresh). Results were expressed as cumulative release in mol% (of the total loaded amount) over the refresh number.[142]

Characterization methods

The samples SrHA**1**-12.9 and SrHA**2**-8.4 were analysed to get ATR-FTIR spectra with Alpha FT IR Bruker spectrometer with ATR diamond module at single reflection, with a resolution of 4 cm^{-1} and 32 scans in the scan range 4000–450 cm^{-1}. The background spectrum was collected before the acquisition of each sample spectrum. HPLC-MS analyses were obtained with an HP1100 instrument Agilent Technologies (ZOBRAX-Eclipse XDB-C8 column, H_2O/CH_3CN, 0.4 mL/min, from 30 to 80 % of CH_3CN in 8 min, 80 % of CH_3CN until 25 min) integrated with a MSD1100 single-quadrupole mass spectrometer (full scan mode, m/z 50-2600, scan time 0.1 s, positive ion mode, ESI spray voltage 4500 V, N_2 35psi, drying gas flow 11.5 mL/min, fragmentor voltage 20 V. ^1H NMR spectra were recorded with an INOVA 400 instrument with a 5mm probe, as $CDCl_3$ or d-4 methanol solutions.[142]
Powder X-ray diffraction patterns were recorded from 10 to 60 2θ° with a step size of 0.1° and time/step of 100 s (PANalytical-X'Pert PRO powder diffractometer equipped with a fast X'Celerator detector, λ = 0.154 nm, 40 mA, 40 kV).
For Transmission Electron Microscopy (Philips CM-100) investigations, a small amount of powder was dispersed in ethanol and submitted to ultrasonication.

Ca and Sr contents in the solid products were monitored by ion cromatography (Dionex ICS-90). Powders were previously dissolved in 0.1 M HCl.
Thermogravimetric analysis was carried out heating under air stream from 40.0 °C at 10.0 °C/min in a TGA7 Perkin Elmer instrument.[142]

In vitro tests

Biological tests were performed on samples of SrHA functionalized with azetidinones **1** or **2** (Y) in different percentage (X). Samples were prepared by pressing 40 mg of SrHA**Y**-X powder into cylindrical molds using a standard evacuable pellet die (Hellma). The obtained disk-shaped samples (diameter = 6 mm, height = 1.5 mm) were sterilized by gamma irradiation (25 kGy).[142]

In vitro co-culture model

The in vitro model was performed culturing together primary osteoclast derived from mononucleated blood cells (OC), and primary mesenchymal stem cells derived from bone marrow (hMSC, ATCC), both from human origin.
Osteoclast precursors were isolated from mononuclear cells of peripheral blood of healthy donor (Ethic Committee approval n.191/2019/Sper/IOR, prot. VIRTOS). Briefly, a volume of peripheral blood, diluted 1:1 with pre-warmed PBS, was carefully layered on an equal volume of Histopaque1077, to separate the mononuclear cells from the other elements of blood by density gradient centrifugation (600 g, room temperature, 30 min). The mononuclear cells at the interface PBS/Histopaque were collected after centrifugation, washed twice in PBS, and seeded on the bottom of 24-wells plates ($4x10^5$ cells/well) using the culture medium (DMEM, Sigma, UK) supplemented with osteoclastogenic factors (macrophage colony-stimulating factor, MCSF, 25 ng/mL, and receptor activator for κB factor ligand, RANKL, 30 ng/mL, DMEM-OC). The plate was maintained for 7 days in standard condition (37 °C ± 0.5 temperature, 5% CO_2 ± 0.2, 95% humidity), to differentiate in osteoclasts (OC).
A culture of hMSC was expanded in their basal medium. After counting, cells were seeded on material samples ($4x10^4$ cells/sample) prepared with different concentrations of β-lactams (SrHA**1**-3.5, SrHA**1**-6.2, SrHA**2**-3.2, SrHA**2**-4.2), and on SrHA without lactams as reference group. Samples with cells were co-cultured in the same wells with OC, as showed in Figure S3, for 14 days. Final medium was a mixture of osteogenic differentiation medium (StemPro Gibco, Termofisher, USA) and DMEM-OC.
Additional control groups with only cells (hMSC and OC cultures) were prepared to verify regular cell proliferation and differentiation, regardless of material presence.[142]

Cell viability and adhesion

Cell viability was tested by Alamar blue dye (Cell Viability Reagent, LIFE Technologies Corp., Oregon, USA). Samples with hMSC were transferred in new empty wells to evaluate hMSC separately from OC, both at 7 and at 14 days of co-culture. The reagent, which was added 1:10 reagent/medium to each well and incubated for further 4 hours at 37 °C, contains a redox indicator that modify the color from blue to pink according to the increasing number of living cells.

Cell colonization of samples was observed after DAPI staining (Sigma Aldrich, Steinheim, Germany), performed on hMSC adherent to material samples, according to manufacturer's instructions. Briefly, after passages in PBS, 4% paraformaldehyde, 0.5% Triton X-100, and DAPI solution, nuclei of cells on samples were observed in fluorescence by inverted microscope (Eclipse TiU, NIKON Europe BV, NITAL SpA, Milan, Italy) equipped with a digital camera.[142]

Cell differentiation and morphology

The evaluation of osteoclast differentiation was performed using TRAP (Tartrate-resistant acid phosphatase) staining (TRAP kit, SIGMA, Buchs, Switzerland), following manufacturer's instructions, on control culture after 4 weeks of culture, and on cells cultured with hMSC, alone or in presence of materials, after 10 days of co-culture.
TRAP staining develops red colour in positive cells, allowing to evaluate osteoclastogenesis. The number of TRAP positive cells, typically showing 3 or more nuclei each positive cell, were counted in 10 fields under the microscope by a semiautomatic software (NIS-Elements AR 4.30.01). Results are given as percentage, considering OC control culture as 100%.
Moreover, osteoclast morphology was evaluated by Phalloidin / DAPI (4′,6-diamidino-2-phenylindole) staining according to manufacturer's instructions, and observed by a computerized image analysis system (Kontron KS 300 software, Kontron Electronic GmbH, Eching bei Munchen, Germany).
FITC-conjugate phalloidin solution shows cytoskeleton and it is useful to visualize cell shape and adhesion onto material surface.
Random samples of materials cultured with hMSC were treated for scanning electron microscopy (SEM) at the end of experimental time and examinated with a Hitachi S-2400 instrument operating at 15 kV.[142]

qPCR

qPCR technique was used to evaluate most common markers of co-cultured hMSC and OC to assess gene expression of cell differentiation and activity. Total RNA was extracted from samples cultured with materials and controls (only cells) both at 7 and 14 days by PureLink RNA Mini Kit (Life Technologies, Carlsbad, CA, USA) and samples were reverse transcribed with SuperScriptVILO cDNA Synthesis Kit (Life Technologies, Carlsbad, CA, USA), following the manufacturer instructions. Semi-quantitative polymerase chain reaction (PCR) analysis was performed for each sample in duplicate in a LightCycler 2.0 Instrument (Roche Diagnostics GmbH, Manheim, Germany) using QuantiTect SYBR Green PCR Kit (Qiagen, Hilden, Germany) and gene-specific primers. After melting curve analysis to check for amplicon specificity, the threshold cycle was determined for each sample and relative gene expression was calculated using the 2-DDCtmethod. For each gene, expression levels were normalized to GAPDH (Glyceraldehyde 3-phosphate dehydrogenase, Invitrogen, CA, USA) using SrHA reference group for each experimental time as calibrator.[142]

1.1.6 Novel ligands for leukocyte integrins

Integrins, as previously anticipated, can be divided into 4 groups in relation to their ligand-binding specificity[8,10] and one of these groups is composed by leukocyte integrins.
Integrins expressed predominantly by leukocytes are made of a β_2 subunit coupled with one of several α subunit counterparts ($\alpha_L\beta_2$, $\alpha_M\beta_2$, $\alpha_X\beta_2$, and $\alpha_D\beta_2$), or an α_4 subunit coupled with its β subunit counterparts ($\alpha_4\beta_1$ and $\alpha_4\beta_7$). These leukocyte integrins are dynamically up- or down-regulated depending on the stage of leukocyte activation and extravasation; moreover, each integrin has specific function contributing to leukocyte movements. Insufficient integrin activity contributes to recurrent infectious episodes and impaired wound healing, while an excessive integrin activity brings to a sustained and exaggerated inflammatory response with associated tissue damage.[150]

Leukocytes are the cells with the highest mobility and their integrins are responsible of several processes such as cell adhesion, migration and the recruitment of other leukocytes; these receptors are therefore also linked to the pathogenesis of autoimmune diseases and inflammations such as multiple sclerosis[151], rheumatoid arthritis[152] and Crohn's disease.[153] Furthermore, the relationship between inflammation and the development of cancer has long been known[154]: in fact, when we reach a chronic level of chemokines or growth factor released due to inflammation, DNA can easily undergo mutations, promoting the development of tumors.[155]

Leukocyte trafficking to sites of injury or infection is strictly regulated by the leukocyte adhesion cascade. The cascade starts with selectin-dependent leukocyte rolling, followed by chemokine-induced leukocyte activation and leukocyte slow rolling, mediated by the cooperation between selectin and integrins and the interactions with their respective ligands. Slow rolling paves the way for the integrin-dependent steps which involve: leukocyte adhesion/arrest, adhesion strengthening and leukocyte crawling on the endothelium, that finally enable the trans-endothelial migration of leukocytes mostly through endothelial junctions to the sub-endothelium.[156]

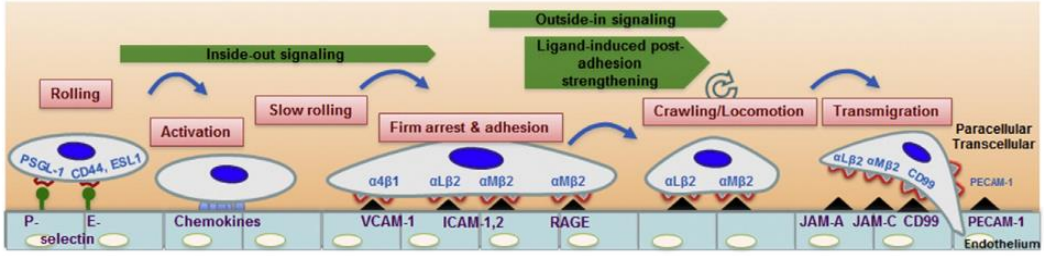

Figure 40. The multistep model of leukocyte recruitment. Figure adapted from ref. 157.

In particular, integrin $\alpha_L\beta_2$ or LFA-1 is expressed exclusively by leukocytes and it is essential for the recruitment of these cells to sites of inflammation. This integrin binds several members of the ICAM family and also with the *Junction Adhesion Molecule* JAM-1. The preferential ligand for $\alpha_L\beta_2$ is ICAM-1 and it has been shown that the amino acid residue Glu34 located in the D1

domain of ICAM-1 binds to the Mg^{2+} ions present in the MIDAS site of the α_LI domain (*Figure 41).*[150]

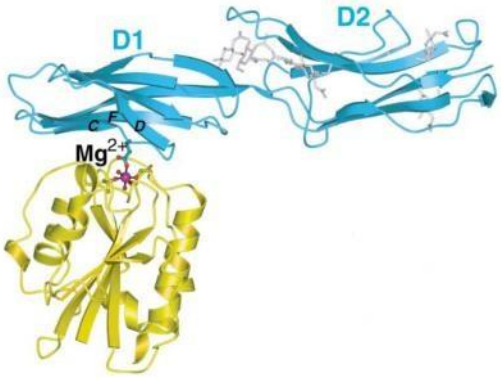

Figure 41. Interaction between α_LI domain (yellow) and D1 domain of ICAM-1(blu).[158]

The effects of the interaction of $\alpha_L\beta_2$ with other ligands was also studied, showing how for example ICAM-2[159] and ICAM-3[160] are respectively involved in leukocyte extravasation and antigen recognition, however no information is available on which are the key amino acids that allow interaction with $\alpha_L\beta_2$.

Integrin $\alpha_M\beta_2$ or Mac-1 is instead expressed by myeloid cells including neutrophils, dendritic cells and macrophages,[161] and becomes overexpressed in response to inflammatory stimuli. The recognition site of the extracellular ligand resides in the α_MI domain. Studies carried out on this domain have shown that three amino acid residues Phe246, Asp254 and Pro257 play a critical role in the recognition of ligands.[162] More than 30 possible natural ligands for Mac-1 have been reported including fibrinogen and members of the ICAM (*IntraCellular Adhesion Molecules*) family; in particular, it is interesting to note how ICAM-1, which usually binds the integrin $\alpha_L\beta_2$ with its D1 domain, in the case of $\alpha_M\beta_2$ interacts through the D3 domain, underlining a possible competition between the two integrins if they were both present on the cell.

Then we have integrin $\alpha_4\beta_1$ or VLA-4, which plays a decisive role in the onset of various types of pathologies; it is mainly expressed by lymphocytes and monocytes[163] and a high presence can be found during the maturation of dendritic cells of monocytic origin.[164] Contrary to the integrins described above, $\alpha_4\beta_1$ does not possess the αI domain and therefore the recognition of its ligands remains dependent on the βI domain. One of these is fibronectin, and through interaction with $\alpha_4\beta_1$ the adhesion between cell and extracellular matrix is activated; in particular $\alpha_4\beta_1$ recognizes the amino acid sequence leucine-aspartic acid-valine (LDV, *Figure 42*) present in a region called CS-1 of fibronectin. Integrin $\alpha_4\beta_1$ is also able to promote adhesion between cells by binding to the amino acid sequence isoleucine-aspartic acid-serine (IDS, *Figure 42*) present on the VCAM-1 protein.[165]

Finally, $\alpha_4\beta_7$ or LPAM, expressed in cells such as T lymphocytes, plays a crucial role in the development of organs of the lymphoid system associated with the mucous membranes, in the

generation of an immunological response in the mucous membranes and in the onset of diseases associated with these are chronic inflammation of tracts of the digestive system and type 1 diabetes.[166] As previously seen for $\alpha_4\beta_1$, the αI domain is also missing in this integrin so the main endogenous ligand, MAdCAM-1, is recognized by the β subunit; the *mucosal vascular addressing cell adhesion molecule 1* (MAdCAM-1), is selectively expressed on mucosal endothelial cells and performs a directing function for the recirculation of T lymphocytes within the mucous membranes. [167] The key amino acidic sequence recognized by $\alpha_4\beta_7$ is a leucine-aspartic acid-threonine triad (LDT, *Figure 42*).[168]

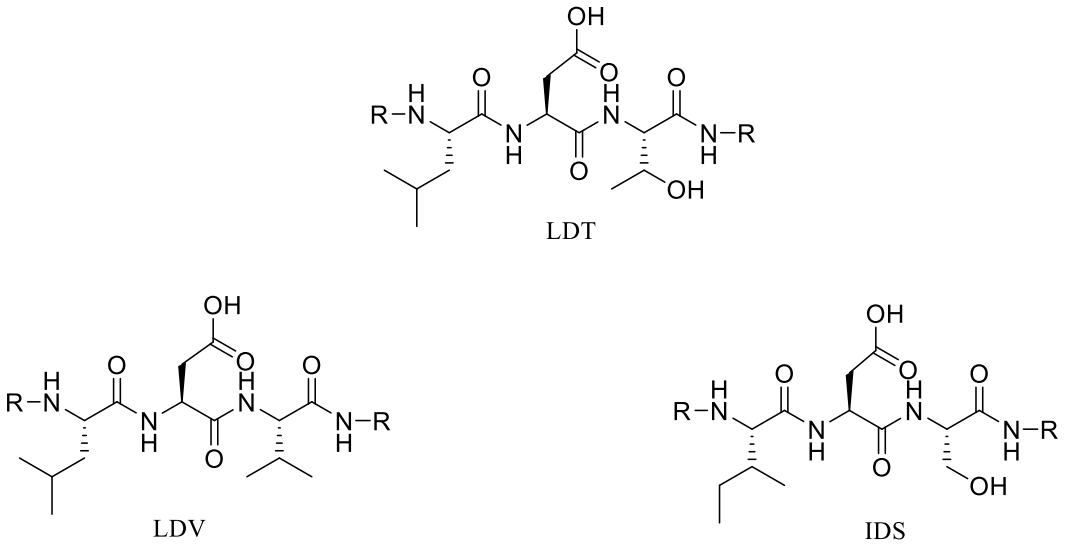

Figure 42. Amino acidic sequences recognized by leukocyte integrins.

Being integrins strictly linked to the pathogenesis of autoimmune diseases and inflammation, they have been chosen as target for pharmacological therapies.

Treatments that we are going to see are made of both antagonist and agonist compounds. Among the main exponents of the first category of drugs we find both antibodies and small molecules, capable of inhibiting the activity of the receptor. Natalizumab is a recombinant humanized antibody, that was the first drug approved by the Food & Drug Administration as a targeted therapy for multiple sclerosis[169] and Crohn's disease[170] with the aim of blocking the activity of α_4 integrins. Although it was revoked from the market due to encephalopathic complications arising in patients[171], it was subsequently reintroduced as a monotherapy for relapsed forms of multiple sclerosis, triggering once again the interest in the development of α_4 integrin antagonists. Vedolizumab and Etrolizumab are two other humanized monoclonal antibodies that have shown good efficacy in the treatment of diseases such as Crohn's disease with a good specificity for $\alpha_4\beta_7$ integrin for the first one and for all β_7 integrins for the other one. [172]
Despite the therapies based on monoclonal antibodies, the prospect of creating small molecules as ligands for integrins remains very interesting.
In the case of β_2 integrins, several potent antagonists have been developed over the years as potential anti-inflammatory agents by various pharmaceutical companies. For example, there is a group of compounds which promote the inhibition of the interaction between $\alpha_L\beta_2$ and ICAM-1

in an allosteric way, binding to the allosteric site and stabilizing the α_LI domain in the low affinity conformation (*Figure 43*).[173]

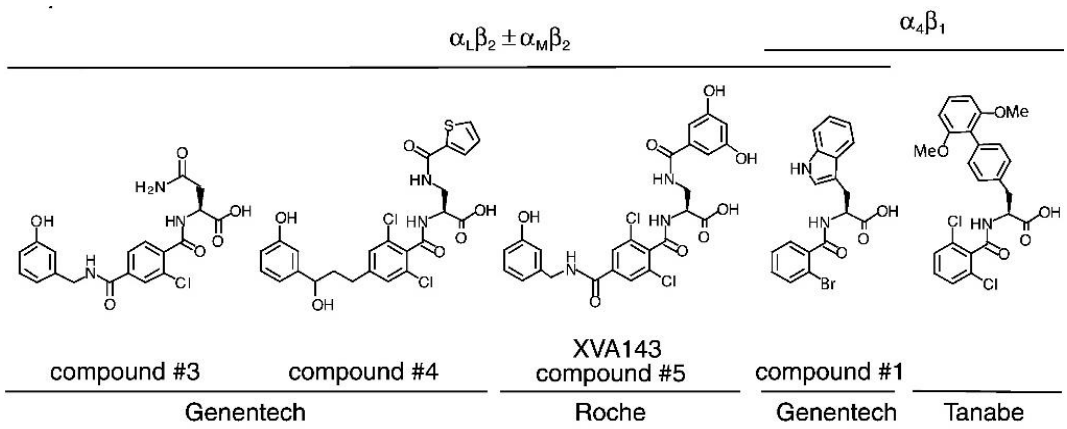

Figure 43. Antagonist ligands towards $\alpha_L\beta_2$ and $\alpha_M\beta_2$. Figure adapted from ref. 174.

Regarding integrins that have the α_4 subunit we can identify two major classes of ligands with antagonist activity towards the receptors: a first class of compounds containing an ureido group have been developed starting from a first study[175] in which it was described the synthesis and activity of a cyclic pentapeptide "**1**" shown in *Figure 44*. In particular, molecules Bio-1211, IVL-745 and TBC-3486 (*Figure 44*) showed interesting activities reaching clinical phase 2. Moreover, following SAR studies conducted on the cyclic peptide "**1**", it was also highlighted how the presence of a phenylalanine function could be useful in order to improve its antagonist activity. On the basis of these studies, the second main class of α_4 integrin antagonists has been developed which presents phenylalanine as a key functional group. Among the main exponents of this category the most important results have been achieved with R-411, which has been shown to be effective in the treatment of asthma up to clinical phase 2, and AJM-300 which reached clinical phase 2 for the treatment of inflammatory diseases of the digestive system (*Figure 44*).[176]

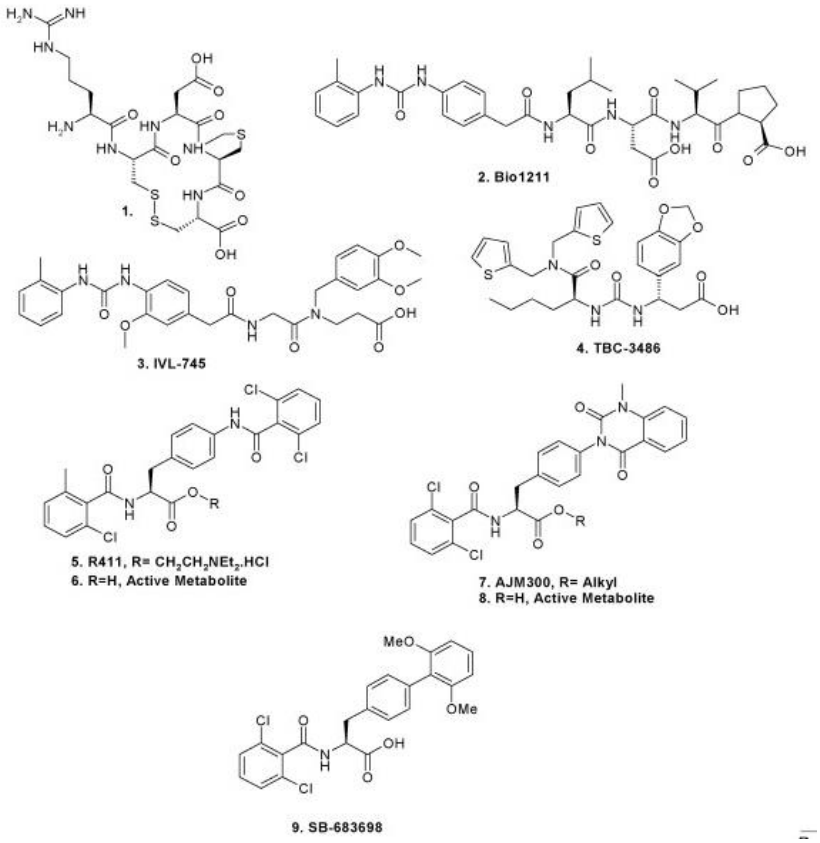

Figure 44. Antagonist ligands towards integrins $\alpha_4\beta_1$ e $\alpha_4\beta_7$. Figure adapted from ref. 176.

On the other hand, there are agonist ligands; for example, following high-throughput phage display screening studies, several integrin ligands with agonist activity towards the β_2 class have been identified (*Figure 45*).

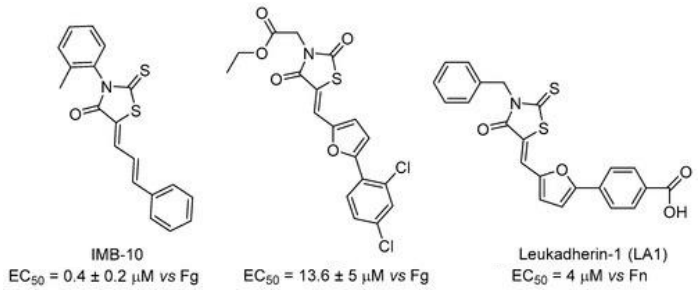

Figure 45. Agonist ligands towards integrins $\alpha_L\beta_2$ e $\alpha_M\beta_2$. Figure adapted from ref. 42.

The IMB-10 compound was able to inhibit the competitive binding of integrin with specific antibodies; it also showed an increased adhesion capacity of the $\alpha_M\beta_2$ receptor toward fibrinogen.[177] Starting from the IBM-10 structure, other drugs were then developed (*Figure 45*); the interaction of these molecules with the receptor in an inactive state promotes its rearrangement in a conformation of partial activity.[178]

Also my research group, as previously described, have developed a new library of integrin ligands[43] and among them, some compounds showed good activity also towards integrins of the immune system (*Figure 46*).

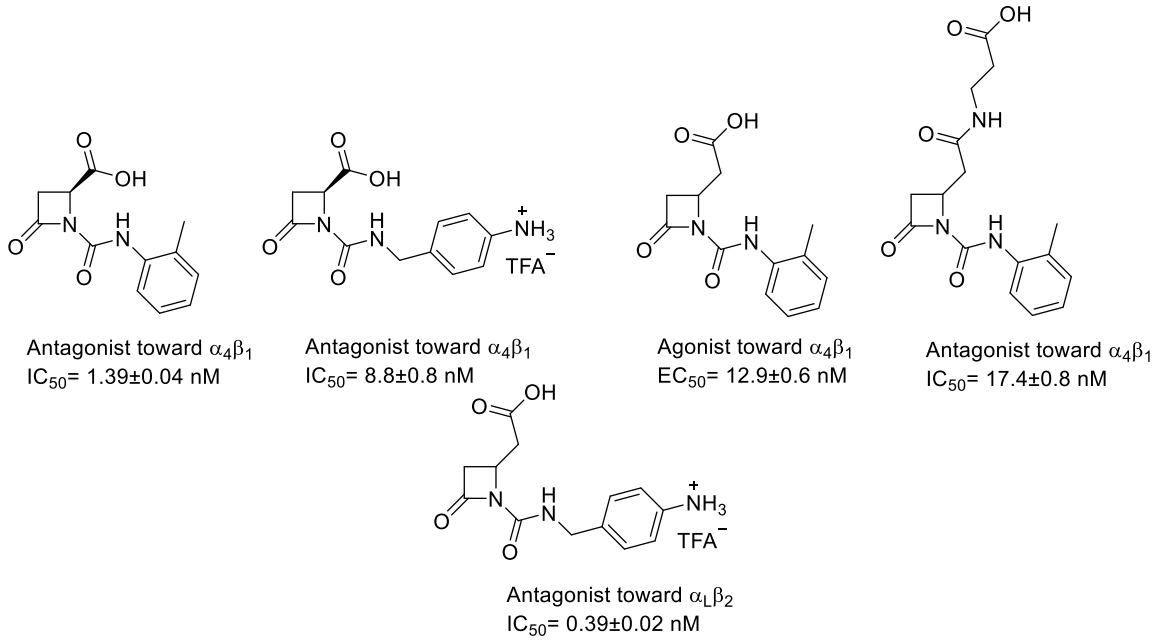

Figure 46. Leukocyte integrin ligands developed by the Giacomini's research team.[43]

Following the good results obtained for this β-lactams towards leukocyte integrins,[43] we decided to expand this library with new compounds able to be recognized by the same class of receptors (*Figure 47*).

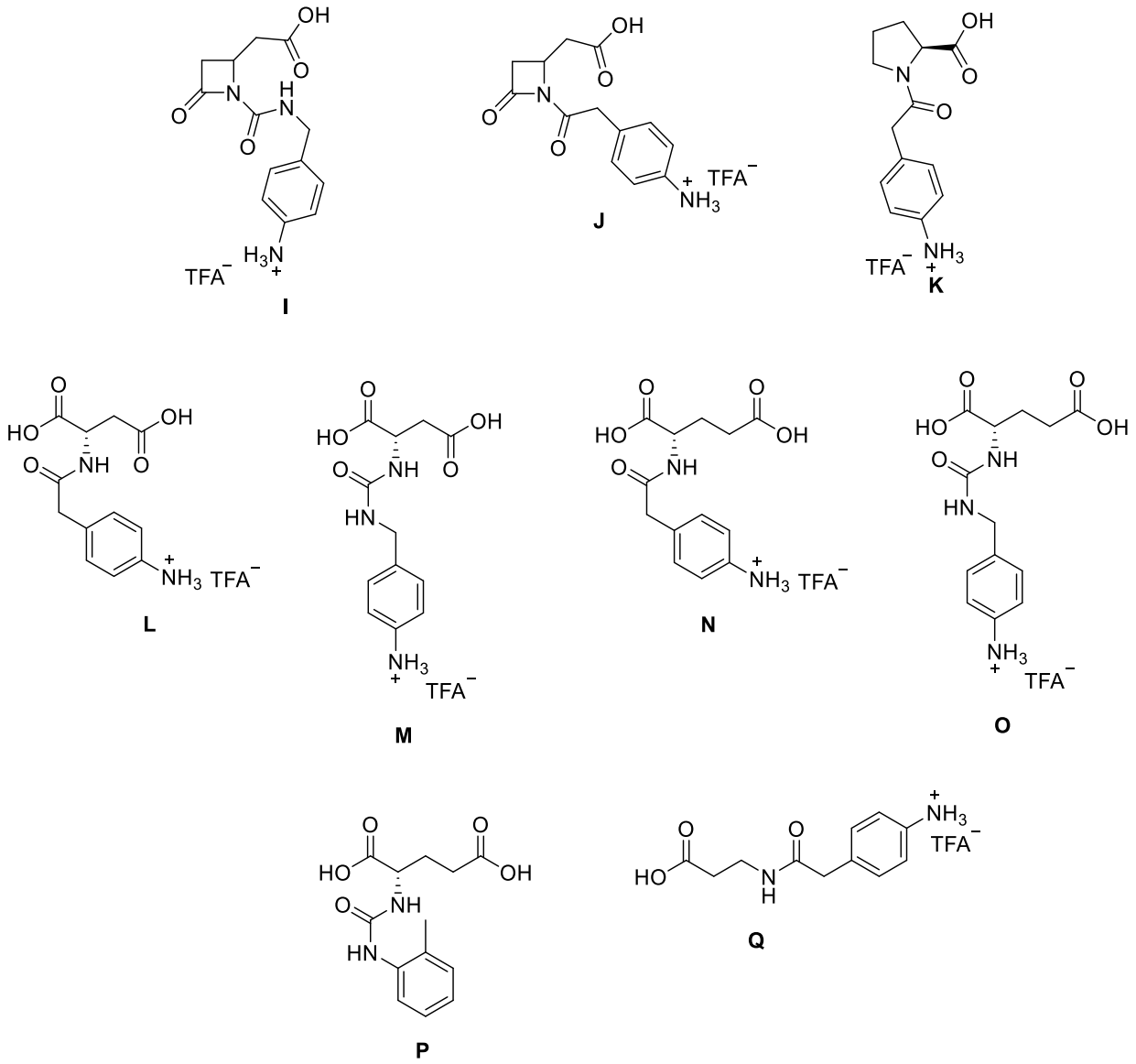

Figure 47. A series new compounds **I-Q** designed and synthesized to target leukocyte integrins evaluated in this study.

Results and discussions

Using compound **I**[43] (antagonist toward $\alpha_L\beta_2$, IC_{50} = 0.39 nM), as a model for the design of the new ligands we know that is necessary a carboxylic acid terminal on the C4 position of the β-lactam scaffold to target the integrin metal ion-dependent adhesion site (MIDAS), and a free aniline. Because of 2-azetidinone ring represents a site of conformational restriction with a cyclic β-amino acid residue which could give a favourable alignment of both the amine and carboxylate moieties on the ligand, we decided to keep the β-lactam scaffold in compound **J** but substituting the *ureidic* portion with an amide in order to evaluate if this functional group is necessary in terms of integrin recognition. In compound **K** instead the β-lactam ring is substituted by a proline, introducing chirality. For compounds **L-Q** the strategy is completely different; we started from L-aspartic or L-glutamic acid and OBn-β-alanine, differently functionalized to have a free aniline or the *o*-tolyl group (able to improve the bioactivity and specificity for $\alpha_4\beta_1$ integrins). In that way we want to study if the conformational restriction of the ring is essential in

terms of integrin interaction and if introducing two free carboxylic acids (**L**-**P**) the bioactivity and the specificity can be enhanced.

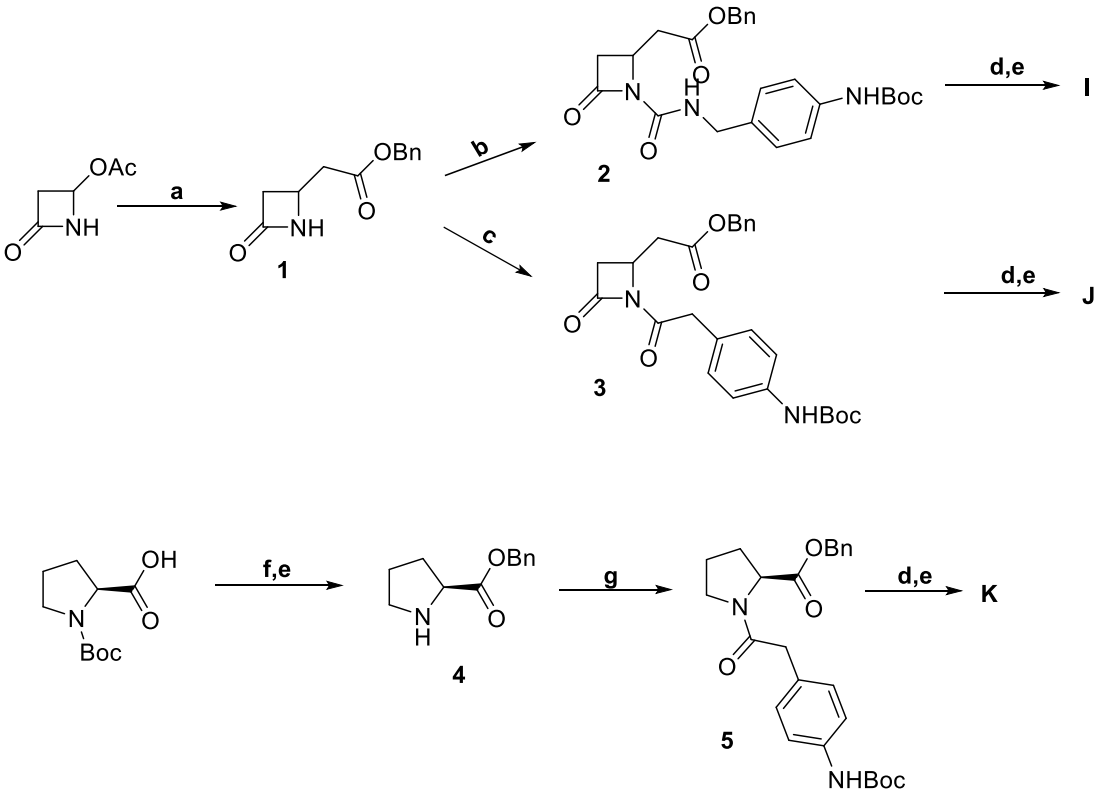

Scheme 13. Synthesis of compounds **I**, **J**, **K**. Reagents and conditions: a) Zn, TMSCl, benzylbromoacetate, THF, 0°C then rt, 3 h; b) 2-(4-((*tert*-butoxycarbonyl)amino)phenyl)acetic acid (**14**), HBTU, DIPEA, DCM, 0°C then rt, 24 h; c) NaHMDSA, *tert*-butyl(4-(isocyanatomethyl)phenyl)carbamate (**15**), THF, -78°C, 1 h; d) H_2, Pd/C (10%), THF/CH_3OH 1:1, rt, 2 h; e) TFA, CH_2Cl_2, 0°C then rt, 1-4 h; f) BnOH, DCC, DMAP, DCM, 0°C then rt, 4 h; g) 2-(4-((*tert*-butoxycarbonyl)amino)phenyl)acetic acid (**14**), DCC, DMAP, DCM, 0°C then rt, 24 h.

The synthesis of β-lactams **I** and **J** starts with a substitution reaction on the 4-acetoxy-2-azetidinone by a Reformatsky reagent; benzyl-bromoacetate was treated with an excess of metallic Zinc in THF to furnish the corresponding Reformatsky reagent, which was then coupled with 4-acetoxyazetidin-2-one to give 4-acetate-azetidin-2-one ester **1** in good overall yields after flash chromatography.[69]

For the synthesis of compound **K** we started from N-Boc Proline. To preserve the carboxylic acid moiety, we need to protect it with benzyl alcohol, in presence of coupling agent DCC and DMAP as base. Subsequently the Boc-group needs to be eliminated with TFA, in order to give compound **4** with the free amine necessary for the following step.

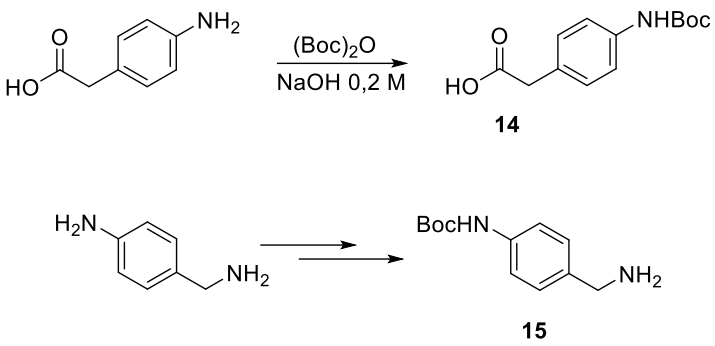

Scheme 14. Synthesis of intermediates **14** and **15**.

As previously anticipated, our target compounds need to have a free aniline for integrin recognition and to introduce this functional group we use two different strategies: starting from *p*-amino phenyl acetic acid or 4-amino benzylamine. In the first case we can easily protect the amine using Boc anhydride in NaOH 0.2 M, obtaining compound **14** with good yields. In the second case instead, we have to plan a orthogonal protection/deprotection strategy of 4-amino benzylamnine in order to obtain *tert*-butyl(4-(isocyanatomethyl)phenyl) carbamate **15** with the free benzyl amine and Boc-protected aniline.

The N-1- side chain was inserted on azetidinone **1** in two different ways: for the synthesis of compound **2** it has been previously deprotonated at −78°C with sodium hexamethyl disilylamide (NaHMDSA), and then reacted with *tert*-butyl(4-(isocyanatomethyl)phenyl) carbamate (*Scheme 13*), which had been obtained in turn from 4-N-Boc-aminobenzylamine **15** with triphosgene; for the synthesis of compound **3** instead we have the coupling reaction with compound **14** in presence of HBTU and DIPEA.

The secondary amine of proline **4** was coupled with **14** too. In this case the coupling reaction was conducted in presence of DCC and DMAP to obtain **5** as a colourless oil.
When intermediates **2-3-5** were subjected to a two-step procedure consisting of hydrogenolysis and treatment with TFA for the final deprotection, compounds **I**-**K** were obtained in very good yields.

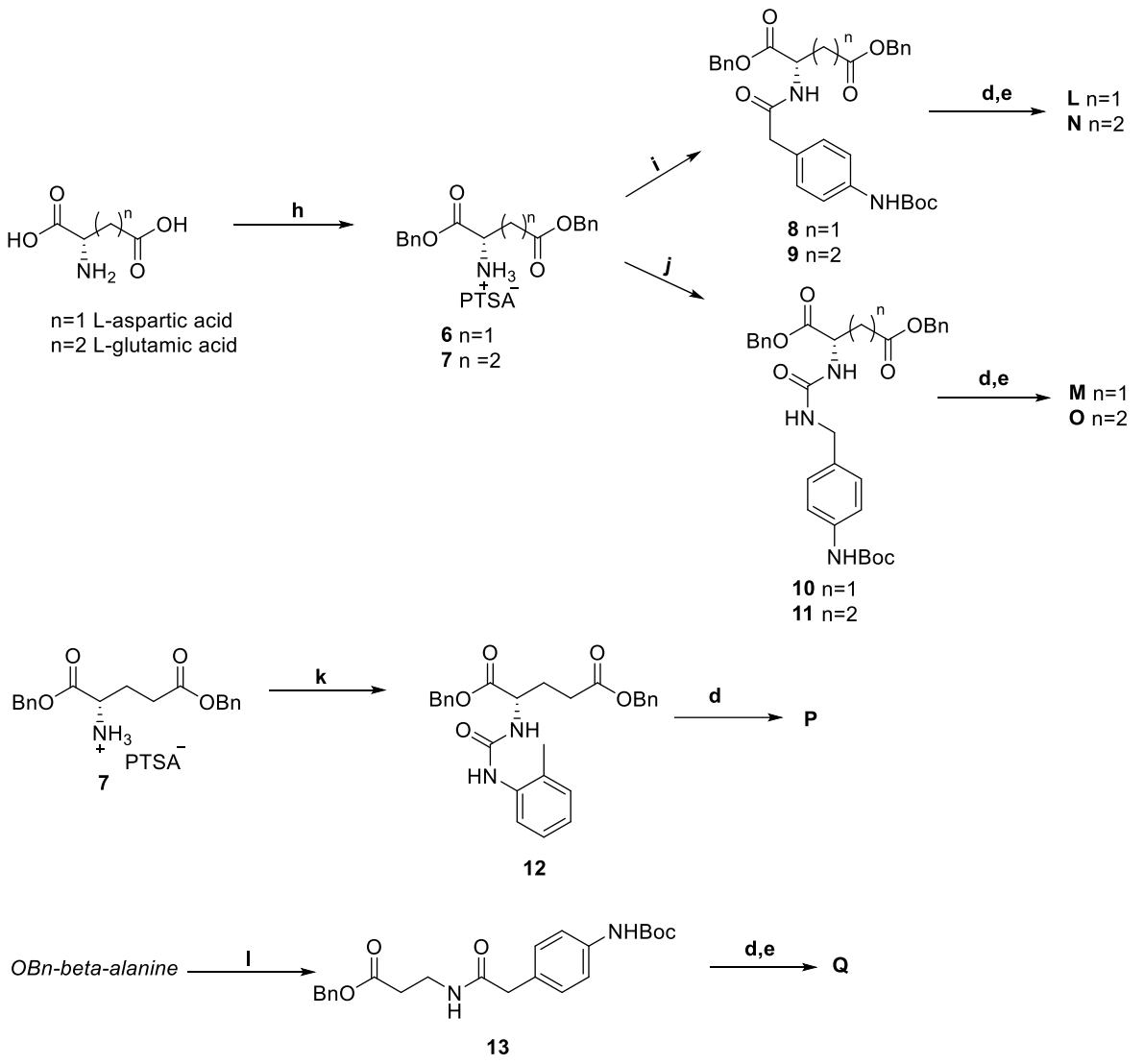

Scheme 15. Synthesis of target compounds **L, M, N, O, P, Q.** Reagents and conditions d) H_2, Pd/C (10%), THF/CH_3OH 1:1, rt, 2 h; e) TFA, CH_2Cl_2, 0°C then rt, 1-4 h; h) BnOH, PTSA, toluene, 110°C, 24 h; i) 2-(4-((*tert*-butoxycarbonyl)amino)phenyl)acetic acid (**14**), HOBt, EDC, TEA, DCM, 0 °C then rt, 18 h; j) TEA, *tert*-butyl(4-(isocyanatomethyl)phenyl)carbamate (**15**), DCM, rt, 18 h; k) *o*-tolylisocyanate, TEA, CH_2Cl_2, rt, 16 h; l) 2-(4-((*tert*-butoxycarbonyl)amino)phenyl)acetic acid (**14**), HOBt, EDC, TEA, DCM, 0°C then rt, 24 h.

A careful strategy for protecting the carboxylic acid and the amine terminus of L-aspartic and L-glutamic acids was developed to preserve these moieties during the synthesis and specific combinations of protecting groups have been chosen to achieve full or partial deprotection depending on the requirements of the synthetic strategy. The protection reaction of the carboxylic acids of L-aspartic and L-glutamic acid provides the use of benzyl alcohol and p-toluensulfonic acid in toluene. Compounds **6** and **7** obtained with yields between 60-70% are ready for the following steps.

After the preparation of the protected starting materials, we can proceed with the assembling of the different portions.
Compounds **6** and **7** have been functionalized both with compound **14**, in presence of HOBt, EDC and TEA, to obtain respectively **8** and **9**, and with *tert*-butyl(4-(isocyanatomethyl)phenyl) carbamate, obtained from compound **15**, in presence of TEA to obtain **10** and **11**.

Moreover, compound **7** was also functionalized with *o*-tolylisocyanate in presence of TEA as base to give compound **12** with the typical *ureidic* portion of a 4([(N-2-methylphenyl)ureido]-phenylacetyl motif (PUPA) that greatly enhanced bioactivity and specificity for $\alpha_4\beta_1$ integrins.
Finally, OBn-β-alanine was coupled with **14** with typical conditions of EDC, HOBt and TEA, to give compound **13** in good yields as a white solid.
Then intermediates **8-9-10-11-12-13** were subjected to a two-step procedure consisting of hydrogenolysis and treatment with TFA for the final deprotection, and compounds **L-Q** were obtained in very good yields.

Conclusions

The molecules **I-Q** have been synthesized and totally characterized and are now being tested in adhesion assays in order to evaluate their real activity in collaboration with Prof. Spampinato and Dr. Baiula of the Department of Pharmacology of the University of Bologna.

Experimental

Commercial reagents were used as received without additional purification. ^{1}H and ^{13}C NMR spectra were recorded with an INOVA 400 instrument with a 5 mm probe. All chemical shifts were quoted relative to deuterated solvent signals (δ in ppm and J in Hz). Polarimetric analyses were conducted on Unipol L 1000 "Schmidt−Haensch" polarimeter at 598 nm. FTIR spectra: Bruker Alpha instrument, measured as films between NaCl plates, wave numbers are reported in cm^{-1}. The purities of the target compounds **I-Q** were assessed as being >95% using HPLC. HPLC-MS: Agilent Technologies HP1100 instrument, equipped with a ZORBAX-Eclipse XDB-C8 Agilent Technologies column; mobile phase, H_2O/CH_3CN, 0.4 mL/min; gradient from 30 to 80% of CH_3CN in 8 min, 80% of CH_3CN until 25 min, coupled with an Agilent Technologies MSD1100 single-quadrupole mass spectrometer, full scan mode from m/z = 50 to 2600, in positive or negative ion mode. Compounds **1**,[179] **2**,[43] **4**,[180,181] **14**,[179] **15**,[43] **I**,[43] are known and were synthesized according to reported procedures, spectroscopic data of the compounds were in accordance to those reported in literature.

General Procedure for OBn-Protection (GP1)

A dicarboxylic acid compound (1 equiv) was dissolved in toluene (2.9 mL/mmol, 1:1 v/v), under a nitrogen atmosphere and benzylic alcohol (6.5 equiv) and *p*-toluensulfonic acid (1.4 equiv) were added. The solution was then stirred at reflux for 24 hours. After a complete consumption of the starting material (TLC monitoring), The reaction mixture was cooled to room temperature and evaporated, then CH_3OH (2 mL) was added and warmed to dissolve the residue, then Et_2O (8 mL) was added, and finally the resulting suspension was filtered.

General Procedure for Hydrogenolysis (GP2)

A benzyl ester (1 equiv) was dissolved in a mixture of THF and CH_3OH (22 mL/mmol, 1:1 v/v), and Pd/C (10% w/w) was added. The solution was then stirred under a H_2 atmosphere (1 atm) at room temperature. After a complete consumption of the starting material (TLC monitoring, 2 h)

the reaction mixture was filtered through Celite and concentrated in vacuum. The crude was then triturated with a few drops of pentane to afford the desired carboxylic acid.

General Procedure for N-Boc-Deprotection (GP3)

A N-Boc-protected compound (1 equiv) was dissolved in CH_2Cl_2 (18.5 mL/mmol) under a nitrogen atmosphere, and trifluoroacetic acid (TFA) (4 equiv) was added dropwise at 0 °C. New TFA aliquots were added each 60 min at 0 °C until a complete conversion (HPLC or TLC monitoring). The solvent was removed under reduced pressure, and the crude was triturated with few drops of pentane to afford the resulting deprotected compound.

Coupling reaction with EDC-HOBt (GP4)

To a solution of amine (1 equiv) dissolved in CH_2Cl_2 (6.5 mL/mmol) under a nitrogen atmosphere, and anhydrous TEA (1.2 equiv) was added dropwise. The reaction was left for 20 min. At the same time, in a second round-bottom flask, the carboxylic acid (1 equiv) was dissolved in DCM (4.5 mL/mmol), and the solution of the first round-bottom flask was dropped. Then HOBt (0.5 equiv) and EDC (1 equiv) were added at 0 °C. The solution was warmed to rt and left under stirring after complete consumption of the starting material (18 h, TLC monitoring). The mixture was quenched with H_2O and extracted with CH_2Cl_2. The organic layer was dried over Na_2SO_4, concentrated in vacuum, and purified by flash chromatography.

*Benzyl 2-(1-(2-(4-((tert-butoxycarbonyl)amino)phenyl)acetyl)-4-oxoazetidin-2-yl)acetate (**3**)*

To a solution of **14** (114 mg, 0.46 mmol, 1 equiv) in 4 mL of DCM, under a nitrogen atmosphere at 0° C, HBTU (383 mg, 0.92 mmol, 2 equiv), DIPEA (320 µL, 1.84 mmol, 4 equiv) and compound **1** (100 mg, 0.46, 1 equiv) were added. The reaction was left under stirring overnight. At completion (TLC monitoring) the mixture was quenched with NH_4Cl and extracted with EtOAc. The organic layer was dried over Na_2SO_4, concentrated in vacuum, and purified by flash chromatography (Cyclohexane/EtOAc = 7:3). Compound **3** (54 mg; 26%) was obtained as colourless oil. ^{1}H NMR (400 MHz, $CDCl_3$) δ: 7.40 – 7.27 (m, 7H), 7.21 (d, *J* = 8.5 Hz, 2H), 6.43 (bs, 1H), 5.10 (d, *J* = 1.4 Hz, 2H), 4.34 – 4.27 (m, 1H), 3.92 (s, 2H), 3.27 (dd, *J* = 9.4, 5.2 Hz, 1H), 3.23 (dd, *J* = 9.3, 5.2 Hz, 1H), 2.85 (dd, *J* = 16.6, 3.4 Hz, 1H), 2.64 (dd, *J* = 16.4, 8.8 Hz, 1H), 1.51 (s, 9).^{13}C NMR (100 MHz, $CDCl_3$) δ: 170.22, 169.61, 164.80, 153.23, 138.11, 135.91, 130.60, 129.18, 129.01, 128.88, 128.10, 119.24, 81.11, 67.31, 47.22, 43.05, 42.63, 37.16, 28.88. HPLC-MS (ESI^+): Rt = 10.7 min, m/z = 470 $[M+H_2O]^+$. IR (film): ν = 3350, 3113, 3062, 3034, 2977, 2930, 2854, 1791, 1702, 1613, 1595, 1525, 1455, 1414, 1366, 1319, 1266, 1235, 1161, 1053, 1027, 1018, 902, 838, 808, 736, 698 cm^{-1}.

*2-(1-(2-(4-((tert-butoxycarbonyl)amino)phenyl)acetyl)-4-oxoazetidin-2-yl)acetic acid (**3a**)*

Following GP2 compound **3** (40 mg, 0.09 mmol, 1 equiv) yielded compound **3a** as withe solid (34 mg, 99%). ^{1}H NMR (400 MHz, CD_3OD) δ: 7.33 (d, *J* = 8.2 Hz, 2H), 7.18 (d, *J* = 8.3 Hz, 2H), 4.31-4.23 (m, 1H), 3.94 (d, *J* = 3.5 Hz, 2H), 3.27 (dd, *J* = 16.4, 8.8 Hz, 1H), 3.09 (dd, *J* = 16.5, 3.5 Hz, 1H), 2.93 (dd, *J* = 16.5, 3.2 Hz, 1H), 2.65 (dd, *J* = 16.4, 8.8 Hz, 1H), 1.51 (s, 9H).

^{13}C NMR (100 MHz, CD_3OD) δ: 171.59, 167.21, 156.03, 140.14, 131.42, 129.63, 120.41, 81.99, 55.49, 43.81, 43.36, 37.16, 29.25. HPLC-MS (ESI^+): Rt = 7.4 min, m/z = 380 $[M+H_2O]^+$. IR (film): ν = 3341, 3057, 2979, 2932, 1790, 1713, 1613, 1596, 1525, 1415, 1392, 1367, 1319, 1268, 1236, 1160, 1056, 1028, 984, 901, 862, 809, 772, 737, 703 cm^{-1}.

*4-(2-(2-(carboxymethyl)-4-oxoazetidin-1-yl)-2-oxoethyl)benzenaminium trfluororacetate (**J**)*

Following GP3 compound **3a** (14 mg, 0.04 mmol, equiv) yielded compound **J** as yellow oil (11 mg, 73%). ^{1}H NMR (400 MHz, CD_3OD) δ: 7.45 (d, *J* = 8.5 Hz, 2H), 7.32 (d, *J* = 1.9 Hz, 2H), 4.30 (ddd, *J* = 10.0, 6.9, 3.6 Hz, 1H), 4.09 (s, 2H), 3.34 (dd, J= 16.6, 8.6 Hz, 1H), 3.08 (dd, *J* = 16.6, 3.8 Hz, 1H), 2.96 (dd, J= 16.6, 3.8 Hz, 1H), 2.71 (dd, *J* = 16.6, 8.6 Hz, 1H). ^{13}C NMR (100 MHz, CD_3OD) δ: 171.35, 167.28, 132.80, 123.72, 52.70, 43.69, 43.19, 37.17. HPLC-MS (ESI^+): Rt = 1.4 min, m/z = 263 $[M+H\text{-}TFA]^+$. IR (film): ν = 2957, 2925, 2865, 2619, 1791, 1681, 1516, 1434, 1410, 1370, 1330, 1309, 1275, 1201, 838, 799, 750, 723 cm^{-1}.

*Benzyl (2-(4-((tert-butoxycarbonyl)amino)phenyl)acetyl)-L-prolinate (**5**)*

To a solution of compound **4** (65 mg, 0.20 mmol, 1 equiv) in 1.8 mL of CH_2Cl_2, under nitrogen atmosphere, compound **14** (51 mg, 0.20 mmol, 1 equiv) and DMAP (12 mg, 0.1 mmol, 0.5 equiv) were added. The mixture was then cooled to 0 °C, and DCC (45 mg, 0.22 mmol, 1.2 equiv) was added; the system was allowed to reach room temperature in 15 min and left under stirring overnight. After 24 h (TLC monitoring), the reaction mixture was filtered washing with CH_2Cl_2 and evaporated. The crude was suspended in EtOAc at 0 °C, and the solid residual dicyclohexylurea was eliminated by filtration. The organic layer was concentrated in vacuum and purified by flash chromatography (Cyclohexane/EtOAc = 6:4). Compound **5** (38 mg; 43%) was obtained as colourless oil. ^{1}H NMR (400 MHz, $CDCl_3$) δ: 7.41 – 7.24 (m, 7H), 7.14 – 7.08 (m, 2H), 6.56 (bs, 1H), 5.93 (bs, 1H), 5.08 (s, 2H), 3.51-3.44 (m, 4H), 2.58 – 2.50 (m, 2H), 1.50 (s, 9H). ^{13}C NMR (100 MHz, $CDCl_3$) δ: 172.16, 171.33, 152.85, 137.78, 135.74, 129.98, 129.22, 128.70, 128.45, 128.30, 119.10, 80.65, 66.57, 43.14, 35.20, 34.11, 28.43. HPLC-MS (ESI^+): Rt = 10.1 min, m/z = 439 $[M+H]^+$. IR (film): ν = 3045, 1728, 1645, 1265, 738, 705 cm^{-1}. $[\alpha]_D^{20}$= 39.5 (c=1, CH_2Cl_2).

*2-(1-((4-((tert-butoxycarbonyl)amino)benzyl)carbamoyl)-4-oxoazetidin-2-yl)acetic acid (**5a**)*

Following GP2 compound **5** (38 mg, 0.09 mmol, 1 equiv) yielded compound **5a** as withe solid (26 mg, 83%).^{1}H NMR (400 MHz, CD_3OD) δ: 7.33 (d, J = 8.0 Hz, 2H), 7.16 (d, J = 8.0 Hz, 2H), 4.87 (s, 2H), 3.47-3.34 (m, 4H), 2.53-2.39 (m, 2H), 1.51 (s, 9H). ^{13}C NMR (100 MHz, CD_3OD) δ: 155.08, 139.17, 130.71, 130.18, 119.78, 80.58, 42.93, 36.43, 34.53, 28.49. IR (film): ν = 2978, 2931, 1720, 1600, 1526, 1451, 1238, 1161, 1028 cm^{-1}. HPLC-MS (ESI^+): Rt = 6.3 min, m/z = 349 $[M+H]^+$. $[\alpha]_D^{20}$= - 129 (c=1.2, MeOH).

*(S)-4-(2-(2-carboxypyrrolidin-1-yl)-2-oxoethyl)benzenaminium trfluororacetate (**K**)*

Following GP3 compound **5a** (26 mg, 0.07 mmol, 1 equiv) yielded compound **K** as yellow oil (25 mg, 99%). ^{1}H NMR (400 MHz, CD_3OD) δ: 7.43 (d, J = 8.0 Hz, 2H), 7.33 (d, J = 8.0 Hz,

2H), 3.55 (s, 2H), 3.43 (t, J = 6.7 Hz, 2H), 2.50 (t, J = 6.6 Hz, 2H).^{13}C NMR (100 MHz, CD_3OD) δ: 175.41, 138.51, 132.10, 130.92, 124.33, 43.08, 36.82, 34.73. IR (film): ν = 3307, 2929, 1715, 1668, 1621, 1516, 1454, 1191, 1141 cm^{-1}. HPLC-MS (ESI^+): Rt = 1.5 min, m/z = 249 $[M+H-TFA]^+$. $[\alpha]_D^{20}$= - 46 (c=1.6, MeOH).

*Dibenzyl L-aspartate p-toluensulfonic acid (**6**)*

Following GP1 L-aspartic acid (100 mg, 0,75 mmol, 1 equiv) yielded compound **6** as withe solid (240 mg, 66%). The spectroscopic data are in accordance to those reported in the literature.[182]

*Dibenzyl L-glutamate p-toluensulfonic acid (**7**)*

Following GP1 L-glutamic acid (100 mg, 0.68 mmol, 1 equiv) yielded compound **7** as withe solid (240 mg, 70%). The spectroscopic data are in accordance to those reported in the literature.[182]

*Dibenzyl (2-(4-((tert-butoxycarbonyl)amino)phenyl)acetyl)L-aspartate (**8**)*

Following GP4 compound **6** (55 mg, 0.11 mmol, 1 equiv) and compound **14** (28 mg, 0.11 mmol, 1 equiv) yielded compound **8** as withe solid (40 mg, 67%). ^{1}H NMR (400 MHz, $CDCl_3$) δ 7.38 – 7.15 (m, 11H), 7.08 (d, *J* = 8.5 Hz, 2H), 6.52 (s, 1H), 6.43 (d, *J* = 8.0 Hz, 1H), 5.06 (s, 2H), 4.99 (s, 2H), 4.89 – 4.83 (m, 1H), 3.47 (s, 2H), 3.01 (dd, *J* = 17.1, 4.6 Hz, 1H), 2.84 (dd, *J* = 17.1, 4.6 Hz, 1H), 1.50 (s, 9H). ^{13}C NMR (100 MHz, $CDCl_3$) δ 171.44, 171.03, 170.85, 153.33, 138.19, 135.87, 135.60, 130.44, 129.19, 129.14, 129.12, 129.00, 128.97, 128.86, 128.81, 119.41, 81.17, 68.09, 67.32, 49.32, 43.31, 36.84, 28.90. HPLC-MS (ESI^+): Rt = 10.7 min, m/z = 547 $[M+H]^+$ IR (film): ν = 3306, 3189, 3089, 3064, 3034, 2977, 2932, 1726, 1659, 1524, 1235, 1162, 1052, 737 cm^{-1}. $[\alpha]^{25}_D$ =11.2 (c=1, CH_2Cl_2).

*(2-(4-((tert-butoxycarbonyl)amino)phenyl)acetyl)L-aspartic acid (**8a**)*

Following GP2 compound **8** (40 mg, 0.073 mmol, 1 equiv) yielded compound **8a** as waxy solid (27 mg, 99%). ^{1}H NMR (400 MHz, CD_3OD) δ 7.34 (d, *J* = 8.2 Hz, 2H), 7.19 (d, *J* = 8.4 Hz, 2H), 4.79-4.68 (m, 1H), 3.51 (s, 2H), 2.91 – 2.75 (m, 2H), 1.51 (s, 9H). ^{13}C NMR (101 MHz, CD_3OD) δ 174.00, 155.28, 139.36, 130.58, 119.93, 80.81, 42.84, 36.90, 28.70. HPLC-MS (ESI^+): Rt = 4.6 min, m/z = 311 $[M+H]^+$. IR (film): ν = 3310, 2957, 2925, 2855, 1719, 1654, 1648, 1524, 1458, 1318, 1233 cm^{-1}. $[\alpha]^{20}_D$ = 5.3 (c=1, MeOH).

*(S)-4-(2-((1,2-dicarboxyethyl)amino)-2-oxoethyl)benzenaminium trfluororacetate (**L**)*

Following GP3 compound **8a** (27 mg, 0.073 mmol, 1 equiv) yielded compound **L** as yellow oil (30 mg, 99%). ^{1}H NMR (400 MHz, CD_3OD) δ 7.37 (d, *J* = 8.2 Hz, 2H), 7.18 (d, *J* = 8.3 Hz, 2H), 4.75 (dd, *J* = 12.4, 6.2 Hz, 1H), 3.60 (s, 2H), 2.89 – 2.75 (m, 2H). ^{13}C NMR (100 MHz, CD_3OD) δ 174.12, 173.17, 135.65, 131.50, 129.28, 129.23, 129.00, 122.20, 68.73, 42.33, 36. HPLC-MS (ESI^+): Rt = 1.2 min, m/z = 267 $[M+H]^+$. IR (film): ν = 3426, 2960, 2624, 1676, 1547, 1514, 1434, 1203, 1143. 59 cm^{-1}. $[\alpha]^{20}_D$ = 0.5 (c=1, MeOH).

*Dibenzyl ((4-((tert-butoxycarbonyl)amino)benzyl)carbamoyl)L-aspartate (**10**)*

To a solution of compound **6** (95 mg, 0.19 mmol, 1 equiv) and TEA (53 μL, 0.38 mmol, 2 equiv) in 1.2 mL of DCM, under a nitrogen atmosphere, the previously synthesized isocyanate **15** was added, and the reaction was left at rt overnight. At completion (TLC monitoring) the mixture was quenched with NH_4Cl and extracted with DCM. The organic layer was dried over Na_2SO_4, concentrated in vacuum, and purified by flash chromatography (from Cyclohexane/EtOAc = 7:3 to Cyclohexane/EtOAc = 6:4). Compound **10** (50 mg; 47%) was obtained as colourless oil. ^{1}H NMR (400 MHz, $CDCl_3$) 7.33-7.28 (m, 7H), 7.27-7.22 (m, 2H), 7.15 (d, *J* = 8.4 Hz, 2H), 6.51 (bs, 1H), 5.07 (s, 2H), 5.00 (d, *J* = 2.9 Hz, 2H), 4.84 (t, *J* = 4.3 Hz, 1H), 4.24 (s, 2H), 3.05 (dd, *J* = 17.1, 4.6 Hz, 1H), 2.88 (dd, *J* = 17.0, 4.6 Hz, 1H), 1.50 (s, 9H).^{13}C NMR (101 MHz, $CDCl_3$) δ 172.25, 171.68, 157.81, 153.61, 138.08, 136.41, 134.38, 129.10, 129.07, 128.89, 128.80, 128.78, 128.72, 119.29, 67.94, 67.23, 50.23, 44.58, 37.72, 28.89. HPLC-MS (ESI+): Rt =10.5 min, m/z = 561 $[M+H]^+$. IR (film): ν = 3360, 2978, 2931, 1729, 1643, 1597, 1526, 1456, 1413, 1356, 1316, 1237, 1163, 1053 cm^{-1}. $[\alpha]_D^{20}$ = 4.7 (c=1, CH_2Cl_2).

*((4-((tert-butoxycarbonyl)amino)benzyl)carbamoyl)L-aspartic acid (**10a**)*

Following GP2 compound **10** (50 mg, 0.09 mmol, 1 equiv) yielded compound **10a** as waxy solid (35 mg, 98%). ^{1}H NMR (400 MHz, CD_3OD) δ 8.82 (s, 1H), 7.33 (d, *J* = 8.0 Hz, 2H), 7.19 (d, *J* = 8.3 Hz, 2H), 4.65 (s, 1H), 4.26 (s, 2H), 2.84 (d, *J* = 16.7 Hz, 2H), 1.51 (s, 9H).^{13}C NMR (101 MHz, CD_3OD) δ 155.79, 139.32, 135.13, 130.57, 128.60, 119.67, 80.56, 44.16, 38.28, 28.61. HPLC-MS (ESI+): Rt=4.4 min, m/z = 382 $[M+H]^+$. IR (film): ν = 3339, 2979, 2931, 1714, 1644, 1616, 1598, 1529, 1414, 1393, 1368, 1316, 1242, 1162, 1056 cm^{-1}. $[\alpha]_D^{20}$ = 12.5 (c=1, MeOH).

*(S)-4-((3-(1,2-dicarboxyethyl)ureido)methyl)benzenaminium benzenaminium trfluororacetate (**M**)*

Following GP3 compound **10a** (35 mg, 0.0926 mmol, 1 equiv) yielded compound **M** as yellow oil (22 mg, 84%). ^{1}H NMR (400 MHz CD_3OD,) δ 7.45 (d, J = 7.7 Hz, 2H), 7.29 (d, J = 7.1 Hz, 2H), 4.61 (s, 1H), 4.38 (s, 2H), 2.84 (m, 2H). ^{13}C NMR (100 MHz, CD_3OD) δ 141.50, 138.33, 129.50, 123.52, 43.85, 42.14, 30.57. HPLC-MS (ESI+): Rt =1.3 min, m/z = 282 $[M+H]^+$. IR (film): ν = 3369, 2926, 2615, 1713, 1672, 1652,1567, 1515, 1199, 1141, 842 cm^{-1}. $[\alpha]_D^{20}$ = 4.6 (c=1, MeOH).

*Dibenzyl (2-(4-((tert-butoxycarbonyl)amino)phenyl)acetyl)L-glutamate (**9**)*

Following GP4 compound **7** (210 mg, 0.48 mmol, 1 equiv) and compound **14** (122 mg, 0.48 mmol, 1 equiv) yielded compound **9** as withe solid (157 mg, 56%). ^{1}H NMR (400 MHz, $CDCl_3$) δ: 7.39 – 7.26 (m, 12H), 7.14 (d, *J* = 8.3 Hz, 2H), 6.54 (bs, 1H), 6.13 (d, *J* = 7.8 Hz, 1H), 5.11 (s, 2H), 5.05 (s,2H), 4.68 – 4.61 (m, 1H), 3.50 (s, 2H), 2.42 – 2.26 (m, 2H), 2.19 (td, *J* = 13.3, 6.7 Hz, 1H), 1.94 (td, *J* = 14.2, 7.8 Hz, 1H), 1.52 (s, 9H).^{13}C NMR (100 MHz, $CDCl_3$) δ: 172.80, 171.78, 171.56, 153.12, 138.07, 136.04, 135.43, 130.26, 129.02, 128.95, 128.90, 128.81, 128.62, 128.58, 128.57, 119.26, 81.13, 67.37, 66.51, 52.13, 43.10, 30.49, 28.68, 27.41. HPLC-MS

(ESI$^+$): Rt = 9.8 min, m/z = 561 [M+H]$^+$. IR (film): ν = 3342, 1728, 1696, 1648, 1521, 1240, 1154, 1056, 807, 734, 695 cm^{-1}. $[\alpha]_D^{20}$= -1.7 (c=1, CH_2Cl_2).

*(2-(4-((tert-butoxycarbonyl)amino)phenyl)acetyl)L-glutamic acid (**9a**)*

Following GP2 compound **9** (150 mg, 0.27 mmol, 1 equiv) yielded compound **9a** as waxy solid (102 mg, 99%). ^{1}H NMR (400 MHz, CD_3OD) δ: 7.34 (d, *J* = 8.1 Hz, 2H), 7.20 (d, *J* = 8.2 Hz, 2H), 4.43 (dd, *J* = 8.6, 4.9 Hz, 1H), 3.51 (s, 2H), 2.37 (t, *J* = 7.4 Hz, 2H), 2.24 – 2.12 (m, 1H), 2.00-1.88 (m, 1H), 1.51 (s, 9H).^{13}C NMR (100 MHz, CD_3OD) δ: 176.59, 174.28, 155.57, 139.44, 139.35, 130.87, 130.46, 119.93, 81.37, 53.17, 42.85, 31.17, 28.70, 27.90. HPLC-MS (ESI$^+$): Rt = 3.9 min, m/z = 381 [M+H]$^+$. IR (film): ν = 2922, 2256, 2113, 1990, 1706, 1524, 1415, 1237, 1160, 814 cm^{-1}. $[\alpha]_D^{20}$= -8 (c=1, MeOH).

*(S)-4-(2-((1,3-dicarboxypropyl)amino)-2-oxoethyl)benzenaminium trfluororacetate (**N**)*

Following GP3 compound **9a** (102 mg, 0.27 mmol, 1 equiv) yielded compound **N** as yellow oil (100 mg, 99%).^{1}H NMR (400 MHz, CD_3OD) δ: 7.46 (d, *J* = 8.1 Hz, 2H), 7.33 (d, *J* = 8.1 Hz, 2H), 4.43 (dd, *J* = 8.9, 4.9 Hz, 1H), 3.64 (s, 2H), 2.38 (t, *J* = 7.4 Hz, 2H), 2.19 (dt, *J* = 13.3, 7.8 Hz, 1H), 1.95 (dt, *J* = 15.0, 7.8 Hz, 1H).^{13}C NMR (100 MHz, CD_3OD) δ: 175.72, 174.54, 173.09, 137.67, 131.45, 130.09, 123.59, 52.95, 42.04, 30.62, 27.23. HPLC-MS (ESI$^+$): Rt = 1.3 min, m/z = 281 [M+H]$^+$. IR (film): ν = 2923, 2620, 1709, 1637, 1543, 1512, 1431, 1180, 1134, 838, 796, 721 cm^{-1}. $[\alpha]_D^{20}$= -8.5 (c=1, MeOH).

*Dibenzyl ((4-((tert-butoxycarbonyl)amino)benzyl)carbamoyl)L-glutamate (**11**)*

To a solution of compound **7** (40 mg, 0.08 mmol, 1 equiv) and TEA (22 μL, 0.16 mmol, 2 equiv) in 0.5 mL of DCM, under a nitrogen atmosphere, the previously synthesized isocyanate **15** was added, and the reaction was left at rt overnight. At completation (TLC monitoring) the mixture was quenched with NH_4Cl and extracted with DCM. The organic layer was dried over Na_2SO_4, concentrated in vacuum, ,and purified by flash chromatography (from Cyclohexane/EtOAc = 7:3 to Cyclohexane/EtOAc = 5:5). Compound **11** (29 mg; 67%) was obtained as colourless oil. ^{1}H NMR (400 MHz, $CDCl_3$) δ: 7.34 – 7.25 (m, 10H), 7.23 (d, *J* = 6.8 Hz, 2H), 7.13 (d, *J* = 8.5 Hz, 2H), 6.48 (bs, 1H), 5.09 (d, *J* = 3.7 Hz, 1H), 5.18 (d, *J* = 8.0 Hz, 2H), 5.04 (s, 2H), 4.88 (t, *J* = 5.7 Hz, 1H), 4.53 (td, *J* = 8.1, 5.1 Hz, 1H), 4.22 (d, *J* = 5.6 Hz, 2H), 2.46 – 2.30 (m, 2H), 2.15 (dt, *J* = 12.5, 7.4 Hz, 1H), 1.94 (dt, *J* = 14.7, 8.1 Hz, 1H), 1.49 (s, 9H).^{13}C NMR (100 MHz, $CDCl_3$) δ: 172.85, 172.76, 157.31, 152.76, 137.49, 135.77, 135.25, 133.47, 128.56, 128.53, 128.37, 128.23, 128.20, 128.17, 118.75, 80.72, 67.16, 66.40, 52.66, 44.01, 30.35, 28.32, 27.75. HPLC-MS (ESI$^+$): Rt = 9.9 min, m/z = 576 [M+H]$^+$. IR (film): ν = 3409, 3372, 3361, 3348, 3323, 3305, 3271, 3040, 2974, 1721, 1654, 1596, 1560, 1522, 1499, 1453, 1411, 1389, 1365, 1314, 1231, 1153, 1093, 1051, 821, 753, 695 cm^{-1}. $[\alpha]_D^{20}$= -0.6 (c=1, CH_2Cl_2).

*((4-((tert-butoxycarbonyl)amino)benzyl)carbamoyl)L-glutamic acid (**11a**)*

Following GP2 compound **11** (29 mg, 0.05 mmol, 1 equiv) yielded compound **11a** as waxy solid (20 mg, 99%). ^{1}H NMR (400 MHz, CD_3OD) δ: 8.78 (s, 1H), 7.29 (d, *J* = 8.2 Hz, 2H), 7.15 (d, *J*

= 8.4 Hz, 2H), 4.33-4.25 (m, 1H), 4.21 (s, 2H), 2.39 (dd, *J* = 17.5, 8.1 Hz, 2H), 2.21 – 2.03 (m, 1H), 1.93-1.81 (m, 1H), 1.47 (s, 9H).^{13}C NMR (100 MHz, CD_3OD) δ: 161.27, 156.27, 139.44, 135.01, 128.71, 119.93, 81.22, 54.56, 44.29, 31.31, 28.97, 28.71. HPLC-MS (ESI^+): Rt = 3.7 min, m/z = 396 $[M+H]^+$. IR (film): ν = 1701, 1633, 1615, 1594, 1522, 1450, 1411, 1393, 1366, 1338, 1314, 1238, 1157, 1094, 1055, 1017 cm^{-1}. $[\alpha]_D^{20}$= +1.5 (c=1, MeOH).

*(S)-4-((3-(1,2-dicarboxypropyl)ureido)methyl)benzenaminium benzenaminium trifluororacetate (**O**)*

Following GP3 compound **11a** (20 mg, 0.05 mmol, 1 equiv) yielded compound **O** as yellow oil (20 mg, 99%). ^{1}H NMR (400 MHz, CD_3OD) δ: 7.45 (d, *J* = 8.4 Hz, 2H), 7.33 (d, *J* = 8.4 Hz, 2H), 4.36 (d, *J* = 3.7 Hz, 2H), 4.33 (dd, *J* = 8.8, 5.0 Hz, 1H), 2.51 – 2.32 (m, 2H), 2.22 – 2.06 (m, 1H), 1.98 – 1.85 (m, 1H).^{13}C NMR (100 MHz, CD_3OD) δ: 176.45, 175.93, 142.83, 131.03, 130.73, 129.77, 123.99, 53.72, 43.88, 31.18, 28.67. HPLC-MS (ESI^+): Rt = 1.1 min, m/z =296 $[M+H\text{-}TFA]^+$. IR (film): ν = 3350, 2924, 2623, 1704, 1656, 1561, 1513, 1430, 1182, 1134, 1019, 839, 798, 775, 722 cm^{-1}. $[\alpha]_D^{20}$= -2 (c=1, CH_2Cl_2).

*Dibenzyl (o-tolylcarbamoyl)L-glutamate (**12**)*

To a solution of compound **7** (100 mg, 0.2 mmol, 1 equiv), dissolved in 2 mL of DCM, in a nitrogen atmosphere, TEA (60 μL, 0.42 mmol, 2.2 equiv) wad added. The reaction was left under stirring for 20 minutes and then *o*-tolyl isocyanate (30 μL, 0.21 mmol, 1.1 equiv) was added. After 4 h (TLC monitoring), the reaction mixture was quenched with NH_4Cl and extracted (x3) with EtOAc. The organic layer was dried over Na_2SO_4, concentrated in vacuum and purified by flash chromatography (Cyclohexane/EtOAc = 8:2). Compound **12** (55 mg; 60%) was obtained as colourless oil. ^{1}H NMR (400 MHz, $CDCl_3$) δ: 7.43 (d, *J* = 7.8 Hz, 1H), 7.36-7.27 (m, 10H), 7.18 (dd, *J* = 10.5, 7.4 Hz, 2H), 7.11 (d, *J* = 7.3 Hz, 1H), 6.52 (bs, 1H), 5.12 (q, *J* = 12.3 Hz, 2H), 5.05 (s, 2H), 4.65 (dd, *J* = 8.2, 5.0 Hz, 1H), 2.51 – 2.33 (m, 2H), 2.23 (s, 3H), 1.97 (dt, *J* = 14.5, 8.2 Hz, 1H). ^{13}C NMR (100 MHz, $CDCl_3$) δ: 172.26, 155.82, 135.38, 134.80, 130.57, 128.22, 128.17, 128.07, 127.88, 127.85, 127.82, 126.68, 125.61, 124.87, 66.91, 66.08, 52.26, 29.98, 27.28, 17.45. HPLC-MS (ESI^+): Rt = 9.3 min, m/z = 461 $[M+H]^+$. IR (film): ν = 2361, 2332, 1749, 1728, 1635, 1606, 1559, 1543, 1534, 1455, 1420, 1378, 1351, 1293, 1257, 1241, 1212, 1178, 1155, 1143, 1113, 967, 950, 753, 732, 694 cm^{-1}. $[\alpha]_D^{20}$= +6 (c=1, CH_2Cl_2).

*(o-tolylcarbamoyl)L-glutamic acid (**P**)*

Following GP2 compound **12** (55 mg, 0.12 mmol, 1 equiv) yielded compound **P** as waxy solid (31 mg, 99%). ^{1}H NMR (400 MHz, CD_3OD) δ: 7.48 (d, *J* = 7.9 Hz, 1H), 7.09 (dd, *J* = 16.7, 7.8 Hz, 2H), 6.96 (d, *J* = 7.4 Hz, 1H), 4.37 (t, J= 4, 1H), 2.47 – 2.32 (m, 2H), 2.21 (s, 3H), 1.93 (dt, *J* = 14.8, 8.0 Hz, 2H). ^{13}C NMR (100 MHz, CD_3OD) δ: 176.81, 158.62, 138.15, 131.79, 131.59, 127.61, 127.57, 125.59, 124.93, 53.87, 31.42, 29.06, 18.23. HPLC-MS (ESI+): Rt = 2.3 min, m/z = 281 $[M+H]^+$. IR (film): ν = 2362, 2342, 1735, 1701, 1686, 1647, 1629, 1618, 1577, 1560, 1509, 1499, 1288, 1228, 1213, 1181, 769, 755, 740, 669 cm^{-1}. $[\alpha]_D^{20}$= +7 (c=1, MeOH).

*Benzyl 3-(2-(4-((tert-butoxycarbonyl)amino)phenyl)acetamido)propanoate (**13**)*

Following GP4 compound **14** (36 mg, 0.14 mmol, 1 equiv) and β-Alanine benzyl ester *p*-toluenesulfonate salt (50 mg, 0.14 mmol, 1 equiv) yielded compound **13** as withe solid (42 mg, 73%). ^{1}H NMR (400 MHz, $CDCl_3$) δ: 7.41 – 7.24 (m, 7H), 7.14 – 7.08 (m, 2H), 6.56 (bs, 1H), 5.93 (bs, 1H), 5.08 (s, 2H), 3.51-3.44 (m, 4H), 2.58 – 2.50 (m, 2H), 1.50 (s, 9H). ^{13}C NMR (100 MHz, $CDCl_3$) δ: 172.16, 171.33, 152.85, 137.78, 135.74, 129.98, 129.22, 128.70, 128.45, 128.30, 119.10, 80.65, 66.57, 43.14, 35.20, 34.11, 28.43. HPLC-MS (ESI^+): Rt = 9.3 min, m/z = 413 $[M+H]^+$. IR (film): ν = 3189, 2978, 2932, 1726, 1654, 1597, 1526, 1240, 1164, 1054, 737 cm^{-1}.

*3-(2-(4-((tert-butoxycarbonyl)amino)phenyl)acetamido)propanoic acid (**13a**)*

Following GP2 compound **13** (42 mg, 0.10 mmol, 1 equiv) yielded compound **13a** as withe solid (22 mg, 68%). ^{1}H NMR (400 MHz, CD_3OD) δ: 7.33 (d, J = 8.0 Hz, 2H), 7.16 (d, J = 8.0 Hz, 2H), 4.87 (s, 2H), 3.47-3.34 (m, 4H), 2.53-2.39 (m, 2H), 1.51 (s, 9H). ^{13}C NMR (100 MHz, CD_3OD) δ: 155.08, 139.17, 130.71, 130.18, 119.78, 80.58, 42.93, 36.43, 34.53, 28.49. HPLC-MS (ESI^+): Rt = 4.6 min, m/z = 340 $[M+H_2O]^+$. IR (film): ν = 2980, 1714, 1651, 1521, 1392, 1239, 1162, 738 cm^{-1}.

*4-(2-((2-carboxyethyl)amino)-2-oxoethyl)benzenaminium trfluororacetate (**Q**)*

Following GP3 compound **13a** (22 mg, 0.07 mmol, 1 equiv) yielded compound **Q** as yellow oil (24 mg, 99%). ^{1}H NMR (400 MHz, CD_3OD) δ: 7.43 (d, J = 8.0 Hz, 2H), 7.33 (d, J = 8.0 Hz, 2H), 3.55 (s, 2H), 3.43 (t, J = 6.7 Hz, 2H), 2.50 (t, J = 6.6 Hz, 2H). ^{13}C NMR (100 MHz, CD_3OD) δ:175.41, 138.51, 132.10, 130.92, 124.33, 43.08, 36.82, 34.73. HPLC-MS (ESI^+): Rt = 1.5 min, m/z = 223 $[M+H\text{-}TFA]^+$. IR (film): ν = 1675, 1514, 1200, 1139, 723 cm-1.

1.2 Novel N-thio substituted azetidinones with a potential activity as antitubercular agents

1.2.1 Tuberculosis

Tuberculosis is an infectious and contagious disease, among the top ten causes of death worldwide and is also the leading cause of death caused by a single infectious agent, the bacillus *Mycobacterium tuberculosis* (MTb). It usually affects the lungs (pulmonary tuberculosis) but can also affect other sites (extrapulmonary tuberculosis). The disease can affect anyone and anywhere, but most of the people with the disease (about 90%) are adults and the male/female ratio is 2/1. Worldwide, approximately 10 million people have tuberculosis every year.[183] In the transmission of the disease, the tubercle bacilli are inhaled and reach the pulmonary alveoli, where they are phagocytosed by macrophages and multiply. The contaminated macrophages create an envelope called granuloma, where the bacilli replicate; after a latent period, they escape and active disease develops (*Figure 48*). The manifestation depends on various factors such as age, the period of latent infection and, above all, on the patient's immune system.[184]

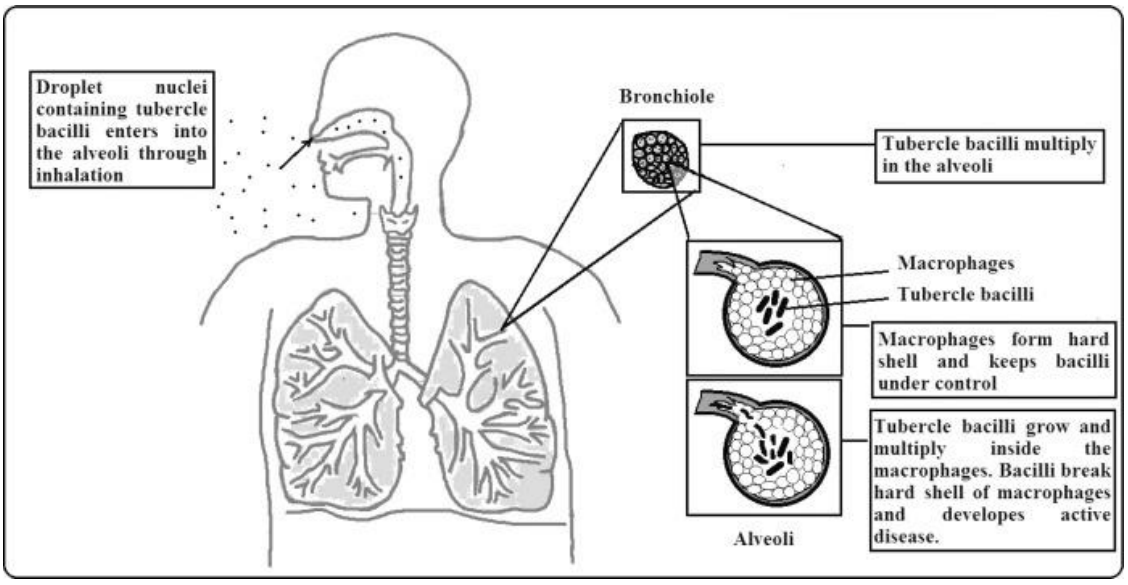

Figure 48. Pathogenesis of tuberculosis. Figure adapted from ref. 184.

The standard treatment regimen for drug-sensitive tuberculosis includes four active drugs: isoniazid, rifampicin, pyrazinamide and ethambutol, which are administered to the patient for a period of at least 6 months. A serious problem associated with the treatment of tuberculosis is the widespread emergence of the phenomenon of drug resistance. The exact cause of resistance is not well understood, but the genetic mutation is thought to be one of the main causes. Strains of *Mycobacterium tuberculosis* are classified according to resistance as: multi-drug resistant (MDR-TB), extensively drug resistant (XDR-TB) or totally drug resistant (TDR-TB). MDR-TB is an infection caused by MTb resistant at least to isoniazid and rifampicin, the two key drugs in therapeutic treatment. In 2006, a more resistant strain emerged, XDR-TB, resistant not only to isoniazid and rifampicin, but also to fluoroquinolones and second-line aminoglycosides. Treatment of XDR-TB requires the use of third-line anti-TB drugs, but these drugs have more side effects than first or second-line anti-TB drugs and hence the need to design selective drugs

for these resistant strains, that do not have too serious side effects on the patient's health, arises.[185]

Badalaquiline and Delamanid are the two new drugs recently approved. The first has a diarylquinoline as an active pharmaceutical ingredient (API) and acts on the mycobacterium by inhibiting the proton pump of the enzyme ATP synthase; it is the first antitubercular agent approved by the U.S. Food and Drug Administration. The second, Delamanid, has a nitroimidazole as API and acts on the mycobacterium by inhibiting the synthesis of mycolic acid, an important molecule for the life of the bacterium; it has been approved by the European Medicines Agency, but not by the FDA.[186] Other APIs such as Pretomanid, Linezolid, Sutezolid, Clofazimine and Carbapenem (imipenem-cilastatin, meropenem) are still in clinical phase II and III.[187] Some of the molecules mentioned and their mechanism of action are shown in *Figure 49*. Each drug has a specific objective and a defined mode of action; they are generally involved in cell wall biosynthesis, protein synthesis, DNA/RNA synthesis or metabolism of the bacterium MTb.

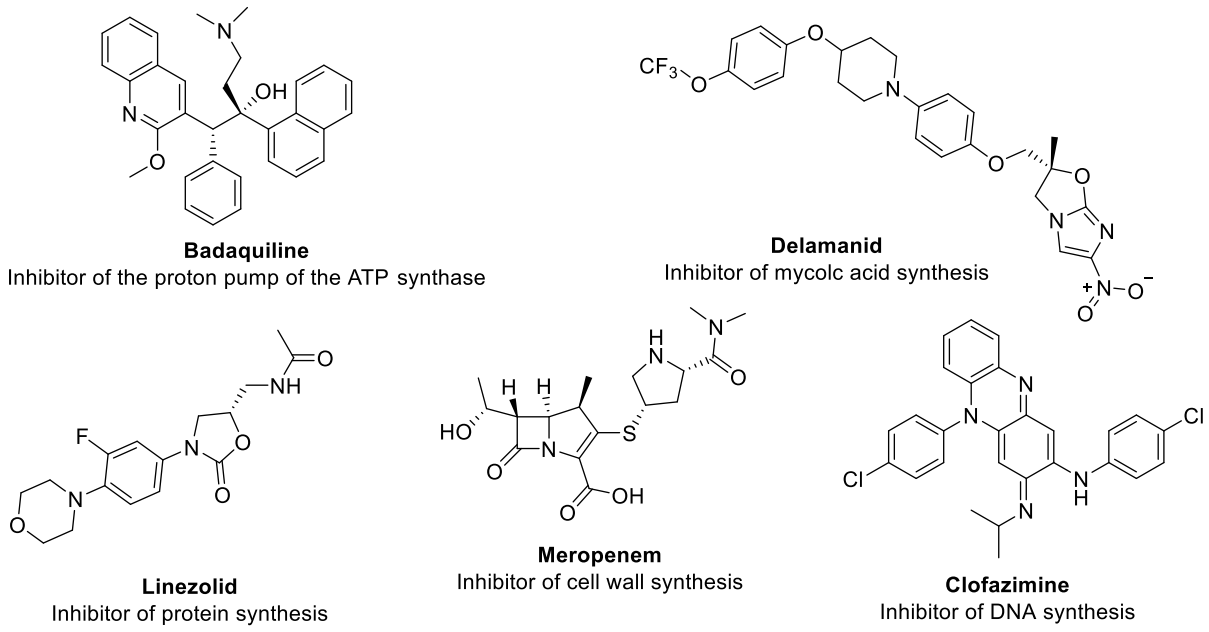

Figure 49. Antitubercular drug and their mechanism of action.

1.2.2 Cell wall of MbT

As previously anticipated, one of the pharmacological targets of tuberculosis is the cell wall of the mycobacterium; it remains beyond the cytoplasmic membrane and is composed of peptidoglycan, a polysaccharide covalently linked to arabinogalactan glycan, which is in turn bound to mycolic acids.[188]

Peptidoglycan (PG) is present in almost all bacteria and gives shape, rigidity and osmotic stability to the bacterial cell. It is a biopolymer and in all bacteria it has the same basic structure: a polysaccharide skeleton to which small cross-linked peptide chains are linked. The

polysaccharide skeleton typically consists of N-acetylglucosamine (NAG) and N-acetylmuramic acid (NAM) units linked by repeating β-1,4 glycosidic bonds.[189]
Mycobacterial peptidoglycan exhibits structural modifications; it has in fact been seen that PG isolated from MTb contains both N-acetylmuramic acid (NAM) and N-glycolylmuramic acid (NGM) (*Figure 50*) and that the presence of the latter increases the resistance of mycobacterial PG to lysozyme, enzyme that catalyzes the hydrolysis of the β-1,4 glycosidic bond between N-acetylmuramic acid and N-acetylglucosamine.[190]

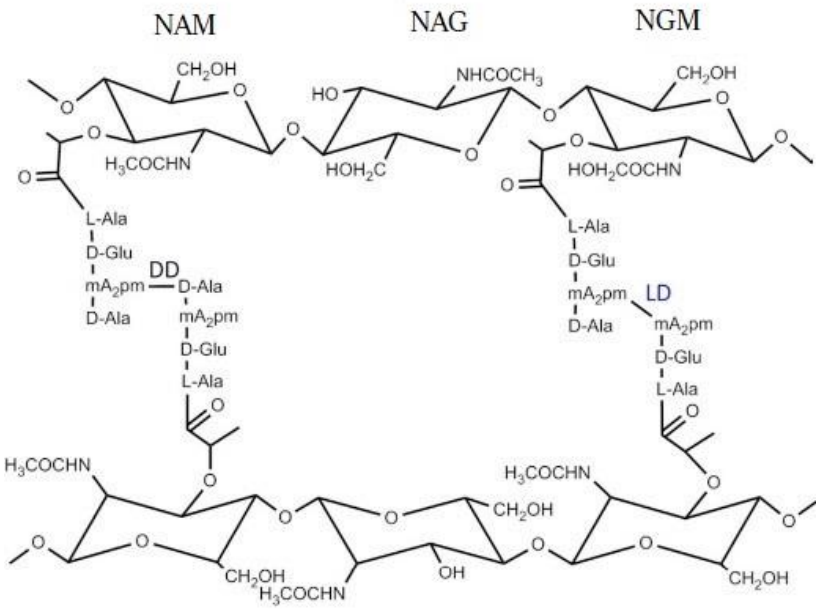

Figure 50. Structure of PG of mycobacterium. Figure adapted from ref. 190.

The pentapeptide chains L-Ala-D-γGlu-meso-DAP-D-Ala-D-Ala (DAP: diaminopimelate) are bound to the glycan filament through the lactic acid portion of NAM or NGM. These chains, empty of one or both of the D-Ala residues, bind to the peptide chains of another glycan filament, forming a cross-linked mesh responsible for the strength and rigidity of the entire structure. The formation of these cross-links is catalysed by D,D-transpeptidases (also called penicillin binding proteins, PBPs) and by L,D-transpeptidases (Ldt), from which 4,3 (D - Ala - DAP) and 3,3 (DAP - DAP) cross-links are obtained (*Figure 51*).[191]
3,3 crosslinks were first identified by Wietzerbin and his collaborators in the peptidoglycan of mycobacteria,[192] but their significance and biosynthetic pathway remained unknown until recently, when their predominance in MTb was demonstrated.[193] Indeed, while most bacteria contain mainly 3,4 crosslinks, the peptidoglycan of MTb contains a high density (up to 80%) of DAP-DAP crosslinks, especially in the stationary phase within the macrophage.[194]
The chromosome of the MTb H37Rv strain encodes five L,D-transpeptidases, indicated from Ldt_{Mt1} to Ldt_{Mt5}. Inactivation of the gene encoding Ldt_{Mt2} results in altered colony morphology, attenuation of persistence and increased susceptibility to amoxicillin in combination with clavulanate both in vitro and in a mouse model of tuberculosis, suggesting that L,D-transpeptidase activity is an important contributor to resistance and that inhibition of Ldt_{Mt2} alone may be sufficient to break 3,3 links even if Ldt_{Mt1} is present.[195]

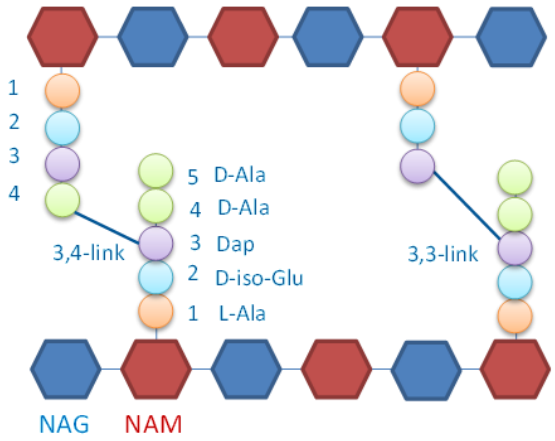

Figure 51. 3,4-peptide crosslinks formed by D,D-transpeptidases and the 3,3-peptide crosslinks dominating in M. tuberculosis cell wall, formed by L,D-transpeptidases. Figure adapted from ref. 196.

1.2.3 β-lactam-based antitubercular drugs

Antibiotics belonging to the β-lactam family for a long time have not been considered for the treatment of tuberculosis due to the presence of a class A (serine-dependent) β-lactamase produced by *Mycobacterium tuberculosis*, called BlaC. The interest in β-lactam derivatives in the treatment of tuberculosis has been renewed thanks to the characterization of BlaC and the evidence that the latter is irreversibly inhibited by clavulanic acid.[197]

Indeed, the mixture of Meropenem, whose target is Ldt_{Mt2}, and clavulanic acid showed activity on a mouse model of tuberculosis.[198] Six patients with severe pulmonary XDR-TB have also been clinically tested and the results were successful.[199] These collective facts brought Ldt_{Mt2} and β-lactam antibiotics in focus for future TB therapy.

The covalent adduct formation between the active-site cysteine of Ldt_{Mt2} and β-lactam type antibiotics (penam, penem, and carbapenem class) was shown by us and by others,[191,200] and it was established that the penem-type β-lactam, Faropenem, is the most effective on Ldt_{Mt2} as target.[200b]

Faropenem was the most successful β-lactam even in the absence of clavulanate in killing *M. tuberculosis* in in vitro cultures and inside macrophage.[201] Mass spectrometry and structural and biochemical analysis shed light on the mechanism of Faropenem (*Figure 52*) action on Ldt_{Mt2}. Following the nucleophilic attack by the active-site cysteine on the lactam ring of Faropenem, the primary adduct decomposes, leaving a small 86-Da fragment of the antibiotic (285 Da) attached to the cysteine in the active site, thus locking the enzyme in a non-reactive, dead-end complex.[191,200b] The detailed mechanism of adduct evolution was described recently;[202] additionally it was revealed that Faropenem follows a classical mechanism without decomposition after acyl-enzyme adduct formation when targeting the D,D-transpeptidase PBP3.[203]

These recent achievements suggest that the inhibition of peptidoglycan biosynthesis by β-lactam antibiotics following the Faropenem-type mechanism of action holds a potential for future TB therapy with Ld_{tMt2} as the target in focus.[196]

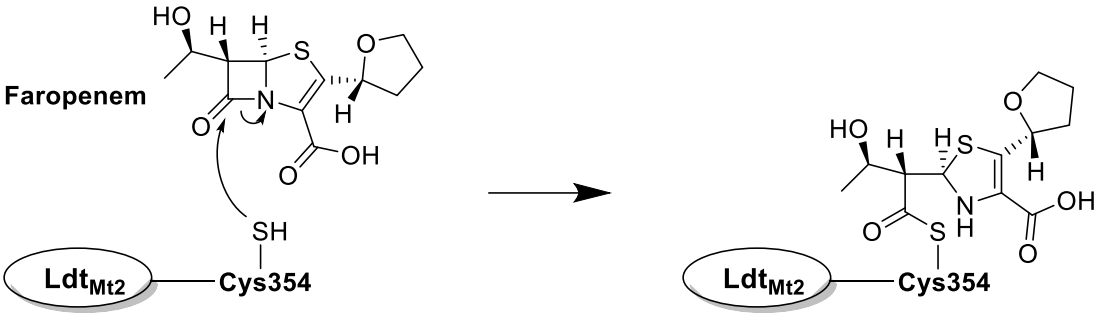

Figure 52. Formation of a stable covalent adduct with Faropenem.

Turos and his team reported the synthesis and biological evaluation of monocyclic β-lactams with an alkylthio group on the nitrogen atom of the ring with antibacterial activity against Bacillus and Staphylococcus species.[204] Their discovery was somewhat coincidental, because the research group was working on the synthesis of structural isomers of Penam (isopenam), but while these isopenams had no antibacterial action, their precursors with a methylthio- group showed a marked highly selective bacteriostatic action against *Staphylococcus aureus*, including the methicillin-resistant strain, commonly known as MRSA. The isopenams and their precursors under examination are shown in *Figure 53*.

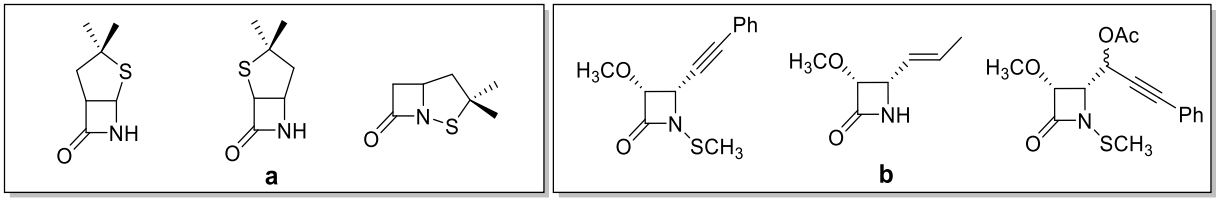

Figure 53. **a**) penam structural isomers; **b**) precursor used for the synthesis of the isopenam.

The results obtained led to the decision to deepen the study of this family of compounds and to understand if other variants of N-thio-β-lactams had antibacterial activity. From structure-activity relationship studies, many pieces of information emerged, the most important of which is that the thioalkyl group is essential to obtain bactericidal action and that these compounds can tolerate a wide range of substituents on C3 and C4 without altering their effects. This feature allows to carefully choose these substituents to regulate the lipophilicity of the molecule and, therefore, modulate its absorption by bacterial cells.[205,206] Further scanning electron microscopy (SEM) studies also revealed that these monocyclic N-thio-β-lactams did not produce alterations of the bacterial cell wall, therefore, differently from the classic β-lactams (eg. Penicillins), which inhibit enzymes responsible for cell wall cross-linking, these N-thio-β-lactams have a profoundly different mechanism of action.[207] To understand the mechanism of action of these N-thio-β-lactams, three pathways were considered, shown in *Figure 54*, of a possible nucleophilic attack by suitable protein residues of the bacterium:

- acylation with opening of the β-lactam ring
- alkylation
- Disulfide formation

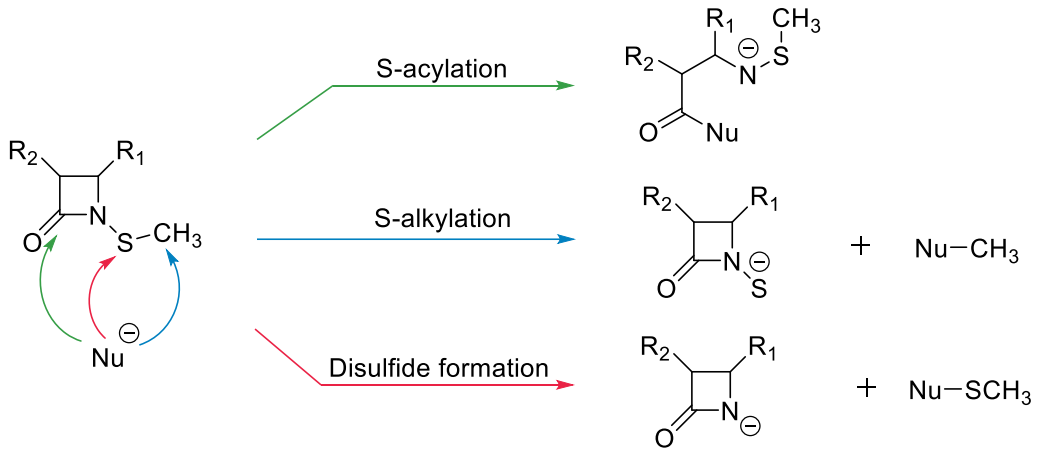

Figure 54. Mechanisms hypothesized for N-thio-β-lactams action.

The first path represented is acylation, the path commonly used by β-lactam antibiotics; the stability of these compounds towards acid or basic hydrolysis and towards β-lactamases demonstrates that this path is not the right mechanism. Subsequently, the second mechanistic possibility was considered, according to which the compounds could serve as alkylating agents towards cell nucleophiles. According to this mechanism, the nucleophilic attack on the carbon of the thioalkyl residue should be prevented by more voluminous and branched alkyl groups. Experimentally, the exact opposite result was found: N-ethylthio, N-isopropylthio and N-secbutylthio β-lactams are always more active than the N-methylthio derivative. Furthermore, also the lack of ability of these N-thioalkyl-β-lactams to alkylate bacterial biological components, such as DNA, confirmed that even the second mechanism is not the correct one.[208] Turos finally proposed that these N-thio-β-lactams exert their bactericidal action thanks to their thioalkylating power, and that their main target could be a cellular thiol (thiophil), with which the β-lactam reacts forming a mixed disulfide. It has been discovered that the thiophile involved is Coenzyme A and that therefore the inhibition of bacterial growth occurs by interrupting the work of CoA-dependent enzymes involved in the bacterial biosynthesis of fatty acids. These results lead to two important observations: the bacterial strains on which these compounds are not active are those deficient or lacking in CoA, which is replaced by glutathione with which the N-thio-β-lactams do not react; these molecules are of fundamental importance as a pro-drug for the formation of mixed disulfides whose direct introduction is not possible due to the hydrophilicity that prevents them from crossing the cell membrane.[209]
Professor Giacomini's research team developed a library of new bioactive N-thio substituted β-lactam compounds (*Figure 55*) which have shown various interesting biological activities as antitubercular agents.[196]

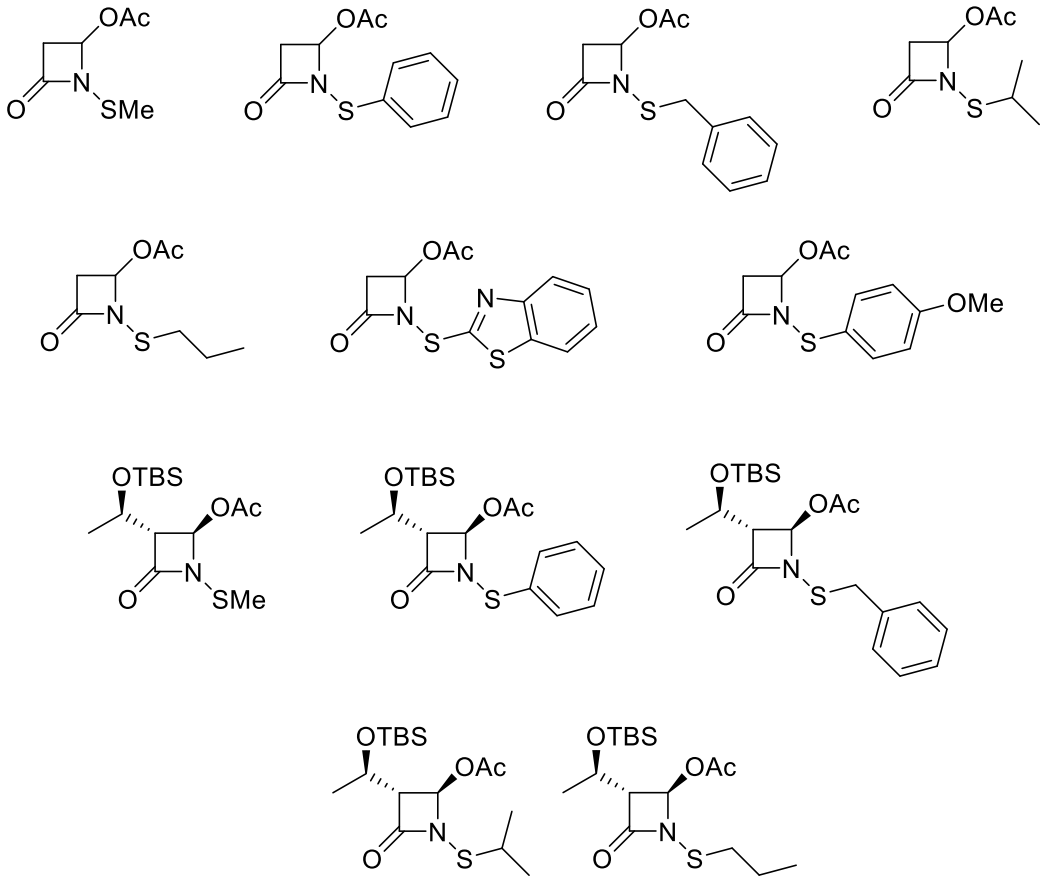

Figure 55. N-thio-β-lactams synthesized by Giacomini's research group.[196]

These new monocyclic N-thio-β-lactam compounds target L,D-transpeptidase-2 (Ldt_{Mt2}). Single-turnover enzyme kinetic data showed that the best candidates are comparable or faster than meropenem and other carbapenems with regards to their binding kinetics when evaluated on the same molecular target Ldt_{Mt2}. The kinetic and mass spectrometric analysis indicated covalent binding of a smaller fragment of the compounds at the active-site cysteine, Cys354 of the target protein. The adduct-mass values pointed at attachment of the alkylthio or aryl-thio moieties from the various N-thio-β-lactams. Five X-ray structures of the protein with the respective adducts bound revealed the nature of these covalent modifications. These N-thio-β-lactam compounds transferred their respective alkylthio or arylthio moieties onto Cys354, resulting in the mixed disulfide adducts, previously anticipated.

The kinetic and mass spectrometric data consistently showed that the adducts exhibit a long lifetime and suggest a long-term stable inactivation of the target protein. The five high-resolution X-ray structures revealed that these small fragments induce the closure of the active-site lid module, thus protecting the covalent modification and blocking the binding site of the substrate, further mitigating the stability of the dead-end complex. Moreover, the X-ray structures will be fruitful in modelling future derivatives. The most active compounds (*Figure 56*) showed growth inhibition in the μg/mL concentration range against *M. tuberculosis* strains in culture, including multidrug-resistant clinical isolates.[196]

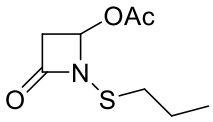

MIC = 20 μg/mL

Figure 56. N-thio-β-lactam synthesized by Giacomini's research group which gave the best results.[196]

Thanks to the aforementioned relevant results obtained by the research group on the development of new N-thio-β-lactam-based antitubercular agents, we decided to expand the library of these compounds. They will be then tested in collaboration with the research group of Prof. Schnell and Dr. Dal Monte and these new results will also be useful to carry out studies of structure-activity relationship.

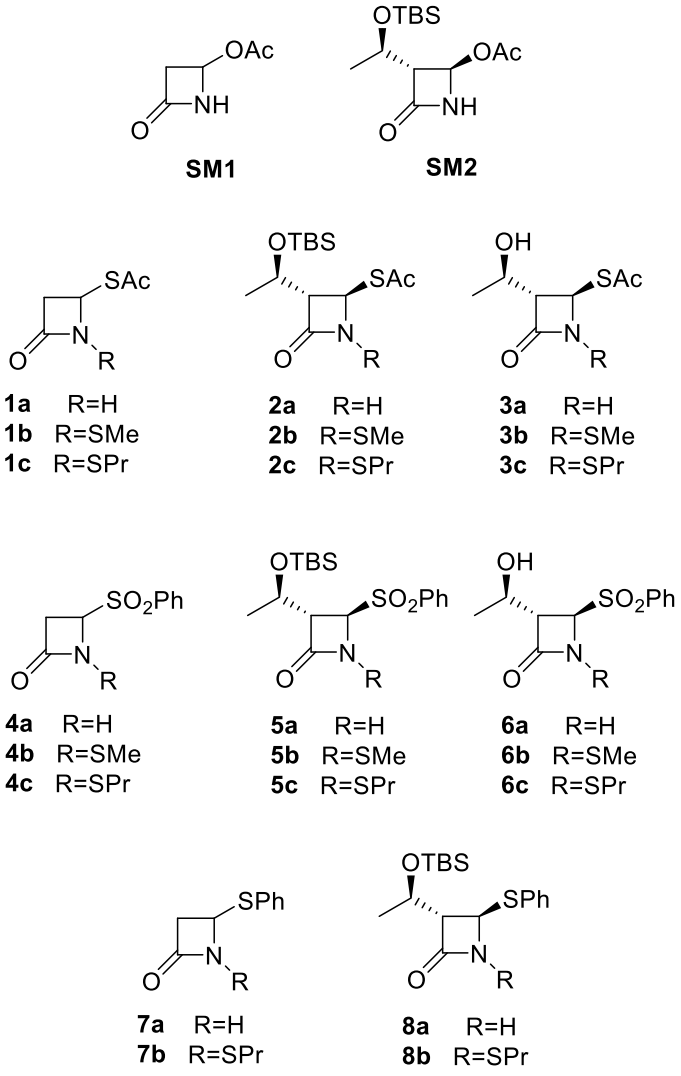

Figure 57. N-thio-β-lactams target molecules of the project.

Results and discussion

We developed and synthesized three series of azetidinones that differ for the functional group at the C4 position of the β-lactam ring. This position, starting from the commercial compounds **SM1** and **SM2**, was in fact functionalized with thioacetate (-SAc), benzenesulfinate (-SO2Ph) and thiophenate (-SPh) groups. In addition, for each series, the N-thiomethylation and N-thiopropylation reactions were carried out, except for the last series on which only N-thiopropylation was tested. Furthermore, the compounds of the first two series containing the *tert*-buthyldimethylsilyl functionality (TBS) underwent the deprotection reaction in order to obtain also the compounds with free alcohol (*Figure 57*).
Furthermore, it is important to specify that structures that have no stereochemical indications are in a racemic mixture and are obtained from **SM1**. Stereochemical details will be evaluated in the following section.

Synthesis of 4–SAc series

The thioacetate derivatives were obtained from the commercially available **SM1** and **SM2** precursors, through a nucleophilic substitution reaction with potassium thioacetate (CH_3COSK).

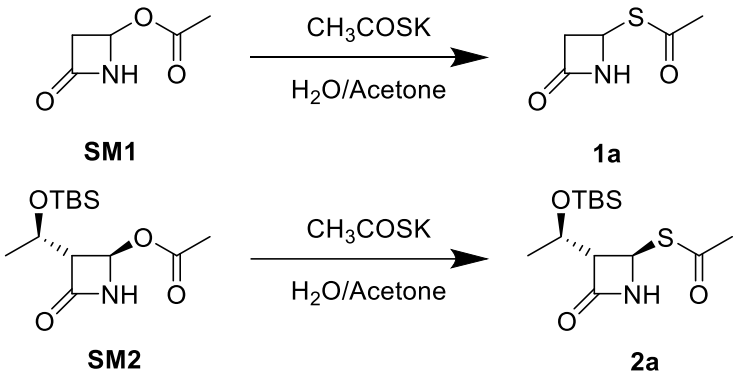

Scheme 16. Synthesis of compound **1a** and **2a**.

For the synthesis of compound **1a**, represented in *Scheme 16*, several tests were carried out in order to optimize the reaction conditions. The results are reported in *Table 4*.

Table 4. Synthesis optimization for compound **1a**.

Entry	SM1 (eq)	CH_3COSK (eq)	Acetone/H_2O	Temperature	Time	Yield (%)
1	1	1.2	1/3	r.t.	16h	45
2	1	1.2	1/3	0°C	1.5h	Mixture **SM**:**1a**=65:35
3	1	1.2	1/3	45°C	1.5h	65
4	1	1.2	1/3	45°C	45min	99

We can observe that four tests were carried out keeping the ratio between the reactants and between the two solvents (acetone/water) constant but changing time and temperature. What emerges is that the best reaction conditions are obtained with a temperature of 45°C for a reaction time of 45 minutes. At room temperature the reaction takes too long (16 h) and moreover a good yield is not obtained, probably due to the low stability of **SM1** in H_2O for such a long time. At 0°C the reaction did not reach the completion and a mixture of **SM1** and **1a** is obtained (*Table 4*, entry 2). On the other hand, in entry 3 (*Table 4*) the low yield can be explained by the formation of a by-product that has been isolated and which derives from the opening of the β-lactam ring **1a** mediated by thioacetate (*Scheme 17*).

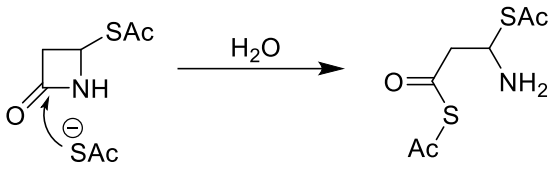

Scheme 17. By-product formation.

The problem of the formation of the by-product was solved by carefully monitoring the progresses of the reaction and reducing its time; in fact, quantitative yields are so obtained (*Table 4*, entry 4) and the raw material of the reaction did not require any purification.

Tests for the optimization of the reaction were also carried out for the synthesis of compound **2a**; they are summarized in *Table 5*.

Table 5. Synthesis optimization for compound **2a**.

Entry	**SM2 (eq)**	**CH_3COSK (eq)**	**Acetone/H_2O**	**Temperature**	**Time**	**Yield (%)**
1	1	1.2	1/2,5	r.t.	20h	Mixture **SM2**:**2a**=45:55
2	1	1.2	1/1	45°C	1.5h	Mixture **SM2**:**2a**=35:65
3	1	1.2	1/1	45°C	6h	99

The azetidinone **SM2** is poorly soluble in H_2O and for this reason it was necessary to increase the amount of acetone in the mixture (*Table 5*, entries 2-3). Moreover, longer reaction times are required respect to **SM1**. However, also in this case excellent yields were obtained, and the raw product did not require any purification.
Once the thioacetate derivatives **1a** and **2a** were obtained, the N-thioalkylation reaction was carried out using a methodology already developed by the research group (*Scheme 18*).

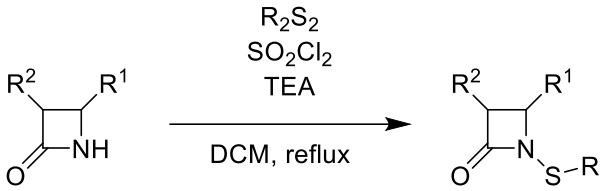

***Scheme 18**. N-thio alkylation.*

This methodology provides the use of the alkyl disulfide (R_2S_2) and of the sulfuryl chloride (SO_2Cl_2) to form the reactive species RSCl *in situ*. Subsequently, β-lactam and TEA were added; the reaction is then brought to reflux to give the N-thioalkylated product.
Sulfuryl chloride is already known as a source of chlorine,[210] for this reason the research group decided to exploit this ability; the hypothesized the reaction mechanism is reported in *Scheme 19*.

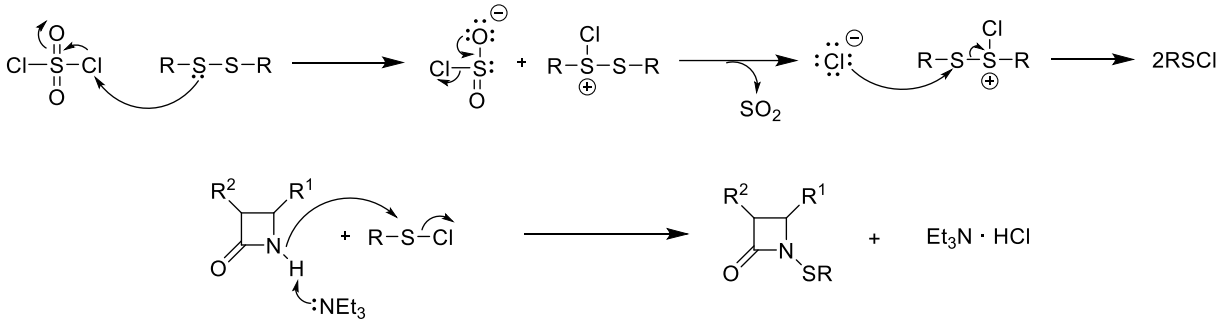

***Scheme 19**. N-thio alkylation mechanism.*

Using this methodology, N-thiomethylation and N-thiopropylation reactions were performed on compounds **1a** and **2a**.

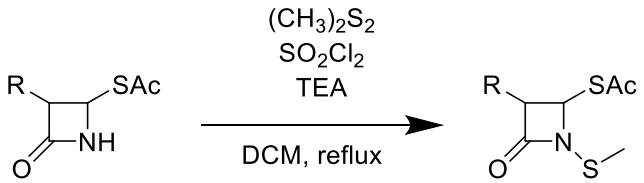

***Scheme 20**. N-thio methylation reaction of 4-SAc series.*

The products **1b** and **2b** were obtained using the reaction conditions optimized by the group: 1 equiv of β-lactam (**1a** or **2a**), 1 equiv of $(CH_3)_2S_2$, 1.5 equiv of SO_2Cl_2 and 2 equiv of TEA. Similarly, the N-thiopropyl compounds **1c** and **2c** were synthesized.

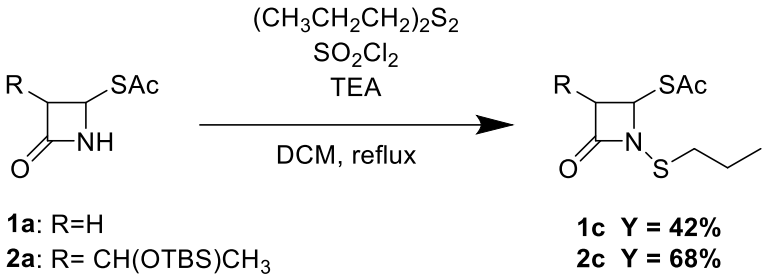

Scheme 21. *N*-thio propylation reaction of 4-SAc series.

Due to the low yields obtained for compound **1b** and **2b**, for the N-thio propylation reaction we decided to increase the equivalents of the reagents (1 equiv of β-lactam **1a** or **2a**, 1.2 equiv of $(CH_3)_2S_2$, 1.8 equiv of SO_2Cl_2 and 2 equiv of TEA). Nevertheless, high yields were not obtained. Finally, the deprotection reaction was carried out on the synthesized compounds **2a**, **2b**, and **2c** (*Scheme 22*). The procedure used has already been optimized by the research group[211] and involves the use of $BF_3 \cdot Et_2O$ in acetonitrile.

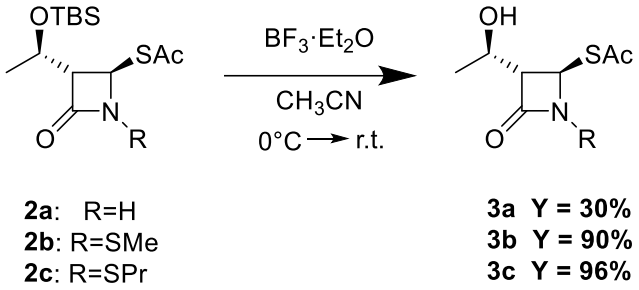

Scheme 22. Deprotection reaction of OTBS of 4-SAc series.

Synthesis 4–SO_2Ph series

The -SO_2Ph group was inserted through a nucleophilic substitution reaction performed by sodium benzenesulfinate ($NaSO_2Ph$) on the 4-acetoxy derivatives **SM1** and **SM2**.
Although the reaction for the **SM1** substrate is already reported in the literature,[212] it showed yield problems and for this reason an optimization process was necessary (*Table 6*).

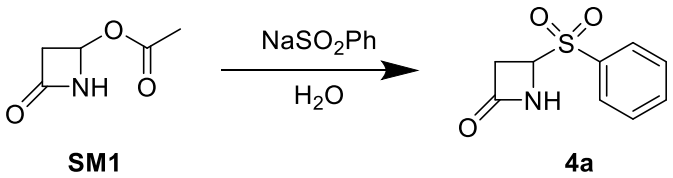

Scheme 23. Synthesis of compound **4a**.

Table 6. Synthesis optimization for compound **4a**.

Entry	SM1 (eq)	$NaSO_2Ph$ (eq)	Solvent	Temperature-time	Filtrate	Extracted	Yield (%)
1[a]	1,1	1,15	H_2O	100°C 20 min	/	45mg (DCM)	19
2[b, d]	1,1	1,15	H_2O/Acetone 3/1	45°C 4h	/	Mixture **SM1**:**4a** 45:55 (DCM)	57
3[b, d]	1,1	1,15	H_2O/Acetone 3/1	45°C 2,5h + overnight r.t.	/	Mixture **SM1**:**4a** 15:85 (DCM)	52
4[b, d]	1	1,2	H_2O/Acetone 3/1	55°C 6h + overnight r.t.	/	Mixture **SM1**:**4a** 25:75 (DCM)	47
5[c]	1	1,5	H_2O	60°C 2h + overnight r.t.	49 mg	97mg (EtOAc)	69
6[c, e]	1	1,5	H_2O	60°C 3h + overnight r.t.	91 mg	21mg (EtOAc)	53

[a] To β-lactam in H_2O, $NaSO_2Ph$ was added and the reaction mixture was brought to 100°C.
[b] To a solution of $NaSO_2Ph$ in H_2O β-lactam was dropped.
[c] H_2O was warmed and then β-lactam e $NaSO_2Ph$ were added.
[d] Yield calculated after trituration.
[e] Filtration at 0°C.

Entry 1 (*Table 6*) was performed following the reaction conditions reported in the literature:[212] $NaSO_2Ph$ is added to a solution of the β-lactam in H_2O and the reaction was brought to 100°C; after 20 minutes the work-up was performed. As anticipated, however, the yields were very low, therefore we decided to try the reaction with the same conditions used in the nucleophilic substitution on the 4-SAc series (*Table 6*, entries 2-3): $NaSO_2Ph$ was solubilized in H_2O, the mixture was brought to 45°C and then the azetidinone solubilized in acetone was dropped into.
To permit the complete consumption of **SM1**, the equivalents of $NaSO_2Ph$ and the temperature were increased, but the problem was not solved (*Table 6*, entry 4). However, thanks to the poor solubility in DCM of the product **4a**, it was possible to eliminate the residues of **SM1** from the mixtures triturating with DCM at 0°C.
For the entries 5-6 (*Table 6)* only H_2O was used as solvent of the reaction to reach higher temperature (60° C). Moreover, the equivalents of $NaSO_2Ph$ were further increased and, considering the sensitivity of **SM1** to temperature, first the solvent was heated and then the reagents were added. Thanks to the absence of acetone compound **4a** was formed as a precipitate recovered by filtration. Moreover, the product remaining in the aqueous filtrate was extracted with EtOAc. These conditions resulted the best (*Table 6*, entry 5) but a last attempt to obtain

higher yields was made as reported in entry 6 (*Table 6)*, increasing the reaction time; but in this case the reaction proved to be time sensitive, showing lower yields.

The synthesis of compound **5a** was not performed under the same conditions due to the poor solubility in H_2O of **SM2**, so acetone was necessary as co-solvent.

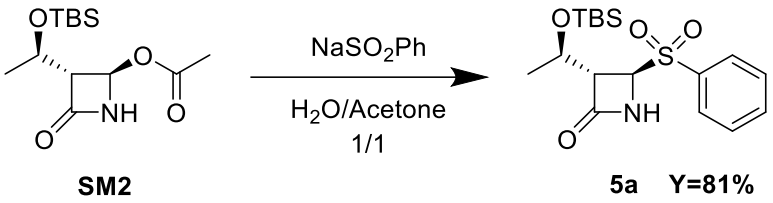

Scheme 24. Synthesis of compound **5a**.

$NaSO_2Ph$ was solubilized in H_2O, and the mixture was brought to 55°C and then the azetidinone **SM2** solubilized in acetone was dropped. The reaction is completed in 3 days and the product did not need any purification.

Similarly, to the 4-SAc series, the N-thioalkylation reaction was carried out on compounds **4a** and **5a**, but with some modification of the procedure.

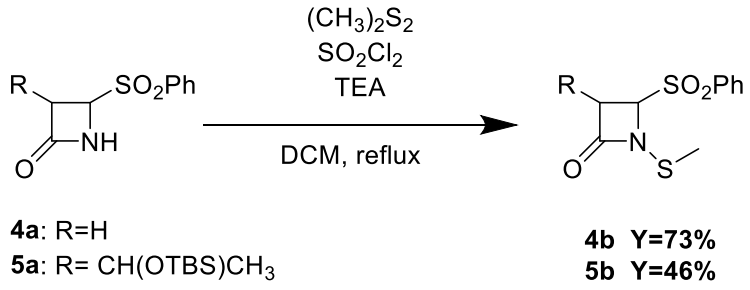

Scheme 25. *N*-thio methylation reaction of 4-SO_2Ph series.

Considering the problem of the persistence of the starting material for the 4-SAc series, it was decided to carry out the same procedure seen before but to make a second addition of the reagents. In fact, in a second flask, at 0°C under inert atmosphere, the disulfide and SO_2Cl_2 were mixed in DCM for 10 minutes. This mixture was then transferred into the reaction flask and TEA was also re-added. In that way, we observed complete conversion by TLC analysis. With this modification of the procedure, compound **4b** was obtained with a good yield, while compound **5b** was isolated with a lower yield; this low yield is caused by the formation of a by-product identified by HPLC-MS and ^1H NMR analyses (*Figure 58*).

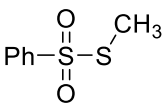

Figure 58. By-product in synthesis of **5b**.

With this optimized technique, the N-thiopropyl β-lactams of this series, **4c** and **5c**, were synthesized with good yields.

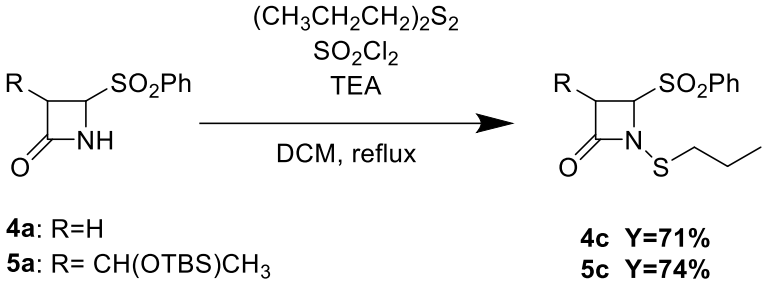

Scheme 26. *N*-thio propylation reaction of 4-SO_2Ph series.

The deprotection reaction was carried out on the products containing the protective group *tert*-buthyldimethylsilyl (**5a**, **5b**, **5c**).

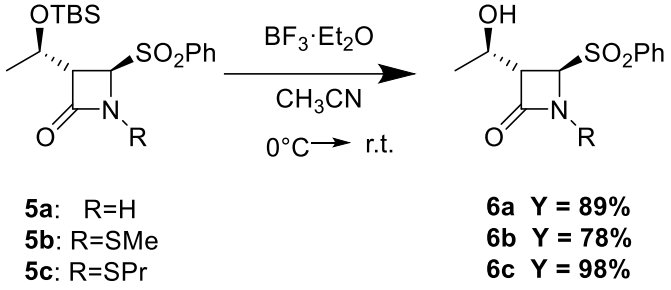

Scheme 27. Deprotection reaction of OTBS of 4-SO_2Ph series.

Sintesi della serie 4–SPh

-SPh group was inserted by a nucleophilic substitution reaction with sodium thiophenate (NaSPh) on 4-acetoxy derivatives **SM1** and **SM2**. The reagent was generated *in situ* starting from the disulfide (Ph_2S_2); it was reduced by sodium borohydride ($NaBH_4$), as reported in literature,[213] and subsequently the β-lactam was added. The reaction was conducted in two different solvents, ethanol e THF, on **SM1** (*Table 7*) and once obtained the best conditions, this procedure was also applied to **SM2**.

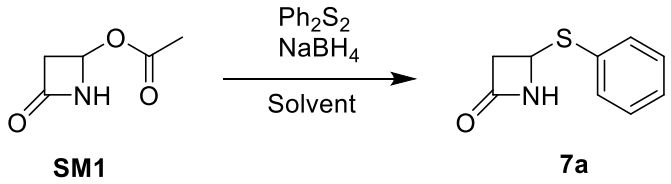

Scheme 28. Synthesis of compound **7a**.

Table 7. Synthesis optimization for compound **7a**.

Entry	Ph_2S_2 (eq)	$NaBH_4$ (eq)	SM1 (eq)	Solvent	Yield (%)
1	1.5	2.0	1.0	Ethanol	66
2	1.5	2.0	1.0	THF	/

In both the entries (*Table 7)*, Ph_2S_2 and $NaBH_4$ were dissolved in the reaction solvent and left under stirring for 3 hours. **SM1** was then added and the reaction monitored by TLC. For entry 1 (*Table 7)*, after 15 minutes, the total formation of the product was observed, then the ethanol was eliminated under vacuum and a liquid-liquid H_2O-EtOAc extraction was performed. The crude thus obtained was purified by flash chromatography, to eliminate the excess of disulfide; the desired product was so obtained with a good yield. In entry 2 (*Table 7*) instead the solvent was modified, using THF, but despite of considerably longer reaction times (1 day) than in entry 1, the presence of a large amount of **SM1** was observed from the analysis of the crude.

As anticipated, this reaction was also carried out on **SM2** using the conditions of entry 1 (*Table 7*).

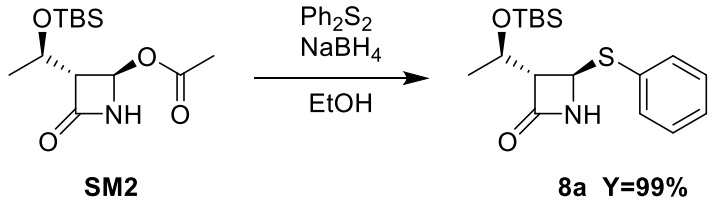

Scheme 29. Synthesis of compound **8a**.

A N-thiopropylation reaction (*Scheme 30*) was performed on compounds **7a** and **8a** with the methodology used for the other target products of this project. Unfortunately, on these substrates the reaction did not give the expected results. From ^1H NMR analysis, in fact, the presence of the desired products is not observed, but there are peaks attributable to polymeric species. Further evidence in support of this hypothesis was provided by the presence high masses in the HPLC-MS spectra. The structure of these species has not been yet identified.

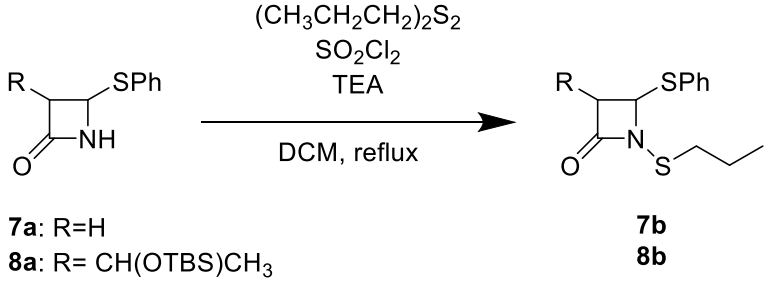

Scheme 30. *N*-thio propylation reaction of compounds **7a**-**8a**.

Conclusions

In this project three series of azetidinones that differ in the group at the C4 position of the β-lactam ring were synthesized to be tested as antitubercular agents, given the need to develop new drugs for the treatment of tuberculosis and in particular to overcome the problems deriving from drug resistance phenomena. Each series contains the products of the N-thiomethylation and N-thiopropylation reactions, except for the last series. Furthermore, the compounds of the first two series containing the *tert*-buthyldimethylsilyl functionality (TBS) were subjected to the deprotection reaction in order to obtain also the compounds with free alcoholic functionality. All synthetic steps were optimized and the products were obtained with good yields and with a high purity (HPLC analysis). Furthermore, both the reaction intermediates and the final molecules have been characterized by ^{1}H NMR, ^{13}C NMR, IR, HPLC-MS and for the chiral molecules also polarimetry has been done. Activity tests will be carried out in collaboration with the research group of Prof. Schnell of the Karolinska Institutet in Stockholm and Dr. Dal Monte of the Azienda Ospedaliero-Universitaria of Bologna. The results of these tests together with those already obtained for the previously tested library will be useful to deepen structure-activity relationship studies.

Experimental

Commercial reagents (reagent grade, >99%) and the commercially available azetidinones **SM1** and **SM2** were used as received (Sigma-Aldrich) without additional purification. Anhydrous solvents were obtained commercially from Sigma-Aldrich. All reactions were performed under an inert atmosphere (N2). TLC: Merck 60 F254 plates. Column chromatography: Merck silica gel 200-300 mesh. ^{1}H and ^{13}C NMR spectra were recorded with an INOVA 400 instrument with a 5 mm probe. All chemical shifts are quoted relative to deuterated solvent signals (δ in ppm and J in Hz). Polarimetric Analyses were conducted on Unipol L 1000 “Schmidt-Haensch” Polarimeter at 598 nm. FTIR spectra: Brucker instrument, measured as films between NaCl plates or CH_2Cl_2 solutions for solid compounds; wave numbers are reported in cm^{-1}. ATR-FTIR spectra: Alpha FT IR Bruker spectrometer with platinum ATR single reflection diamond module. As reference, the background spectrum of air was collected before the acquisition of each sample spectrum. Spectra were recorded with a resolution of 4 cm^{-1}, and 32 scans were averaged for each spectrum (scan range 4000–450 cm^{-1}). The purities of the target compounds were assessed as being >95% using HPLC-MS. Elemental analysis were performed on a Thermo Flash 2000 CHNS/O Analyzer. HPLC-MS: Agilent Technologies HP1100 instrument, equipped with a ZOBRAX-Eclipse XDB-C8 Agilent Technologies column; mobile phase: H_2O/CH_3CN, 0.4 mL/min, gradient from 30 to 80% of CH_3CN in 8 min, 80% of CH_3CN until 25 min, coupled with an Agilent Technologies MSD1100 single-quadrupole mass spectrometer, full scan mode from m/z = 50 to 2600, in positive ion mode, ESI spray voltage 4500 V, nitrogen gas 35psi, drying gas flow 11.5mL/min, fragmentor voltage 20 V.

S-(4-oxazetidin-2-yl) ethanthioate (**1a**)

To a solution of potassium thioacetate (1.2 mmol, 1.2 equiv) dissolved in H_2O (7.5 mL) and wormed at 45°C, **SM1** (1 mmol, 1 equiv) in acetone (2.5 mL) was added. The mixture was

stirred at room temperature until consumption of starting materials (45 min, TLC monitoring). After acetone elimination, the solution was extracted with EtOAc (x3) and the combined organic layers were dried over Na_2SO_4, filtered off, and concentrated under vacuo to give the product **1a** as a yellow oil (144 mg, 99%).
Spectroscopic data are in accordance to those reported in literature.[214]

S-((2R,3R)-3-(1-((tert-butyldimethylsilyl)oxy)ethyl)-4-oxoazetidin-2-yl) ethanethioate (**2a**)

To a solution of potassium thioacetate (1.2 mmol, 1.2 equiv) dissolved in H_2O (7.5 mL) and wormed at 45°C, **SM1** (1 mmol, 1 equiv) in acetone (2.5 mL) was added. The mixture was stirred at room temperature until consumption of starting materials (6 h, TLC monitoring). After acetone elimination, the solution was extracted with EtOAc (x3). and the combined organic layers were dried over Na_2SO_4, filtered off, and concentrated under vacuo to give the product **2a** as a yellow oil (302 mg, 99%).
Spectroscopic data are in accordance to those reported in literature.[215]

GP1: N-thio-alkylation (method A)

To a solution of disulfide (1-1.2 equiv) in DCM (2 mL/mmol) under a nitrogen atmosphere, SO_2Cl_2 (1,5-1.8 equiv) was added dropwise at a 0°C. After 10 minutes the β-lactam in DCM (2 mL/mmol), and TEA (2-2.4 equiv) were added. The mixture was warmed to room temperature and then stirred at reflux until consumption of starting materials (TLC monitoring). The reaction was quenched with NH_4Cl and extracted with DCM (x3). The combined organic layers were dried over Na_2SO_4, filtered off, and concentrated under vacuo. The crude compound was purified by flash chromatography.

GP2: N-thio-alkylation (method B)

To a solution of disulfide (1 equiv) in DCM (2 mL/mmol) under a nitrogen atmosphere, SO_2Cl_2 (1.5 equiv) was added dropwise at a 0°C. After 10 minutes the β-lactam in DCM (2 mL/mmol), and TEA (2 equiv) were added. The mixture was warmed to room temperature and then stirred at reflux. To favour the consumption of starting materials a second aliquot of thio-alkylation reagent was prepared in a second round bottom flask and added to the mixture at 0°C together with TEA. Then the mixture was warmed to room temperature and then stirred at reflux until consumption of starting materials (TLC monitoring). The reaction was quenched with NH_4Cl and extracted with DCM (x3). The combined organic layers were dried over Na2SO4, filtered off, and concentrated under vacuo. The crude compound was purified by flash chromatography.

GP3: OTBS-deprotection

To the desired β-lactam (1equiv) in CH_3CN (10 mL/mmol), under a nitrogen atmosphere at 0°C, $BF_3{\cdot}Et_2O$ (1.15 equiv) was added. The mixture was left under stirring for 45 minutes at 0°C and ther at room temperature until consumption of starting materials (TLC monitoring). The reaction was quenched with water and extracted with DCM (x3). The combined organic layers were dried over Na_2SO_4, filtered off, and concentrated under vacuo. The crude compound was purified by flash chromatography.

S-(1-(methylthio)-4-oxoazetidin-2-yl) ethanethioate (**1b**)

Following GP1, dimethyl disulfide and β-lactam **1a** (0.9 mmol), yielded compound **1b** (90 mg, 52%) as a brown oil.
Spectroscopic data are in accordance to those reported in literature.[211]

S-((2R,3R)-3-(1-((tert-butyldimethylsilyl)oxy)ethyl)-1-(methylthio)-4-oxoazetidin-2-yl) ethanethioate (**2b**)

Following GP1, dimethyl disulfide and β-lactam **2a** (0.3 mmol), yielded compound **2b** (45 mg, 43%) as a brown oil.
Spectroscopic data are in accordance to those reported in literature.[211]

S-(4-oxo-1-(propylthio)azetidin-2-yl) ethanethioate (**1c**)

Following GP1, diisopropyl disulfide and β-lactam **1a** (0.98 mmol), yielded compound **1c** (90 mg, 42%) as a brown oil. ^{1}H NMR: (400 MHz, $CDCl_3$) δ 5.43 (dd, J = 5.6, 2.9 Hz, 1H), 3.55 (dd, J = 15.4, 5.6 Hz, 1H), 3.07 (dd, J= 15.4, 2.9 Hz, 1H), 2.78 – 2.63 (m, 2H), 2.39 (s, 3H), 1.67 – 1.56 (m, 2H), 0.98 (t, J = 7.3 Hz, 3H).^{13}C NMR: (100 MHz, $CDCl_3$) δ 194.23, 169.38, 58.92, 46.03, 41.10, 31.56, 22.57, 13.54. IR (film): ν = 2962.6, 2931.4, 2872.8, 1768.4, 1697.0, 1457.8, 1410.4, 1354.8, 1280.1, 1238.3, 1154.5, 1125.1, 1040.7, 1009.7, 967.4, 947.2, 830.0, 619.1, 548.0 cm^{-1}. HPLC-MS (ESI^+): Rt = 6.5 min, m/z = 220 $[M+H]^+$.

S-((2R,3S)-3-((R)-1-((tert-butyldimethylsilyl)oxy)ethyl)-4-oxo-1-(propylthio)azetidin-2-yl) ethanethioate (**2c**)

Following GP1, diisopropyl disulfide and β-lactam **2a** (0.5 mmol), yielded compound **2c** (129 mg, 68%) as a brown solid. ^{1}H NMR (400 MHz, $CDCl_3$) δ 5.54 (d, J = 2.8 Hz, 1H), 4.27 – 4.15 (m, 1H), 3.25 (t, J = 3.2 Hz, 1H), 2.79 – 2.57 (m, 2H), 2.38 (s, 3H), 1.69 – 1.50 (m, 2H), 1.14 (d, J = 6.3 Hz, 3H), 0.95 (t, J = 7.3 Hz, 3H), 0.83 (s, 9H), 0.03 (s, 3H), 0.01 (s, 3H).^{13}C NMR (100 MHz, $CDCl_3$) δ 193.25, 169.82, 65.55, 64.52, 60.09, 40.55, 30.82, 25.54, 21.99, 21.88, 17.78, 12.93, -4.69, -5.09. IR (film): ν = 2958.9, 2929.0, 2881.4, 2855.7, 1772.3, 1701.6, 1459.6, 1329.35, 1281.5, 1254.8, 1124.3, 1069.2, 1039.2, 969.5, 952.7, 831.2, 776.1, 732.9, 664.9, 623.6 cm^{-1}. HPLC-MS (ESI^+): Rt = 12.0 min, m/z = 300 $[M+Na]^+$. $[\alpha]_D^{20}$ = + 33 (c=1, CH_2Cl_2). m.p. = 43-45°C.

S-((2R,3S)-3-((R)-1-hydroxyethyl)-4-oxoazetidin-2-yl) ethanethioate (**3a**)

Following GP3, β-lactam **2a** (0.99 mmol), yielded compound **3a** (54 mg, 30%) as a yellow solid.
Spectroscopic data are in accordance to those reported in literature**.**[216]

S-((2R,3R)-3-(1-hydroxyethyl)-1-(methylthio)-4-oxoazetidin-2-yl) ethanethioate (**3b**)

Following GP3, β-lactam **2b** (0.2 mmol), yielded compound **3b** (46 mg, 90%) as a yellow solid.
Spectroscopic data are in accordance to those reported in literature.[211]

S-((2R,3S)-3-((R)-1-hydroxyethyl)-4-oxo-1-(propylthio)azetidin-2-yl) ethanethioate (**3c**)

Following GP3, β-lactam **2c** (0.54 mmol), yelded compound **3c** (136 mg, 96%) as a yellow solid. ^{1}H NMR (400 MHz, $CDCl_3$) δ 5.49 (d, *J* = 2.7 Hz, 1H), 4.25 – 4.17 (m, 1H), 3.32 (dd, *J* = 4.8, 2.7 Hz, 1H), 3.06 (bs, 1H), 2.83 – 2.74 (m, 1H), 2.68 – 2.60 (m, 1H), 2.40 (s, 3H), 1.70 – 1.56 (m, 2H), 1.24 (d, *J* = 6.4 Hz, 3H), 0.97 (t, *J* = 7.3 Hz, 3H).^{13}C NMR (100 MHz, $CDCl_3$) δ 194.48, 170.49, 66.18, 64.57, 60.83, 40.74, 31.33, 22.16, 21.33, 13.30. IR (film): ν = 3414.5, 2963.3, 2931.2, 2871.5, 1750.0, 1694.2, 1332.1, 1301.36, 1280.7, 1126.0, 1037.8, 833.7, 626.7, 555.4 cm^{-1}. HPLC-MS (ESI^+): Rt = 5.5 min, m/z = 286 $[M+Na]^+$. $[\alpha]_D^{20}$ = - 12 (c=1, CH_2Cl_2). m.p. = 70-73°C.

4-(phenylsulfonyl)azetidin-2-one (**4a**)

In a two neck-round-bottom flask, H_2O (5 mL) was warmed at 60°C, and then **SM1** (1 mmol, 1 equiv) and il $NaSO_2Ph$ (1.5 mmol, 1.5 equiv) were added. The reaction was left under stirring for 2,5 h at 60°C and the cooled at room temperature and left overnight. The desired product precipitated in the flask was filtered ad collected. To the aqueous layer, NaCl was added until saturation and the mixture was extracted with EtOAc (x3). the combined organic layers were dried over Na_2SO_4, filtered off, and concentrated under vacuo to give the product **4a** as a white solid (146 mg, 69%).
Spectroscopic data are in accordance to those reported in literature.[212]

(3S,4R)-3-((R)-1-((tert-butyldimethylsilyl)oxy)ethyl)-4-(phenylsulfonyl)azetidin-2-one (**5a**)

In a two neck-round-bottom flask, a solution $NaSO_2Ph$ (1.5 mmol, 1.5 equiv) in H_2O (2.5 mL) was wormed at 55°C and **SM2** (1 mmol, 1 equiv) in acetone (2.5 mL) was added. The reaction was left under stirring for 3 days and monitored by TLC. The desired product precipitated in the flask was filtered ad collected. To the aqueous layer, NaCl was added until saturation and the mixture was extracted with EtOAc (x3). the combined organic layers were dried over Na_2SO_4, filtered off, and concentrated under vacuo to give the title product as a withe solid (146 mg, 69%). After acetone elimination, the solution was dried over Na_2SO_4, filtered off, and concentrated under vacuo to give the product **5a** as a white solid (300 mg, 81%).
Spectroscopic data are in accordance to those reported in literature.[217]

1-(methylthio)-4-(phenylsulfonyl)azetidin-2-one (**4b**)

Following GP2, dimethyl disulfide and β-lactam **4a** (0.45 mmol), yielded compound **4b** (84 mg, 73%) as a yellow oil. Spectroscopic data are in accordance to those reported in literature.[211]

(3S,4R)-3-((R)-1-((tert-butyldimethylsilyl)oxy)ethyl)-1-(methylthio)-4-(phenylsulfonyl)azetidin-2-one (**5b**)

Following GP2, dimethyl disulfide and β-lactam **5a** (0.5 mmol), yielded compound **5b** (96 mg, 46%) as a yellow oil. Spectroscopic data are in accordance to those reported in literature.[211]

4-(phenylsulfonyl)-1-(propylthio)azetidin-2-one (**4c**)

Following GP2, diisopropyl disulfide and β-lactam **4a** (0.43 mmol), yielded compound **4c** (87 mg, 71%) as a yellow oil. ^{1}H NMR (400 MHz, $CDCl_3$) δ 7.96-7.91 (m, 2H), 7.75-7.69 (m, 1H), 7.64-7.58 (m, 2H), 4.71 (dd, *J* = 4.5, 3.7 Hz, 1H), 3.32 – 3.28 (m, 2H), 2.99 (ddd, *J* = 13.6, 8.0, 5.9 Hz, 1H), 2.57 (ddd, *J* = 13.3, 8.1, 7.1 Hz, 1H), 1.70 – 1.50 (m, 2H), 0.96 (t, *J* = 7.3 Hz, 3H). ^{13}C NMR (100 MHz, $CDCl_3$) δ 168.25, 136.24, 136.24, 129.98, 129.53, 71.95, 42.24, 41.58, 22.17, 13.23. IR (film): ν = 2409.4, 2370.5, 2346.0, 2331.1, 1775.1, 1308.5, 1233.9, 1152.5, 1139.4, 776.0, 718.1, 695.4, 592.9, 529.6 cm^{-1}. HPLC-MS (ESI^+): Rt = 7.4 min, m/z =303 $[M+H_2O]^+$. m.p. = 94-96°C

(3S,4R)-3-((R)-1-((tert-butyldimethylsilyl)oxy)ethyl)-4-(phenylsulfonyl)-1-(propylthio)azetidin-2-one (**5c**)

Following GP2, diisopropyl disulfide and β-lactam **5a** (0.78 mmol), yielded compound **5c** (275 mg, 74%) as a yellow oil. ^{1}H NMR (400 MHz, $CDCl_3$) δ 7.94-7.90 (m, 2H), 7.70 – 7.65 (m, 1 H), 7.60-7.54 (m, 2H), 4.77 (d, *J* = 2.4 Hz, 1H), 4.18 (qd, *J* = 6.3, 1.9 Hz, 1H), 3.42 (dd, *J* = 5.5, 3.3 Hz 1H), 3.06 – 2.98 (m, 1H), 2.46 (ddd, *J* = 13.1, 8.3, 7.2 Hz, 1H), 1.66 – 1.46 (m, 2H), 0.89 (t, *J* = 7.4 Hz, 3H), 0.80 (d, *J* = 6.4 Hz, 3H), 0.77 (s, 9H), -0.03 (s, 3H), -0.05 (s, 3H). ^{13}C NMR (100 MHz, $CDCl_3$) δ 170.02, 136.85, 135.06, 129.89, 129.57, 74.08, 64.09, 63.39, 41.76, 26.03, 22.36, 22.13, 18.19, 13.28, -4.34, -4.64. IR (film): ν = 2956.8, 2930.0, 2883.1, 2856.8, 1787.9, 1462.3, 1447.4, 1324.1, 1259.3, 1147.4, 1108.1, 1053.0, 967.3, 827.7.6, 778.9, 716.7, 687.5, 620.4, 582.2, 550.2 cm^{-1}. HPLC-MS (ESI^+): Rt = 13.0 min, m/z =461 $[M+H_2O]^+$. $[\alpha]_D^{20}$ = - 41 (c=1, CH_2Cl_2).

(3S,4R)-3-((R)-1-hydroxyethyl)-4-(phenylsulfonyl)azetidin-2-oneone (**6a**)

Following GP3, compound **5a** (0.48 mmol), yielded compound **6a** (110 mg, 89%) as a white solid. Spectroscopic data are in accordance to those reported in literature.[218]

(3S,4R)-3-((R)-1-hydroxyethyl)-1-(methylthio)-4-(phenylsulfonyl)azetidin-2-one (**6b**)

Following GP3, compound **5b** (0.22 mmol), yielded compound **6b** (52 mg, 78%) as a white solid.

^{1}H NMR (400 MHz, $CDCl_3$) δ 7.97–8.00 (m, 1H), 7.73–7.77 (m, 1 H), 7.62–7.66 (m, 2 H), 4.86 (d, J=2.8 Hz, 1 H), 4.30 (dq, J=6.8, 4.4, 3.2 Hz, 1 H), 3.59 (dd, J=3.2, 2.8, 1H), 2.48 (s, 3H), 1.85 (d, J=4.4 Hz, 1 H), 1.14 (d, J=6.8 Hz, 3 H).

(3S,4R)-3-((R)-1-hydroxyethyl)-4-(phenylsulfonyl)-1-(propylthio)azetidin-2-one (**6c**)

Following GP3, compound **5c** (0.33 mmol), yielded compound **6c** (108 mg, 98%) as a white solid. ^{1}H NMR (400 MHz, $CDCl_3$) δ 7.97-7.92 (m, 2H), 7.73 – 7.68 (m, 1H), 7.63-7.56 (m, 2H), 4.86 (d, *J* = 2.4 Hz, 1H), 4.23 (qd, *J* = 6.4, 3.2 Hz, 1H), 3.54 (t, *J* = 3.0 Hz, 1H), 2.87 (ddd, *J* =

13.7, 7.9, 6.1 Hz, 1H), 2.54 (ddd, *J* = 13.4, 8.0, 6.9 Hz, 1H), 1.66 – 1.46 (m, 2H), 1.07 (d, *J* = 6.4 Hz, 3H), 0.89 (t, *J* = 7.3 Hz, 3H). ^{13}C NMR (100 MHz, $CDCl_3$) δ 170.87, 136.96, 135.55, 130.27, 130.02, 73.92, 63.93, 62.87, 41.80, 22.43, 22.18, 13.57. IR (film): ν = 3485.0, 3061.3, 3023.2, 3003.8, 2963.6, 1788.6, 1449.9, 1301.3, 1141.6, 1105.3, 1071.7, 720.7, 688.6, 625.9, 535.2 cm^{-1} HPLC-MS (ESI^+): Rt = 6.8min, m/z = 347 $[M+H_2O]^+$. $[\alpha]_D^{20}$ = - 76 (c=1, CH_2Cl_2). m.p. = 105-108°C.

Synthesis of 4-(phenylthio)azetidin-2-one (**7a**)

To a solution of diphenyl disulfide (1.5 mmol, 1.5 equiv) in ethanol (2.5 mL), under a nitrogen atmosphere, $NaBH_4$ (2 mmol, 2 equiv) was added dropwise and the reaction was stirred for 3 h. Then at 0°C, **SM1** was added (1 mmol, 1 equiv) and the mixture was stirred at room temperature until consumption of starting materials (5 min, TLC monitoring). After ethanol elimination, the solution was extracted with EtOAc (x3) and the combined organic layers were dried over Na_2SO_4, filtered off, and concentrated under vacuo. Compound **7a** was obtained as a white solid (118 mg, 66%) after flash chromatography (from Cyclohexane/EtOAc = 95:5 to 80:20). Spectroscopic data are in accordance to those reported in letteratura.[219]

Synthesis of (3S,4R)-3-((R)-1-((tert-butyldimethylsilyl)oxy)ethyl)-4-(phenylthio)azetidin-2-one (**8a**)

To a solution of diphenyldisulfide (1.5 mmol, 1.5 equiv) in ethanol (2.5 mL), under a nitrogen atmosphere, $NaBH_4$ (2 mmol, 2 equiv) was added drop-wise and the reaction was stirred for 3 h. Then at 0°C, **SM1** was added (1 mmol, equiv) and the mixture was stirred at room temperature until consumption of starting materials (5 min, TLC monitoring). After ethanol elimination, the solution was extracted with EtOAc (x3) and the combined organic layers were dried over Na_2SO_4, filtered off, and concentrated under vacuo. Compound **8a** was obtained as a white solid (337 mg, 99%) after flash chromatography (from Cyclohexane/EtOAc = 95:5 to 80:20)
Spectroscopic data are in accordance to those reported in literature.[220]

Section 2. β-lactam compounds properties

In this second section, we will focus on two projects which consider two different proprieties of β-lactams:

- Stereochemistry
- Reactivity at C-4 position of the ring

In the first case we want to obtain enantiomerically pure 4-acetoxy-2-azetidinone, useful for synthesis of stereo-chemically defined bioactive β-lactams, while in the second case we want to study in which conditions the nucleophilic substitution at C4 position of azetidinones occurs.

2.1 Chemoenzymatic enantioselective synthesis route of (+) and (-) 4-acetoxy-azetidin-2-one by Lipase-catalysed kinetic resolution and their applications

2.1.1 Biocatalysis

Biocatalysis is an enabling technology for chemists that provide the use of isolated enzymes or whole cells, giving access to a broad range of selective transformations often inaccessible with 'chemical' catalysts.[221] Biocatalysis indeed has many attractive features in the context of green chemistry and sustainable development thanks to the fact that enzymes derive from renewable resources and are biocompatible, biodegradable, and essentially non-toxic.[222]
Moreover, biocatalysis has now become a standard technology applied to the industrial production of both bulk and fine chemicals. In fact, biocatalytic systems are today used not only in organic synthesis, but also in textile, food and paper industries, as well as in the production of biosensors (*Figure 59*).
Biocatalysts and microorganisms can indeed be used to obtain building blocks for chemical industry from plants and waste materials derived from agriculture. However, the pharmaceutical sector is that involving the major number of biocatalytic process; this reflects the need of pharma-industry to synthetize enantiomerically pure drugs.[223] We know that enantiomers could have dramatically different biological activities such as pharmacokinetic, pharmacology or toxicology;[224,225] in fact, they could show different spatial distributions on the same receptor or even bind two diverse receptors, producing other biological pathways. Thus, it is of fundamental importance to know the biological response of single stereoisomers and to separately obtain two enantiomers of a new bioactive molecule; biocatalysis in this field have a prominent role.[222]

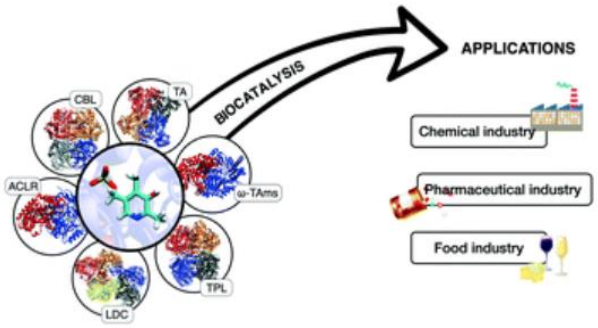

Figure 59. Biocatalysis and its applications.

2.1.2 Enzymes: lipases

Enzymes are globular proteins containing, among the others, two fundamental structural portions: the active site, in which the catalysis actually takes place, and the recognition pockets (binding sites), where the substrate binds and positions properly with a complementary interaction.[226] Moreover, enzymes are highly selective catalysts in terms of chemo-, regio-, and stereo- selectivity, and highly specific toward substrates and reactions.[222]
Processes involving the use of enzymes operate in mild conditions and do not require protections of functional groups; they also avoid the use of hazardous materials, reduce the energy demanding, rarely performing endo- or exothermic processes, and require catalytic amounts rather than stoichiometric.[227] However, the effect of defined conditions due to the protein nature of the enzyme can also limit their use: changes in solvent, pH, mechanical stresses (such as an agitation system), reduce or cancel its activity, also reducing the yield of the process.
The fact that enzymes, given their nature, are mostly active in aqueous at neutral pH is often considered an added value on industrial processes (therefore on a large scale) due to the legislative restrictions on organic solvents. However, most organic molecules are scarcely or not at all soluble in aqueous solvents and this requires the adoption of alternative strategies to improve their solubility such as the addition of co-solvents or immiscible solvents (biphasic systems). In recent decades, the study of enzymes in organic solvents has been deepening, thus overcoming the problem of the solubility of substrates while maintaining the activity of the catalyst. Furthermore, the different structure of the organic substrates compared to the natural ones, could generate a limited catalytic efficiency of the enzymes, but thanks to the protein engineering techniques that modify the active site appropriately it was possible to expand the number of organic compounds to be used as substrates.[228]

In this thesis work we will focus particularly on a specific type of enzyme: lipase.
Lipases (triacylglycerol hydrolase, EC 3.1.1.3) are enzymes widely distributed among animals, plants and microorganisms that catalyze the hydrolysis of glycerol ester bonds at fat water interfaces. In anhydrous water-immiscible organic solvents they are also able to catalyze the reverse reactions of synthesis and group exchange of esters and the resolution of racemic mixtures into optically active alcohols or acids.[229] Many organisms like fungi, bacteria, yeast, animals etc. produce lipases; but lipases generated by bacteria and fungi are of commercial

interest because they are easier to product, to recovery and are characterised by cheaper production costs as compared to other sources. Lipases along with other enzymes have wide range of applications because of their versatility like tolerance to wide pH and temperature range.[230]

Most of the known lipases displays a serine-depending mechanism performed by a serine, aspartic acid and histidine catalytic triad. Histidine acts as proton shuttle between serine and aspartic acid residues, allowing the enzyme active site to maintain its three-dimensional conformation. The active site is covered by a peptide lid that remains closed in the absence of substrate. Conversely, when the lipase is in contact with a lipid-water interface, the lid undergoes conformational changes letting the active site open and accessible for the substrate (lid effect, *Figure 60*).[231]

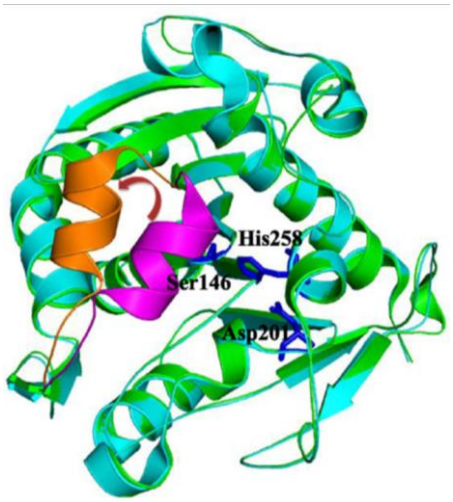

Figure 60. Lipase active site and lid effect (superimposition of close and open conformations of Thermomyces lanuginosus lipase). Figure adapted from ref. 232.

2.1.3 Kinetic resolution with lipases

As previously mentioned, lipases are used for the kinetic resolution of racemic mixtures and can be exploited both for the formation of the ester bond and for its hydrolysis.

Since the active site is chiral, one enantiomer of alcohol or ester adapts better than the other and is converted at a faster rate, thus obtaining what is called kinetic resolution (*Figure 61*).

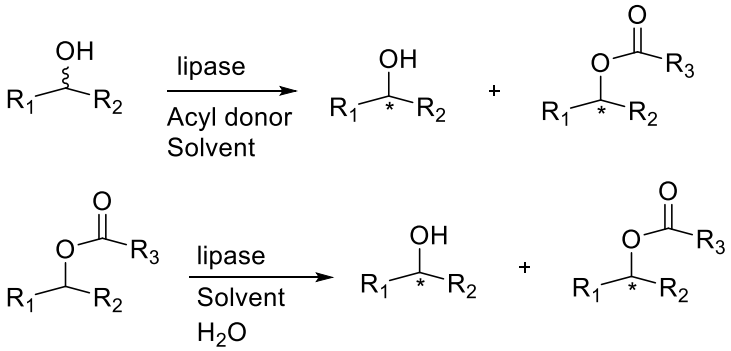

Figure 61. Generic scheme of kinetic resolution with lipases.

The ideal result occurs when the reaction rates for the two enantiomers conversion is so different that only one is processed by the enzyme at acceptable times, thus obtaining the maximum 50% yield and elevate enantiomeric excesses (ee). In this optimal case, the enzyme possesses a high enzymatic selectivity (E), a dimensionless parameter corresponding to the ratio of the relative rate constants for the single enantiomers (*Figure 62*).

$$E = \frac{v_A}{v_B} = \frac{(\frac{k_{cat}}{k_m})_A}{(\frac{k_{cat}}{k_m})_B}$$

Figure 62. Equation for Enzymatic selectivity E.

E values superior to 20 are excellent, while values between 10 and 15 are considered satisfactory.[233] When E is below 10, the biocatylic process is not selective and leads to insignificant enantiomeric excesses (*Figure 63*).

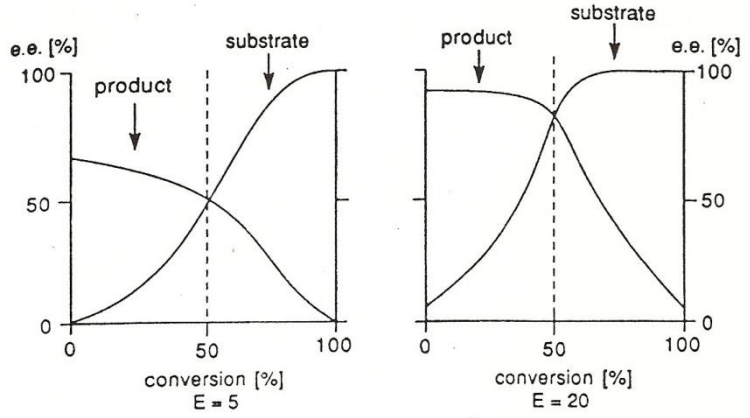

Figure 63. Conversion vs ee in kinetic resolutions; E=5 (left) and when E=20 (right).

The optimal result of a kinetic resolution showing moderate selectivity can be obtained in two steps (*Figure 64*): the reaction is stopped at the conversion of 40% where the product curve reaches the maximum of enantiomeric excess with the maximum yield, around the range conversion X shown in the *Figure 64*. The product is then isolated and the residual substrate showing low conversion level and enantiomeric excess undergoes a second esterification step (or hydrolysis) until a conversion of around 60% is reached. At this point the substrate is separated with its maximum enantiomeric excess and its maximum yield. In any case, at least 20% of the product from the second step is lost.

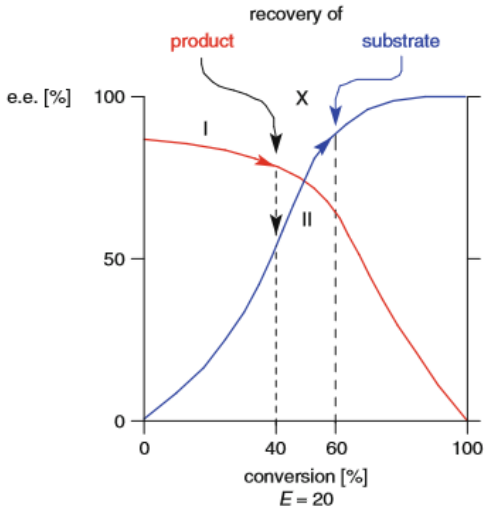

Figure 64. Two-steps kinetic resolution.

As useful β-lactam intermediates, 4-acetoxy azetidin-2-one (**SM1**) and (3R,4R)-4-acetoxy-3-[(1R)-1-(*tert*-butyldimethylsilyloxy)-ethyl]-azetidin-2-one (**SM2**) are commercially available and have been widely used as starting materials for the synthesis of important bioactive compounds (*Figure 65*).[234]

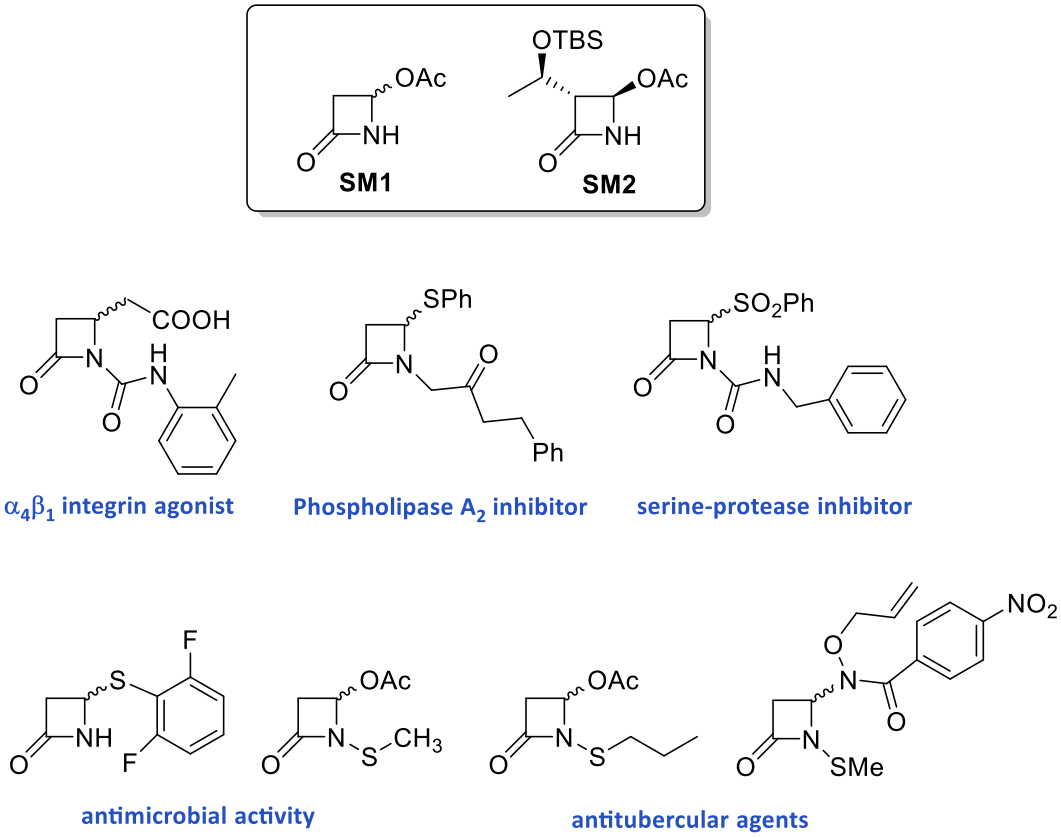

Figure 65. 4-acetoxy-azetidinones **SM1** and **SM2**, and some selected racemic bioactive β-lactam compounds obtained from **SM1**. Figure adapted form ref. 235.

Intermediate **SM2** is available as enantiopure compound, **SM1** instead is purchased only as a racemic mixture. Although the great usefulness of **SM1** as starting material in the synthesis of new bioactive β-lactam compounds,[43,48,143,196,211,236] this reactant could only provide racemic derivatives (selected examples in *Figure 65*). However, we know the importance to have these molecule enantiomerically pure.

About that, my research group exploited the kinetic resolution with lipases to obtain the two enantiomers of a β-lactam intermediate, precursor of novel integrin ligands and to determine how theycould differently interact with the receptor in terms of activity as agonists or antagonists, and potency (*Figure 66*).[222]

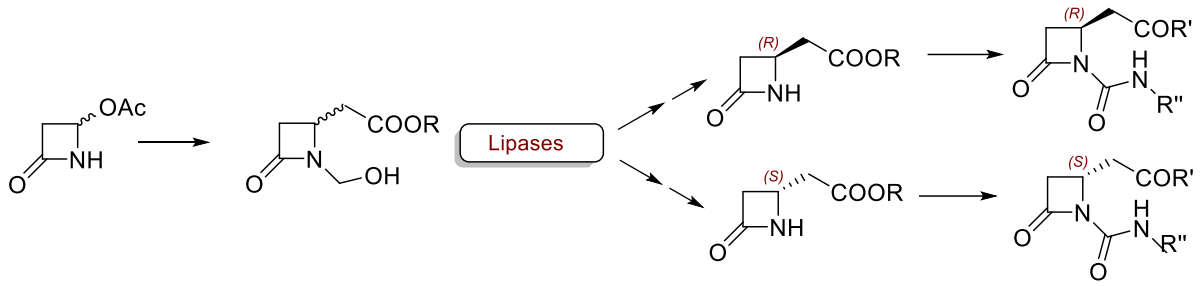

Figure 66. Strategy for the synthesis of enantiomerically pure β-lactam derivatives.

Among a series of Lipases, *Burkholderia Cepacia Lipase* (BCL) was selected as the most suitable enzyme for the kinetic resolution. After optimization of the biocatalytic protocol (enzymes and acylating agents) and of the synthetic procedures, the two enantiomers (+)S and (−)R were obtained in excellent enantiomeric excesses. Assignment of the absolute configurations was assessed by chemical transformation in to a known compound. Four chiral β-lactams **(S)-11**, **(R)-11**, **(S)-12**, and **(R)-12** were obtainedand finally evaluated in cell adhesion assays (*Figure 67*). Pharmacological tests on Jurkat cell line expressing $\alpha_4\beta_1$ integrin and K562 cell line expressing $\alpha_5\beta_1$ integrin, revealed that th eactivity as agonists with a nanomolar potency was fully maintained only in case of (S)-enantiomers, while (R)-derivatives were completely inactive, thus revealing an important stereochemical requirement for further developments of the new β-lactam-based integrin ligands.[222]

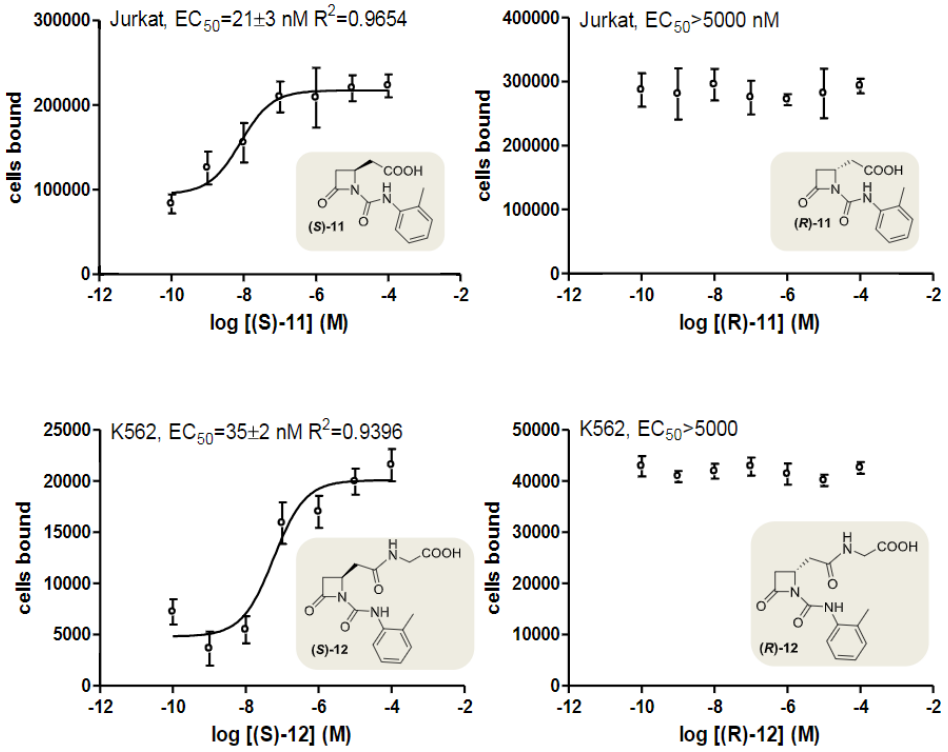

Figure 67. Effects of β-lactams **(S)-11** and **(R)-11** in cell adhesion assays on Jurkat cell line expressing $\alpha_4\beta_1$integrin, and **(S)-12**, and **(R)-12** on K562 cell line expressing $\alpha_5\beta_1$ integrin. Figure adaperd from ref. 222.

With these results it was confirmed that two enantiomeric drugs could give different pharmacologic responses. However, even in this case the possibility to gain access to the enantiopure form of 4-acetoxy-azetidinone **SM1** is not achieved, and as previously mentioned, it would be of utmost importance in the synthesis of stereo-chemically defined bioactive β-lactams.[237] For that reason, the aim of this work was to establish a chemoenzymatic route starting from the commercially available **SM1** to obtain the two enantiomers of 4-acetoxyazetidin-2-one from the racemic **rac-2** by means of a kinetic resolution by lipases. Moreover, we also want to conduct preliminary tests on the single enantiomers of some typical reactions as C4 substitutions and N-thioalkylation in order to evaluate the stereochemical integrity of the corresponding products (*Figure 68*).[235]

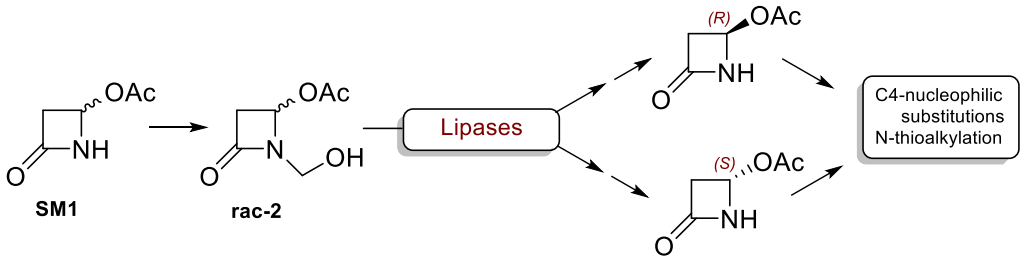

Figure 68. Enzymatic kinetic resolution on functionalized 4-acetoxy-azetidinone and evaluation of the stereochemical outcome in C4 and N-functionalization. Figure adapted form ref. 235.

Results and discussion

To approach the resolution of **SM1**, the possibility to directly perform a lipase-mediated hydrolytic kinetic resolution on the 4-acetoxy ester group was excluded because of an alleged low stability of the corresponding 4-hydroxy-azetidinone which could undergo a ring-opening reaction *via* breakdown of the N-C4 bond.[238] In the previous work, as aforementioned, we took advantage of an N-hydroxymethyl- functionalization to successfully develop a KR on a racemic β-lactam intermediate for the synthesis of enantiopure integrin ligands (*Scheme 31*).[222]

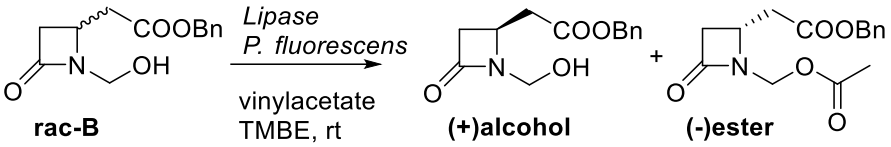

Scheme 31. Kinetic enzymatic resolution on the β-lactam intermediate **rac-B** previously reported.[235]

Thus, it was applied the same strategy on the racemic 4-acetoxy-azetidinone **SM1**, which was accordingly treated with paraformaldehyde and catalytic potassium carbonate under microwave irradiation to obtain the *N*-methylene-hydroxy derivative **rac-2** in excellent yields (*Scheme 32*).

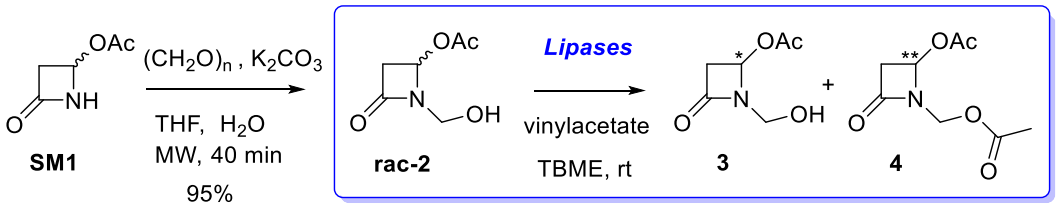

Scheme 32. Synthesis of *N*-methylene-hydroxy-azetidinone **rac-2** and its enzymatic KR by transesterification reaction. [235]

In order to perform a KR on **rac-2**, some lipases were tested in the transesterification reaction with vinyl acetate in *t*-butylmethylether (TBME) at room temperature. After filtration of the enzymes, the crude reaction mixtures were monitored by chiral HPLC analysis for evaluating conversions and enantiomeric excesses (*Table 8*).[235]

Table 8. Screening of lipases in KR on **rac-2**.[a]

Entry	*Lipases* (activity)[b]	Enzyme (U)	Time (h)	Conv. (%)[c]	3 ee%[c]	4 ee%[c]
1	*Burkholderia cepacia* (30 U/mg)	300	20	3.5	6	>99
2	*Burkholderia cepacia* (30 U/mg)	300	72	13	24	>99
3	CAL B (10 U/mg)	75	16	>99	0	0
4	CAL B (10 U/mg)	75	6	84	>99	22
5	CAL B (10 U/mg)	75	2	65	>99	65
6	CAL B (10 U/mg)	75	1	54	78	60
7	*Pseudomonas fluorescens* (20 U/mg)	223	72	51	>99	91
8	*Pseudomonas fluorescens* (36 U/mg)	48	48	55	89	96
9	*Pseudomonas fluorescens* (309 U/mg)	150	23	55	>99	90
10	*Pseudomonas fluorescens* (309 U/mg)	117	8	52	>99	90

[a] Reaction conditions: **rac-2** (0.063 mmol), vinyl acetate (0.38 mmol), TBME (1.5 mL), enzyme (U in table), rt.
[b] Activity of the commercial enzymes.
[c] Determined by chiral HPLC analysis on the crude.

Lipase from *Burkholderia cepacia* or *Candida antarctica B* (*CAL B*) which achieved very good results with other *N*-hydroxymethyl-azetidinones[239,240], behaved differently on **rac-2**: *Burkholderia cepacia* gave low conversions with poor ee % of the unreacted alcohol **3**, even after 72 h (*Table 8*, entries 1 and 2); on the contrary, CAL B showed high conversions but null or poor enantioselectivities in the ester **4** even at lower conversions (*Table 8*, entries 3-6). The best results were obtained with *Pseudomonas fluorescens* lipase and some conditions were then studied (*Table 8*, entries 7-10). Three *Pseudomonas fluorescens* lipase preparations with different activities (20, 36, and 309 U/mg) were tested, and on changing activity, units and reaction time, satisfactory conversions (45-55%) and good to excellent ee% for both **3** and **4** were obtained.

The conditions of *Table 8* entry 7 were then applied in a preparative KR in order to isolate discrete amounts of **3** and **4**.

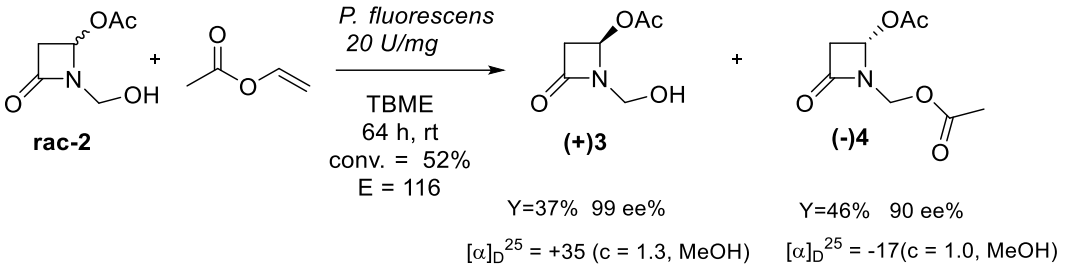

Scheme 33. Kinetic resolution of β-lactam **rac-2**; isolated yields % after column chromatography, ee% and specific optical rotations for compounds **3** and **4** are reported. The enzymatic selectivity E was calculated by the ENANTIO tool of the Elk group Graz University. [235]

The reaction was stopped at a 52% conversion: the two products were isolated and separated by flash-chromatography, characterized and analysed by chiral HPLC analysis and polarimetry; their specific optical rotations and enantiomeric excesses resulted as **(+)3** (99 % ee) and **(-)4** (90 % ee) with an excellent enzymatic selectivity (E) of 116 (*Scheme 33*).

Concerning the absolute configuration of the two enantiomers, it can be only tentatively attributed according to the enantio-preference of lipases on some C-3 unsubstituted β-lactam compounds bearing primary alcohols with a β-stereocenter.[222,241] As above mentioned for the kinetic resolution on the racemic β-lactam **rac-B**[222], *P. fluorescens* gave (*S*)-ester as the preferred enantiomer (*Scheme 32*). In that case the absolute configuration was assigned by comparison with an already known chiral azetidinone obtained from (*S*)-aspartic acid.[242] On assuming the same (*S*)-enantio-preference by *P. fluorescens* for the C4 substituent, it could be tentatively assigned a (*S*) configuration to the **(-)4** ester as the preferred enantiomer also in this KR.

Alcohol **(+)3** and ester **(-)4** were then further elaborated in order to eliminate the substituents on the β-lactam nitrogen atom and to obtain the final separated enantiomers **(+)5** and **(-)5** (*Scheme 34).*[235]

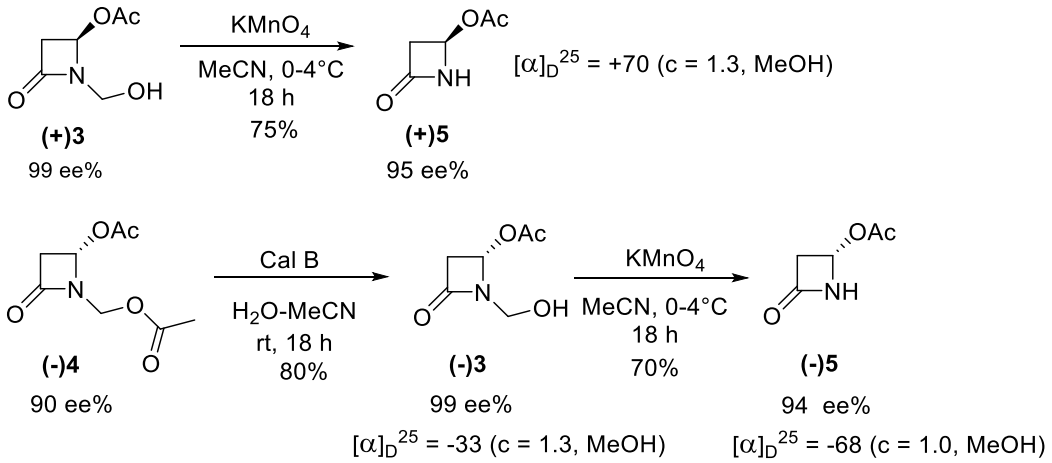

Scheme 34. Synthesis of β-lactam enantiomers **(+)5** and **(-)5**. Isolated yields, ee%, and specific optical rotation powers are reported.[235]

For this purpose, it was necessary to eliminate the *N*-hydroxymethyl group on **(+)3** and different conditions were tested: NH_4OH (25%)/MeOH, $KMnO_4$/acetone-H_2O, and $KMnO_4$/MeCN.[243] Only oxidative conditions were effective, and the use of $KMnO_4$ in acetonitrile allowed to isolate compound **(+)5** in satisfactory yields. As mentioned in the introduction, the (+)4-acetoxy-

azetidinone **(+)5** has been already reported in the literature, as an enantiopure compound obtained by means of host-guest inclusion complexes.[244] However, we observed a higher specific rotation for **(+)5** $[\alpha]_D^{25}$ = +70 (c = 1.3, MeOH) than that reported in the literature:[245] $[\alpha]_D^{25}$ = +6.5 (c = 0.68, MeOH), but the latter has a lower concentration and its enantiomeric purity as ee% by chiral chromatography was not reported.[235]

The **(-)5** enantiomer was obtained from **(-)4** with a two steps procedure: ester hydrolysis to get intermediate **(-)3** followed by oxidative cleavage of the oxymethylene group. Concerning the hydrolysis, biocatalysis fulfilled the requirement of a high regioselectivity among the two acetates present on **(-)5**. The effectiveness of lipases to satisfy this requirement was preliminary evaluated on the racemic ester **rac-4** (*Table 9*), easily obtained from **rac-2** with acetic anhydride and triethylamine and used as racemic standard for chiral HPLC analyses.[235]

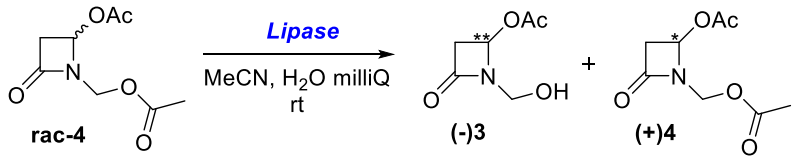

Table 9. Screening of lipases for enzymatic hydrolysis on **rac-4**.[a]

Entry	*Lipases* (U/mg)[b]	Enzyme amount (U)	Time (h)	T (°C)	Conv. (%)[c]	(-)3 ee%[b]	(+)4 ee%[b]
1	*Burkholderia cepacia* (30 U/mg)	180	144	rt	30	>99	40
2	*Pseudomonas fluorescens* (309 U/mg)	326	21	rt	25	>99	24
3[d]	*CAL B* (10 U/mg)	100	3	rt	55	>99	66
4[d]	*CAL B (10 U/mg)*	100	24	rt	99	>99	-
5	*CAL B* (10 U/mg)	35	24	rt	95	96	99
6[d, e]	*CAL B* (10 U/mg)	100	3	60	95	>99	99
7[d, e]	*CAL B* (10 U/mg)	100	1	60	58	>99	30

[a] Reaction conditions: **rac-4** (0.06 mmol), H_2O/MeCN 11:1 (2.5 mL), enzyme (U in table), rt.
[b] Activity of the commercial enzymes.
[c] Determined by chiral HPLC analysis on the crude.
[d] Reaction conditions: **rac-4** (0.174 mmol), H_2O/MeCN 11:1 (3 mL), enzyme (U in table), rt.
[e] The recovery of the organic fraction is around 60%.

Burkholderia cepacia and *Pseudomonas fluorescens* lipases (*Table 9*, entries 1-2) gave unsatisfactory results with low conversions even for longer reaction time. *CAL B* was instead successful and furnished a 55% conversion and excellent enantiomeric excess (>99 %) for the

alcohol **3** in only 3 hours (*Table 9*, entry 3). The result obtained with *CAL B* is quite interesting: the excellent ee for the product **(-)3** >99% at a conversion exceeding the 50% (i.e. 55 %) and a lower ee (66%) for the ester **(+)4** catches a glimpse of a possible racemization of the reactant via a C-4 cation (see *Scheme 35*), thus revealing the possibility of a prospective dynamic kinetic resolution under controlled conditions. On extending the hydrolysis for 24 h with *CAL B*, the conversion was quantitative, only the alcohol **3** was isolated as single enantiomer with ee >99 %, but no traces of the ester **4** were isolated in the organic fraction (*Table 9*, entry 4). This could probably be due to a hydrolysis of the β-lactam ring in the ester **(+)4** and its further degradation in the aqueous phase. The hydrolysis with *CAL B* was further examined at 60 °C at short reaction time, 3 and 1 h (*Table 9*, entries 6 and 7) obtaining 95% and 58% conversion, respectively. The product **3** was isolated with high ee%, but with a poor recovery in the organic extract (60%).[235]

The hydrolysis was repeated with *CAL B* on the enantiomerically enriched ester **(-)4** (*Scheme 34*). The process was carried out in MilliQ water with a small amount of acetonitrile necessary to dissolve **(-)4** (H_2O/CH_3CN = 11:1). Alcohol **(-3)** was obtained in an 80% yield with a 99% optical purity; remarkably, its enantiomeric excess was greatly enriched if compared to that of the starting ester **(-)4** (90% ee). The final oxidation of **(-)3** with $KMnO_4$ in acetonitrile afforded chiral (-)4-acetoxy-azetidinone **(-)5** in good yields (*Scheme 34*). Careful attention should be paid for a cold aqueous work-up of the crude because lowering of the enantiomeric excess was otherwise observed, and an ee = 88% was reached instead of 94%.

Introduction or transformation of functional groups on C4 position of azetidinones is a common step in the synthesis of β-lactam-based compounds.[234] Once obtained the enantiomerically pure 4-acetoxy-azetidinones **(+)5** and **(-)5**, some nucleophilic substitution reactions were tested on these substrates. We then examined the stereochemical outcome in two C4 substitution reactions (*Scheme 35*) on enantiomer **(+)5**, with potassium thioacetate and with Reformatsky reagent $BrZnCH_2COOBn$, previously applied for the synthesis of integrin ligands with a β-lactam scaffold.[43,246]

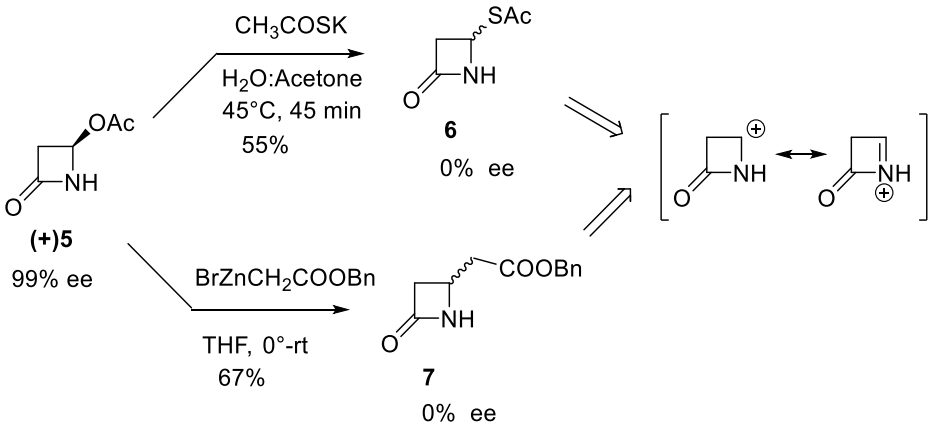

Scheme 35. Nucleophilic substitution reactions at C4 position of the enantiomerically pure 4-acetoxy-azetidinone **(+)5**.[235]

However, starting from enantiopure compound **(+)5**, the C4 substitution products **6** and **7** were obtained as racemic mixtures, confirming the mechanism of this substitution as an addition-

elimination pathway *via* the short-living intermediate 1-azetin-2-one (*Scheme 35*), as determined by Gavina *et al.*[247]

As a further stereochemical investigation, the **(+)5** and **(-)5** enantiomers were considered for a functionalization on the nitrogen atom of the β-lactam ring (*Scheme 34*). For this purpose, we selected a *N*-thioalkylation reaction, since *N*-alkyl-thio-4-acetoxy-azetidinones demonstrated to have interesting antibacterial activities[169,211] and were also successfully applied in the development of new antibacterial functional materials. Enantiomers **(+)5** and **(-)5** were separately subjected to a *N*-thiolation reaction using dimethyl disulfide in the presence of sulfuryl chloride and triethylamine (TEA) in DCM (*Scheme 36*), according to a previously reported procedure.[143]

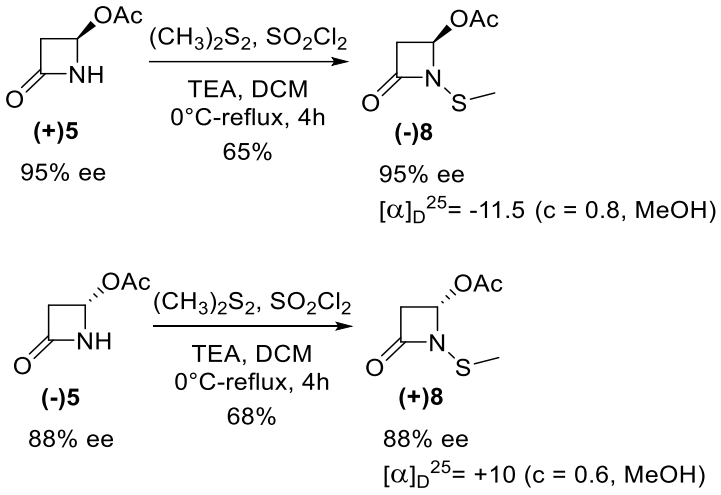

Scheme 36. *N*-thiomethylation on enantiopure 4-acetoxy-azetidinone **(-)5**.[235]

Compounds **(-)8** and **(+)8** were isolated by flash chromatography and then analysed by chiral HPLC. The chromatographic analysis showed the preservation of the ee at 95% and 88%, as that of the precursors **(+)5** and **(-)5**, respectively, thus confirming that the *N*-thioalkylation reaction did not affect the configuration at C4 of the β-lactam. The optical rotations of the *N*-methylthio derivatives **(-)8** and **(+)8** have opposite signs compared to the starting compounds **(+)5** and **(-)5**, however, optical power is an inherent property of a molecule, and a change in sign between different molecules does not entail an inversion of the configuration.[248,249]

Conclusions

The syntheses of several biologically active β-lactam-based compounds share as starting material the 4-acetoxy-azetidin-2-one, a cheap and readily available compound, but commercially available as a racemic mixture. Given the effect of chirality on biological activity and the need to synthesize enantiopure β-lactams for pharmacological use it would be worthwhile to obtain 4-acetoxy-azetidin-2-one as separated single enantiomers. Biocatalysis is becoming a valid and an increasingly employed technique for achieving enantiomerically pure products. Among a series of lipases, *Pseudomonas fluorescens* was selected as the most suitable enzyme for performing a kinetic resolution by transesterification on the *N*-hydroxymethyl β-lactam **rac-2**, giving the corresponding ester **(−)4** and the residual starting alcohol **(+)3** with excellent enantiomeric excesses. The successful ester hydrolysis of **(−)4** was obtained with *Candida antarctica lipase B*

(*CAL B*) with a significant enrichment of the enantiomeric excess of the *N*-hydroxymethyl-azetidinone **(-)3**. The potential dynamic kinetic resolution of the β-lactam **rac-4** by *CAL B* is currently under investigation. Following the optimized deprotection steps, 4-acetoxy-azetidin-2-ones **(+)5** and **(−)5** were thus obtained as single enantiomers with excellent optical purities. Nucleophilic substitution reactions were then studied on the pure enantiomers in order to evaluate their stereochemical outcome. The C4 substitution on the enantiomer **(+)5** with potassium thioacetate or $BrZnCH_2COOBn$ gave the corresponding products **6** and **7** as racemic mixtures, confirming the propensity of 4-acetoxy-azetidinones to undergo a S_N1 mechanism. On the contrary, the C4 configuration is not affected by functionalization of the β-lactam nitrogen atom upon sulfenylation reaction, and optically active *N*-methylthio-4-acetoxy- β-lactams were successfully obtained. With this result we report for the first time the synthesis of an enantiopure *N*-alkylthio-4-acetoxy-azetidinone, hence paving the way to the development of novel chiral β-lactams that could be employed in medicinal chemistry as antimicrobial agents as pure enantiomers instead of racemic mixtures.[235]

Experimental

Solvents and reagents were obtained commercially and used as received. Deionized water was obtained from a Millipore analytical deionization system (MilliQ). For TLC monitoring Merck 60 F254 plates were used and for liquid chromatography Merck silica gel 200–300 mesh was used. ^1H and ^{13}C NMR spectra were recorded with an INOVA 400 instrument with a 5 mm probe. All chemical shifts are quoted relative to deuterated solvent signals (δ in ppm and J in Hz). FTIR spectra were recorded with Alpha FT IR Bruker spectrometer. Polarimetric analyses were conducted on Unipol L 1000 Polarimeter at 598 nm. The purities of the target compounds were assessed as being > 95% using HPLC-MS. HPLC-MS: Agilent Technologies HP1100 instrument, equipped with a ZORBAX-Eclipse XDB-C8 Agilent Technologies column; mobile phase: H_2O/CH_3CN, 0.4 mL/min, gradient from 30 to 80% of CH_3CN in 8 min, 80% of CH_3CN until 25 min, coupled with an Agilent Technologies MSD1100 single-quadrupole mass spectrometer, full scan mode from m/z = 50 to 2600, in positive ion mode, ESI spray voltage 4500 V, nitrogen gas 35psi, drying gas flow 11.5 mL/min, fragmentor voltage 20 V. Enantiomeric excesses were determined by chiral-HPLC: Agilent Technologies 1200 instrument equipped with a diode array UV detector on Daicel Chiralcel column IA (25 cm, I.D. 0.46 cm, 5 μm) with HPLC grade isopropanol and *n*-hexane as eluting solvents. Racemic compounds were used for comparison. The commercially available enzymes used in this work are: *Burkholderia cepacia lipase* (BCL) powder, ≥30 U/mg by Sigma Aldrich; Lipase from *Pseudomonas fluorescens*, powder, 309 U/mg by Fluka; Lipase from *Pseudomonas fluorescens*, powder, 20-36 U/mg by Sigma Aldrich; Lipase from *Candida antarctica B*, immobilized on acrylic resin, 10 U/mg, by Sigma Aldrich; Lipase B from *Candida antarctica*, immobilized on Immobead 150, 4.4 U/mg, by Sigma Aldrich.

1-(hydroxymethyl)-4-oxoazetidin-2-yl acetate (**rac-2**)

To a solution of compound **SM1** (200 mg, 1.55 mmol, 1 equiv) in THF (3.4 mL), paraformaldehyde (72 mg, 2.48 mmol, 1.6 equiv), K_2CO_3 (2 mg, 0.05 mmol, 0.03 equiv) and water (140 μL) were added. The system was subjected to microwave irradiation at 180 W for 40

minutes**.** At completion, the reaction mixture was diluted with EtOAc (2.5 mL), dried on anhydrous Na_2SO_4, filtered and concentrated to yield compound **rac-2** as a colorless oil (240 mg, 95%) without further purifications. ^{1}H NMR (400 MHz, $CDCl_3$) δ (ppm) 6.01 (dd, *J* = 4.2, 1.2 Hz, 1H), 4.78 (d, *J* = 11.5 Hz, 1H), 4.49 (d, *J* = 11.5 Hz, 1H), 3.23 (dd, *J* = 15.3, 4.2 Hz, 1H), 2.96 (dd, *J* = 15.3, 1.2 Hz, 1H), 2.10 (s, 3H).^{13}C NMR (100 MHz, $CDCl_3$) δ (ppm) 171.6, 165.3, 74.5, 64.1, 44.3, 20.7. IR (film): ν = 3425, 2950, 1752, 1649, 1378, 1241, 1120, 1043 cm^{-1}. HPLC-MS (ESI^+) Rt =2.9 min, m/z = 100 $[M\text{-}OAc]^+$, 160 $[M+H]^+$, 177 $[M+H_2O]^+$, 182 $[M+Na]^+$.

*Procedure for lipases screening in enzymatic kinetic resolution on **rac-2***

In a glass vial with a screw cap, to a solution of alcohol **rac-2** (10 mg, 0.063 mmol, 1 equiv) and vinyl acetate (45 μL, 0.38 mmol, 6 equiv) in TBME (1.5 mL), the selected enzyme (see Units in Table 1) was added. The mixture was stirred at room temperature. At set time intervals, the substrate conversion and the enantiomeric excesses of unreacted alcohol **(+)3** and ester product **(-)4** were monitored by chiral HPLC. Chiral HPLC samples were prepared as follows: 0.5 mL of mixture was filtered through regenerated cellulose syringe filters (diameter = 25 mm, pore diameter = 0.45 μm); the filtrate was then concentrated, re-suspended in a solution of *n*-hexane/isopropanol 1:1 and directly analysed.

*Preparative enzymatic KR of compound **rac-2***

In a glass vial with a screw cap, to a solution of alcohol **rac-2** (164 mg, 1.03 mmol, 1 equiv) and vinyl acetate (0.57 mL, 6.18 mmol, 6 equiv) in TBME (24.5 mL), Amano Lipase from *Pseudomonas fluorescens (20 U/mg*, 1640 U, 82 mg*)* was added. The mixture was then kept under magnetic stirring at room temperature and monitored by chiral HPLC. At 52% conversion, after 64 h, the mixture was filtered through regenerated cellulose syringe filters and the organic solvent was removed under reduced pressure. Compounds **(+)3** and **(-)4** were separated by flash chromatography (Cyclohexane/EtOAc 1:1 then 35:65); target ester **(-)4** was obtained as a colorless oil (46%, ee = 90%, $[\alpha]_D^{25} = -17$ (c = 1.0, MeOH)) and residual alcohol **(+)3** was isolated as a colorless oil (37%, ee = 99%, $[\alpha]_D^{25} = +35$ (c = 1.3, MeOH)).

*Procedure for lipases screening in the enzymatic hydrolysis on **rac-4***

In a glass vial with a screw cap, to a solution of **rac-4** (12 mg, 0.06 mmol) in CH_3CN and Milli Q H_2O (1:11 ratio, total volume 2.5 mL), the selected enzyme (see Units in Table 2) was added. The mixture was stirred at room temperature under orbital shaking (450 rpm). The conversion and the enantiomeric excesses of **(-)3** and **(+)4** were monitored by chiral HPLC at set time intervals. Chiral HPLC samples were prepared as follows: 200 μL of the mixture were extracted with 0.5 mL EtOAc, organic solvent was dried, re-suspended in a solution of *n*-hexane/isopropanol 1:1 and directly analysed.

*Preparative enzymatic hydrolysis of compound **(−)4***

In a glass vial with a screw cap, to a solution of ester **(-)4** (102 mg, 0.51 mmol, 1 equiv) in CH_3CN and Milli Q H_2O (1:11 ratio, total volume 17 mL), *Lipase B from Candida Antarctica immobilized on Immobead 150* (4.4 U/mg, 224 U, 51 mg) was added. The mixture was stirred at room temperature under orbital shaking (450 rpm) overnight and monitored by chiral HPLC. At reaction completion (18 h), the enzyme was filtered and the aqueous mixture was saturated with brine and extracted with EtOAc (3×10 mL). The collected organic phases were dried over anhydrous Na_2SO_4, filtered and concentrated under vacuum. The target alcohol **(-)3** was obtained without further purification as a colorless oil (65 mg, Y =80%, ee = 99%, $[\alpha]_D^{25} = -33$ (c = 1.3, MeOH). Spectroscopic data of **(−)3** were in fully accordance with those reported for its corresponding racemic analogue **rac-2**.

*Oxidation with $KMnO_4$ to give **(+)5** and **(−)5***

To a solution of the alcohol **(+)3** or **(−)3** (1 equiv) in CH_3CN (30 mL/mmol), $KMnO_4$ (6 equiv) was added portionwise at 0°C. The reaction flask was maintained at 4°C overnight (refrigerator). The reaction mixture was quenched at 0°C with a saturated solution of $Na_2S_2O_5$ until complete decoloring. The mixture was then filtered and acetonitrile evaporated under reduced pressure. The residual aqueous solution was then extracted with DCM (3×10 mL). The collected organic phases were dried over anhydrous Na_2SO_4, filtered and concentrated. The desired products **(+)5** and **(-)5** were obtained without further purification as sticky solid. **(+)5**: Y = 75%, ee = 99%, $[\alpha]_D^{25} = +70$ (c = 1.3, MeOH); **(−)5**: 70%, ee = 99%, $[\alpha]_D^{25} = -68$ (c = 1.0, MeOH). Spectroscopic data of **(+)5** and **(−)5** were in fully accordance with those reported for their corresponding racemic analogue **SM1**.

*Synthesis of S-(4-oxoazetidin-2-yl) ethanethioate (**6**)*

To a solution of CH_3COSK (27 mg, 0.24 mmol, 1.2 equiv) in H_2O (1.5 mL) warmed at 45°C, compound **(+)5** (25 mg, 0.2 mmol, 1 equiv) dissolved in acetone (0.5 mL) was added dropwise. At completion (50 min, TLC monitoring), acetone was evaporated under reduced pressure and the residual aqueous solution was then extracted with EtOAc (5×10 mL). The collected organic phases were dried over anhydrous Na_2SO_4, filtered and concentrated. Compound **6** was yielded as a yellow oil (16 mg, 55%) without further purification. Spectroscopic data were in fully accordance with those reported in literature.[211]

*Synthesis of benzyl 2-(4-oxo-azetidin-2-yl) acetate (**7**)*

In a 25 mL 3-neck flask under inert atmosphere (N_2), Zn powder (203 mg, 3.12 mmol, 8 equiv) and THF (1 mL) were introduced followed by TMSCl (20 µL, 0.155 mmol, 0.39 equiv). After 30 min of stirring the temperature was raised to 30-32 °C and a solution of benzylbromoacetate (247 µL, 1.56 mmol, 4 equiv) in THF (2 mL) was slowly added dropwise. After 30 min of stirring the mixture was cooled to rt and decanted. The limpid grey supernatant was slowly added dropwise into a 25 mL flask under nitrogen containing a solution of **(+)5** (50 mg, 0.39 mmol, 1 equiv) in anhydrous THF (2.2 mL) at 0°C. The mixture was stirred at rt for 3 h, quenched with a saturated

Seignette salt (potassium sodium tartrate) solution and extracted with EtOAc (3x10 mL). The organic layers were dried on Na_2SO_4, filtered and concentrated in vacuum. The crude was purified by flash chromatography (Cyclohexane/EtOAc = 1:1) yielding **7** as a white solid (57 mg, 67%). Spectroscopic data were in fully accordance with those reported in literature.[43]

*Synthesis of compounds **(+) 8** and **(-) 8***

In a round bottom flask under inert atmosphere (N_2), to a solution of dimethyl disulfide (10 μL, 0.11 mmol, 1 equiv) in dry DCM (1 mL), SO_2Cl_2 (13 μL, 0.16 mmol, 1.5 equiv) was slowly added at 0°C. After 10 minutes, **(+) 5** or **(-) 5** (14 mg, 0.11 mmol, 1 equiv) dissolved in DCM (1 mL) was added, followed by dropwise addiction of TEA (28 μL, 0.22 mmol, 2 equiv). After 10 minutes at 0°C, the reaction mixture was warmed to rt and then refluxed for 4 h. At completion (TLC monitoring), the reaction was quenched with saturated aqueous solution of NH_4Cl and the mixture extracted with DCM (3x5 mL). The collected organic phases were dried over anhydrous Na_2SO_4, filtered and concentrated under vacuum. The desired product was obtained as a yellow oil after purification by flash chromatography on silica gel (Cyclohexane/EtOAc = 7:3). **(+)8**: 13 mg, Y=68%, ee = 88%, $[\alpha]_D^{20}$ = +10 (c = 0.6, MeOH); **(−)8**: 12.5 mg, Y=65%, ee = 95%, $[\alpha]_D^{25}$ = −11.5 (c = 0.8, MeOH). Spectroscopic data were in fully accordance with those reported in literature.[143,211]

2.2 Study of nucleophilic substitutions at C4 positions of β-lactam compounds

As previously discussed, one of the most important intermediates on the synthesis of monocyclic β-lactams, as demonstrated in *Chapter 2.1*, is the 4-acetoxy-2-azetidinone. It can be functionalised at the amidic nitrogen or/and at the C-4 position to develop new compounds having different activities.

Specifically, the C4 position can be functionalised by a nucleophilic substitution reaction following an S_N1 pathway. Nucleophilic substitution reaction with a base as catalyst, is widely known for this type of compounds and follows the mechanism reported in *Figure 69*.[250]

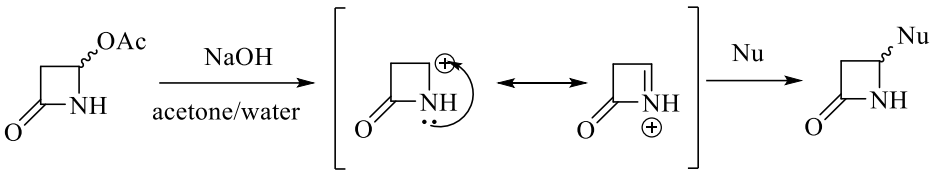

Figure 69. General nucleophilic substitution at C4 position of β-lactam compounds using bases.

My research team conducted a study on C3 and C4 disubstituted β-lactams, that underwent nucleophilic substitution at C4 position, showing a retention of configuration. This means that probably a S_N1 reaction mechanism occurs. The Rate Determining Step of a S_N1 reaction is the formation of the carbocation and the reaction rate depends on its formation. In our case, the carbocation at the C4 position is a secondary one and it can undergo a S_N1 reaction with the possible stabilization by a lone-pair back donation and formation of a N1-C4 double bond (*Figure 97*).

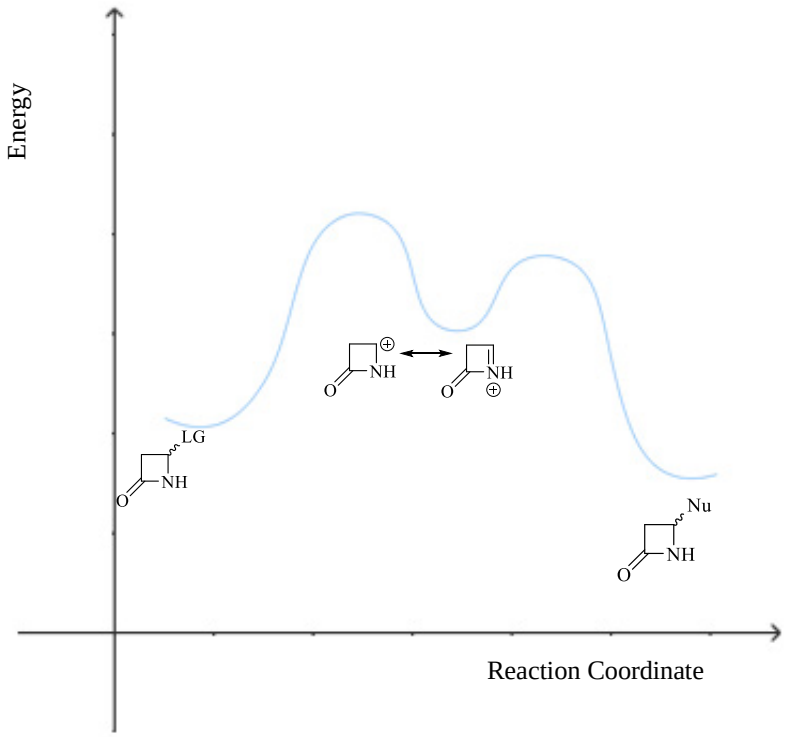

Figure 70. Energy diagram for a S_N1 reaction.

This intermediate with a N1-C4 double bond is similar to the oxonium ion which is formed during a glycosidation reaction; in fact, the positive charge on C1 was stabilized for back-donation of the lone-pair on the oxygen atom and the subsequent formation of an oxonium ion. This intermediate is formed as a consequence of the elimination of the anomeric leaving group during a S_N1 reaction (*Figure 71).*[251]

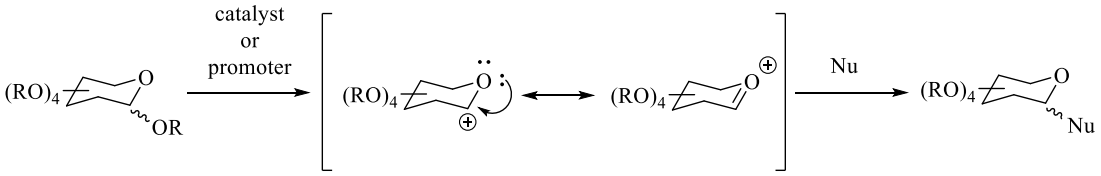

Figure 71. General scheme of a glycosidation reaction.

Therefore, the β-lactam C4 position can be compared to the glycosidic C1 position, having both an electrophilic character; the cationic intermediate of the glycosidation could be instead compared to the one of nucleophilic substitution reaction.

Figure 72. Intermediates in comparison.

Considering this information, the aim of our study is to further explore the reactivity at the C4 position of β-lactam based compounds through nucleophilic substitutions S_N1, under different conditions; moreover, thanks to the aforementioned similarity between the cationic intermediate of β-lactams and the oxonium ion of glycosides we want to apply typical reaction conditions of glycosidation to S_N1 reactions on azetidinones.

Results and discussion

We will divide this study in three main paragraphs:

1- Non-catalysed reactions
2- Catalysed reactions
3- Glycosidation reaction conditions

Initially, we studied the reactivity at C4 position using benzyl alcohol or 4-methoxybenzylamine as nucleophiles in two different solvents: water and DCM, without any catalyst. In addition, selected alcohols were employed both as nucleophile and solvent.
Subsequently, we employed acid or basic catalysts to promote the S_N1 reaction. Polymeric resins were used as acid catalyst, while several amines having different basicity were used as basic catalyst. The nucleophiles chosen are the benzyl alcohol and different amines.

Finally, to extend our study, we compared the reactivity at C4 position of β-lactams to the reactivity at the anomeric position of glycosides. To do that, S_N1 reactions were conducted on selected β-lactams employing reaction conditions characteristic of glycosidation; they involve the use of lewis acids such as $BF_3 \cdot Et_2O$, $TiCl_4$, and $AlCl_3$, and promoters such as NBS and triflates. Moreover, to imitate an O-glycoside synthesis, alcohols were employed as nucleophiles.

1. Non-catalysed reactions

1.1 Benzyl alcohol as nucleophile

The experiments described in this section provide the use of benzyl alcohol as nucleophile in water and DCM.

Table 10. Benzyl alcohol as nucleophile.[a]

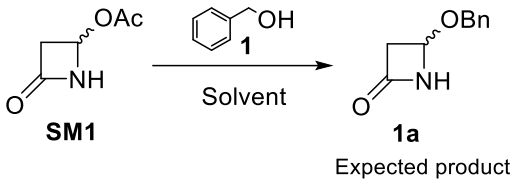

Reaction	1 (equiv)	Solvent	Temperature	Time	Conversion (%)	Crude *(mg)*	SM1:1:1a[b]
reac-97	2	H_2O	65°C	1h	0	25.4	1:1:0
reac-128	1.1	H_2O	rt	17h	0	34.4	1:1:0
reac-126	1.1	DCM	-20°C	6h	0	36.9	1:1.5:0
reac-46	1.1	DCM	0°C	5h	~0	10.5	1:2:traces
reac-131	1.1	DCM	rt	24h	0	34	1:1:0
reac-132	1.1	DCM	rt	23h	0	29.7	1:2:0

[a] Reaction conditions: SM (0.155 mmol), solvent (1.5 mL).
[b] Composition of the crude was determined via ^1H NMR analysis.

The 4-acetoxy-2-azetidinone is well soluble in H_2O, but it did not undergo any reaction with benzyl alcohol in this solvent (*Table 10*, reac-97-reac-128). Regarding DCM as solvent instead, only in reac-46 (*Table 10*), conducted at 0°C, the expected product **1a** was observed, but in traces.

1.2 4-methoxybenzylamine as nucleophile

4-Methoxybenzylamine (**2**) was also tested as nucleophile both in water and DCM.

Table 11. 4-methoxybenzylamine as nucleophile.[a]

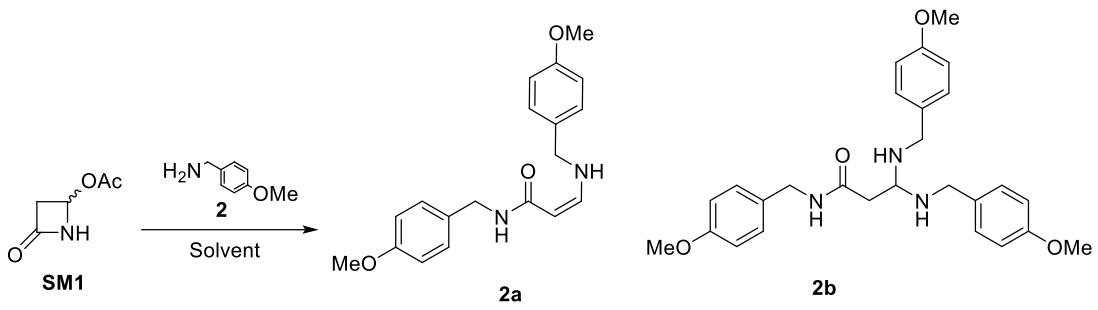

Reaction	2 (equiv)	Solvent	Temperature	Time	Conv. (%)	Crude (mg)	SM1:2:2a-2b[b]
reac-112	0.5	H_2O	rt	30min	100	12	1:2:1.5
reac-137	1	DCM	rt	22h	35	43.5	Complex mixture
reac-99	2	H_2O	65°C	1h	100	28.9	0:1:1
reac-100	2	H_2O	rt	30min	100	34.6	0:1:1
reac-133	2	H_2O	rt	30min	100	31.4	0:1:0
reac-146	2	H_2O	rt	3min	100	21.3	0:0:1
reac-103	2	DCM	rt	5h	75	33.1	1:1:4
reac-104	2	DCM	0°C	25h	100	28.9	0:1:1
reac-145	2	DCM	rt	18h	65	62.4	1:2.5:1.5

[a] Reaction conditions: SM (0.155 mmol), solvent (1.5 mL).
[b] Composition of the crude was determined via ^{1}H NMR analysis.

With 4-methoxybenzylamine as nucleophile and H_2O as solvent, the starting 4-acetoxy-2-azetidinone disappeared immediately affording a full conversion (*Table 10*, reac-112) but crude is presented in a complex mixture. We were able to trace compounds **2a** and **2b** whose structures were deduced by careful analysis of ^{1}H NMR, ^{13}C NMR, COSY, HSQC, IR and HPLC-MS data. On the other hand, reactions conducted in DCM did not show full conversions (except for reac-104); moreover, the crude mixtures were similar to those obtained in water.

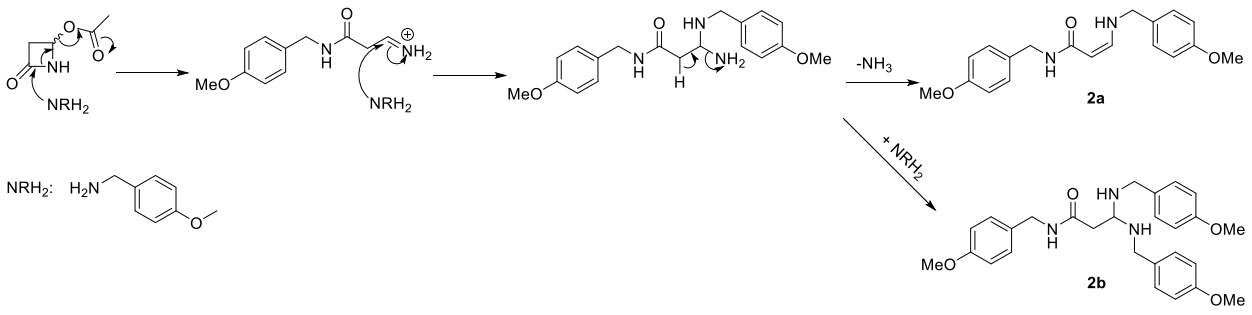

Scheme 37. 4-methoxybenzylamine hypothesised nucleophilic attack to give **2a** and **2b.**

In general, 4-methoxybenzylamine is a good nucleophile and probably it attacks the carboxylic carbon of the ring, which is extremely electrophile. **2a** and **2b** derive from different reaction pathways (*Scheme 37*): **2a** could derive from the nucleophilic attack at the carboxylic carbon which led to the ring opening followed by a nucleophilic substitution at C4 position; only subsequently there could be the formation of the α,β-unsaturated compound. On the other hand, **2b** could derive from nucleophilic attack at the carboxylic centre followed by a double substitution at C4 position. Compounds **2a** at ^{1}H NMR showed 8.0Hz vicinal coupling between vinyl hydrogens, thus confirming a Z geometry of the C=C bond. This geometry is probably due to an intramolecular hydrogen bond (*Figure 73*).

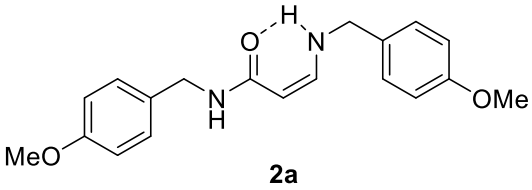

Figure 73. Intramolecular hydrogen bond which could favour Z geometry.

1.3 Acetone and acetonitrile as solvents

We wanted to extend our study using different solvents as acetone and acetonitrile in the absence of a catalyst. We followed the procedure previously described.

Table 12. Reactions conducted using different solvents.[a]

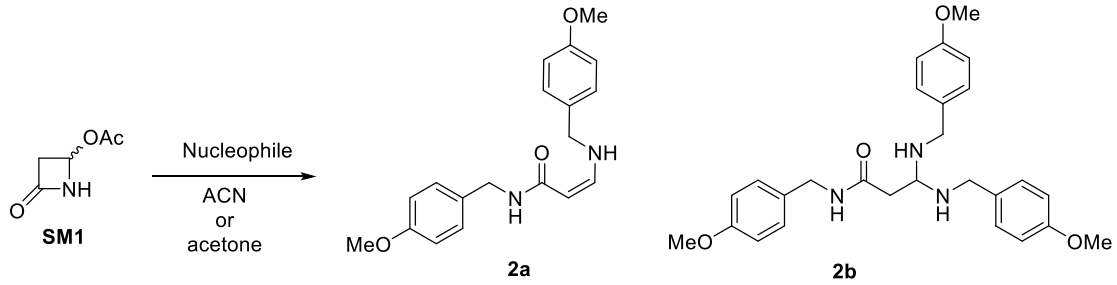

Reaction	Nucleophile (equiv)	Solvent	Time	Conv. (%)	Crude (mg)	SM1:Nu:Product[b]
reac-124	BnOH (1.1)	Acetone	19h	0	35.7	1:2:0
reac-125	BnOH (1.1)	ACN	19h	0	31.1	2:3:0
reac-135	4-methoxybenzylamine (2)	ACN	22h	100	68.5	0:0:1**(2a - 2b)**

[a] Reaction conditions: SM (0.155 mmol), solvent (1.5mL).

[b] The composition of the crude was determined via ^{1}H NMR analysis.

Experiments conducted with benzyl alcohol **1**, did not give any product. Probably the solvation of the nucleophile benzyl alcohol in those solvents lowered its nucleophilicity. On the contrary, as for reactions in water and DCM, the nucleophile 4-methoxybenzylamine **2** gave a complete conversion (*Table 12*, reac-135) but lading to **2a** and **2b.**

1.4 Nucleophiles as solvent

We extend our study also using Methanol and Ethanol both as solvents and as nucleophiles.

Table 13. Methanol and ethanol used as nucleophiles and solvents.[a]

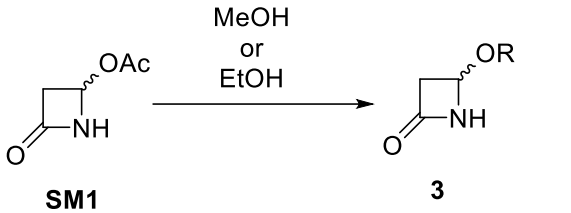

Reaction	Nucleophile	Time	Temperature	Conv. (%)	Crude (mg)	SM1:Nu:Product[b]
reac-129	MeOH	19h	rt	5	19.1	1:1:0.05(**3a)**
reac-130	EtOH	24h	rt	10	17.9	1:1:0.10(**3b)**
reac-134	EtOH	7h	60°C	30	14.7	1:0:0.30(**3b**)

[a] Reaction conditions: SM (0.155 mmol), solvent (1mL).
[b] Composition of the crude was determined via ^{1}H NMR analysis.

Reaction in pure methanol showed low conversion, 5%, with only traces of the methyl ether (**3a**). Analog results were obtained with ethanol, at two different temperatures (r.t. and 60°C) giving the ethyl ether (**3b**) in traces. We noticed that higher is the temperature higher is the starting material conversion. However, the highest conversion of 30% is still poor and it means that a catalyst is required.

2. Catalysed reactions

The experiments in which the nucleophile was employed as solvent allow us to understand that this type of reaction needs a catalyst; so, we decide to test different types of catalysts, acids and bases. The procedure employed was the same used for reactions reported before, the only variation is that the catalyst was added as last reactant.

2.1 Acid-catalysed reactions

Initially we chosen an acid polymeric resin as catalyst because it can provide acid conditions and it can be easily removed from the reaction mixture by filtration.

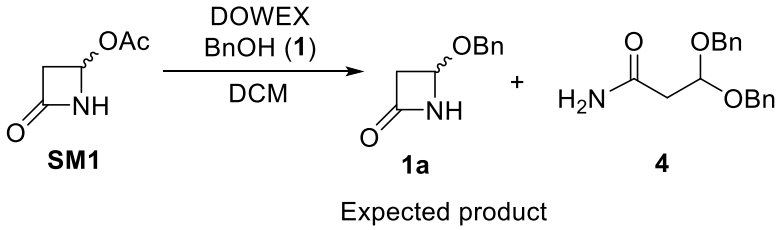

Scheme 38. DOWEX as acid catalyst.

DOWEX (50WX2-200(H)) was employed as catalyst and it led to the formation of **4** with a starting material conversion of 30% in 21 hours. The crude (25.8 mg) composition was determined by ^{1}H NMR; thanks to the latter we have hypothesised the molecular structure of compound **4** and then confirmed it by IR, HPLC-MS, ^{13}C NMR, COSY, and HSQC analysis.

2.2 Base-catalysed reactions

We also tried reactions using some selected tertiary amines as base catalysts to promote the nucleophilic substitution reaction.

Table 14. Amines as catalysts.[a]

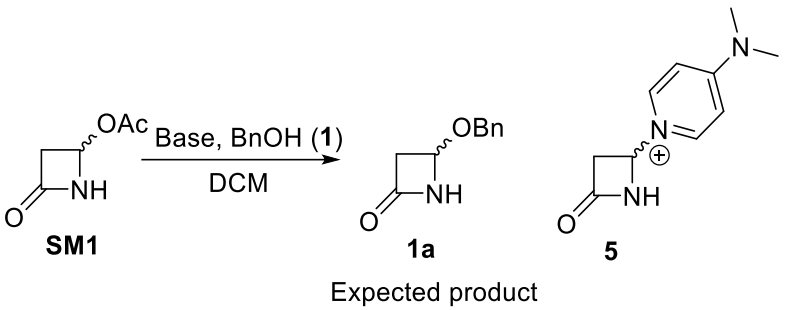

Reaction	1 (equiv)	Catalyst (equiv)	Temperature	Time	Conv. (%)	Crude (mg)	SM1:1:1a:5[b]
reac-132	1.1	DMAP (cat.)	rt	23h	0%	29.7	1:2:0:0
reac-151	2	DMAP (1)	rt	3 days	100	65.9	1:2:0:traces
reac-153	2	DMAP (1)	rt	2h 15min	100	69.5	1:8:0:2
reac-136	-	TEA (1)	rt	22h	0	19.8	1:1:0:0[c]
reac-149	2	TEA (1)	rt	23h	50	37.2	1:3:1:0
reac-154	2	TEA (1)	reflux	21h 45min	75	59.3	2:8:1:0
reac-152	2	DIPEA (1)	rt	3 days	10	53.4	1:2:0.10:0
reac-156	2	Morpholine (1)	rt	22h	0	51.3	1:1:0:0
reac-158	2	Quinine (1)	rt	22h 30min	0	91.6	1:1:0:0
reac-161	2	L-(-)-Norephedrine (1)	rt	29h	0	57.5	1:1:0:0

[a] Reaction conditions: SM (0.155 mmol), DCM (1.5mL).
[b] Composition of the crude was determined via ^{1}H NMR analysis.

We chose different bases as catalysts, such as 4-Dimethylaminopyridine (DMAP), Triethylamine (TEA), N,N-Diisopropylethylamine (DIPEA), morpholine, and two chiral bases as quinine, and L-(-)-norephedrine. Reac-151 and reac-153 (*Table 14*) were conducted using 1 equivalent of DMAP and led to a starting material conversion of 100%; both crudes showed a ^{1}H NMR spectrum in which is detectable compound **5,** but further studies are required to confirm the molecular structures and its formation mechanism. TEA as catalyst, in reac-149 and reac-154**,** led to a significant starting material conversion. Reac-149 showed a SM conversion equal to 50% giving the compound **1**. To improve the starting material conversion, the same reaction was conducted at reflux (*Table 14*, reac-154) with an increased conversion (75%). TEA was also used without any nucleophile to study its effect on the starting material (*Table 14*, reac-136). By ^{1}H NMR analysis of the crude it was observed the formation of ammonium acetate thus confirming the effect of TEA in promoting the exit of the acetate group at C4. Other amines such as DIPEA, morpholine, quinine, and L-(-)-norephedrine did not give any relevant result.

2.3 Amines as nucleophiles

To extend the scope decided to extend our screening using selected amines as nucleophile.

Table 15. Amines as nucleophile.[a]

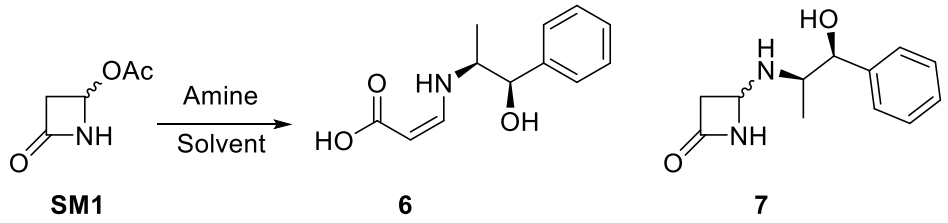

SM1 **6** **7**

Reaction	Nucleophile (equiv)	Solvent	Time	Conv. (%)	Crude (mg)	SM1:Nu:Product[b]
reac-167	4-metoxy aniline (1)	DCM	23h	0	29	1:1:0
reac-162	L-(-)-norephedrine (1)	H_2O	29h	16	27.8	1:0:traces (**6**)
reac-168	L-(-)-norephedrine (1)	DCM	2h	50	7.0	1:1:1 (**7**)
reac-172	L-(-)-norephedrine (2)	DCM	15h 30min	100	37.4	0:1:1 (**6**)
reac-171	L-(-)-amphetamine (1)	H_2O	22h	0	21.5	1:0:0
reac-165	L-(-)-amphetamine (1)	DCM	29h	0	8.0	1:0:0
reac-166[c]	L-(-)-amphetamine (1)	DCM	23h	0	12.1	1:0:0
reac-169	L-(-)-ephedrine (1)	H_2O	22h	0	8.2	1:0:0
reac-170[d]	L-(-)-ephedrine (1)	H_2O	23h	0	11.2	1:0:0
reac-173	L-(-)-ephedrine (2)	H_2O	15h	0	4.	1:0:0

[a] Reaction conditions: SM (0.155 mmol), Solvent (1.5mL), rt.
[b] Composition of the crude was determined via ^{1}H NMR analysis.
[c] Amphetamine sulfate as nucleophile
[d] Ephedrine hydrochloride as nucleophile

Reac-162 (*Table 15*) gave an interesting result, giving the derivate **6** that could be compared to **2a** (similar ^{1}H NMR spectrum). Compound **6** have not been isolated, but its structure was obtained by ^{1}H NMR analysis which showed 8.0 Hz vicinal coupling between vinyl hydrogens, thus confirming a Z geometry of the C=C bond. This geometry is probably due to an intramolecular hydrogen bond (*Figure 74*).

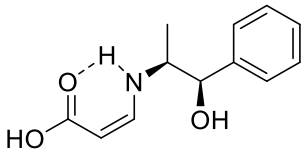

6

Figure 74. Intramolecular hydrogen bond favours Z geometry.

On the other hand, reac-172 (*Table 15*) was conducted using 2 equivalents of L-(-)-norephedrine and showed a ^{1}H NMR spectrum that showed the presence of compound **6**. In reac-168 (*Table 15*) the crude ^{1}H NMR analysis revealed the presence of two β-lactam systems, one corresponds to the starting material and the other one could be the N-substituted one (**7**). Nevertheless, crudes weights are smaller than we expected and for this reason it was necessary an ^{1}H NMR analysis of the aqueous layers, which revealed for reac-168, reac-169, reac-172, and reac-173 (*Table 15*) the presence of correspondent ammonium acetates, indicating that the acetoxy group leaved the C4 position. Thus, the most promising amines are the L-(-)-norephedrine which led to compounds **6** and **7.**

3. Glycosidation reaction conditions: Lewis acids and promoters as catalysts

To extend the study of the mechanism that occurs at C4 position of β-lactams, we made a screening using lewis acids and promoters as catalysts. The lewis acids screened are $BF_3{\cdot}Et_2O$, $AlCl_3$, $TiCl_4$; then we used triflates such as AgOTf, TMSOTf, $Zn(OTf)_2$ and NBS; moreover, different β-lactam-based starting materials have been used (such as 4-acetoxy-2-azetidinone and 4-(phenylthio)azetidin-2-one)

3.1 4-acetoxy-2-azetidinone

$BF_3{\cdot}Et_2O$

Table 16. $BF_3{\cdot}Et_2O$ as Lewis Acid.[a]

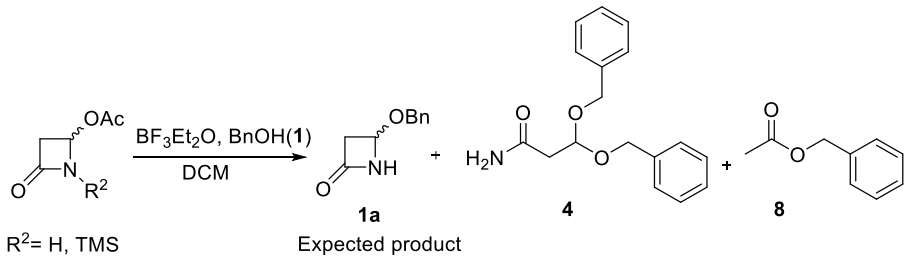

Reaction	$BF_3{\cdot}Et_2O$ (equiv)	BnOH (equiv)	Time	Conv. (%)	Crude (mg)	SM:1:1a:4:8 [b]
reac-46	-	1.1	5h	0	10.5	1:2:traces:0:0
reac-58	-	1.1	overnight	0	22.1	1:2:0:0:0
reac-119[c]	-	1.1	3h	0	35	1:4:0:0:0
reac-120[c]	-	1.1	5h 30min		29.3	1:1:0:0:0
reac-122[c]	-	1.1	7h	0	30.4	1:1:0:0:0
reac-50	2	-	5h	0	15.5	1:0:0:0:0
reac-45	cat.	1.1	5h	50	18.6	2:1:0:2:0
reac-73	cat.	1.1	5h	50	27.8	1:2:0:1:0
reac-95	cat.	1.1	48h	100	26.3	0:1:0:0:0
reac-44	1	1.1	5h	67	15.4	1:4:0:2:0
reac-36	2	1.1	20min	100	38.4	0:1:0:0:1
reac-40[d]	2	2	2h	50	23.1	1:3:0:1:0
reac-42	2	1.1	2h	100	30.9	0:1:0:1:0
reac-47[e]	2	1.1	4h	100	80.2	0:0:0:1:0
reac-48	2	1.1	4h	100	28.8	0:2:0:1:0
reac-49	2	1.1	4h	100	21.4	0:1:0:1:0
reac-59	2	1.1	5h	100	21.2	0:3:0:1:0
reac-88[d]	2	1.1	23h	100	20.2	0:17:0:1:0
reac-96[f]	2	1.1	48h	50	26.6	2:3:0:2:0
reac-102[g]	2	1.1	48h	45	20.2	1:1.5:0:0.45:0
reac-114	2	2	overnight	100	38.6	0:0:0:0:1
reac-117	2	2	35min	100	36.1	0:1:0:0:1
reac-121	2	2	2h	100	40.4	0:3:0:2:0

[a] Reaction conditions: SM (0.155 mmol), DCM (1.5mL).
[b] Composition of the crude was determined via ^1H NMR analysis.
[c] No work-up.
[d] Silylated SM.
[e] SM (0.38mmol), DCM 3mL.
[f] Molecular Sieves 4A (1-2mm beads).
[g] Molecular sieves 4A (activated powder).

We wanted to study possible reactions between our starting material and the selected nucleophiles in absence of lewis acid. With this scope, in experiments reac-46, reac-58, reac-119, reac-120, and reac-122 the lewis acid was not added in the attempt to study the nucleophile behaviour towards the 4-acetoxy-2-azetidinone under different reaction conditions.
Only reac-46 showed the formation of **1a** in traces and was performed in 5 hours. Other experiments did not show any reactions between starting material and benzyl alcohol. A similar strategy was employed with the experiment reac-50 in which the nucleophile was not added in the attempt to study the lewis acid behaviour towards the starting 4-acetoxy-2-azetidinone; no reaction was observed. Experiments reac-40, reac-44, reac-45, reac-73, reac-96, and reac-102 led to **4**. Among these experiments, reac-44 is the only one that showed an higher starting material conversion (67%). It was conducted employing 1 equivalent of $BF_3{\cdot}Et_2O$, 1.1 equivalent of benzyl alcohol with a reaction time of 5 hours. Experiments reac-42, reac-47, reac-48, reac-49, reac-59, reac-88, and reac-121 led to the total conversion of the starting material giving **4** as

product. These reactions were all performed using 2 equivalents of $BF_3{\cdot}Et_2O$ and 1.1 equivalent of benzyl alcohol with variable reaction times. It is evident that employing 2 equivalents of $BF_3{\cdot}Et_2O$ instead of 1, led to the full conversion of the starting material. Experiments reac-36, reac-114, and reac-117 were conducted using 2 equivalents of $BF_3{\cdot}Et_2O$ and 2 equivalents of benzyl alcohol; it was observed that these conditions led to the total conversion of the starting material giving **8** as product, probably as result of a transesterification that occurred between the acetoxy group and the benzyl alcohol. Furthermore, we wanted to test if the 4-acetoxy-2-azetidinone reactivity could be influenced by a previous silylation at the amidic nitrogen; reac-40 and reac-88 were conducted on a pre-silylated starting material. We noticed that the silylation do not prevent the ring opening reaction; however, at longer reaction time (reac-88) is evident the full conversion of the starting material. Generally, the experiments in which lewis acid was employed showed an unexpected reactivity, and there is not a comparable reactivity with the anomeric position of sugars. Almost all reactions have **4** as product, which was isolated characterized by ^1H NMR, ^{13}C NMR, HPLC-MS, IR. To extend our knowledge about compound **4,** we wanted to conduct a reaction scope using different nucleophiles. Reac-42 gave the best result to obtain **4**, so we decided to use these conditions to conduct the following Scope.

*Reaction Scope: Compound **4***

To extend the study on the ring opening reaction by $BF_3{\cdot}Et_2O$ we tested some alcohols as nucleophiles:

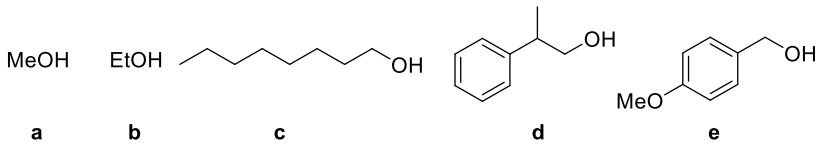

Figure 75. Nucleophiles employed.

The best result was obtained adopting 4-acetoxy-2-azetidinone as starting material, $BF_3{\cdot}Et_2O$ as lewis acid, and benzyl alcohol as nucleophile (*Table 16*, reac-42).

Table 17. Reaction scope experiments.[a]

Entry	$BF_3{\cdot}Et_2O$ (equiv)	Nucleophile (equiv)	Time	Conv. (%)	Crude (mg)	SM1:Nu:Product[b]
reac-105	2	**a** (1.1)	4h 20min	100	3.0	0:1:1
reac-106	2	**b** (1.1)	4h 20min	100	4.0	0:1:1
reac-55	2	**c** (1.1)	overnight	0	19.8	0:1:0
reac-108	2	**d** (1.1)	4h 20min	100	26.5	0:1:0
reac-107	2	**e** (1.1)	4h 20min	100	27.8	Complex mixture
reac-111	2	**a** (2)	4h 40min	0	18.3	1:1:0
reac-118	2	**c** (2)	2h	100	58.6	0:1:1
reac-108	2	**d** (2)	4h 20min	100	26.5	0:1:0
reac-109	2	**e** (2)	40min	100	43.1	Complex mixture

[a] Reaction conditions: SM (0.155 mmol), DCM (1.5mL).
[b] Composition of the crude was determined via ^{1}H NMR analysis.

All the experiments have been made both using 1.1 or 2 equivalents of the nucleophile. In most cases it is evident that a higher concentration of nucleophile gave faster reactions, only methanol, ethanol, and octanol gave the opened derivates **4a**, **4b**, and **4c**.

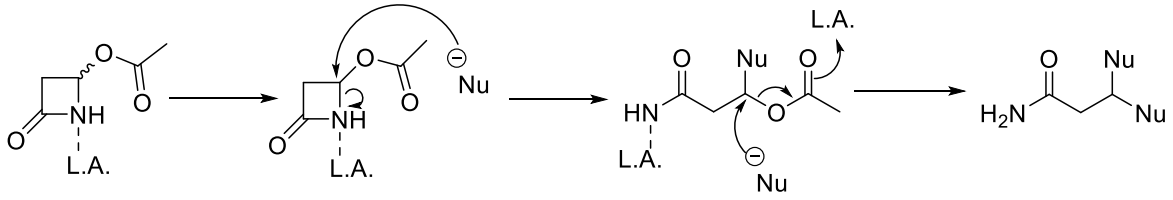

Scheme 39. Hypothetical mechanism for the nucleophilic attack at C-4 position.

The mechanism that probably occurs is reported in *Scheme 39*. The C-N bond (184 Kcal/mol) is weaker than the C-O (257 Kcal/mol) and this weakness is increased by the nitrogen-lewis acid coordination, thus the C-N bond-breaking could be the first step of the reaction.
To get information, we have synthetized the 4-oxoazetidin-2-yl benzoate, compound **1a**, employing known procedures.

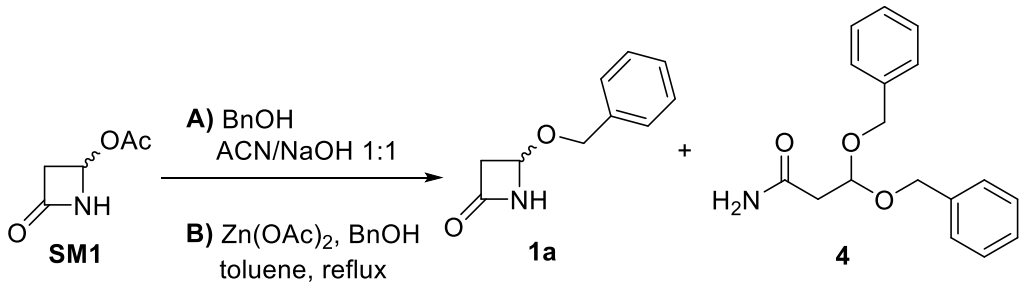

Scheme 40. Two ways to synthetize **1a**.

For preparation of compound **1a** two procedures were tested. In the first procedure, NaOH is used as base to activate benzyl alcohol; the starting material did not completely disappear and after a ^{1}H NMR analysis it was evident that the starting material and the compound **1a** ratio is

1:1. It is also evident the presence of the compound **4** and benzyl alcohol. Using the second procedure, the crude ^{1}H NMR spectrum showed only the presence of compound **1a** and benzyl alcohol, but when the crude was purified by flash-chromatography it was evident the presence of a third by-product. The latter was isolated and then analysed; the spectrum was comparable to the one of compound **4**. The best result to synthetize **1a** was obtained using the second procedure and **1a** was then used for the reaction with BnOH (**1**) and $BF_3{\cdot}Et_2O$.

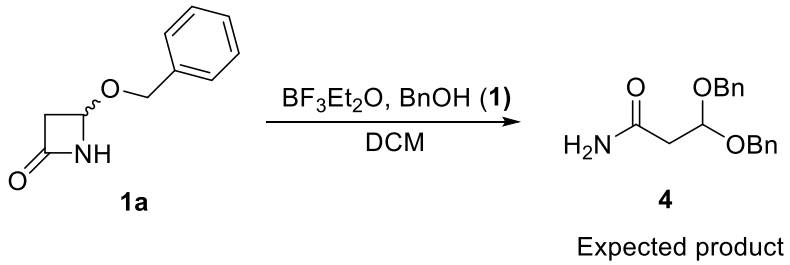

Scheme 41. **1a** treated with BnOH and $BF_3{\cdot}Et_2O$.

The ^{1}H NMR spectrum revealed the total conversion of the starting material, but it was observed the formation of **4** only in traces**.** Thus, to evaluate its formation mechanism further studies are required.

$TiCl_4$

Table 18. $TiCl_4$ as lewis acid.[a]

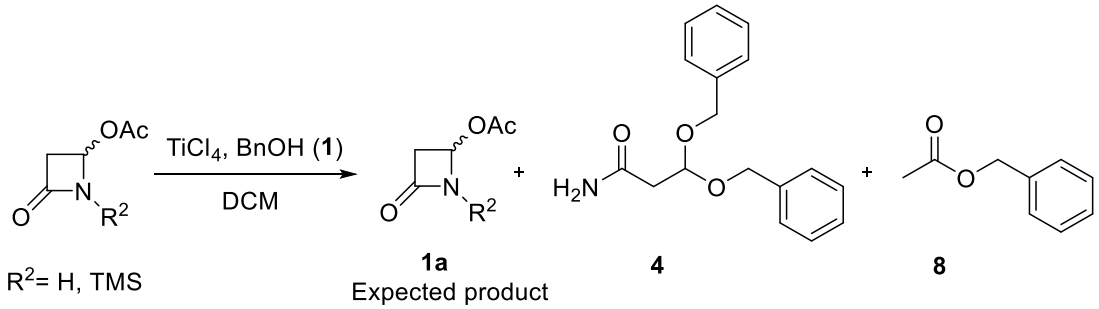

Reaction	$TiCl_4$ (equiv)	1 (equiv)	Time	Conv. (%)	Crude (mg)	SM:1:1a:4:8[b]
reac-38	2	2	2h 30min	50	29.8	1:3:0:2:0
reac-39[c]	2	2	overnight	50	34.7	1:2:0:1:0
reac-90[c]	2	1.1	overnight	0	35	1:6:0:0:0
reac-91	2	1.1	overnight	50	23.1	0:0:0:0:1

[a] Reaction conditions: SM (0.155 mmol), DCM (1.5mL), 0°C.

[b] Composition of the crude was determined via ^{1}H NMR analysis.

[c] Sylilated starting material.

Both experiments reac-38 and reac-39 led to **4** (the second one was conducted on a pre-silylated starting material at the amidic nitrogen). When the SM is previously silylated the amount of product **4** is less. Similarly, we have reac-90 and reac-91: the first one involved the previous silylation of the starting material; in those experiments were employed 1.1 equivalents of benzyl alcohol instead of 2. Reac-90 was useful to confirm that the silylation prevents the formation of **4**, using $TiCl_4$ as catalyst. Reac-91 led to the formation of **8**; the latter is a consequence of a transesterification that occured between benzyl alcohol and the acetate at C-4 position of 4-acetoxy-2-azetidinone. Probably, during the work-up the benzyl acetate remained in the organic layer, while the 4-acetoxy-2-azetidinone probably underwent ring-opening reaction and stays in aqueous layer.

$AlCl_3$

Table 19. $AlCl_3$ as Lewis Acid.[a]

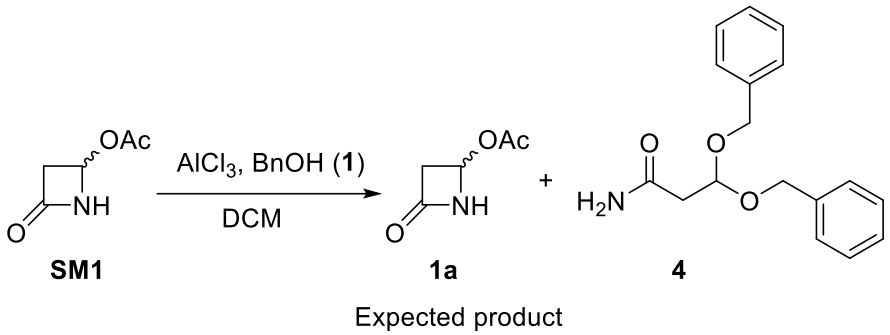

Reaction	$AlCl_3$ (equiv)	1 (equiv)	Time	Conv. (%)	Crude (mg)	SM1:1:1a:4[b]
reac-72	2	-	5h	0	11.7	1:0:0:0
reac-81	cat.	1.1	overnight	0	37.6	1:2:0:0
reac-80	1	1.1	overnight	0	32.9	0:1:0:0
reac-51	2	1.1	overnight	0	38.1	1:1:0:traces
reac-53	2	1.1	overnight	0	16	3:1:0:0
reac-60	2	1.1	overnight	0	38.7	1:1:0:0
reac-70	2	1.1	5h	0	30.2	1:1:0:0

[a] Reaction conditions: SM (0.155 mmol), DCM (1.5mL), 0°C.
[b] Composition of the crude was determined via ^1H NMR analysis.

In reac-72 the nucleophile was not added in the attempt to study the $AlCl_3$ behaviour towards the 4-acetoxy-2-azetidinone; it revealed that there were no interactions. All reactions conducted in the presence of $AlCl_3$ as lewis acids did not show any reactivity, even if they have been

performed using different amounts of $AlCl_3$ and variating the reaction time. Reac-51 is the only experiment in which the starting material was partially converted giving **4** in traces.

TMSOTf

Table 20. *TMSOTf as promoter.*[a]

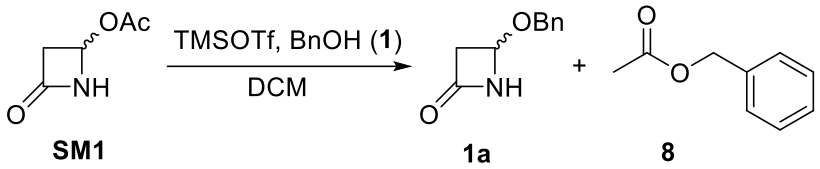

Reaction	TMSOTf (equiv)	1 (equiv)	Time	Conv. (%)	Crude (mg)	SM1:1:1a:8[b]
reac-86	cat.	1.1	overnight	100	15.7	0:0:0:1
reac-139[c]	cat.	1.1	45h	100	27.3	0:0:0:1
reac-85	1	1.1	overnight	100	20.5	0:0:0:1
reac-56	2.5	1.1	15h	100	17.4	0:0:0:1

[a] Reaction conditions: SM (0.155 mmol), DCM (1.5mL), 0°C.
[b] Composition of the crude was determined via ^{1}H NMR analysis
[c] No work-up

All reactions that involved TMSOTf as promoter gave benzyl acetate **8** as product and this is a consequence of a transesterification that occurs between benzyl alcohol and the acetate at C4 position of 4-acetoxy-2-azetidinone. Probably, during the work-up the 4-acetoxy-2-azetidinone underwent ring-opening reaction and stays in aqueous layer.

AgOTf

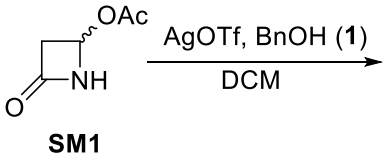

Scheme 42. AgOTf as promoter.

Using AgOTf as promoter, the reaction did not work, in fact, the starting material conversion was 0%.

NBS

Table 21. NBS as promoter.[a]

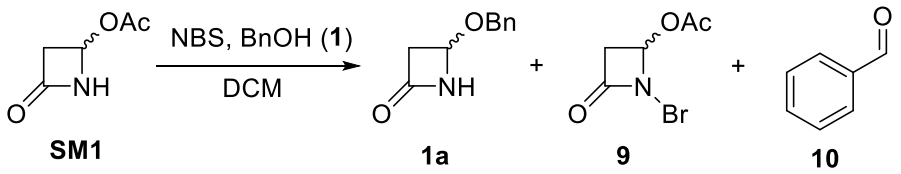

Reaction	NBS (equiv)	1 (equiv)	Time	Conv. (%)	Crude (mg)	SM1:1:1a:9:10[b]	Yield after purification[c]
reac-93	2	-	2h 30min	100	34	**0:0:0:1:0**	
reac-140	2	-	1h 30min	100	66.1	0:0:0:1:0	Y=95%
reac-142[d]	2	-	2h	100	52.3	0:0:0:1:0	Y=95%
reac-66	2	1.1	2h 30min	100	24.7	0:0:0:0:1	
reac-144	2	1.1	2h	100	27.1	0:0:0:0:1	

[a] Reaction conditions: SM (0.155 mmol), DCM (1.5mL), 0°C.

[b] Composition of the crude was determined via ^{1}H NMR analysis.

[c] Flash-chromatography Cyclohexane/EtOAc 7:3 then 1:1

[d] SM (0.39mmol)

In reac-93 the nucleophile was not added in the attempt to study the NBS behaviour towards the 4-acetoxy-2-azetidinone. In addition to the reactivity shown by the formation of **4**, another type of relevant reactivity was observed using NBS. In fact, the NBS oxidize the benzyl alcohol to benzaldehyde (**10**) when it was employed as nucleophile (reac-66 and reac-144); on the other hand, when the nucleophile was not employed, the NBS brominates the amidic nitrogen of the starting material (reac-93, reac-140, and reac-142). The oxidizing activity of NBS towards some alcohols is known, but we wanted to focus on the bromination reaction. The brominated product corresponds to the structure **9**, and from this molecule we would find new synthetic pathways to obtain different β-lactam based-compounds. Consequently, reac-140 and reac-142 were useful to obtain the compound **9**, necessary to conduct reactions in presence of benzyl alcohol and $BF_3{\cdot}Et_2O$ (*Scheme 43*, procedure as *Table 16*, reac-48).

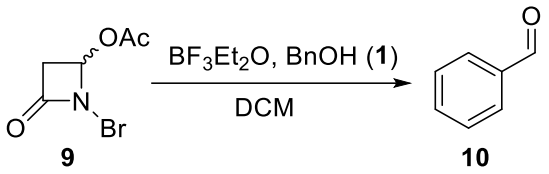

Scheme 43. Compound **9** as SM.

What we can see is that 4-acetoxy-2-azetidinone underwent ring opening reaction. In addition, it is evident the formation of benzaldehyde (**10**) derived from the oxidation of benzyl alcohol. The latter have been oxidized by the brominated β-lactam at the amidic nitrogen which acted as the NBS releasing the Br^+ ion which is an oxidant agent.

3.2 4-(phenylthio)azetidin-2-one

We decided to extend our study using a different staring material: the 4-(phenylthiol)azetidin-2-one. Previous work conducted by the research group demonstrated a higher reactivity at C4 position of this compound compared to the one of 4-acetoxy-2-azetidinone.

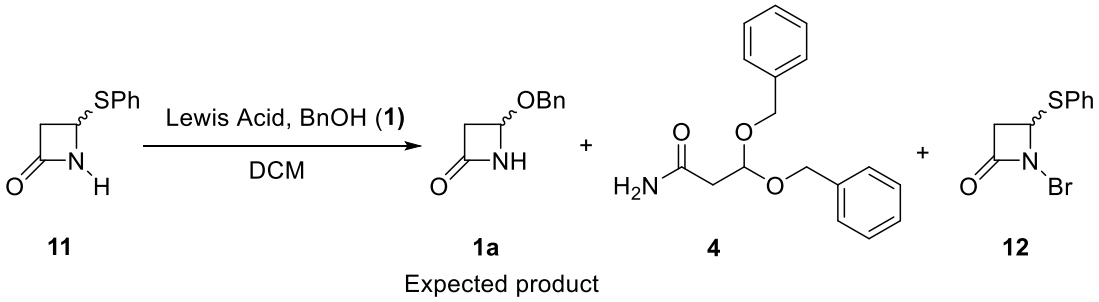

Scheme 44. 4-(phenylthio)azetidin-2-one as starting material reacts with lewis acids or promoters.

$BF_3{\cdot}Et_2O$

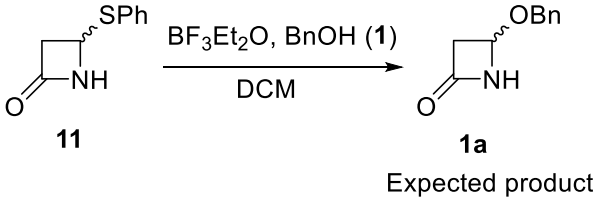

Scheme 45. $BF_3{\cdot}Et_2O$ as lewis acid.

The reaction was conducted using $BF_3{\cdot}Et_2O$, for 72 hours. ^1H NMR spectrum of the organic layer only showed the presence of benzyl alcohol, probably because the 4-(phenylthio)azetidin-2-one underwent ring-opening reaction and it remained in the aqueous layer.

AgOTf

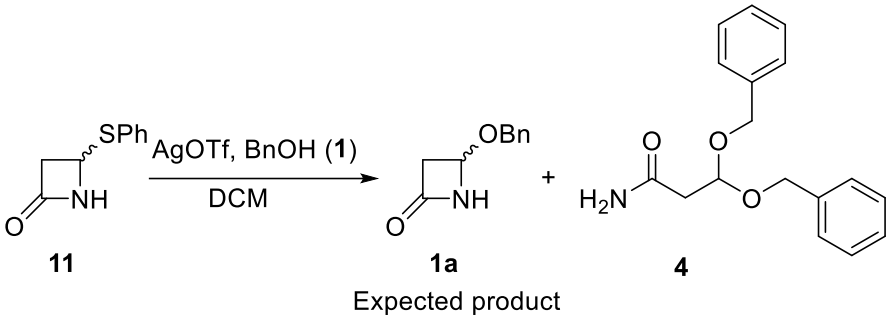

Scheme 46. AgOTf as promoter.

The reaction was conducted using AgOTf as promoter, for 4 hours. The ^{1}H NMR spectrum showed the formation of **4** with a SM conversion of 50%. The **11**:**1**:**1a** ratio is equal to 1:3:1.

NBS

Table 22. NBS as promoter.[a]

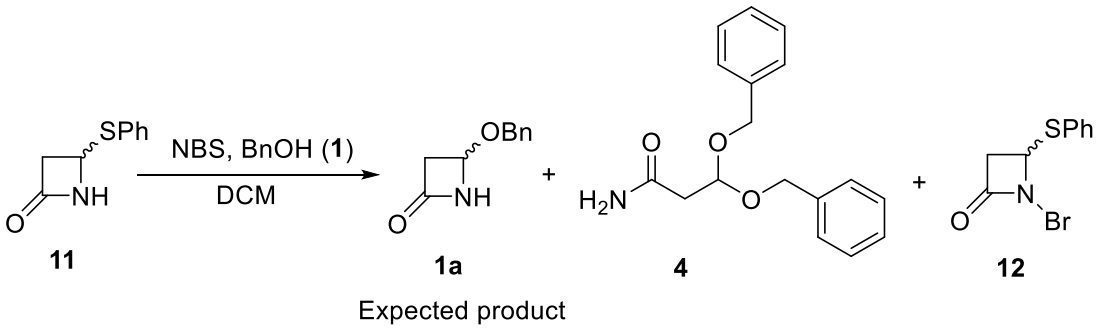

Reaction	NBS (equiv)	1 (equiv)	Time	Conv. (%)	Crude (mg)	11:1:1a:4:12[b]
reac-79	cat.	1.1	4h 40min	0	36.6	1:2:0:0:0
reac-77 [c]	1	1.1	2h 30min	80	62.9	1:14:0:2:2
reac-67	2	1.1	2h 30min	100	24.7	0:4:0:0:1
reac-71 [d]	2	1.1	1h 30min	100	96.4	0:1:0:0:0
reac-75	2	1.1	2h 30min	100	46.3	0:1:0:0:0
reac-78 [c]	2	1.1	2h 30min	100	97.1	0:1:0:0:1
reac-143	2	1.1	2h	100	47.5	0:1:0:0:0.30

[a] Reaction conditions: **11** (0.111 mmol), DCM (1.5mL), 0°C.

[b] Composition of the crude was determined via ^{1}H NMR analysis.

[c] **11** (0.279 mmol), DCM (1.5mL), -20°C (proc. 2). Crude purified by flash-chromatography (Cyclohexane/EtOAc 7:3 then 1:1).

[d] **11** (0.335 mmol), DCM (1.5mL), 0°C.

As seen for the 4-acetoxy-2-azetidinone, even the 4-(phenylthio)azetidin-2-one underwent ring-opening reaction giving compound **4**. Differently from the 4-acetoxy-2-azetidinone, that gave this results employing $BF_3{\cdot}Et_2O$ and $TiCl_4$, the 4-(phenylthio)azetidin-2-one led to the same product using AgOTf and NBS. This is probably related to the HSAB theory because the harder oxygen atom coordinates harder lewis acids, as $BF_3{\cdot}Et_2O$ and $TiCl_4$, and thus favours the exit of the leaving group. At the same time, the softer sulphur atom coordinates softer promoters (AgOTf and NBS), favouring the exit of the leaving group.
Reac-67, reac-77, and reac-78 showed a different ^1H NMR spectra. In fact, they showed an interesting β-lactam system; it was hypothesized that the β-lactam nitrogen could have been brominated by the NBS, and the spectra could be referred to the structure **12**.

Conclusions

This study allowed us to extend our knowledge about the reactivity at C4 position of β-lactam based compounds through nucleophilic substitution reactions (S_N1). Although the S_N1 reaction intermediate of β-lactams looks like the glycosidic reaction one, they do not have the same reactivity. In fact, employing glycosidation reaction conditions on selected β-lactam based compounds, we did not obtain the expected results, however β-lactams revealed an unexpected and interesting reactivity.

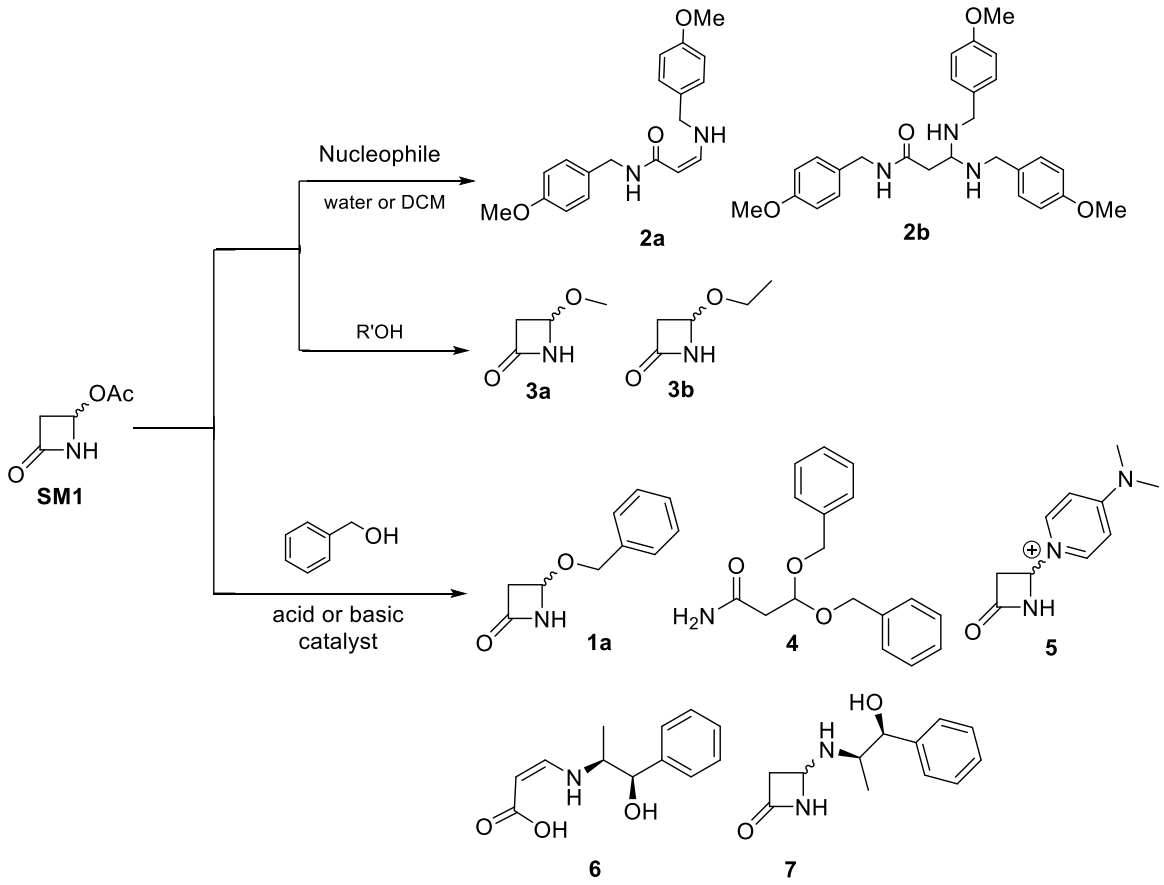

Figure 76. Non catalyzed and catalyzed reactions.

The 4-methoxybenzylamine turned out to be a strong nucleophile both in water and in DCM without needing the use of a catalyst; this nucleophile brought to compound **2a** and **2b**. In addition, methanol and ethanol employed both as nucleophiles and solvents, gave compounds **3a** and **3b** even though in very limited amount. This confirm that it is required a catalyst to promote the reaction with alcohols. To this aim, we used the Dowex resin (as acid catalyst) and TEA (as basic catalyst) which respectively gave compound **4** and compound **1a**. Among the amines employed both as nucleophiles and catalysts, the most promising was the L-(-)-norephedrine, which gave **6** and **7**. These products will be studied in depth by the research group. Furthermore, they are potential optically active compounds because they derive from an optically active amine, thus further studies will be done to isolate them and to assess their potential use.

To extend our work, we explored the reactivity at C4 position of 4-acetoxy-2-azetidinone and 4-(phenylthio)azetidin-2-one applying the glycosylation reaction conditions. These two different starting materials led to different compounds according to the type of catalyst employed (*Figure 77*).

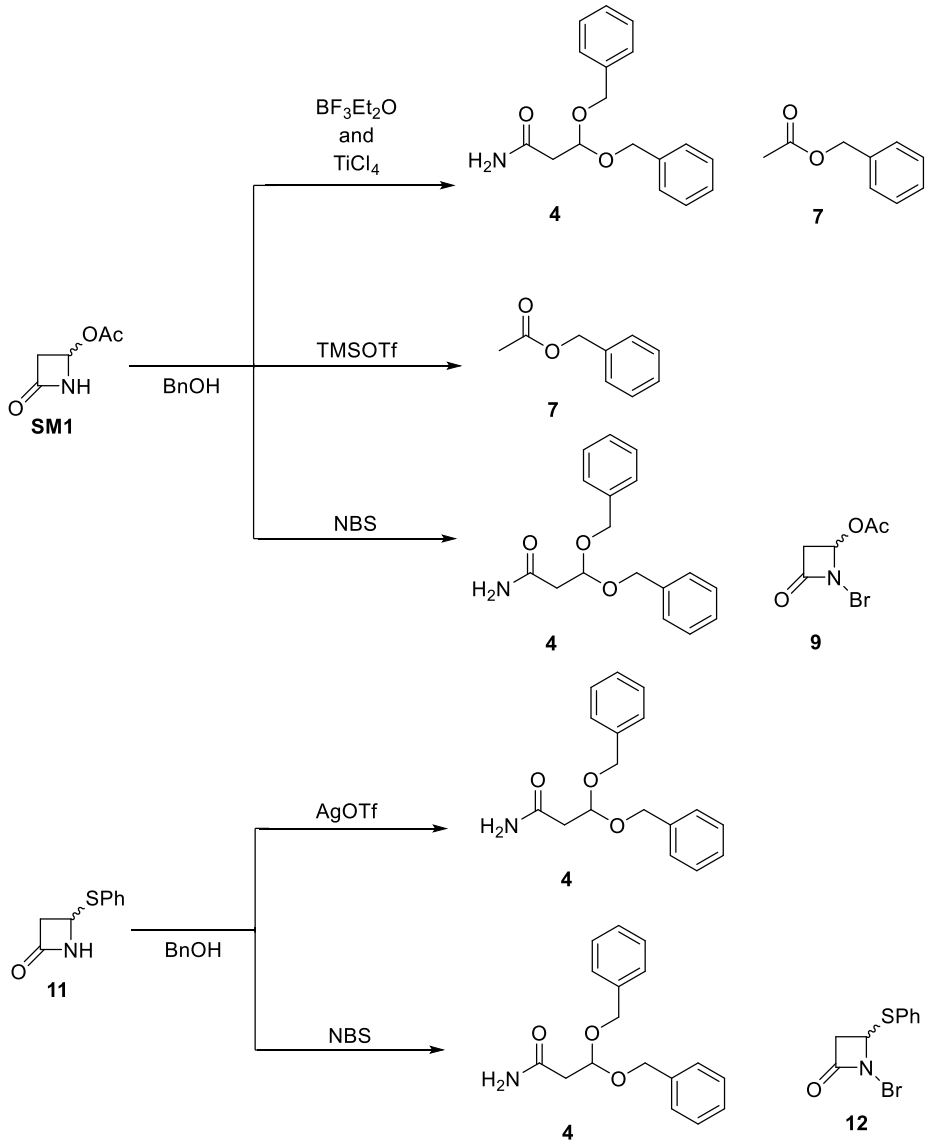

Figure 77. Products obtained from 4-acetoxy-2-azetidinone (up) and products obtained from 4-(phenylthio) azetidin-2-one (down).

In conclusion, it is evident that to promote a nucleophilic substitution at C4 position of β-lactam based compounds is required a basic catalyst like TEA, while an acid one led to the β-lactam ring opening giving compound **4,** and derivatives, using different alcohols as nucleophiles. Both polymeric resins, lewis acids and NBS employed in reactions in which the 4-acetoxy-2-azetidinone is the starting material and the benzyl alcohol is utilized as nucleophile, led to compound **4**. Even in reactions in which the 4-(phenylthio)azetidin-2-one is the starting material and the benzyl alcohol is utilized as nucleophile, compound **4** is obtained, employing both catalysts such as AgOTf, and NBS. However, even if we did not obtain the expected reactivity, two promising products **9** and **12** resulted, in which the amidic nitrogen was brominated by the NBS; they could be the subject of future study by the research group to synthesise new β-lactam based compounds.

Experimental

All reactions were performed using normal organic chemistry laboratory equipment, as standard Pyrex glassware, magnetic stirrers, and rotavapors. Every reagent employed, where not specified, is commercially available and was employed without further purification procedures.
The triethylamine (TEA) was distilled under nitrogen atmosphere, and it is kept anhydrous by potassium hydroxide pellets. The Thin Layer Chromatography (TLC) was performed on plates precoated with silica gel, Kieselgel 60 F254, while products were purified by flash-chromatography on silica gel Merk 230-400 mesh. The ^{1}H NMR spectra were recorded on a Varian Gemini 400, in $CDCl_3$ or CD_3OD solution. The FTIR analysis were recorded in transmittance in the mid-IR (range 4000-400cm^{-1}), in ATR mode (Attenuated Total Reflectance) at room temperature, using a spectrophotometer Bruker Alpha.
HPLC-MS: Agilent Technologies HP1100 instrument, equipped with a ZORBAX-Eclipse XDB-C8 Agilent Technologies column; mobile phase: H_2O/CH_3CN, 0.4 mL/min, gradient from 30 to 80% of CH_3CN in 8 min, 80% of CH_3CN until 25 min, coupled with an Agilent Technologies MSD1100 single-quadrupole mass spectrometer, full scan mode from m/z = 50 to 2600, in positive ion mode, ESI spray voltage 4500 V, nitrogen gas 35psi, drying gas flow 11.5 mL/min, fragmentor voltage 20 V.

4-(benzyloxy)azetidin-2-one (**1a**)

Under nitrogen atmosphere, $Zn(OAc)_2$ (0.155 mmol) was dissolved in toluene (3 mL), and 4-acetoxy-2-azetidinone (**SM1**, 0.31 mmol) and then the benzyl alcohol (35 μL) were added. The reaction mixture was refluxed until the **SM1** disappearance (~24 h). Then the reaction mixture was cooled at room temperature, and it was filtrated using celite and washed using DCM. After that, the filtrate was evaporated. The crude was purified by flash-chromatography, with an eluent mixture of Cyclohexane/EtOAc =1:1. (Compound **1a**: 29.9 mg, Y = 54%).
Spectroscopic data are in accordance to those reported in literature.[252]

*1-bromo-4-oxoazetidin-2-yl acetate (***9**)

4-acetoxy-2-azetidinone (**SM1**, 0.155 mmol) commercially available, under nitrogen atmosphere, was dissolved in anhydrous dichloromethane (1.5 mL). The mixture was cooled at 0°C and NBS was added. The reaction was conducted at 0°C and monitored by TLC analysis.
The reaction mixture was stirred until starting material disappearance and then the mixture was concentrated at rotavapor to eliminate the solvent. The crude was purified by flash-chromatography (eluent mixture: Cyclohexane/EtOAc = 7:3 then 1:1). (Compound **9**: 30.5 mg, Y = 95%).

4-(phenylthio)azetidin-2-one (**11**)

The diphenildisulphide was solubilized in anhydrous EtOH, under nitrogen atmosphere, then $NaBH_4$ (2 mmol) was slowly added. The reaction mixture was stirred for 3 hours, then at 0°C the 4-acetoxy-2-azetidinone (**SM1**, 1 mmol) was added and the mixture was stirred for 25 minutes until starting material disappearance. Then, the EtOH was concentrated at the rotavapor and the reaction mixture was extracted using H_2O and EtOAc (x3). The organic layer was dried with Na_2SO_4, filtered, and concentrated. The reaction was monitored by TLC.
The crude was purified by gradient flash-chromatography, using as eluent mixture Cyclohexane/EtOAc = 95:5 then 8:2, and in the end using only EtOAc. (Compound **11**: 150 mg, Y = 84%).
Spectroscopic data are in accordance to those reported in literature.[219]

Non-catalysed reactions

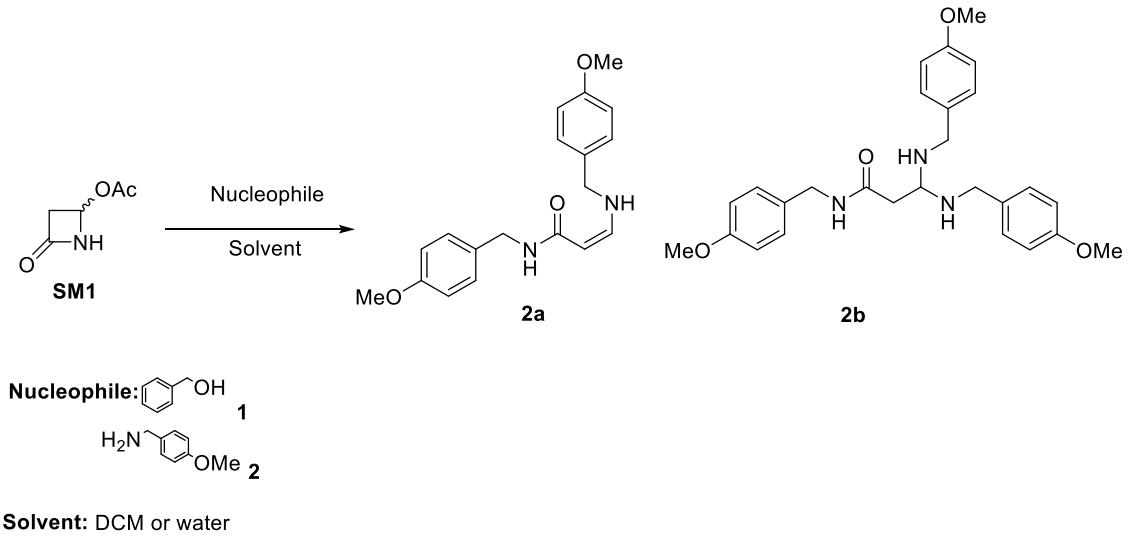

In a 2-neck flask, the 4-acetoxy-2-azetidinone (**SM1**, 0.155mmol) was dissolved in the selected solvent (1.5 mL), then the nucleophile (0.31 mmol) was added to the mixture and stirred until starting material disappearance.
Then, the reaction mixture was transferred to a separatory funnel and extracted with DCM (x3) and Brine. The organic layer was dried with Na_2SO_4, filtered, and concentrated.

*(Z)-N-(4-methoxybenzyl)-3-((4-methoxybenzyl)amino)acrylamide (**2a**)*

^{1}H NMR (400 MHz, $CDCl_3$) δ 8.58 (bs, 1H), 7.15 – 7.18 (m, 4H), 6.94 – 6.70 (m, 4H), 6.54 (dd, J = 12.7, 8.0 Hz, 1H), 4.39 (d, J = 8.0 Hz, 1H), 4.28 (d, J = 5.5 Hz, 2H), 4.23 (d, J = 6.0 Hz, 2H), 4.10 (d, J = 5.3 Hz, 1H), 3.77 (s, 9H). HPLC-MS (ESI+): m/z = 327.17 $[M+H]^+$.

*N-(4-methoxybenzyl)-3,3-bis((4-methoxybenzyl)amino)propenamide (**2b**)*

HPLC-MS (ESI+): m/z = 463.58 $[M+H]^+$.

Nucleophile as solvent

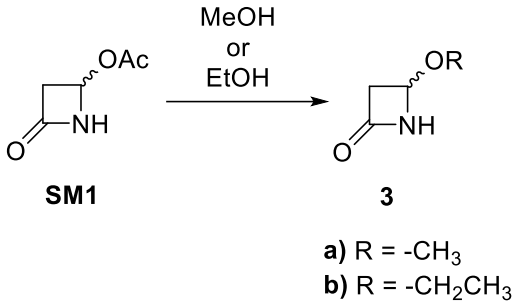

The 4-acetoxy-2-azetidinone (**SM1**, 0.155 mmol), commercially available, was dissolved in methanol or ethanol (1 mL), under nitrogen atmosphere. The reaction was conducted at room temperature. The alcohol was then evaporated using rotavapor.

*4-methoxyazetidin-2-one (**3a**)*

(Crude: 19 mg, SM1 conversion 5%). ^{1}H NMR: (400 MHz, $CDCl_3$) δ 5.01 (d, *J* = 3.7, 1H) 3.05 (dd, *J* = 15.1, *J* = 3.7 Hz, 1H), 2.84 (d, *J* = 15.1 Hz, 1H), 2.03 (s, 3H).

*4-ethoxyazetidin-2-one (**3b**)*

(Crude: 15 mg, SM1 conversion 30%). ^{1}H NMR: (400 MHz, $CDCl_3$) δ 5.04 (d, *J* = 1.2 Hz, 1H), 3.5-3.4 (q, *J* = 4 Hz, 2H), 3.08 (dd, *J* = 15.0, *J* = 1.2 Hz, 1H), 2.86 (dd, *J* = 15.0, *J* = 1.2 Hz, 1H), 1.23 (t, *J* = 4 Hz, 3H).

Acid-base-catalysed reactions

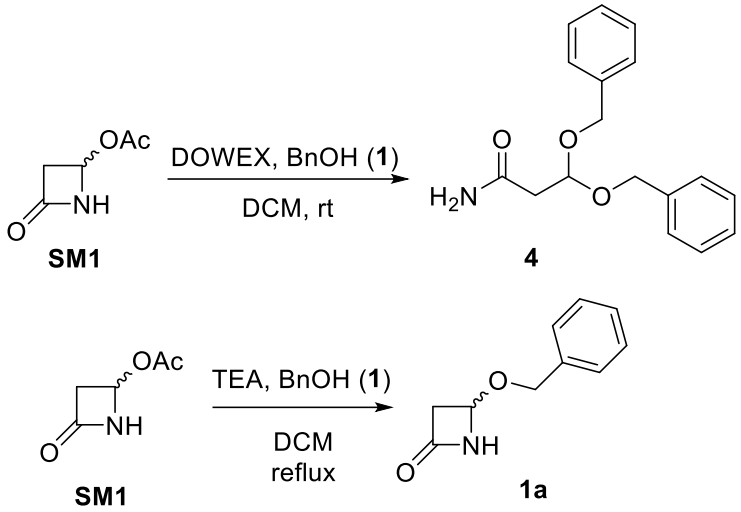

The 4-acetoxy-2-azetidinone (**SM1**, 0.155 mmol), commercially available, was dissolved in DCM (1.5 mL) under nitrogen atmosphere. The benzyl alcohol was slowly added, then the catalyst (0.155 mmol) was added.
The reaction was conducted at room temperature. The DCM was then evaporated using rotavapor.

*3,3-bis(benzyloxy)-1-(methyl-l4-azaneyl)propan-1-one (**4**)*

(7mg, 0.025mmol, Y=16%). ^{1}H NMR: (400 MHz, $CDCl_3$) δ 7.40 – 7.26 (m, 10H), 6.12 (bs, 1H), 5.36 (bs, 1H), 5.05 (t, *J* = 5.1 Hz, 1H), 4.69 (dd, *J* = 11.6, *J* = 44 Hz, 2H), 4.58 (dd, *J* = 11.6, *J* = 44 Hz, 2H), 2.68 (d, *J* = 5.1 Hz, 2H). ^{13}C NMR: (100 MHz, $CDCl_3$) δ 171.52, 137.40, 130.20, 127.14, 99.38, 69.06, 65.57, 41.37. HPLC-MS (ESI^+): m/z = 308.12 $[M+Na]^+$.

Amines as catalysts or nucleophiles

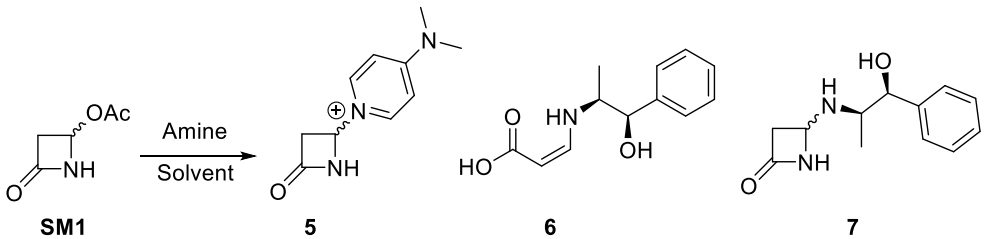

The 4-acetoxy-2-azetidinone (**SM1**, 0.155 mmol), commercially available, was dissolved in DCM (1.5 mL) under nitrogen atmosphere. The amine was slowly added, then the catalyst (0.155 mmol) was added.
The reaction was conducted at room temperature. The DCM was then evaporated using rotavapor.

*(Z)-3-((1-hydroxy-1-phenylpropan-2-yl)amino)acrylic acid (**6**)*

^{1}H NMR (400 MHz, $CDCl_3$) δ 7.41 – 7.14 (m, 5H), 6.46 (dd, J = 12.8, 8.0 Hz, 1H), 4.65 (d, J = 4.2 Hz, 1H), 4.29 (d, J = 8.0 Hz, 1H), 3.60 – 3.64 (m, 1H), 1.06 (d, J = 6.8 Hz, 3H).
HPLC-MS (ESI+): m/z = 222.11 $[M+H]^+$.

4-(((1S,2R)-1-hydroxy-1-phenylpropan-2-yl)amino)azetidin-2-one (7)

^{1}H NMR (400 MHz, $CDCl_3$) δ 7.41 – 7.26 (m, 5H), 6.46 (bs, 1H), 4.58 (d, J = 4.5 Hz, 1H), 3.92 - 3.95 (m, 1H), 3.14 (dd, J = 16.5, 4.5 Hz, 1H), 2.77 (dd, J = 16.5, 4.5 Hz, 1H), 2.10 (d, 3H).

Lewis acids and promoters catalysed reactions

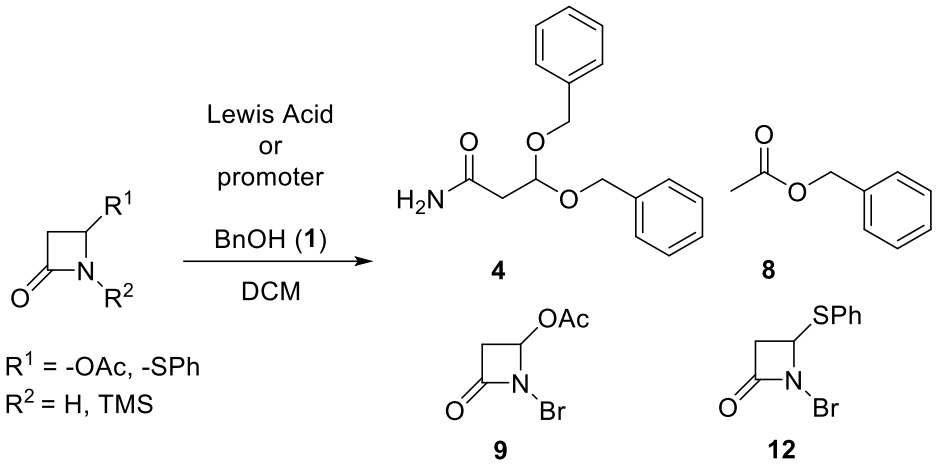

Lewis Acids and Promoters:
BF_3Et_2O, $TiCl_4$, $AlCl_3$, TMSOTf, AgOTf, NBS

Procedures:

1. The β-lactam (1 equiv) was dissolved in anhydrous dichloromethane (1.5 mL) under nitrogen atmosphere. The mixture was cooled at 0°C and the lewis acid was added. Afterwards the nucleophile was added dropwise, and the reaction was conducted at room temperature. The reaction mixture was stirred until starting material disappearance, then the mixture was quenched using H_2O at 0°C. The mixture was transferred to a separatory funnel and extracted with DCM (x3). The organic layer was dried with Na_2SO_4, filtered, and concentrate.
2. The β-lactam (1 equiv) was dissolved in anhydrous dichloromethane (1.5 mL) under nitrogen atmosphere. The mixture was cooled at 0°C and the lewis acid was added, after 20 minutes the nucleophile was added dropwise, and the reaction was conducted at 0°C. The reaction mixture was stirred until starting material disappearance, then the mixture was quenched using H_2O at 0°C. The reaction mixture was transferred to a separatory funnel and extracted with DCM (x3) and Brine. The organic layer was dried with Na_2SO_4, filtered, and concentrated.
3. The β-lactam (1 equiv) was dissolved in anhydrous dichloromethane (1.5mL) under nitrogen atmosphere. The mixture was cooled at 0°C and the lewis acid was added, then the mixture has been kept at room temperature for 30 minutes and then the nucleophile was added dropwise at 0°C. The reaction was stirred at 0°C until starting material disappearance. Then the mixture was quenched using H_2O at 0°C. The reaction mixture was transferred to a separatory funnel and

extracted with DCM (x3) and Brine. The organic layer was dried with Na_2SO_4, filtered, and concentrated.

*3,3-bis(benzyloxy)-1-(methyl-l4-azaneyl)propan-1-one (**4**)*

(7mg, 0.025 mmol, Y=16%). ^{1}H NMR: (400 MHz,$CDCl_3$) δ 7.40 – 7.26 (m, 10H), 6.12 (bs, 1H), 5.36 (bs, 1H), 5.05 (t, *J* = 5.1 Hz, 1H), 4.69 (dd, *J* = 11.6, *J* = 44 Hz, 2H), 4.58 (dd, *J* = 11.6, *J* = 44 Hz, 2H), 2.68 (d, *J* = 5.1 Hz, 2H). ^{13}C NMR: (100 MHz, $CDCl_3$) δ 171.52, 137.40, 130.20, 127.14, 99.38, 69.06, 65.57, 41.37. HPLC-MS (ESI+): m/z 308.12 $[M+Na]^+$.

*1-bromo-4-oxoazetidin-2-yl acetate (**9**)*

(30.5mg, 0.146 mmol, Y=95%). ^{1}H NMR: (400 MHz, $CDCl_3$) δ 6.10 (d, *J* = 4.2, Hz, 1H), 3.43 (dd, *J* = 13.8, 1.3 Hz, 1H), 3.19 (dd, *J* = 13.8, 1.3 Hz, 1H), 2.15 (s, 3H). ^{13}C NMR: (100 MHz, $CDCl_3$) δ 169.71, 164.89, 79.63, 45.90, 20.56. HPLC-MS (ESI^+): Rt 2.64 min, m/z = 227 $[M+H_3O]^+$.

*1-bromo-4-(phenylthio)azetidin-2-one (**12**)*

(Crude: 24.7 mg, SM conversion 100%). *^{1}H NMR:* (400 MHz, $CDCl_3$) δ 7.42 – 7.11 (m, 6H), 5.66 (d, *J* = 4.5 Hz, 1H), 3.77 (dd, *J* = 15.7, 4.5 Hz, 1H), 3.49 (dd, *J* = 15.7, 4.5 Hz, 1H).

Reaction Scope: Compound 4

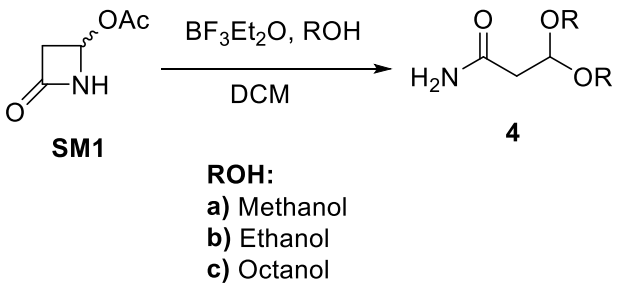

All reactions were conducted using 2 equivalents of $BF_3{\cdot}Et_2O$ and 2 equivalents of benzyl alcohol.

*3,3-dimethoxypropanamide (**4a**)*

(Crude: 4 mg, SM1 conversion 100%, Y=20%). ^{1}H NMR**:** (400 MHz, $CDCl_3$) δ 4.67 (t, J = 5.1 Hz, 1H), 2.94 (s, 3H), 2.87 (s, 3H), 2.57 (d, J = 5.1 Hz, 2H).

*3,3-diethoxypropanamide (**4b**)*

(Crude: 4 mg, SM1 conversion 100%, Y=15%). ^{1}H NMR: (400 MHz, $CDCl_3$) δ 4.82 (t, *J* = 5.1 Hz, 1H), 3.72 – 3.65 (m, 2H), 3.64 - 3.56 (m, 2H), 2.60 (d, *J* = 5.1 Hz, 2H), 1.35 (m, 6H).

*3,3-bis(octyloxy)propanamide (**4c**)*

(Crude: 58.6 mg, SM1 conversion 100%)**.** ^{1}H NMR: (400 MHz, $CDCl_3$) δ 4.74 (t, *J* = 5.1 Hz, 1H), 3.47 – 3.41 (m, 4H), 2.56 (d, *J* = 5.1 Hz, 2H), 1.50-1.57 (m, 8H), 1.32 - 1.25 (m, 16H), 0.87 – 0.84 (m, 6H).

1a and 9 as starting materials

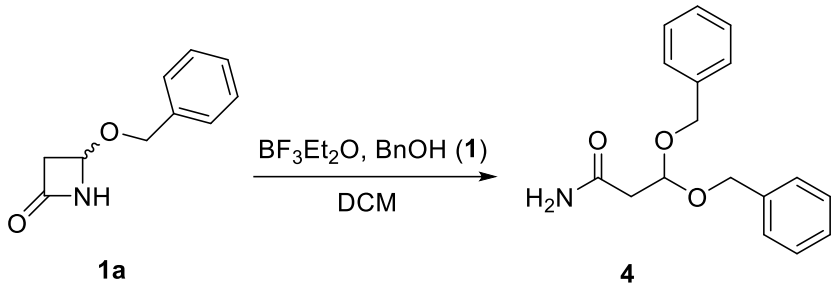

1a **4**

The 4-benzoloxy-2-azetidinone (0.16 mmol), was dissolved in anhydrous dichloromethane (1.5 mL) under nitrogen atmosphere. The mixture was cooled at 0°C and $BF_3{\cdot}Et_2O$ (0.338 mmol) was added, after 20 minutes the alcohol (0.338mmol) was added dropwise and the reaction was conducted at 0°C. The reaction mixture was stirred until starting material disappearance (22h, monitored by TLC) and then the mixture was quenched using H_2O at 0°C. The reaction mixture was transferred to a separatory funnel and extracted with DCM (x3). The organic layer was dried with Na_2SO_4, filtered, and concentrated. (Crude reac-123: 50.6 mg)

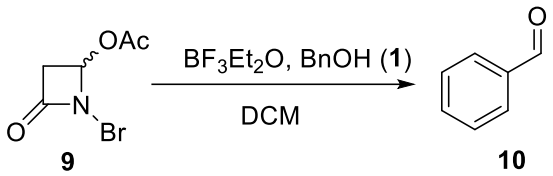

9 **10**

Compound **9** (0.147 mmol), was dissolved in anhydrous dichloromethane (2 mL) under nitrogen atmosphere. The mixture was cooled at 0°C and $BF_3{\cdot}Et_2O$ (0.294 mmol) was added; after 20 minutes the alcohol (0.161 mmol, 2 equiv) was added dropwise and the reaction was conducted at 0°C till the starting material disappearance. The reaction was monitored by TLC, and finally quenched using H_2O at 0°C.

The reaction mixture was transferred to a separatory funnel and extracted with DCM (x3). The organic layer was dried with Na_2SO_4, filtered, and concentrated.

Section 3. Disulfide linkers for small molecule drug conjugates

During my PhD period abroad, I had the great opportunity to join the research team of Prof. Dario Neri and Dr. Samuele Cazzamalli in Philochem AG, Zurich. During this six-months period I was lucky to work together with the team on a very stimulating project based on the study of different cleavable linkers for small molecule drug conjugates, designed to target Fibroblast Activation Protein (FAP).

FAP is a type II integral membrane serine protease with a dual action both as a dipeptidyl peptidase and as an endopeptidase.[253] Moreover, despite of endogenous FAP dipeptidyl peptidase substrates are un-known, several results with coumarin-based dipeptide substrates show that FAP cleaves P2-Pro1-coumarins with broad P2 specificity.[254-256]

FAP is 760 amino acids long with residues 1–4 composing the intracellular domain, 5–25 composing the transmembrane domain, and 26–760 composing the extracellular domain. Residues 27–53 and 493–760 include the α/β-hydrolase domain while residues 54–492 contain the β-propeller domain that is believed to serve as filter for the selective entry of peptides into the catalytic domain. It is also thought to act as the scaffolding region of FAP as certain β-sheets are the site for homodimerization, heterodimerization or interaction with other cell surface molecules such as integrins. FAP's catalytic triad is located at the interface of the β-propeller domain and the α/β-hydroxylase domain (*Figure 78*).[257]

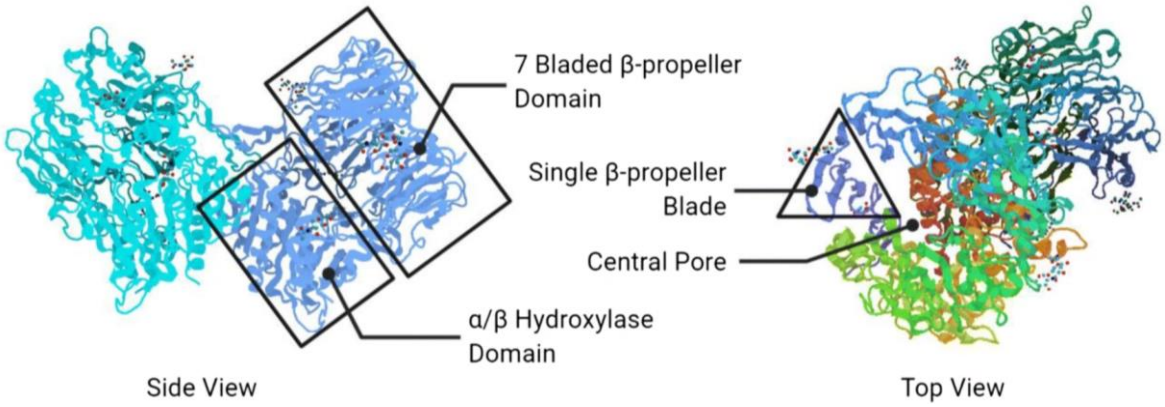

Figure 78. Ribbon model of FAP structure. Figure adapted from ref. 257.

Furthermore, FAP resulted as a specific marker of tumor-associated fibroblasts (TAFs).[258] It is richly expressed in the stroma of more than 90% of the epithelial cancers, including malignant breast, colorectal, skin, prostate, and pancreatic cancers,[259,260] while exhibiting a restricted expression in normal adult tissues.[261] This data makes this protease a potential therapeutic target;[262] in fact, Haberkorn and coworkers[263-265] have recently described a series of FAP ligands capable of accumulating selectively in FAP positive tumors in mice and in patients.

Also the research team of Philochem AG has developed a FAP ligand with a dissociation constant in the sub-nanomolar concentration range. This ligand exhibited a strikingly selective and efficient tumor-targeting performance when equipped with various types of payloads, such as cytotoxic drugs.[261] This opens the door to the development of small molecule–drug conjugates (SMDCs), targeting FAP.

The research group of Prof. Dario Neri, in a previous study has developed and synthesised a new SMDC, having a FAP ligand as carrier for the selective binding at the tumor site. This molecule (see *Figure 79*) contains the Monomethyl Auristatin E (MMAE) payload as cytotoxic drug, and the Valine-Citrulline (*Val-Cit*) cleavable linker, as well as para-aminobenzyloxy carbonyl (PABC) as self-immolative moiety.[261] MMAE is a cytotoxic agent that binds to microtubules and prevent cell proliferation by inhibiting mitosis.[32]

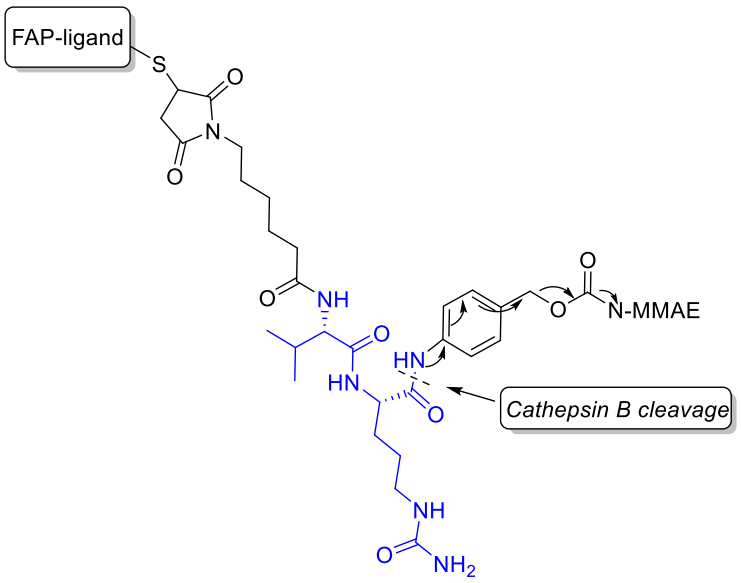

Figure 79. SMDC developed by Philochem research team. In blu the *Val-Cit* linker is highlighted, and the Cathepsin B cleavage is indicated.[261]

Preliminary studies demonstrated that the amount of MMAE released is very small compared to the intact SMDC at the tumor site. This can be explained by the fact that generally, *Val-Cit*-PBAC can be preferentially cleaved by intracellular proteases of the lysosomal degradation pathway.[266] Consequently in internalizing systems the release of MMAE mediated by the cleavage of *Val-Cit* linker occurs successfully, while in case of non-internalizing SMDCs such as in the case of FAP targeting conjugates the release is not so efficient. For that reason, what we want to achieve with this project, is to find new cleavable linkers able to guarantee a better release of the payload.

The strategy that we decided to apply is based on the use of redox responsive disulfide linkers, whose cleavage and subsequent release of the cytotoxic drug is mediated by Glutathione (GSH); it is the most abundant thiol and reducing agent in the intracellular space, both in normal cells and in tumors, which often contain higher concentrations of these species.[267-268] For that reason, molecules having disulfide linkers have been designed for the intracellular release of the payload in internalizing antibody drug conjugates (ADC) or SMDCs.

About this, one of the most important examples is the one of EC1169 developed by Endocyte; this novel tubulysin B-containing therapeutic agent was developed for the treatment of PSMA-expressing cancer. It emerged as a lead candidate for preclinical development and phase I clinical testing.[269]

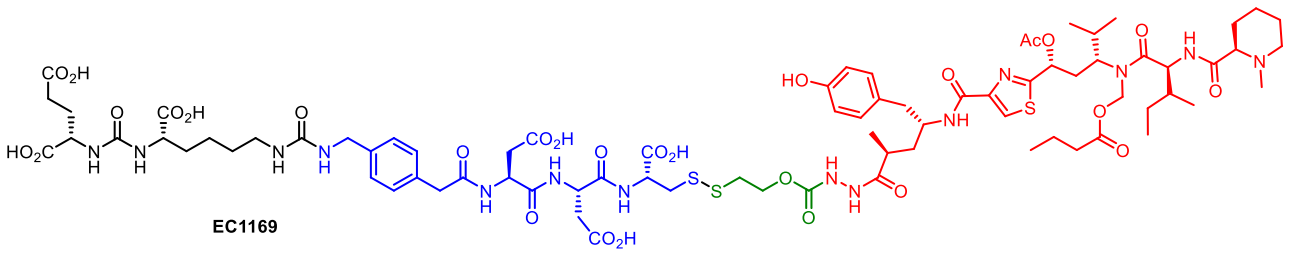

Figure 80. Chemical structure of EC1169.[269]

However, the use of disulfide linkers can be extended to non-internalizing systems, hypothesizing that the extracellular drug release process at the tumor site would be facilitated by the death of tumor cells which permit the release of GSH (Glutathione) into the tumor extracellular space, where it can act as reducing agent on disulfide bonds, favouring an amplified cascade of drug release and tumor cell death.[270]

About this, the team of Prof. Dario Neri developed and synthesized a SMDC with disulfide linker, targeting Carbonic anhydrase IX (CAIX), and using DM1 as payload.[271]

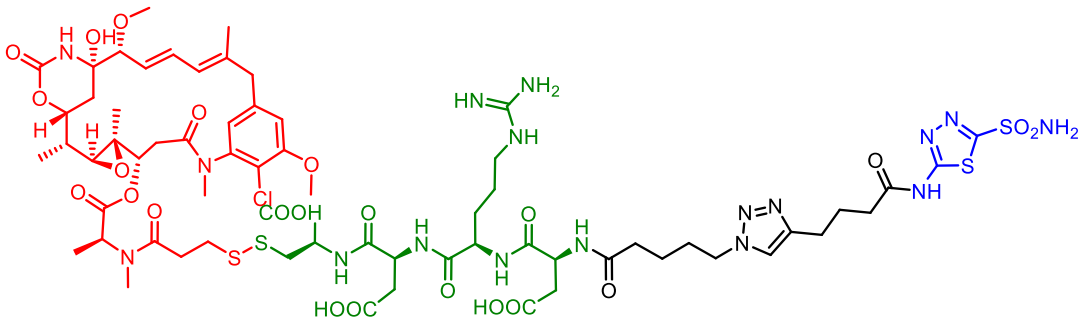

Figure 81. Chemical structure of the SMDC developed by Neri's group for the treatment of carbonic anhydrase IX expressing solid tumors.[271]

This compound exhibited a potent antitumor effect in SKRC52 renal cell carcinoma in mice, but elevate doses were necessary.[271]

What we want to do in this project is evaluate if the presence of a disulfide linker can eventually improve the release of MMAE, that compared with DM1 of the previous example is less metabolizing. Therefore, we developed and synthesized two different SMDCs which differ in the presence of methyl groups on the disulfide chain. The addition of methyl groups is important to identify the possible effect of the increasing steric hindrance on the stability of the conjugates and on the MMAE release.

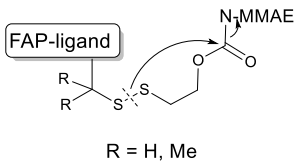

Figure 82. General structure of our SMDCs and mechanism of release of MMAE mediated by GSH cleavage.

Results and discussions

We will study the redox responsive disulfide linkers shown in *Figure 83*.

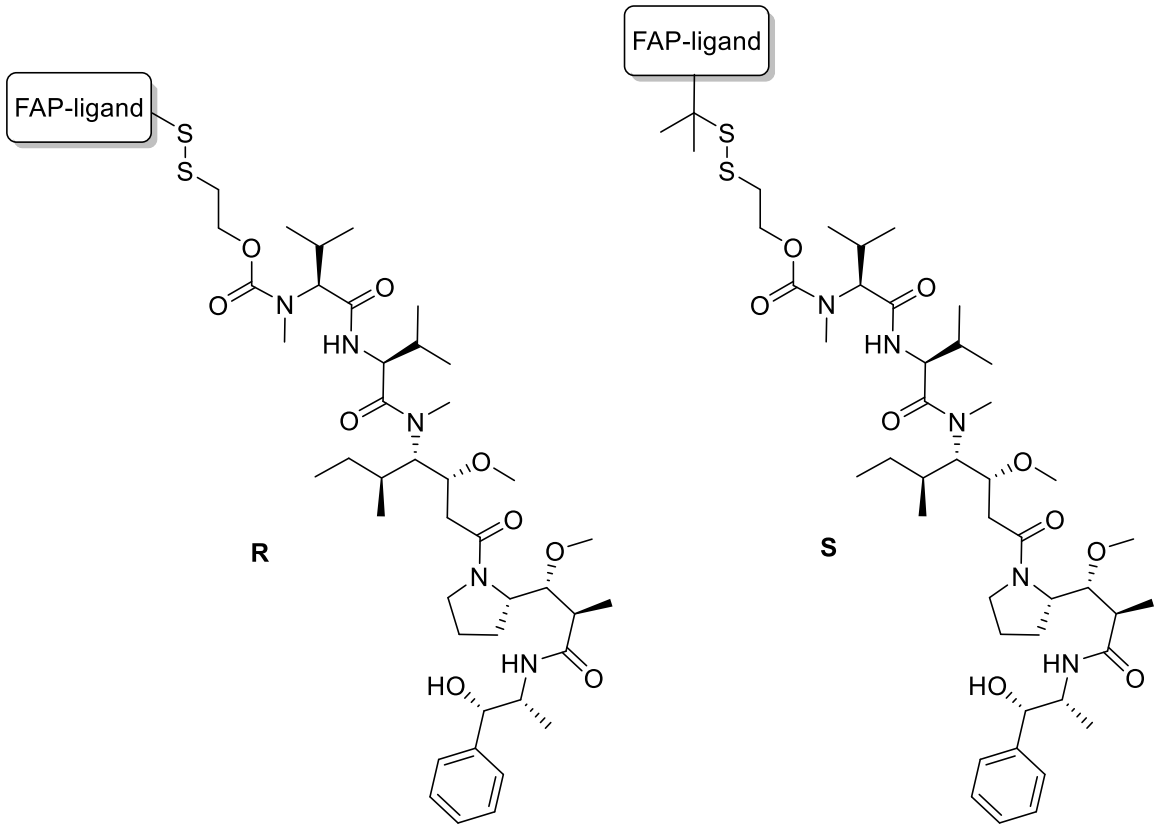

Figure 83. Small molecule drug conjugates **R** and **S** with disulfide linkers.

Even in this case the two target molecules **R** and **S** have in common the carrier, the FAP ligand previously developed by Philochem AG, and the MMAE as cytotoxic drug; however, we decided to use disulfide molecules as linkers whose cleavage and subsequent release of MMAE is mediated by GSH, expressed at high level in different type of tumors. Moreover, the difference between compound **R** and compound **S** consists in the presence of methyl groups on the disulfide chain. The addition of methyl groups is important to evaluate if increasing the steric hindrance, the stability increases too.
The synthesis of SMDCs **R** and **S** is described in *Scheme 47*.

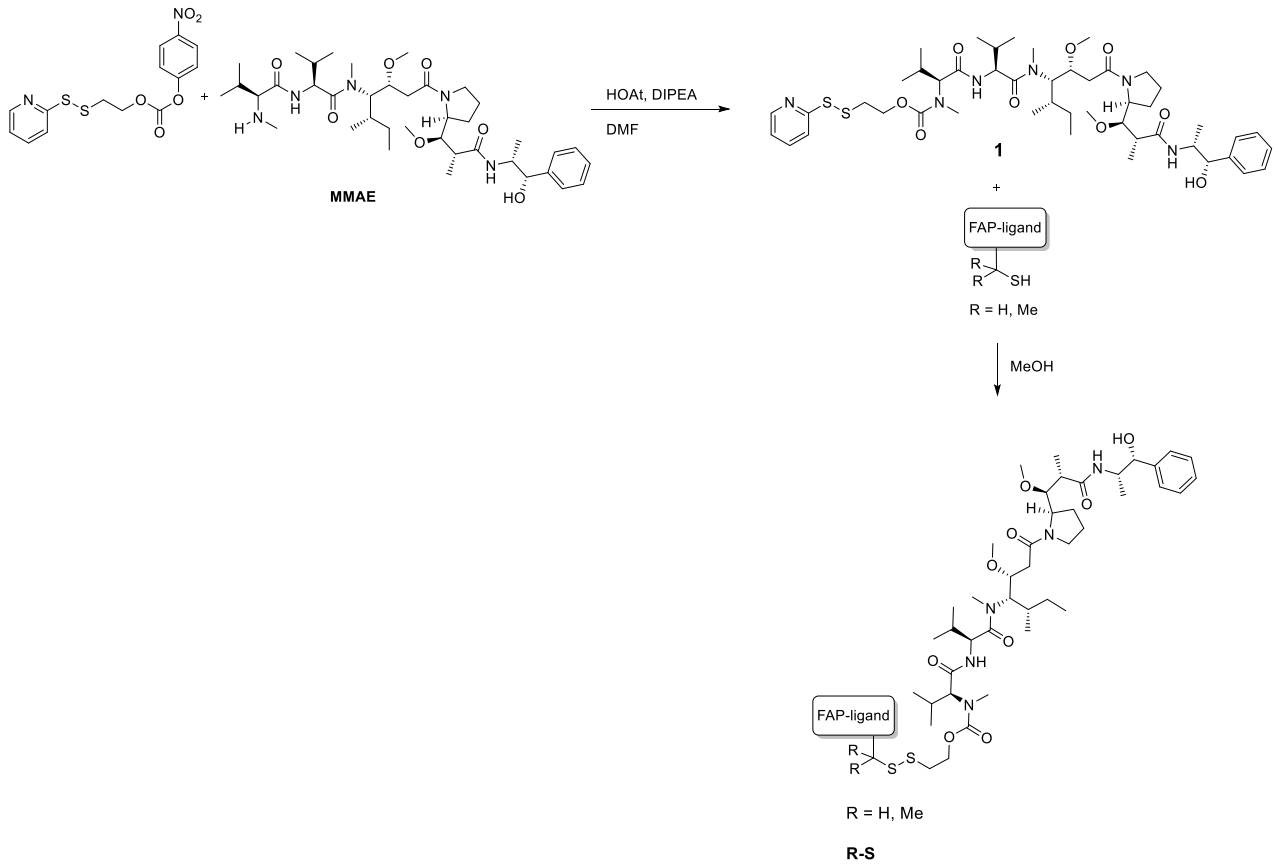

Scheme 47. Synthesis of target compounds **R** and **S**.

We start from a commercially available compound, the *4-nitrophenyl (2-(pyridin-2-yldisulfaneyl)ethyl) carbonate* who have a *p*-nitrophenyl leaving group that permit the insertion of the secondary amine of MMAE in presence of HOAt and DIPEA in DMF in order to give compound **1**. The latter undergoes a disulfide exchange reaction in methanol with the free thiol of the FAP ligand to give target molecule **R** and **S**. We synthesized two different FAP-ligand in order to have the one with no methyl groups and the one with two methyl groups.
Finally, this two SMDCs have been purified by HPLC and obtained in a milligram scale ready to be tested. The purity and the identity were evaluated by LC-MS.
Preliminary studies have been conducted to evaluate the release of MMAE from compounds **R** and **S**, after the incubation with GSH by HPLC. First, we generated a calibration curve of MMAE at different concentration (5, 10, 15, 20, 25, 30 μM), incubated in PBS (pH = 7.4) with GSH at 37°C.

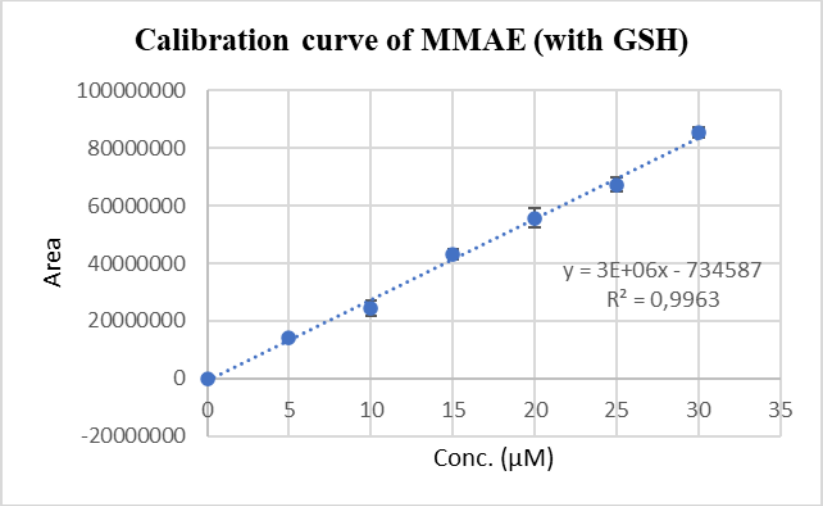

Figure 84. Calibration curve of MMAE incubated with GSH.

Then a first study was conducted on compound **R**, that was dissolved in PBS (pH = 7.4) and incubated with GSH at 37°C. Release of MMAE was evaluated by HPLC at different time points. In this case three different conditions in terms of ratio between **R** and GSH have been screened:

- 1:1 **R**:GSH
- 1:10 **R**:GSH
- 1:100 **R**:GSH

A better release of MMAE has been obtained with a ratio of 1:10 between **R** (50 µM) and GSH (500 µM) so this test has been repeated in triplicate at 0, 2, 4, 6 and 24 h. In *Figure 85* we can see the results obtained in two graphics: the one on the left refers to the increase of MMAE during time, while the one on the right refers to the decrease of **R** during time.

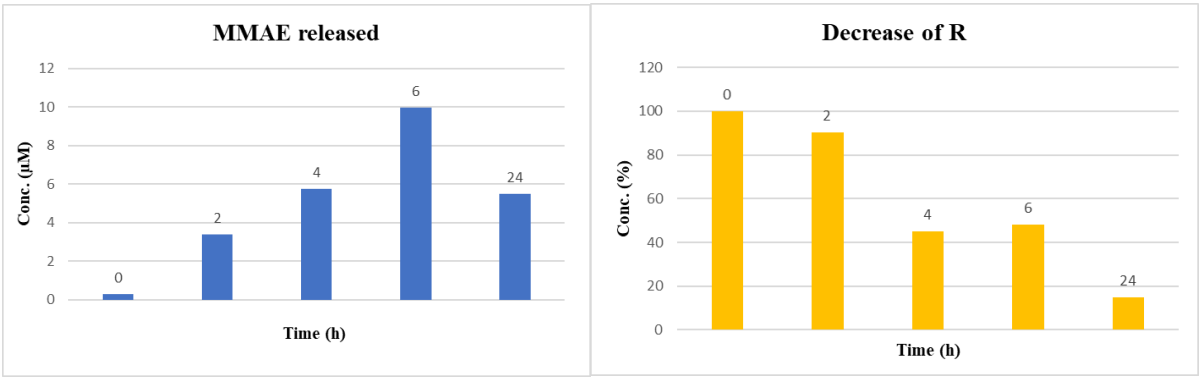

Figure 85. Incubation of **R** with GSH in PBS (pH = 7.4) at 37°C; on the left) increase of MMAE during time (in µM); on the right) decrease of **R** during time (conc.% respect to t = 0).

We can see that after 6 hours we have 10 µM of MMAE released and after 24 hours only 15% of **R** is intact.

However, we can notice that despite of the great decrease in concentration (%) of compound **R** we do not have a quantitative release of MMAE, but only 10 µM of the released drug can be

observed; by LC-MS analysis we discovered that after the reductive cleavage of GSH there was the formation of a MMAE-GSH adduct, that decreased the amount of free MMAE.

The same study was conducted on compound **S** with a ratio of 1:10 between **S** (50 µM) and GSH (500 µM). The concentration of MMAE released was evaluated at 0, 2, 4 and 6 h by HPLC.

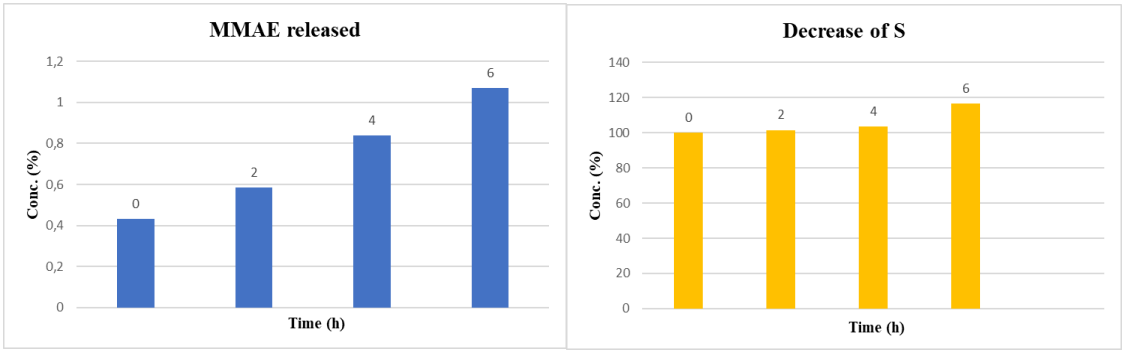

Figure 86. Incubation of **S** with GSH in PBS (pH = 7.4) at 37°C; on the left) increase of MMAE during time (in µM); on the right) decrease of **S** during time (conc.% respect to t = 0).

From *Figure 86* we can see that for compound **S** there is no release of MMAE after 6 hours; this can be explained by the enhanced steric hindrance of compound **S** respect to compound **R** due to the presence of the two methyl groups which can interfere with the reductive action of GSH.

For this two SMDCs **R** and **S** a similar test was conducted in presence of *tris(2-carboxyethyl)phosphine* (TCEP) instead of GSH. TCEP is a potent reducing agent often used to break disulfide bonds in biochemical and molecular biology applications. Even in this case we incubated **R** and **S** in PBS (pH = 7.4) with TCEP and moreover we decided to keep the ratio of 1:10 between our compounds and the reducing agent.

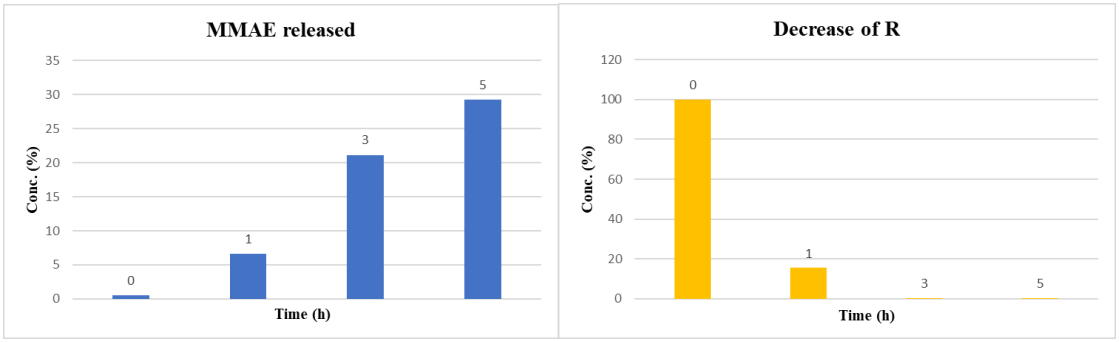

Figure 87. Incubation of **R** with TCEP in PBS (pH = 7.4) at 37°C; on the left) increase of MMAE during time (in µM); on the right) decrease of **R** during time (conc.% respect to t = 0).

In *Figure 87* we can see that after 5 hours in incubation with TCEP, all the compound **R** disappear, and 29 µM of MMAE are released. Comparing this result with the one obtained after incubation with GSH we can say that a stronger reducing agent like TCEP favour the release of MMAE also in a shorter time.

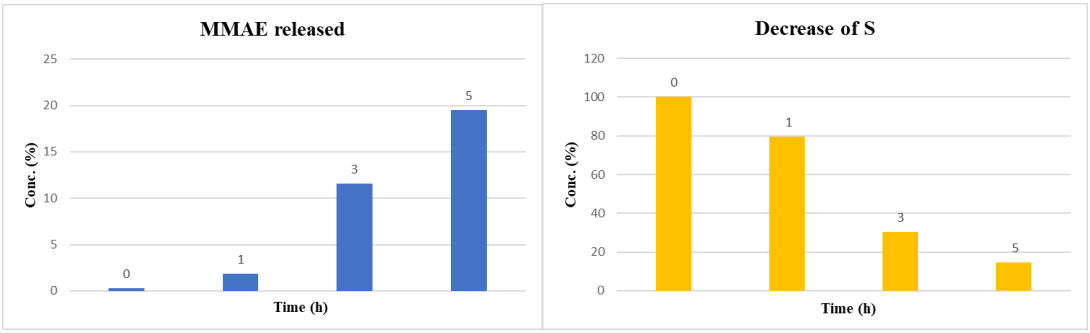

Figure 88. Incubation of **S** with TCEP in PBS (pH = 7.4) at 37°C; On the left) increase of MMAE during time (in µM); On the right) decrease of **S** during time (conc.% respect to t = 0).

Even for compound **S** we can see that the incubation with TCEP favour the release of MMAE, that in 5 hours reach a concentration of 19.5 µM, differently from the incubation with GSH, where no drug was released.
However, it is also important to highlight the fact that also with TCEP, differently from **R**, compound **S**, is not completely consumed, but after 5 hours we have it at a concentration of 14.6% respect to time 0. The explanation can be the same as before and so that the steric hindrance brough by the two dimethyl groups make the cleavage of the disulfide bond more difficult aver for a strongest reducing agent.

Conclusions

The two compounds **R** and **S** have been synthesized and obtained with excellent purity, so they are now ready for in vitro and in vivo validation. Regarding the in vitro tests, preliminary studies have been conducted to evaluate the release of MMAE from compounds **R** and **S**, after the incubation with GSH and TCEP by HPLC.

Experimental

*Synthesis of 2-(pyridin-2-yldisulfaneyl)ethyl ((S)-1-(((S)-1-(((3R,4S,5S)-1-((S)-2-((1R,2R)-3-(((1S,2R)-1-hydroxy-1-phenylpropan-2-yl)amino)-1-methoxy-2-methyl-3-oxopropyl)pyrrolidin-1-yl)-3-methoxy-5-methyl-1-oxoheptan-4-yl)(methyl)amino)-3-methyl-1-oxobutan-2-yl)amino)-3-methyl-1-oxobutan-2-yl)(methyl)carbamate (**1**)*

MMAE (1 equiv) was dissolved in DMF and HOAt (0.5 equiv) and *4-nitrophenyl (2-(pyridin-2-yldisulfaneyl)ethyl) carbonate* were (1 equiv) added and finally DIPEA (2 equiv) was dropped. After complete conversion of starting material (analysed by LC-MS) the crude was directly purified by RP-HPLC (90:10 to 0:100 water/MeCN in 12 min). The factions containing the desired product were collected and lyophilized overnight to afford compound **1** as a white solid. (Y > 80%)

*Synthesis of final compounds **R**-**S**.*

FAP-ligand (2 equiv) and disulfide-MMAE **8** (1 equiv) were dissolved in degassed MeOH, and the reaction was left under stirring at room temperature for 3h. Then the mixture was diluted

with water/ACN 1:1 and purified via RP-HPLC (water/ACN 90:10 to 0:100 in 10 min). The factions containing the desired product were collected and lyophilized overnight to afford final compound **R-S** as a white solid. (Y > 60%)

Abbreviation list:

5-FU: 5-Fluoro Uracil
ACN: Acetonitrile
ACP5: Acid phosphatase 5
ADC: Antibody drug conjugates
ALP: Alkaline phosphatase
API: Active pharmaceutical ingredient
ATR: Attenuated total reflectance
BCL: *Burkholderia Cepacia Lipase*
BGLAP: Bone Gamma-Carboxyglutamate Protein
Boc: *tert*-butyloxycarbonyl
BODIPY: 4,4-difluoro-4-bora-3a,4a-diaza-s-indacene
CAIX: Carbonic anhydrase IX
CAL B: *Candida antarctica B*
CCP: Clathrin-coated pit
CDE: Clathrin-dependent endocytosis
CIE: Clathrinin-independent endocytosis
CoA: Coenzyme A
COLL1: Type I collagen
COSY: Homonuclear correlation spectroscopy
CTSK: Cathepsin K
DAP: diaminopimelate
DAPI: 4′,6-diamidino-2-phenylindole
DCC: N,N′-Dicyclohexylcarbodiimide
DCM: Dichloromethane
DIC: N,N′-Diisopropylcarbodiimide
DIPEA: N,N-Diisopropylethylamine
DMAP: 4-Dimethylaminopyridine
DMF: Dimethylformamide
EC_{50}: Half maximal effective concentration
EDC: 1-Ethyl-3-(3-dimethylaminopropyl)carbodiimide
EGFP: Enhanced Green Fluorescent Protein
ESI: Electronspray ionization
FAP: Fibroblast Activation Protein
FBS: Fetal Bovine Serum
FDA: Food and Drug Administration
FITC: Fluorescein isothiocyanate
FN: Fibronectin
FTIR: Fourier-transform infrared spectroscopy
GSH: Glutathione
HBTU: 2-(1H-benzotriazol-1-yl)-1,1,3,3-tetramethyluronium hexafluorophosphate
hMSC: Human primary mesenchymal stem cells
HOAt: 1-Hydroxy-7-azabenzotriazole
HOBt: Hydroxybenzotriazole
HPLC: High-performance liquid chromatography
HSQC: Heteronuclear Single Quantum Coherence
IC_{50}: Half maximal inhibitory concentration
ICAM: IntraCellular Adhesion Molecules
IDS: Isoleucine-Aspartic acid-Serine
JAM: Junction Adhesion Molecule

KR: kinetic resolution
LDT: Leucine-Aspartic acid-Threonine
LDV: Leucine-Aspartic acid-Valine
MAdCAM-1: Mucosal vascular addressing cell adhesion molecule 1
MDR-TB: Multi-drug resistant
MFI: Mean fluorescence intensity
MIDAS: metal ion-dependent adhesion sites
MMAE: Monomethyl Auristatin E
MNPs: Magnetic nanoparticles
MS: Mass spectrometry
MSCs: Mesenchymal stem cells
MTb: Mycobacterium tuberculosis
NAG: N-acetylglucosamine
NaHMDSA: Sodium hexamethyl disilylamide
NAM: N-acetylmuramic acid
NBS: N-Bromosuccinimide
NGM: N-glycolylmuramic acid
NHS: N-Hydroxysuccinimide
NMR: Nuclear magnetic resonance
OC: Osteoclasts
OSTC: Osteocalcin
PABC: *p*-aminobenzyloxy carbonyl
PBS: Phosphate Buffer Solution
PCR: Polymerase chain reaction
PF: *Pseudomonas Fluorescens*
PG: Peptidoglycan
PS: Photosensitizer
PTD: Photodynamic therapy
PTSA: *p*-Toluenesulfonic acid
PTT: Photothermal therapy
Rab: Ras-associated binding
RGD: Arginine-Glycine-Aspartic acid
ROS: Reactive oxygen species
Rt: Ritention time
RUNX2: Runt-related transcription factor 2
SD: Standard deviation
SEM: Scanning electron microscopy
SM: Starting material
SMDCs: Small molecule–drug conjugates
SrHA: Strontium substituted hydroxyapatite
TAFs: Tumor-associated fibroblasts
TB: Tuberclulosis
TBDMCl: *tert*-butyldimethylsilylchloride
TBME: *tert*-butylmethylether
TBS: *tert*-buthyldimethylsilyl
TCEP: tris(2-carboxyethyl)phosphine
TDDS: Targeted drug delivery systems
TDR-TB: Totally drug resistant
TEA: Triethylamine
TEM: Transmission electron microscopy
TFA: Trifluoroacetic acid
TGA: Thermogravimetric analysis

THF: Tetrahydrofuran
TLC: Thin layer chromatography
TRAP: Tartrate-resistant acid phosphatase
XDR-TB: Extensively drug resistant

Bibliography

1. D-J. Fu, Y-F. Zhang, A-Q. Chang, J. Li, *Eur. J. Med. Chem.*, 2020**, 201**, 112510;

2. P. Galletti, D. Giacomini, *Curr. Med. Chem.*, 2011, **18**, 4265-4283;

3. P.D. Mehta, N. P. Sengar, A. K. Pathak, *Eur. J. Med. Chem.*, 2010, **45**, 5541-5560;

4. a) N. Arya, A. Y. Jagdale, T. A. Patil, S. S. Yeramwar, S. S. Holikatti, J. Dwivedi, C. J. Shishoo, K. S. Jain, Eur. *J. Med. Chem.*, 2014, **74**, 619-656; b) P. D. Mehta, N. P. S. Sengar, A. K. Pathak, Eur. *J. Med. Chem*., 2010, **45**, 5541-5560;

5. a) H. Wolfenson, I. Lavelin, B. Geiger, *Dev. Cell*, 2013, **24**, 447-458; b) M. Barczyk, S. Carracedo, D. Gullberg, *Cell Tissue Res.*, 2010, **339**, 269-280; c) M. A. Arnaout, S. L. Goodman, J-P. Xiong, *Curr. Op. Cell Biol.*, 2007, **19**, 495-507; d) N. J. Anthis, I. D. Campbell, *Trends Biochem. Sci.*, 2011, **36**, 191–198; e) R. Zaidel-Bar, B. Geiger, *J. Cell. Science*, 2010, **123**, 1385–1388; f) M. A. Arnaout, B. Mahalingam, J. P. Xiong, *Ann. Rev. Cell. Dev. Biol*., 2005, **21**, 381–410;

6. R. O. Hynes, *Cell*, 2002, **110**, 673-687;

7. M. J. Humphries, *Biochem. Soc. Trans*., 2000, **28**, 311-339;

8. I. D. Campbell, M. J. Humphries, *Cold Spring Harb. Perspect. Biol.*, 2011, **3**, a004994;

9. A. Tolomelli, P.Galletti, M. Baiula, D. Giacomini, *Cancers*, 2017, **9**,78;

10. J. D. Humphries, A. Byron, M. J. Humphries, *J. Cell Sci.*, 2006. **119**, 3901-3903*;*

11. T. A. Springer, M. L. Dustin, *Curr. Opin. Cell Biol.*, 2012, **24**, 107-115;

12. N. Beglova, S. C. Blacklow, J. Takagi, T. A. Springer, *Nat. Struct. Biol.*, 2002, **9**, 282-287;

13. A. A. P. Mansur, S. M. Carvalho, Z. I. P. Lobato, M. de Fátima Leite, A. da Silva Cunha, Jr., H. S. Mansur; *Bioconjugate Chem.*, 2018, **29**, 1973-2000;

14. S. L. Goodman, M. Picard, *Trends Pharmacol. Sci.*, 2012, **33**, 405-412;

15. N. R. Paul, G. Jacquemet, P. T. Caswell, *Curr. Biol*, 2015, **25**, R1092-R1105;

16. M. Moser, K. R. Legate, R. Zent, R. Fässler, *Science*, 2009, **324**, 895;

17. C. Le Roy, J. L. Wrana, *Nat. Rev. Mol. Cell Biol.*, 2005, **6**, 112-126;

18. a) K. Ley, J. Rivera-Nieves, W. J. Sandborn, S. Shattil, *Nat. Rev. Drug Discov.*, 2016, **15**, 173-183; b) S. E. Winograd-Katz, R. Fassler, B. Geiger, K. R. Legate, *Nat. Rev. Mol. Cell Biol.*, 2014, **15**, 273-288;

19. S. J. Shattil, C. Kim, M. H. Ginsberg, *Nat. Rev. Mol. Cell Biol*., 2010, **11**, 288-300;

20. C. Margadant, H. N. Monsuur, J. C. Norman, A. Sonnenberg, *Curr. Opin. Cell Biol.*, 2011, **23**, 607-614;

21. a) W. J. Chia, B. L. Tang, *Biochim. Biophys. Acta-Reviews on Cancer*, 2009, **1795**, 110-116; b) H. Stenmark, *Nat. Rev. Mol. Cell Biol.*, 2009, **10**, 513-525;

22. A. G. Ramsay, J. F. Marshall, I. R. Hart, *Cancer Metastasis Rev.*, 2007, **26**, 567-578;

23. P. Hassanzadeh, F. Atyabi, R. Dinarvand, *J. Controlled Release*, 2018, **270**, 260-267;

24. W. Guo, Y. Pylayeva, A. Pepe, T. Yoshioka, W. J. Muller, G. Inghirami, F. G. Giancotti, *Cell*, 2006, **126**, 489-502;

25. C. Le Roy, J. L. Wrana, *Nat. Rev. Mol. Cell Biol.*, 2005, **6**, 112-126;

26. a) P. T. Caswell, S. Vadrevu, J. C. Norman, *Nat. Rev. Mol. Cell Biol.*, 2009, **10**, 843-853; b) P. Caswell, J. Norman, *Trends Cell Biol.*, 2008, **18**, 257-263; c) P. T. Caswell, J. C. Norman, *Traffic*, 2006, **7**, 14-21

27. G. J. Doherty, H. T. McMahon, *Annu. Rev. Biochem.*, 2009, **78**, 857-902

28. S. Shin, L. Wolgamott, S-O. Yoon, *Int. J. Cell Biol.*, 2012, **2012**, 516789;

29. P. T. Caswell, S. Vadrevu, J. C. Norman, *Mol. Cell Bio.*, 2009, **10**, 843-853;

30. D. I. Simon, *Circ. Res.*, 2011, **109**, 1199-1201;

31. M. Aumailley, M. Gurrath, G. Müller, J. Calvete, R. Timpl, H. Kessler, *FEBS Lett.*, 1991, **291**, 50-54;

32. M. Cirillo, D. Giacomini, *Cancers*, 2021, **13**, 299;

33. H. M. Sheldrake, L. H. Patterson, *J. Med. Chem.*, 2014, **57**, 6301-6315;

34. U. K. Marelli, F. Rechenmacher, T. R. Sobahi, C. Mas-Moruno, H. Kessler, *Front. Oncol*., 2013, **3**, 222;

35. E. F. Plow, T. A. Haas, L. Zhang, J. Loftus, J. W. Smith, *J. Biol. Chem.*, 2000, **275**, 21785-21788;

36. C. Mas-Moruno, F. Rechenmeier, H. Kessler, *Anticancer Agents Med. Chem.*, 2010, **10**, 753-768;

37. E. Celik, M. H. Faridi, V. Kumar, S. Deep, V. T. Moy, V. A. Gupta, *Biophys. J.*, 2013, **105**, 2517-2727;

38. S. Q. Khan, L. Guo, D. J. Cimbaluk, H. Elshabrawy, M. H. Faridi, M. Jolly, J. F. George, A. Agarwal, V. A. Gupta, *Front. Med.*, 2014, **1**, 45;

39. W. Yang, C. V. Carman, M. Kim, A. Salas, M Shimaoka, T. A. Springer, *J. Biol.Chem*., 2006, **281**, 37904-37912;

40. P. Vanderslice, R. J. Biediger, D. G. Woodside, W. S. Brown, S. Khounlo, N. D. Warier, C. W. Gundlach, A. R. Caivano, W. G. Bornmann, S. D. Maxwell, B. W. McIntyre, J. T. Willerson, R. A. Dixon, *J. Biol. Chem.*, 2013, **288**,19414-19428;

41. a) J. M. Aizpurua, J. I. Ganboa, C. Palomo, I. Loinaz, J. Oyarbide, X. Fernandez, E. Balentova, R. M. Fratila, A. Jimenez, J. I. Miranda, A. Laso, S. Avila, J. L. Castrillo, *ChemBioChem*, 2011, **12**, 401-405; b) J. M. Aizpurua, J. Oyarbide, X. Fernandez, J. I. Miranda, J. I. Ganboa, S. Avila, J. L. Castrillo, *Eur. Pat. Appl*., 2012, EP 2407478 A1 20120118; c) J. M. Aizpurua, J. I. Ganboa, C. Palomo, I. Loinaz, J. I. Miranda, *PCT Int. Appl.*, 2006, WO 2006048473 A1 20060511;

42. P. Galletti, R. Soldati, M. Pori, M. Durso, A. Tolomelli, L. Gentilucci, S. D. Dattoli, M. Baiula, S. M. Spampinato, D. Giacomini, *Eur. J. Med. Chem.*, 2014, **83**, 284-293;

43. M. Baiula, P. Galletti, G. Martelli, R. Soldati, L. Belvisi, M. Civera, S. D. Dattoli, Santi M. Sampinato, D. Giacomini, *J. Med. Chem.*, 2016, **59**, 9721-9742;

44. Z. Pourmanouchehri, M. Jafarzadeh, S. Kakaei, E. S. Khameneh, *J. Inorg. Organomet. Polym. Mater.*, 2018, **28**, 1980-1990;

45. S. Thysiadis, S. Katsamakas, P. Dalezis, T. Chatzisideri, D. Trafalis, V. Sarli, *Future Med. Chem.,* 2017, **9** (18), 2181-2196;

46. Q.Hu, Q. Chen, Z. Gu, *Biomaterials*, 2018, **178**, 546-558;

47. G. Casi and D. Neri, *J. Med. Chem.*, 2015, **58**, 8751-8761;

48. D. Böhme, A. G. Beck-Sickinger, *J. Pept. Sci.*, 2015, **21**, 186-200;

49. P. S. Low, W. A. Henne, D. D. Doorneweerd, *Acc. Chem. Res.* 2008, **41**, 120-129;

50. S. M. Hillier, K. P. Maresca, F. J. Femia, J. C. Marquis, C. A. Foss, N. Nguyen, C. N. Zimmerman, J. A. Barrett, W. C. Eckelman, M. G. Pomper, J. L. Joyal, J. W. Babich, *Cancer Res.,* 2009, **69**, 6932-6940;

51. S. Vallabhajosula, A. Nikolopoulou, J. W. Babich, J. R. Osborne, S. T. Tagawa, I. Lipai, L. Solnes, K. P. Maresca, T. Armor, J. L. Joyal, R. Crummet, J. B. Stubbs, S. J. Goldsmith, *J. Nucl. Med.*, 2014, **55**, 1791-1798;

52. S. M. Hillier, K. J. Maresca, G. Lu, R. D. Merkin, J. C. Marquis, C. N. Zimmerman, W. C. Eckelman, J. L. Joyal, J. W. Babich, *J. Nucl. Med.,* 2013, **54**, 1369-1376;

53. M. Ginj, H. Zhang, B. Waser, R. Cescato, D. Wild, X. Wang, J. Erchegyi, J.Rivier, H. R. Maecke, J. C. Reubi, *Proc. Natl. Acad. Sci. U.S.A.,* 2006, **103**, 16436-16441;

54. N. Krall, F. Pretto, W. Decurtins, G. J. L. Bernardes, C. T. Supuran, D. Neri, *Angew. Chem., Int. Ed*., 2014, **53**, 4231-4235;

55. D. Neri, C. T. Supuran, Nat. *Rev. Drug Discovery*, 2011, **10**, 767-777;

56. N. Krall, F. Pretto, D. Neri, *Chem. Sci.*, 2014, **5**, 3640-3644;

57. M. Wichert, N. Krall, W. Decurtins, R. M. Franzini, F. Pretto, P. Schneider, D. Neri, J. Scheuermann, *Nat. Chem.*, 2015, **7**, 241-249;

58. M. Doss, H. C. Kolb, J. C. Walsh, V. P. Mocharla, Z. H. Zhu, M. Haka, R. K. Alpaugh, D. Y. T. Chen, J. Q. Yu, *Mol. Imaging Biol.*, 2014, **16**, 739−746;

59. F. Kratz, I. Muller, C. Ryppa, A. Warnecke, *ChemMedChem*, 2008, **3**, 20-53;

60. http://www.farmacista33.it/cont/download-center-files/24740/cap-farmaci-antitumorali-x27385allp1.pdf

61. S. Thysiadis, S. Katsamakas, P. Dalezis, T. Chatzisideri, D. Trafalis, V. Sarli, *Future Med. Chem.,* 2017, **9**, 2181-2196;

62. S. Thysiadis, S. Katsamakas, P. Dalezis, T. Chatzisideri, D. Trafalis, V. Sarli, *Future Med.Chem.* 2017, **9**, 2181-2196;

63. M. P. Cook, S. Ando, K. Koide, *Tetrahedron Lett.,* 2012, **53**, 5284-5286;

64. P. Gobbo, P. Gunawardene, W. Luo, S. Workenti, *Synlett*, 2015, **26**, 1169-1174;

65. E. Riva, M. Mattarella, S. Borrelli, M. S. Christodoulou, D. Cartelli, M. Main, S. Faulkner, D. Sykes, G. Cappelletti, J. S. Snaith, D. Passarella, *ChemPlusChem*, 2013, **78**, 222-226;

66. X. Chen, Q. Wu, L. Henschke, G. Weber, T. Weil, *Dyes and Pigments*, 2012, **94**, 296-303;

67. X. Yi, F. Wang, W. Qin, X. Yang, J. Yuan, *Int. J. Nanomedicine*, 2014, **9**, 1347-1365;

68. M. Baiula, M. Cirillo, G. Martelli, V. Giraldi, E. Gasparini, A. C. Anelli, S. M. Spampinato, D. Giacomini, *ACS Pharmacol. Transl. Sci.,* 2021, **4**, 1528-1542;

69. R. Soldati, R. Cervellati, G. Martelli, E. Greco, A. Demma, D. Giacomini, *Chemistry Select*, 2016, **1**, 3232-3238;

70. D-W. Li, F-F.; Tian, Y-S. Ge, X-L. Ding, , J-H. Li, Z-Q. Xu, M-F. Zhang, , X-L. Han, R. Li, F-L. Jiang, Y. Liu, *Chem. Commun.,* 2011, **47**, 10713-10715;

71. Y-F Wen, K-H. Lee, P-T. Huang, M-H.Chen, W-C. Shin, L-J. Huang, M-H. Hsu, C-J Chen, S-C. Kuo, *Bioorg. Med. Chem. Lett.,* 2007, **17**, 2908-2912;

72. Z-Y.; Tian, G-J Du, S-Q. Xie, J. Zhao, W-Y Gao, C.-J. Wang, *Molecules*, 2007, **12**, 2450-2457;

73. F. Bianchini, E. Portioli, F. Ferlenghi, F. Vacondio, E. Andreucci, A. Biagioni, J. Ruzzolini, S. Peppicelli, M. Lulli, L. Calorini, L. Battistini, F. Zanardi, A, Sartori, *Cancer Lett.,* 2019, **446**, 25-37;

74. J. S. Desgrosellier, D. A. Cheresh, *Nat. Rev. Cancer*, 2010, **10**, 9−22;

75. P. H. Wu, A. E. Opadele, Y. Onodera, J. M. Nam, *Cancers*, 2019, **11**, 1783;

76. K. M. Ignatoski, T. Maehama, S. M. Markwart, J. E. Dixon, D. L. Livant, S. P. Ethier, *Br*. J. *Cancer,* 2000, **82**, 666-674;

77. F. Aoudjit, K. Vuori, *Oncogene,* 2001, **20**, 4995-5004;

78. H. Lahlou, W. J. Muller, *Breast Cancer Res.*, 2011, **13**, 229;

79. J. Cheng, M. Haas, *Mol. Cell. Biol.*, 1990, **10**, 5502-5509;

80. D. M. Aresvik, R. D. Pettersen, T. G. Abrahamsen, M. S. Wright, *Anticancer Res.*, 2010, **30**, 3879-3887;

81. A. R. Qasem, C. Bucolo, M. Baiula, A. Sparta, P. Govoni, A. Bedini, D. Fascì, S. M. Spampinato, *Biochem. Pharmacol.*, 2008, **76**, 751-762;

82. L. Ferrazzano, D. Corbisiero, E. Potenza, M. Baiula, S. D. Dattoli, S. M. Spampinato, L. Belvisi, M. Civera, A. Tolomelli, *Sci. Rep.*, 2020, **10**, 7410;

83. E. Ruoslahti, *Drug Delivery Rev.*, 2017, **110-111**, 3-12;

84. C. M. Hu, L. Zhang, *Curr. Drug Metab.*, 2009, **10**, 836-841;

85. J. Huwyler, A. Cerletti, G. Fricker, A. N. Eberle, J. Drewe, *J. Drug Target.*, 2002, **10**, 73-79;

86. Y. Wang, A. G. Cheetham, G. Angacian, H. Su, L. Xie, H. Cui, Adv. *Drug Delivery Rev.*, 2017, **110**, 112-126;

87. L. Ma, C. Wang, Z. He, B. Cheng, L. Zheng, K. Huang, *Curr. Med. Chem.*, 2017, **24**, 3373-3396;

88. C. J. Avraamides, B. Garmy-Susini, Varner, *Nat. Rev. Cancer,* 2008, **8**, 604-617;

89. D. Arosio, C. Casagrande, *Adv. Drug Delivery Rev.*, 2016, **97**, 111-143;

90. S. Cressman, Y. Sun, E. J. Maxwell, N. Fang, D. D. Y. Chen, P. R. Cullis, *Int. J. Pept. Res. Ther*., 2009, **15**, 49-59;

91. G. Martelli, M. Baiula, A. Caligiana, P. Galletti, L. Gentilucci, R. Artali, S. M. Spampinato, D. Giacomini, *J. Med. Chem.*, 2019, **62**, 10156-10166;

92. B. K. Gan, K. Rullah, C. Y. Yong, K. L. Ho, A. R. Omar, N. B. Alitheen, W. S. Tan, *Sci. Rep.*, 2020, **10**, 16867;

93. S. D. Dattoli, M. Baiula, R. De Marco, A. Bedini, M. Anselmi, L. Gentilucci, S. M. Spampinato, *Br. J. Pharmacol.*, 2018, **175**, 3891-3910;

94. M. Baiula, A. Caligiana, A Bedini, J. Zhao, F. Santino, M. Cirillo, L. Gentilucci, D. Giacomini, S. M. Spampinato, *Front. Pharmacol.*, 2021, **11**, 617836;

95. E. Terreno, F. Uggeri, S. Aime, *J. Control. Release*, 2012, **161**, 328-337;

96. K. Kenry, K. C. Chong, B. Liu, *Acc. Chem. Res.*, 2019, **52**, 3051-3063;

97. M. Tasior, D. Kim, S. Singha, M. Krzeszewski, K. H. Ahn, D.T. Gryko, *J. Mater. Chem. C*, 2015, **3**, 1421-1446;

98. G. Signore, R. Nifosì, L. Albertazzi, B. Storti, R. Bizzarri, *J. Am. Chem. Soc.*, 2010, **132**, 1276-1288;

99. K. Sivakumar, F. Xie, B. M. Cash, S. Long, H. N. Barnhill, Q. Wang, *Org. Lett.*, 2004, **6**, 4603-4606;

100. S.S Matikonda, J. Ivanic, M. Gomez, G. Hammersley, M. J. Schnermann, *Chem. Sci*., 2020, **11**, 7302-7307;

101. A. Aggarwal, D. Samaroo, I. Radivojevic Jovanovic, S. Singh, M. P. Tuz M. Rampersad Mackiewicz, J. *Porphyrins and Phthalocyanines*, 2019, **23**, 729-765;

102. Y. Yuan, C-J. Zhang, M. Gao, R. Zhang, B. Z. Tang, B. Liu. *Angew. Chemie - Int. Ed.*, 2015, **54**, 1780-1786;

103. J. Sun, F. Xing, J. Braun, F. Traub, P. M. Rommens, Z. Xiang, U. Ritz, *Int. J. Mol. Sci.*, 2021, **22**, 11354;

104. A. Kamkaew, S. H. Lim, H. B. Lee, L. V. Kiew, L. Y. Chung, K. Burgess, *Chem. Soc. Rev.*, 2013, **42**, 77-88;

105. H. Lu, J. MacK, Y. Yang, Z. Shen, Chem. *Soc. Rev.*, 2014, **43**, 4778-4823;

106. Y. Long, S. Jie; G. Shuang, L. Shibo, N. Congwei, X. Zhen, *Tetrahedron Lett.*, 2009, **50**, 759-762;

107. J. L. Donnelly, D. Offenbartl-Stiegert, J. M. Marín-Beloqui, L. Rizzello, G. Battaglia, T. M. Clarke, S. Howorka, J. D. Wilden, *Chemistry - A European Journal*, 2020, **26**, 863-872;

108. M. Delor, J. Dai, T. D. Roberts, J. R. Rogers, S. M. Hamed, J. B. Neaton, P. L. Geissler, M. B. Francis, N. S. Ginsberg, *J. Am. Chem. Soc.*, 2018, **140**, 6278-6287;

109. L. Clima, B. G. Craciun, A. Angeli, A. Petreni, A. Bonardi, A. Nocentini, F. Carta, P. Gratteri, M. Pinteala, C. T. Supuran, *ChemMedChem*, 2020, **15**, 2052-2057;

110. S. Bua, L. Di Cesare Mannelli, D. Vullo, C. Ghelardini, G. Bartolucci, A. Scozzafava, C. T. Supuran, F. Carta, *J. Med. Chem.*, 2017, **60**, 1159-1170;

111. A. Bigi, E. Boanini, *J. Appl. Biomater. Funct. Mater.*, 2017, **15**, e313-e325;

112. S.V. Dorozhkin, *J. Mater. Chem. B*, 2019, **7**, 7471-7489;

113. V. Uskokovic, *Ceram. Int.*, 2020, **46**, 11443-11465;

114. P. J. Marie, *Osteoporos. Int.*, 2005, **16**, S7-S10;

115. V. Uskokovic, I. Jankovic-Castvan, V. M. Wu, *ACS Biomater. Sci. Eng.*, 2019, **5**, 3483-3498;

116. N. Neves, D. Linhares, G. Costa, C. C. Ribeiro, M. A. Barbosa, *Bone Joint Res.*, 2017, **6**, 366-375;

117. C. Capuccini, P. Torricelli, E. Boanini, M. Gazzano, R. Giardino, A. Bigi, *J. Biomed. Mater. Res. Part A*, 2009, **89**, 594-600;

118. E. Boanini, P. Torricelli, M. Fini, A. Bigi, *J. Mater. Sci. Mater. Med.*, 2011, **22**, 2079-2088;

119. Y. F. Li, X. P. Shui, L. Zhang, J. Hu, *J. Biomed. Mater. Res. B Appl. Biomater.*, 2016, **104**, 476-481;

120. F. Salamanna, G. Giavaresi, A. Parrilli, P. Torricelli, E. Boanini, A. Bigi, M. Fini, *Mater. Sci. Eng. C*, 2019, **95**, 355-362;

121. E. Boanini, P. Torricelli, F. Sima, E. Axente, M. Fini, I. N. Mihailescu, A. Bigi, *J. Inorg. Biochem.*, 2018, **183**, 1-8;

122. S. Bagherifard, *Mater. Sci. Eng. C*, 2017, **71**, 1241-1252;

123. E. Boanini, P. Torricelli, M. Gazzano, E. Della Bella, M. Fini, A. Bigi, *Biomaterials*, 2014, **35**, 5619-5626;

124. Q. Wei, T.L.M. Pohl, A. Seckinger, J.P. Spatz, E.A. Cavalcanti-Adam, *Beilstein J. Org. Chem.*, 2015, **11**, 773-783;

125. L. T. Duong, P. Lakkakorpi, I. Nakamura, G. A. Rodan, *Matrix Biol.*, 2000, **19**, 97-105;

126. a) C. H. Damsky, Bone, 1999, **25**, 95-96; b) M. Brunner, N. Mandier, T. Gautier, G. Chevalier, A. S. Ribba, P. Guardiola, M. R. Block, D. Bouvard, *PLoS One*, 2018, **13**, e0196021;

127. a) R. K. Globus, D. Amblard, Y. Nishimura, U. T. Iwaniec, J.-B. Kim, E. A. C. Almeida, C. D. Damsky, T. J. Wronski, M. C. H. van der Meulen, *Calcif. Tissue Int.*, 2005, **76**, 39-49; b) H. B. Lopes, G. P. Freitas, C. N. Elias, C. Tye, J. L. Stein, G. S. Stein, J. B. Lian, A. L. Rosa, M. M. Beloti, *J. Biomed. Mater. Res. Part A*, 2019, **107A**, 1303-1313; c) U. T. Iwaniec, T. J. Wronski, D. Amblard, Y. Nishimura, M. C. H. van der Meulen, C. E. Wade, M. A. Bourgeois, C. D. Damsky, R. K. Globus, J. *Appl. Physiol.*, 2005, **98**, 690-696;

128. C. R. Yeh, J. J. Chiu, C. I. Lee, P. L. Lee, Y. T. Shih, J. S. Sun, S. Chien, C. K. Cheng, *J. Bone Miner. Res.*, 2010, **25**, 627-639;

129. S. J. Park, J. Gadi, K. W. Cho, K. J. Kim, S. H. Kim, H. S. Jung, S. K. Lim, *Bone*, 2011, **49**, 428-438;

130. R. Dimitriou, E. Jones, D. McGonagle, P.V. Giannoudis, *BMC Med.*, 2011, **9**, 66;

131. R. M. Samsonraj, M. Raghunath, V. Nurcombe, J. H. Hui, A.J. van Wijnen, S. M. Cool, *Stem Cells Transl. Med.*, 2017, **6**, 2173-2185;

132. J. E. Frith, R. J. Mills, J. E. Hudson, J. J. Cooper-White, *Stem. Cells Dev.*, 2012, **21**, 2442-2456;

133. S. Gronthos, P. J. Simmons, S. E. Graves, P. G. Robey, *Bone*, 2001, **28**, 174-181;

134. Z. Hamidouche, O. Fromigue, J. Ringe, T. Haupl, P. Vaudin, J.-C. Pages, S. Srouji, E. Livne, P. J. Marie, *Proc. Natl. Acad. Sci. U. S. A.*, 2009, **106**, 18587-18591;

135. S. Mukherjee, N. Raje, J. A. Schoonmaker, J. C. Liu, T. Hideshima, M. N. Wein, D. C. Jones, S. Vallet, M. L. Bouxsein, S. Pozzi, S. Chhetri, Y. D. Seo, J. P.

Aronson, C. Patel, M. Fulciniti, L. E. Purton, L. H. Glimcher, J. B. Lian, G. Stein, K. C. Anderson, D. T. Scadden, *J. Clin. Invest.,* 2008, **118**, 491-504;

136. N. Huettner, T. R. Dargaville, A. Forget, *Trends Biotechnol.*, 2018, **36**, 372-383;

137. a) P. J. Marie, *Nat. Rev Endocrinol.*, 2013, **9**, 288-295; b) I. P. Geoghegan, D. A. Hoey, L. M. Mc Namara, *Curr. Osteoporos. Rep.*, 2019, **17**, 195-206;

138. D. Puleo, R. Bizios, *Bone*, 1991, **12**, 271-276;

139. A. Mardilovich, E. Kokkoli, *Biomacromolecules*, 2004, **5**, 950-957;

140. K. M. Hennessy, W. C. Clem, M. C. Phipps, A. A. Sawyer, F. M. Shaikh, S. L. Bellis, *Biomaterials*, 2008, **29**, 3075-3083;

141. S. L. Bellis, *Biomaterials*, 2011, **32**, 4205-4210;

142. M. Cirillo, G. Martelli, E. Boanini, K. Rubini, M. Di Filippo, P. Torricelli, S. Pagani, M. Fini, A. Bigi, D. Giacomini, *Colloids Surf. B: Biointerfaces*, 2021, **200**, 111580;

143. D. Giacomini, P. Torricelli, G.A. Gentilomi, E. Boanini, M. Gazzano, F. Bonvicini, E. Benetti, R. Soldati, G. Martelli, K. Rubini, A. Bigi, *Sci. Rep.*, 2017, **7**, 2712;

144. L. R. Snyder, J. *Chromatogr*., 1974, **92**, 223-230;

145. B. N. Bhadra, K. H. Cho, N. A. Khan, D. Y. Hong, S. H. Jhung, *J. Phys. Chem. C*, 2015, **119**, 26620-26627;

146. G. B. Deacon, R. J. Phillips, *Coord. Chem. Rev.*, 1980, **33**, 227-250;

147. M. Fonovic, B. Turk, *Biochim. Biophys. Acta*, 2014, **1840**, 2560-2570;

148. X. Ren, W.H. Shan, L. L. Wei, C. C. Gong, D. S. Pei, *Anticancer Agents Med. Chem.*, 2018, **18**, 1082-1090;

149. M. N. Kozhevnikova, A. S. Mikaelyan, V. I. Starostin, *Biol. Bull. Russ. Acad. Sci.*, 2008, **35**, 223-232;

150. Y-M. Hyun, C. T. Lefort, M. Kim, *Immunol Res.*, 2010, **45**, 195-208;

151. M. Niino, C. Bodner, M. L. Simard, S. Alatab, D. Gano, H. J. Kim, M. Trigueiro, D. Racicot, C. Guérette, J. P. Antel, A. Fournier, F. Grand'Maison, A. Bar-Or, *Ann. Neurol.*, 2006, **59**, 748-754;

152. A. Laffon, R. Garcia-Vicuna, A. Humbria, A. Postigo, A. L. Corbi, M. O. de Landazuri, *J. Clin. Invest.,* 1991, **88**, 546-552;

153. S. Ghosh, E. Goldin, F. H. Gordon, H. A. Malchow, J. Rask-Madsen, P. Rutgeerts, *N. Engl. J. Med.,* 2003, **348**, 24-32;

154. L. M. Coussens, Z. Werb, *Nature*, 2002, **420**, 860-867;

155. C. J. Avraamides, B. Garmy-Susini, J. A. Varner, *Nat. Rev. Cancer*, 2008, **8**, 604-617;

156. I. Mitroulis, V. I. Alexaki, I. Kourtzelis, A. Ziogas, G. Hajishengallis, T. Chavakis, *Pharmacol Ther.*, 2015, **0**, 123-135;

157. I. Mitroulis, V. I. Alexaki, I. Kourtzelis, A. Ziogas, G. Hajishengallis, T. Chavakis, *Pharmacol. Ther.*, 2015, **147**, 123-135;

158. M. Shimaoka, T. Xiao, J-H. Liu, Y. Yang, Y. Dong, C-D. Jun, A. McCormack, R. Zhang, A. Joachimiak, J. Takagi, J-H. Wang, T. A. Springer, *Cell.,* 2003, **112**, 99-111;

159. A. R. de Fougerolles, S. A. Stacker, R. Schwarting, T. A. Springer, J. *Exp. Med.*, 1991, **174**, 253-267;

160. A. R. de Fougerolles, X. Qin, T. A. Springer, *J. Exp. Med.*, 1994, **179**, 619-629;

161. T. Springer, G. Galfre, D. S. Secher, C. Milstein, *Eur. J. Immunol.*, 1979, **9**, 301-306;

162. V. P. Yakubenko, V. K. Lishko, S. C. Lam, T. P. Ugarova, *J. Biol. Chem.*, 2002, **277**, 48635-48642;

163. R. R. Lobb, M. E. Hemler, *J. Clin. Invest.*, 1994, **94**, 1722-1728;

164. A. Puig-Kroger, F. Sanz-Rodriguez, N. Longo, P. Sanchez-Mateos, L. Botella, J. Teixido C. Bernabeu, A. Corbi, *J. Immunol.*, 2000, **165**, 4338-4345;

165. Y. Hyun, C. T. Lefort, M. Kim, *Immunol. Res.*, 2009, **45**, 195-208;

166. J. Boer, D. Gottschling, A. Schuster, M. Semmrich, B. Holzmann, H. Kessler, *J. Med. Chem.*, 2001, **44** (16), 2586-2592;

167. A. Petrovic, O. Alpdogan, L. M. Willis, J. M. Eng, A. S. Greenberg, B. J. Kappel, C. Liu G. J. Murphy G. Heller, M. R. van den Brink, *Blood*, 2004, **103**, 1542-1547;

168. M. J. Briskin, L. Rott, E. C. Butcher, *J. Immunol.*, 1996, **156**, p. 719-726;

169. L. Steinman, *Nat. Rev. Drug Discov.*, 2005, **4**, 510-518;

170. B. K. Kleinschmidt-DeMasters, K. L. Tyler, *N. Engl. J. Med.*, 2005, **353**, 369-374;

171. W. J. Sandborn, J. F. Colombel, R. Enns, B. G. Feagan, S. B. Hanauer, I. C. Lawrance R. Panaccione, M. Sanders, S. Schreiber, S. Targan, S. van Deventer, R. Goldblum, D. Despain, G. S. Hogge, P. Rutgeerts, *N. Engl. J. Med.*, 2005, **353**, 1912-1925;

172. L. P. McLean, R. K. Cross, *Expert Opin. Investig. Drugs*, 2016, **25**, 263-273;

173. C. Lu, M. Shimaoka, Q. Zang, J. Takagi, T. A. Springer, *Proc. Natl. Acad. Sci.*, 2001, **98**, 2393-2398;

174. M. Shimaoka, A. Salas, W. Yang, G. Weitz-Schmidt, T. A. Springer, *Immunity*, 2003, **19**, 391-402;

175. D. M. Nowlin, F. Gorcsan, M: Moscinski, S-L. Chiang, T. J. Lobl, P. M. Cardarelli, *J. Biol. Chem.*, 1993, **268,** 20352-20359;

176. R. J. Davenport, J. R. Munday, *Drug Discov. Today*, 2007, **12**, 569-576;

177. M. Björklund, O. Aitio, M. Stefanidakis, J. Suojanen, T. Salo, T. Sorsa, E. Koivunem, *Biochemistry*, 2006, **45**, 2862-2871;

178. S. Q. Khan, L. Guo, D. J. Cimbaluk, H. Elshabrawy, M. H. Faridi, M. Jolly, J. F. George, A. Agarwal, V. Gupta, *Front. Med.*, 2014, **1**, 45;

179. Y. Huang, P. S. Hammond, B. R. Whirrett, R. J. Kuhner, L. Wu, S. R. Childers, R. H. Mach, *J. Med. Chem.*, 1998, **41**, 2361-2370;

180. I. Bae, D. Kim, J. Choi, J. Kim, M. Kim, B. Park, Y. H. Kim, Y. G. Ahn, H. Hyung Kim, D. K. Kim, *Bioorg. Med. Chem. Lett.*, 2021, **34**, 127676;

181. T. M. Bräuer, Q. Zhang, K. Tiefenbacher, *Angew. Chem. Int. Ed.*, 2016, **55**, 7698-7701;

182. C. Bolchi, E. Valoti, L. Fumagalli, V. Straniero, P. Ruggeri, M. Pallavicini, *Org. Proc. Res. Dev.*, 2015, **19**, 878-883;

183. WHO World Health Organization TUBERCULOSIS GLOBAL REPORT 2019. 2019.

184. K. Patil, S. Bagade, S. Bonde, S. Sharma, G. Saraogi, *Biomed. Pharmacother.*, 2018, **99**, 735-745;

185. A. Bahuguna, D. S. Rawat, *Med. Res. Rev.*, 2020, **40**, 263-292;

186. Y. Li, F. Sun, W. Zhang, *Drug Dev. Res.*, 2019, **80**, 98-105;

187. J. Furin, H. Cox, M. Pai, *The Lancet*, 2019, **393**, 1642-1656;

188. P. J. Brennan, *Tuberculosis*, 2003, **83**, 91-97;

189. M. Jankute, J. A. G. Cox, J. Harrison, G. S. Besra, *Annu. Rev. Microbiol.*, 2015, **69**, 405-423;

190. A. Maitra, T. Munshi, J. Healy, L. T. Martin, W. Vollmer, N. H. Keep, S. Bhakta, *FEMS Microbiol. Rev.*, 2019, **43**, 548-575;

191. P. Kumar, K. Arora, J. R. Lloyd, I. Y. Lee, V. Nair, E. Fischer, H. I. M. Boshoff, C. E. Barry, *Mol. Microbiol.*, 2012, **86**, 367-381;

192. J. Wietzerbin, J. Wietzerbin, E. Lederer, B. C. Das, E. Lederer, M. Leyh-Bouille, *Biochemistry*, 1974, **13**, 3471-3476;

193. S. B. Erdemli, R. Gupta, W. R. Bishai, G. Lamichhane, L. M. Amzel, M. A. Bianchet, *Structure*, 2012, **20**, 2103-2115;

194. M. Lavollay, M. Arthur, M. Fourgeaud, L. Dubost, A. Marie, N. Veziris, D. Blanot, L. Gutmann, J. L. Mainardi, *J. Bacteriol.*, 2008, **190**, 4360-4366;

195. R. Gupta, M. Lavollay, J. L. Mainardi, M. Arthur, W. R. Bishai, G. Lamichhane, *Nat. Med.*, 2010, **16**, 466-469;

196. G. Martelli, T. B. Pessatti, E. M. Steiner, M. Cirillo, C. Caso, F. Bisognin, M. Landreh, P. Dal Monte, D. Giacomini, R. Schnell, *Cell Chem. Biol.*, 2021, **28**, 1321-1332.e5;

197. J. E. Hugonnet, J. S. Blanchard, *Biochemistry*, 2007, **46**, 11998-12004;

198. K. England, H. I. M. Boshoff, K. Arora, D. Weiner, E. Dayao, D. Schimel, L. E. Via, C. E. Barry, *Antimicrob. Agents and Chemother.*, 2012, **56**, 3384-3387;

199. M. C. Payen, S. De Wit, C. Martin, R. Sergysels, I. Muylle, Y. Van Laethem, N. Clumeck, *Int. J. Tuberc. Lung Dis.*, 2012, **16**, 558-560;

200. a) M. Cordillot V. Dubée, S. Triboulet, L. Dubost, A. Marie, J. E. Hugonnet, M. Arthur, J. L. Mainardi, *Antimicrob. Agents Chemother.*, 2013, **57**, 5940-5945; b) E. M. Steiner, G. Schneider, R. Schnell, *FEBS J.*, 2017, **284**, 725-741; c) L. Iannazzo, D. Soroka, S. Triboulet, M. Fonvielle, F. Compain, V. Dubée, J. L. Mainardi, J. E. Hugonnet, E. Braud, M. Arthur, M. Etheve-Quelquejeu, *J. Med. Chem.*, 2016, **59**, 3427-38; d) X. Wang, X. Gu, C. Zhang, F. Zhao, K. Deng, *Biochem. Biophys. Res. Commun.*, 2020, **523**, 6-9;

201. N. Dhar, V. Dubée, L. Ballell, G. Cuinet, J. E. Hugonnet, F. Signorino-Gelo, D. Barros, M. Arthur, J. D. McKinney, *Antimicrob. Agents Chemother.*, 2015, **59**, 1308-19;

202. a) C. T. Lohans, E. van Groesen, K. Kumar, C. L. Tooke, J. Spencer, R. S. Paton, J. Brem, C. J. Schofield, *Angew. Chem. Int. Ed. Engl.*, 2018, **57**, 1282-1285; b) C. T. Lohans, H. T. H. Chan, T. R. Malla, K. Kumar, J. J. A. G. Kamps, D. J. B. McArdle, E. van Groesen, M. de Munnik, C. L. Tooke, J. Spencer, R. S. Paton, J. Brem, C. J. Schofield, *Angew. Chem. Int. Ed. Engl.*, 2019, **58**, 1990-1994;

203. Z. Lu, H. Wang, A. Zhang, X. Liu, W. Zhou, C. Yang, L. Guddat, H. Yang, C. J. Schofield, Z. Rao, *Mol. Pharmacol.*, 2020, **7**, 287-294;

204. E. Turos, M. I. Konaklieva, R. X. F. Ren, H. Shi, J. Gonzalez, S. Dickey, D. Lim, *Tetrahedron*, 2000, **56**, 5571-5578;

205. E. Turos, C. Coates, J. Y. Shim, Y. Wang, J. M. Leslie, T. E. Long, G. S. K. Reddy, A. Ortiz, M. Culbreath, M. S. Dickey, D. V. Lim, E. Alonso, J. Gonzalez, *Bioorg. Med. Chem.*, 2005, **13**, 6289-6308;

206. B. Heldreth, T. E. Long, S. Jang, G. S. K. Reddy, E. Turos, S. Dickey, D. V. Lim, *Bioorg. Med. Chem.*, 2006, **14**, 3775-3784;

207. K. D. Revell, B. Heldreth, T. E. Long, S. Jang, E. Turos, *Bioorg. Med. Chem.*, 2007, **15**, 2453-2467;

208. B. Bhattacharya, E. Turos, *Tetrahedron*, 2012, **68**, 10665-10685;

209. K. D. Revell, B. Heldreth, T. E. Long, S. Jang, E. Turos, *Bioorg. Med. Chem.*, 2007, **15**, 2453-2467;

210. W. E. Truce, G. H. Birum, E. T. McBee, *J. Am. Chem. Soc*., 1952, **74**, 3594-3599;

211. P. Galletti, C. E. A. Cocuzza, M. Pori, A. Quintavalla, R. Musumeci, D. Giacomini, *ChemMedChem*, 2011, **6**, 1919-1927;

212. S. Meiries, R. Marquez, *J. Org. Chem.*, 2008, **73**, 5015-5021;

213. A. L. Amorim, M. M. Peterle, A. Guerreiro, D. F. Coimbra, R. S. Heying, G. F. Caramori, A. L. Braga, A. J. Bortoluzzi, A. Neves, G. J. L.Bernardes, R. A. Peralta, *Dalton Transactions*, 2019, **48**, 5574-5584;

214. I. Ernest, J. Gosteli, R. B. Woodward, *J. Am. Chem. Soc*., 1979, **101**, 6301-6305;

215. W. Cabri, I. Candiani, F. Zarini, A. Bedeschi, *Tetrahedron Lett.*, 1994, **35**, 3379-3382;

216. M. Alpegiani, A. Bedeschi, M. Foglio, F. Giudici, E. Pewone, *Tetrahedron Lett.*, 1983, **24**, 1627-1630;

217. P. Galletti, A. Quintavalla, C. Ventrici, G. Giannini, W. Cabri, D. Giacomini, *New J. Chem.*, 2010, **34**, 2861-2866;

218. S. Masao, H. Tetsuo, Y. Hiroaki, M. Hiroshi, K. Naoyuki; O. Osamu, *Heterocycle*s, 1986, **24**, 1007-1012;

219. T. N. Beck, D. Lloyd, R. Kuskovsky, J. Minah, K. Arora, B. J. Plotkin, J. M. Green, I. H. Boshoff, C. Barry, J. Deschamps, M. I. Konaklieva, *Bioorg. Med. Chem.*, 2015, **23**, 632-647;

220. C. Jacopin, M. Laurent, M. Belmans, L. Kemps, M. Cérésiat, J. and Marchand-Brynaert, *Tetrahedron*, 2001, **57**, 10383-10389;

221. G. Torrelo, U. Hanefeld, F. Hollmann, *Catal. Lett.*, 2015, **145**, 309-345;

222. G. Martelli, P. Galletti, M. Baiula, L. Calcinari, G. Boschi, D. Giacomini, *Bioorg Chem*., 2019, **88**, 102975;

223. R. A. Sheldon, P. C. Pereira, *Chem. Soc. Rev.*, 2017, **46**, 2678-2691;

224. H. Y. Aboul-Enein, I. W. Wainer, *The impact of Stereochemistry on Drug Development and Use*, 1997, Wiley-Interscience;

225. S. W. Smith, *Toxicol. Sci.*, 2009, **110**, 4-30;

226. T. Palmer (editor), *Understanding Enzymes* (3rd edition), 1991, Ellis Horwood Ltd;

227. T. A. Springer, J-H. Wang, *Adv. Protein Chem.*, 2004, **68**, 29-63;

228. R. de Regil, G. Sandoval, *Biomolecules*, 2013, **3**, 812-847;

229. M. A. Taipa, M. R. Aires-Barros, J. M. S. Cabral, *Journal of Biotechnology*, 1992, **26**, 111-142;

230. S. J. Swapnil, H. J. Arpana, *Res. J. Biotechnol.*, 2019, **14**, 130-138;

231. A. Guldhe, B. Singh, T. Mutanda, *Renew. Sustain. Energy Rev.*, 2015, **41**, 1447-1464;

232. F. I. Khan, D. Lan, R. Durrani, W. Huan, Z. Zhao, Y. Wang, *Front. Bioeng. Biotechnol*., 2017, **5**, 16;

233. K. Faber, *Biotransformations in Organic Chemistry* (5th edition), 2004, Springer;

234. H. Wild, *in The Organic Chemistry of β-Lactams*, 1993, Georg, G. I., Ed., VCH Publishers, Inc.: New York.

235. G. Martelli, M. Cirillo, V. Giraldi, D. Giacomini, *Bioorg. Chem.*, 2022, **120**, 105580;

236. a) D. G. Tew, H. F. Boyd, S. Ashman, C. Theobald, C. A. Leach, *Biochemistry*, 1998, **37**, 10087-10093; b) J. Mulchande, L. Martins, R. Moreira, M. Archer, T. F. Oliveira, J. Iley, *Org. Biomol. Chem.*, 2007, **5**, 2617-2626; c) M. B. Kostova, C. J. Myers, T. N. Beck, B. J. Plotkin, J. M. Green, H. I. M. Boshoff, C. E. Barry, J. R. Deschamps, M. I. Konaklieva, *Bioorg Med Chem.*, 2011, **19**, 6842-6852; d) M. W. Majewski, K. D. Watson, S. Cho, P. A. Miller, S. G. Franzblau, M. J. Miller, *Med. Chem. Comm.*, 2016, *7*, 141-147;

237. R. Kuskovsky, D. Lloyd, K. Arora, B. J. Plotkin, J. M. Green, H. I. Boshoff, C. Barry, J. Deschamps, M. I. Konaklieva, *Bioorg. Med. Chem.*, 2019, **27**, 115050;

238. W. J. Tenn 3rd, J. L. Murphy, J. K. Bim-Merle, J. A. Brown, A. J. Junia, M. A. Price, R. W. Nagorski, *J. Org. Chem.*, 2007, **72**, 6075-6083;

239. X.-G. Li, L. T. Kanerva, *Tetrahedron: Asymmetry*, 2007, **18**, 2468-2472;

240. E. Forrò, F. Fülöp, *Tetrahedron: Asymmetry*, 2001, **12**, 2351-2358;

241. X.-G. Li, L. Kanerva, *Adv. Synthesis Catalysis*, 2006, **348**, 197-205;

242. N. Ikota, H. Shibata, K. Koga, *Chem. Pharm. Bull.*, 1985, **33**, 3299-3306;

243. A. Shaabani, F. Tavasoli-Rad, D. G. Lee, *Synth. Commun.*, 2005, **35**, 571-580;

244. A. Calcaterra, I. D'Acquarica, *J. Pharm. Biomed. Anal.*, 2018, **147**, 323-340;

245. F. Toda, K. Tanaka, M. Yagi, Z. Stein, I. Goldberg, *J. Chem. Soc. Perkin Transactions,* 1990, **1**, 1215-1216;

246. P. D. Mehta, N. P. S. Sengar, A. K. Pathak, *Eur. J. Med. Chem.,* 2010, **45**, 5541-5560;

247. F. Gavina, A. M. Costero, M. R. Andreu, *J. Org. Chem.,* 1990, **55**, 434-437;

248. E. L. Eliel, S. H. Wilen, *Stereochemistry of organic compounds*, 1994, New York: John Wiley & Sons;

249. A. Mándi, T. Kurtán, *Nat. Prod. Rep.*, 2019, **36**, 889-918;

250. S. S. Tang, A. Apisarnthanarak, L. Yang Hsu, *Adv. Drug Deliv. Rev.*, 2014, **78**, 3-13;

251. D. L. Nelson and M. M. Cox, *Principles of Biochemistry*, 6th edition, 2012, Leningher;

252. A. Basak and U. Khamrai, *Synth. Commun.*, 1994, **24**, 131-135;

253. J. E. Park, M. C. Lenter, R. N. Zimmerman, P. Garin-Chesa, L. J. Old, W. J. Rettig, *Biol. Chem.*, 1999, **274**, 36505-36512;

254. M. A. Huber, N. Kraut, J. E. Park, R. D. Schubert, W. J. Rettig, R. U. Peter, P. Garin-Chesa, *J. Invest. Dermatol.*, 2003, **120**, 182-8;

255. M. Levy, G. McCaughan, C. Abbott, J. E. Park, A. Cunningham, E. Muller, W. J. Rettig, M. Gorrell, *Hepatology*, 1999, **29**, 1768-1778;

256. C. Edosada, C. Quan, C. Wiesmann, T. Tran, D. Sutherlin, M. Reynolds, J. Elliott, H. Raab, W. Fairbrother, B. Wolf, *J. Biol. Chem.*, 2006, **281**, 7437-44;

257. A. A. Fitzgerald, L. M. Weiner, *Cancer Metastasis Rev.*, 2020, **39**, 783-803;

258. L. Dongmei, L. Ma, W. Fangyuan, *Int. J. Oncol.*, 2021, **41**, 541-550;

259. P. Garin-Chesa, L. J. Old, W. J. Rettig, *Proc. Natl. Acad. Sci.*, 1990, **87**, 7235-7239;

260. J. A. Tuxhorn, G. E. Ayala, M. J. Smith, V. C. Smith, T. D. Dang, D. R. Rowley, *Clin. Cancer Res*., 2002, **8**, 2912-2923;

261. J. Millul, G. Bassi, J. Mock, A. Elsayed, C. Pellegrino, A. Zana, S. Dakhel Plaza, L. Nadal, A. Gloger, E. Schmidt, I. Biancofiore, E. J. Donckele, F. Samain, D. Neri, S. Cazzamalli, *PNAS*, 2021, **118**, e2101852118;

262. C. Y. Edosada, C. Quan, T. Tran, V. Pham, C. Wiesmann, W. Fairbrother, B. B. Wolf, *FEBS Lett.*, 2006, **580**, 1581-6;

263. C. Kratochwil, P. Flechsig, T. Lindner, L. Abderrahim, A. Altmann, W. Mier, S. Adeberg, H. Rathke, M. Röhrich, H. Winter, P. K. Plinkert, F. Marme, M. Lang, H-U. Kauczor, D. Jäger, J. Debus, U. Haberkorn, F. L. Giesel, *J. Nucl. Med.*, 2019, **60**, 801-805;

264. M. Syed, P. Flechsig, J. Liermann, P. Windisch, F. Staudinger, S. Akbaba, S. A. Koerber, C. Freudlsperger, P. K. Plinkert, J. Debus, F. Giesel, U. Haberkorn, S. Adeberg, *Eur. J. Nucl. Med. Mol. Imaging*, 2020, **47**, 2836-2845;

265. C. Meyer, M. Dahlbom, T. Lindner, S. Vauclin, C. Mona, R. Slavik, J. Czernin, U. Haberkorn, J. Calais, *J. Nucl. Med.*, 2020, **61**, 1171-1177;

266. M. Dorywalska, R. Dushin, L. Moine, S. E. Farias, D. Zhou, T. Navaratnam, V. Lui, A. Hasa-Moreno, M. G. Casas, T-T. Tran, K. Delaria, S-H. Liu, D. Foletti, C. J. O'Donnell, J. Pons, D. L. Shelton, A. Rajpal P. Strop, *Mol. Cancer Ther.*, 2016, **15**, 958-970;

267. M. P. Gamcsik, M. S. Kasibhatla, S. D. Teeter, O. M. Colvin, *Biomarkers*, 2012, **17**, 671-91;

268. B. J. Mills, C. A. Lang, *Biochem. Pharmacol.*, 1996, **52**, 401-6;

269. C. P. Leamon, J. A. Reddy, A. Bloomfield, R. Dorton, M. Nelson, M. Vetzel, P. Kleindl, S. Hahn, K. Wang, I. R. Vlahov, *Bioconjugate Chem.* 2019, **30**, 1805-1813;

270. S. Cazzamalli, A. Dal Corso, D. Neri, *Mol. Cancer Ther.*, 2016, **15**, 2926-2935;

271. N. Krall, F. Pretto, W. Decurtins, J. L. G. J. L. Bernardes, C. T. Supuran, D. Neri, *Angew. Chem. Int. Ed.*, 2014, **53**, 4231-4235;